RMIT UNIVERSITY

# Trends and Variability in Climate Extremes in the Western Pacific

A thesis submitted in fulfilment of the requirements for the degree of Doctor of Philosophy

**Simon John McGree**
Master of Science in Geography, University of Auckland

Postgraduate Diploma in Geography, University of the South Pacific

Bachelor of Science, Earth Sciences and Geography, University of the South Pacific

School of Science
College of Science, Technology, Engineering and Maths
RMIT University

October 2020

# Declaration

I certify that except where due acknowledgement has been made, the work is that of the author alone; the work has not been submitted previously, in whole or in part, to qualify for any other academic award; the content of the thesis is the result of work which has been carried out since the official commencement date of the approved research program; any editorial work, paid or unpaid, carried out by a third party is acknowledged; and, ethics procedures and guidelines have been followed.

I acknowledge the support I have received for my research through the provision of an Australian Government Research Training Program Scholarship, publication funding from the RMIT School of Science and study leave and publication funding from the DFAT funded Pacific-Australia Climate Change Science Adaptation Planning Program and Climate and Oceans Support Program in the Pacific via the Bureau of Meteorology.

Simon McGree
30 October 2020

# Acknowledgements

Firstly, I wish to acknowledge and thank my past and present managers at the Bureau of Meteorology, Dr David Jones, Mr Neil Plummer, Ms Janita Pahalad, and Ms Celine Becker for firstly recommending I undertake this task, approving my study leave and/or providing financial assistance. A special thank you to numerous friends and colleagues especially Mr Neil Conning for advice, analytical and/or editorial assistance. Your support was a great help and truly appreciated.

Secondly, I would like to acknowledge and thank Associate Professor Sergei Schreider, Adjunct Professor Yuriy Kuleshov and more recently Professor Asha Rao. I was privileged to have excellent supervisors, who have supercharged my climate science analytical abilities. I truly appreciate the guidance and support provided throughout this journey. Thank you for your patience, allowing me to work independently and at my own pace, enabling me to mature as a researcher, and enhancing the final product of this thesis.

Finally, thank you to my family and Bear the golden retriever (kept me company many nights) who have supported me on this journey. Your support, understanding and love is greatly appreciated. To my very special daughter, Helena. Life hasn’t been easy for you these last few years. High school was difficult for me too. By completing this task, I hope you can see that it is possible to achieve even if Y12 in 2020 doesn’t go your way.

# Table of Contents

# List of Figures

# List of Tables

# Summary of Research

This research is focused on examining interannual and long-term change in precipitation and temperature extremes in the western Pacific. The Pacific Islands have been identified as being among the most vulnerable to climate change and climate extremes with changes in climate extremes likely to impact many sectors. In addition, smallness renders island the countries at risk of high proportionate losses and despite the known impacts, relatively little is known about changes in climate extremes in the region.

In Chapter 2, precipitation records for 21 countries and territories in the western Pacific for the period 1951 to 2010 were examined to identify trends in drought occurrence, duration and magnitude. The strength of the relationship between the main climate drivers of variability in the Pacific, El Niño–Southern Oscillation (ENSO), Interdecadal Pacific Oscillation (IPO) and Pacific Decadal Oscillation (PDO) and precipitation were also examined. Station scale drought trends were largely positive but the majority were statistically non-significant with the significant trends mainly in the subtropics. Spatially, trend patterns were largely heterogeneous. A significant relationship between the oceanic component of ENSO and precipitation was confirmed for a large part of the Pacific Islands and east Australia with a strong lagged relationship in the year after the El Niño onset at locations southwest of the South Pacific Convergence Zone (SPCZ) and north of the Intertropical Convergence Zone (ITCZ). Similarly, a strong relationship was found with IPO and PDO at most locations. Drought was found to be longer and more severe southwest of the SPCZ and north of the ITCZ during the positive phase of the IPO and PDO.

In Chapter 3, trends in mean and extreme annual and seasonal temperature and precipitation over the 1951–2015 period were calculated for 57 stations in 20 western Pacific Island countries and territories. The extremes indices are those of the World Meteorological Organization Expert Team on Sector-specific Climate Indices. The purpose of expert team and indices is to promote the use of globally consistent climate indices to highlight variability and trends in climate extremes which are of particular interest to socio-economic sectors, and to help characterise the climate sensitivity of various sectors. Prior

to the calculation of the monthly means and indices, the data underwent quality control and homogeneity assessment. A rise in mean temperature occurred at most stations, in all seasons and in both halves of the study period. The temperature indices also showed strong warming, which for the majority of stations was strongest in December to February and weakest in June to August. The absolute and percentile-based indices show the greatest warming at the upper end of distribution. While changes in precipitation were less consistent and trends generally weak at most locations, declines in both total and extreme precipitation were found in Southwest French Polynesia and the Southern subtropics. There was a decrease in moderate to high intensity precipitation events, especially those experienced over multiple days, in Southwest French Polynesia from December to February. Strong drying trends have also been identified in the low to moderate extreme indices in the June to August and September to November periods. These negative trends contributed to an increase in the magnitude of meteorological drought in both subregions. The relationship between total and extreme precipitation and Pacific basin sea surface temperatures were investigated with a focus on the influence of the ENSO. A strong relationship between ENSO and total precipitation is substantiated and similar relationships for the threshold extreme indices established. The percentile-based and absolute extreme indices are influenced by ENSO to a lesser extent and in some cases the influence is marginal.

The primary objective of Chapter 4 was determining the magnitude of the influence of mean and extreme climate on agricultural productivity in the western Pacific using sugarcane and sugar yield in western Fiji as a case study. Sugarcane is one of Fiji's largest commercial agricultural crops and greater than 80% of the raw sugar produced is exported. Few sugar producing countries are as dependant on the contribution of sugar to the export market as Fiji. There has been a statistically significant decline in sugar yield since 1975. The proportion of sugar extracted from sugarcane has also declined as shown by a positive trend in the tonnes cane to tonnes sugar ratio. The role of climate in these changes was investigated by first using principal component analysis then stepwise regression to predict sugarcane and sugar yield. ‘Mild drought conditions’, an increase in the diurnal temperature range and cool conditions during the ripening and maturation period are favourable for sugar yield. The

impact of future warmer, wetter and drier conditions on sugar yield was also examined, in the absence of adaptive measures. Results show declines in sugar yield with an increase in mean and extreme temperature. Results also show an increase in the number of rain days in March offsets the increase in temperature suggesting that an increase the number of rain days in the late growing season in a future climate may counter the influence of higher temperatures. Irrigation in the late growing season may be an option to increase yields and/or adapt to a warmer climate.

# 1 Introduction

## 1.1 Outline of the Problem

Global and regional climates have varied on spatial and temporal timescales. Associated with orbital changes, paleoclimatic records document a sequence of glacial-interglacial cycles covering the last 740,000 years in ice cores and several million years in deep oceanic sediments. The past 430,000 years show major swings in global climate between four cooler periods of widespread glaciation (ice ages), interspersed with warmer interglacial periods lasting from 10,000 to 30,000 years (IPCC, 2007; 2013). Warming of the global climate by 4–7°C since the last glacial maximum about 21,000 years ago is estimated to have occurred at a rate 10 times slower than the warming of the 20th century (IPCC, 2007; 2013; Kaufman et al. 2020).

Human influence on climate has been the dominant cause of observed warming since the mid-20th century, with global average surface temperature increasing by 0.85°C between 1880 and 2012 (IPCC, 2013). Each of the last three decades has been successively warmer at the Earth’s surface than any preceding decade since 1850. The period since 1983 is likely to be the warmest 30-year period of the last 1400 years in the northern hemisphere, where such assessment is possible (IPCC, 2014a). The main contributor to the positive radiative forcing is anthropogenic greenhouse gas emissions which since the pre-industrial era have driven large increases in the atmospheric concentrations of carbon dioxide, methane and nitrous oxide. About half of the anthropogenic carbon dioxide emissions since 1750 have occurred in the last 40 years (IPCC, 2014a).

Climate also varies on interannual to decadal timescales due to a range of forcings that are internal (such as El Niño–Southern Oscillation (ENSO) and North Atlantic Oscillation) or external (such as volcanic aerosols, amount of incoming solar radiation) to the climate system (IPCC, 2007).

Temperature rise to date has already resulted in profound alterations to human and natural systems, including increases in droughts, floods, and some other types of extreme weather; sea level rise; and biodiversity loss – these changes are causing unprecedented risks to vulnerable persons and populations (IPCC, 2012, 2014b). The rate of warming has been twice as fast for land masses compared to oceans and, in the northern hemisphere, for high versus low latitude regions. Warming of the ocean varies between basins, with that of the Pacific being ‘punctuated’ by El Niño events and Pacific decadal variability compared to the steadier observed warming of, for example, the Indian Ocean (IPCC, 2007; Lough et al., 2011).

The Pacific Islands (Figure 1.1) are immensely diverse in terms of their history, geography, climate, natural resource base and culture. As part of the group of small island developing states, they share many similar sustainable development challenges such as small populations, limited resources, remoteness, susceptibility to natural disasters, vulnerability to external shocks and dependence on international trade (Australian Bureau of Meteorology and CSIRO, 2011; 2014). The ecosystems that Pacific Island countries and territories rely on for economic development, food security and livelihood opportunities for their people, have adapted to the prevailing climate conditions and their normal seasonal variations (Bell et al., 2011).

There is general agreement amongst the communities of the Pacific Islands that changes in weather and climate are occurring in their region. More change is believed to have occurred over the past decades than at any other time in human memory. Pacific Islanders have described local perceptions of climate change in their countries. These include: shifts in seasonal patterns of precipitation and tropical cyclones, more frequent and extreme precipitation causing flooding and mudslides, more droughts and fires, more hot days, more coral bleaching, more storm surges, coastal erosion and salt water contamination of freshwater springs and taro swamps (Australian Bureau of Meteorology and CSIRO, 2011).

Research into exposure and risk from climate change has found the environmental, socio-economic and cultural factors contribute to the increase in vulnerability (Hay et al., 2019; Salmon et al., 2019). There are multiple stresses that affect the vulnerability of small islands to climate change. In Tuvalu, for example, economic stressors, food related stressors, and overcrowding makes the islands much more vulnerable to climate change impacts including precipitation patterns (McCubbin et al., 2015). Culturally, the people of Tuvalu are obligated to support extended family members, which is one of the main

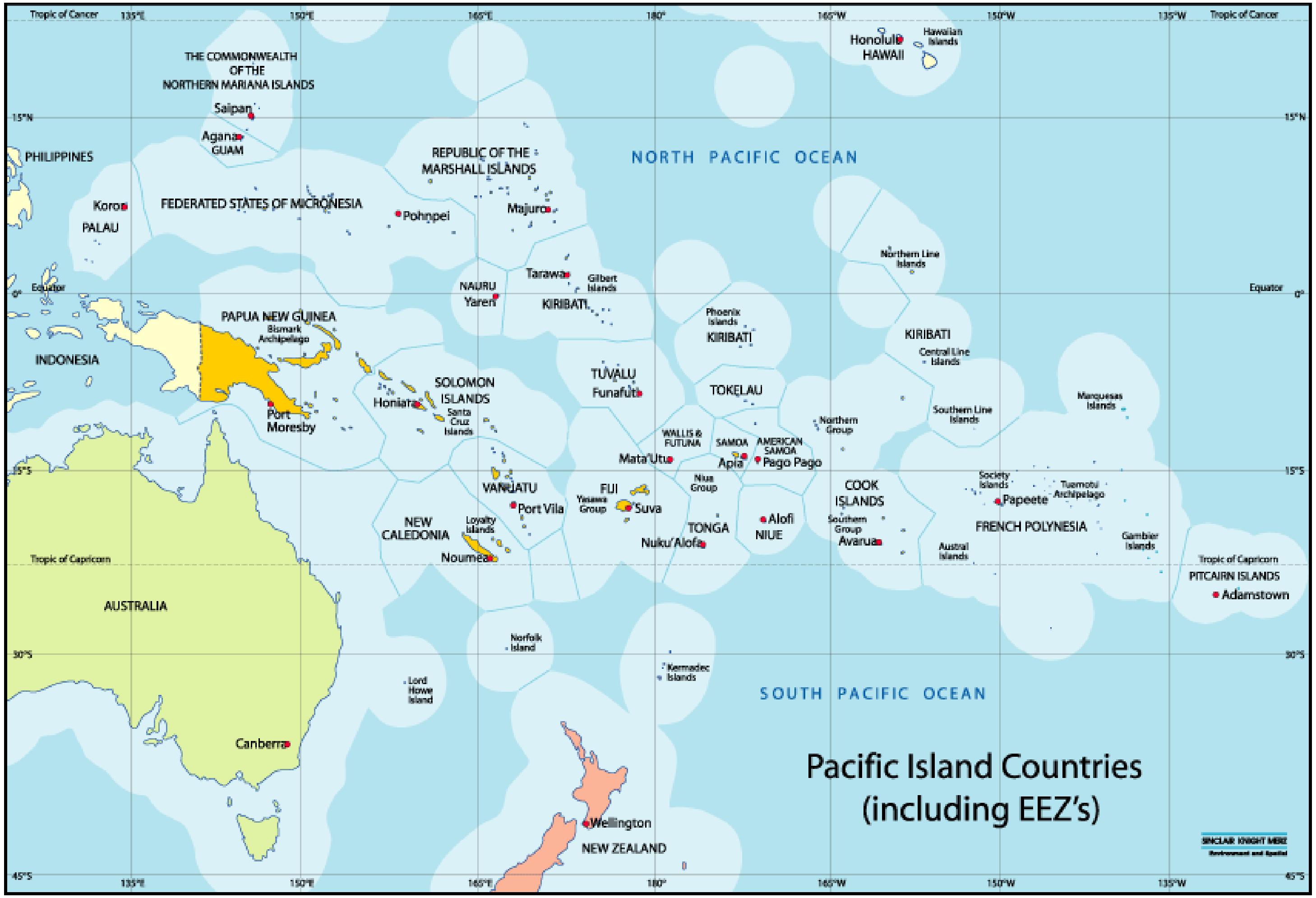


Figure 1.1 Map of the Pacific Islands (source: www.pinterest.com.au)

reasons for overcrowding and large households. However, the high number of people living in these households makes them more vulnerable to drought (Benns, 2011; Manhire, 2011) and because they generate a high demand for water, short-term water saving measures are insufficient. In addition, because of the poverty, people do not have the resources to build more tanks to increase their capacity to store water (McCubbin et al., 2015).

A better understanding the past climate helps to inform more robust projections of future climate which are essential for underpinning climate change adaptation strategies and contributing to the sustainable development of Pacific Island countries (Australian Bureau of Meteorology and CSIRO, 2014).

## 1.2 Changes in Climate Extremes

Global warming is manifested particularly in changes of weather and climate extremes and their impacts on natural and human systems, for instance more intense heat waves leading to more people suffering from heat stress or more intense heavy precipitation events often leading to devastating flash floods or river floods costing lives and property (Donat et al., 2020).

An extreme weather or climate event is generally defined as the occurrence of a value of a weather or climate variable above (or below) a threshold value near the upper (or lower) ends of the range of observed values of the variable (IPCC, 2012). Extremes are rare by definition and this means it takes longer time periods and often better resolution in both space and time to properly characterise long-term changes in extreme events (Alexander, 2016). Climate extremes (e.g., droughts, floods) can be the result of an accumulation of weather or climate events that are, individually, not extreme themselves. As well, weather or climate events, even if not extreme in a statistical sense, can still lead to extreme conditions or impacts, either by crossing a critical threshold in a social, ecological, or physical system, or by occurring simultaneously with other events. Conversely, not all extremes necessarily lead to serious impacts (IPCC, 2012).

Many weather and climate extremes are the result of natural climate variability (including phenomena such as the ENSO), and natural decadal or multi-decadal variations in the climate provide the backdrop for anthropogenic climate changes. Even if there were no anthropogenic changes in climate, a wide variety of natural weather and climate extremes would still occur (IPCC, 2012). It is important to note that only when extremes occur, do we notice the differences. Weather and natural variability dominate all events, but there is a small, significant, and growing anthropogenic component. The times when extremes break records are especially the cases when natural variability, such as the ENSO, is working in the same direction as human-induced warming (Trenberth, 2011).

A changing climate leads to changes in the frequency, intensity, spatial extent, duration, and timing of weather and climate extremes, and can result in unprecedented extremes. Changes in extremes can also be directly related to changes in mean climate, because mean future conditions in some variables are projected to lie within the tails of present-day conditions. Nevertheless, changes in extremes of a climate or weather variable are not always related in a simple way to changes in the mean of the same variable, and in some cases can be of opposite sign to a change in the mean of the variable (IPCC, 2012). Both the Fourth (AR4; IPCC, 2007) and Fifth (AR5; IPCC, 2013) IPCC Assessment Reports highlight the importance of understanding changes in extreme climate events because of their disproportionate impact on society and ecosystems compared to changes in mean climate.

Many factors affect confidence in observed and projected changes in extremes. Confidence in observed changes in extremes depends on the quality and quantity of available data. Before undertaking any analyses of extremes, whether it is at a regional or global level, it is particularly important to ensure that the input data are of high quality and free from artificial inconsistencies (so-called inhomogeneities). Nicholls (1996) observed that a major problem undermining our ability to determine whether extreme weather and climate events were changing was that it is more difficult to maintain the long-term homogeneity of observations required to observe changes in extremes, compared to monitoring changes in means of variables (Alexander, 2016).

There is evidence that some extremes have changed as a result of anthropogenic influences, including increases in atmospheric concentrations of greenhouse gases. It is likely that anthropogenic influences have led to warming of extreme daily minimum and maximum temperatures at the global scale. There is medium confidence that anthropogenic influences have contributed to intensification of extreme precipitation at the global scale. The uncertainties in the historical tropical cyclone records, the incomplete understanding of the physical mechanisms linking tropical cyclone metrics to climate change, and the degree of tropical cyclone variability provide only low confidence for the attribution of any detectable changes in tropical cyclone activity to anthropogenic influences. Attribution of single extreme events to anthropogenic climate change is challenging (IPCC, 2013, 2012, 2007).

The Pacific Islands have been identified as being among the most vulnerable to climate change and climate extremes (Pelling and Uitto, 2001; UNISDR, 2005; Campbell, 2014; Veron et al., 2019). Changes in climate extremes are likely to impact many sectors (IPCC, 2018, 2014b) including human health (McMichael et al., 2003), agriculture (Barnett, 2011), and fisheries (Singh et al., 2001). In the light of current experience and model-based projections, Pacific Islands with high vulnerability and low adaptive capacity, have substantial future risks (Nurse et al., 2007). Smallness renders island countries at risk of high proportionate losses when impacted by a climate extreme (Pelling and Uitto, 2001). Despite the known impacts, relatively little is known about more recent trends in climate extremes in the region (Whan et al., 2014).

## 1.3 Recent Global Changes in Temperature and Precipitation Extremes

According to AR4 it was very likely a large majority of global land areas had experienced decreases in indices of cold extremes and increases in indices of warm extremes, since the middle of the 20th century, consistent with warming of the climate. In addition, globally averaged multi-day heat events had likely exhibited increases over a similar period.

Additional evidence presented in AR5 increased the level of confidence that the majority of warm and cool extremes show warming. Global average time series showed substantial decreases in the frequency of cool nights and cold days and increases in warm nights and warm days since 1951, with the strongest changes occurring after 1970. It was demonstrated that for most of these trends at continental to global scales, a climate change signal could be detected, that is, the trends were larger than expected from internal variability (Fischer and Knutti, 2014; Zwiers et al., 2011). Nevertheless, internal variability should not be discounted as ENSO influences on maximum and minimum temperature are significant especially within and around the Pacific, dampening or enhancing positive trends (Nicholls et al., 2005; Whan et al., 2014) and affecting cold and warm extremes differently (Alexander et al., 2009).

AR5 concluded that it was likely warming of the climate extremes had occurred across most of North America, Europe, Asia and Australia. There was low to medium confidence in historical trends in daily temperature extremes in Africa and South America as there was either insufficient data or trends varied across these regions. This, combined with issues with defining events, led to the assessment that there was medium confidence that globally the length and frequency of warm spells, including heat waves, had increased since the middle of the 20th century although it is likely that heatwave frequency had increased during this period in large parts of Europe, Asia and Australia.

Changes in extreme precipitation have generally been more spatially heterogeneous compared to changes in the temperature extremes. The Special Report on Managing the Risks of Extreme Events and Disasters to Advance Climate Change Adaptation (SREX; IPCC, 2012) and AR5 resolved that it was likely that since 1951 there have been statistically significant increases in the number of heavy precipitation events in more regions than there have been statistically significant decreases. There were, however, strong regional and subregional variations in the precipitation trends. The strongest of these were in South America, where over the Andes and the eastern Amazon there were reductions, but increases in a swath from northern Argentina up to the Caribbean coast. A uniform and moderate increase in the number of days of heavy precipitation was observed over North America, along with the Eurasian high latitudes. Larger increases were seen in south-east Asia and through into central Australia. Several regions showed negative trends e.g., around the Mediterranean and through the Middle East (Dunn et al., 2020). Where seasonal changes were assessed, there were also variations between seasons e.g., more consistent trends in winter than in summer in Europe (IPCC, 2013).

The estimates of past to present changes in droughts have been shown to be sensitive to the drought indices and datasets used (Trenberth et al., 2014). In particular, assessments using the Palmer Drought Severity Index (PDSI) often report global increases in drought (e.g., Dai, 2013). It has, however, been argued that these increases were overestimated due to simplistic calculation of potential evaporation in the PDSI (Sheffield et al., 2012), and calculations using more physically realistic principles indicate little change in drought since 1950. Considering the duration of dry periods [measured as consecutive dry days (CDD)], no robust changes across observations-based datasets could be detected at the global scale, although gridded observations show increases in the duration of dry spells in southern Africa and along the west coasts of North and South America since the mid-20th century (Donat et al., 2016).

Evidence of anthropogenic influence on various aspects of the global hydrological cycle is increasing (e.g., Min et al., 2011; Stott et al., 2010), which is directly relevant to extreme precipitation changes. In particular, an anthropogenic influence on atmospheric moisture content is detectable (Santer et al., 2007). Model projections suggest that the thermodynamic constraint based on the Clausius-Clapeyron relation is a good predictor for extreme precipitation changes in a warmer world in regions where the nature of the ambient flows change little (Pall et al., 2007). This indicates that in some cases but not all (e.g., Emori and Brown, 2005) the observed increase in extreme precipitation in many regions is consistent with the expected extreme precipitation response to anthropogenic influences.

Changes in Pacific Islands extreme temperature and precipitation in recent decades are discussed in detail in Chapters 2–4.

## 1.4 Projected Changes in Temperature and Precipitation Extremes

Models project substantial warming of the temperature extremes by the end of the 21st century. It is virtually certain that increases in the frequency and magnitude of warm days and nights and decreases in the cold days and nights will occur through the 21st century at the global scale. This is mostly linked with mean changes in temperatures, although changes in temperature variability can play an important role in some regions. Moderate temperature extremes on land are projected to warm faster than global annual mean temperature in many regions and seasons (IPCC, 2012). The IPCC special report on the impacts of global warming of 1.5°C above pre-industrial levels has clearly shown that the impacts from weather and climate extremes are more severe in a 1.5°C warmer world compared to current conditions, and are even more pronounced in a 2°C warmer world (IPCC, 2018)

Specifically, for the Pacific Islands, average temperatures will increase, bringing more extremely hot days and warm nights (by 2030, the projected warming is likely to be around +0.5–1.0°C, relative to 1986–2005, regardless of the emissions scenario, and by 2090 a very high emissions scenario could increase temperatures by +2.0–4.0°C). Extreme temperatures that occur once every 20 years on average are projected to increase in line with average temperatures by up to +2.0–4.0°C by 2090 under the very high emissions scenario (Australian Bureau of Meteorology and CSIRO, 2014).

Projected changes from both global and regional studies indicate that it is likely that the frequency of heavy precipitation or proportion of total precipitation from heavy falls will increase in the 21st century over many areas on the globe, especially in the high latitudes and tropical regions, and northern mid-latitudes in winter. Heavy precipitation is projected to increase in some but not all regions (IPCC, 2012). Pacific Islands average annual precipitation is expected to increase with fewer droughts in most areas. Extreme precipitation events that occur once every 20 years on average during 1986–2005 are projected to occur once every seven to 10 years by 2090 under a very low emissions scenario, and every four to six years by 2090 under a very high emissions scenario (Australian Bureau of Meteorology and CSIRO, 2014).

Extreme precipitation from tropical cyclones have a major impact on some Pacific Islands. There is a growing level of consistency between models which favour fewer tropical cyclones globally in a warmer late-twenty-first-century climate, but also an increase in average cyclone intensity, precipitation rates, and the number and occurrence days of very intense category 4 and 5 storms. While these changes are apparent in the globally averaged tropical cyclone statistics, they are not necessarily present in each individual basin. The interbasin variation of changes in most of the tropical cyclone metrics is directly correlated to the variation in magnitude of sea surface temperature (SST) increases between the basins. (Knutson et al., 2010; 2015).

## 1.5 Aims of this research

This research questions/objectives are:

1. Determine if there has been a statistically significant change in drought occurrence, duration, and magnitude, and examine the strength of the relationship between the main climate drivers and Pacific and northeast Australia precipitation on regional and subregional scales. The study region for this component covers the Pacific from 127°E to 130°W and 23°N to 32°S, excluding Indonesia and most of western and southern Australia;
2. Examine trends in mean temperature, total precipitation and the WMO Sector-specific Climate Indices (ET-SCI) relevant indices over 1951–2015, on an annual and seasonal basis using quality-controlled and homogenised daily temperature and precipitation data from the western Pacific. Analyse past variability in total and extreme precipitation in the western Pacific. Investigate possible causal mechanisms underlying the observed variability. The study region for this component covers the Pacific from about 134°E to 135°W and from 15°N to 32°S, excluding Indonesia and the Australian mainland;
3. Examine sugarcane and sugar yield patterns for the last four decades for the Lautoka Mill, Fiji sugar district and model sugarcane and sugar yield using the ET-SCI indices created for Nadi Airport, Fiji in the previous study. Use the sugar model to create a baseline (yield) centred on 1995 and use the baseline to examine the impact of a warmer, wetter and drier future climate on sugar production. The purpose of this study is to demonstrate how interannual variability in extreme temperature and precipitation impact sugarcane production.

## 1.6 The PCCSP, PACCSAP Program, WMO ET-SCI and COSPPac

The research objectives were motivated by work undertaken during the AusAID funded the Pacific Climate Change Science Program (PCCSP) and the Pacific-Australia Climate Change Science and Adaptation Planning (PACCSAP) Program (2008-2014) delivered largely by the Bureau of Meteorology (BoM) and Commonwealth and Scientific Research Organisation (CSIRO). At the start of this research in 2014, the main objective was to extend work undertaken during the PACCSAP Program to better understand Pacific climate variability and change in the last century.

In the process of working on the second research question, I was invited to participate as a facilitator at a World Meteorological Organization (WMO) Expert Team on Sector-specific Climate Indices (ET-SCI) workshop www.wmo.int/pages/prog/wcp/ccl/opace/opace4/ET-SCI-4-1.php in Nadi, Fiji in December 2015. The objectives of the workshop were similar to those of my PhD and timing was perfect with regard to beginning work on Chapter 3. The workshop presented the opportunity to gain access to the latest analytical techniques and software to examine change in climate extremes. At the conclusion of the workshop, I offered to produce two research papers. The objective of the first was to extend previous work on examining trends in mean and extreme temperature and precipitation on annual and seasonal timescales and the second to examine the influence of climate extremes on climate sensitive sectors (the primary focus of the ET-SCI). These became Chapters 3 and 4. Some of the content of Chapter 3 is associated with analyses I conducted during the PACCSAP Program that forms a logical extension to the ET-SCI analyses.

Since the conclusion of PACCSAP in 2014, I have been associated with the Australian Aid funded Climate and Oceans Support Program in the Pacific (COSPPac), now in its second phase (2018–22). Chapter 4 closely aligns with the objectives of COSPPac2 which include using climate information to build community resilience to the impacts of climate variability and change and climate associated disasters.

## 1.7 Thesis Outline

This thesis has five chapters and an appendix. Chapters 2–4 are made up of four scientific papers, published in peer-reviewed journals. Chapter 5 contains concluding remarks, possible improvements and extensions of work presented here. The appendix contains further details on the homogenisation processes associated with Chapter 3.

## References

Alexander, L. V, 2016. Global observed long-term changes in temperature and precipitation extremes: A review of progress and limitations in IPCC assessments and beyond. Weather Clim. Extrem. 11, 4–16. https://doi.org/http://dx.doi.org/10.1016/j.wace.2015.10.007

Alexander, L. V, Uotila, P., Nicholls, N., 2009. Influence of sea surface temperature variability on global temperature and precipitation extremes. J. Geophys. Res. Atmos. 114. https://doi.org/10.1029/2009JD012301

Australian Bureau of Meteorology, CSIRO, 2014. Climate Variability, Extremes and Change in the Western Tropical Pacific: New Science and Updated Country Reports, Pacific-Australia Climate Change Science and Adaptation Planning Program Technical Report. Australian Bureau of Meteorology and Commonwealth Scientific and Industrial Research Organisation, Melbourne, Australia.

Australian Bureau of Meteorology, CSIRO, 2011. Climate Change in the Pacific: Scientific Assessment and New Research. Volume 1: Regional Review. Volume 2: Country Reports. Melbourne, Australia.

Barnett, J., 2011. Dangerous climate change in the Pacific Islands: food production and food security. Reg. Environ. Chang. 11, 229–237. https://doi.org/10.1007/s10113-010-0160-2

Bell, J., Johnson, J., Ganachaud, A., Gehrke, P., Hobday, A., Hoegh-Guldberg, O., Le Borgne, R., Lehodey, P., Lough, J., Pickering, T., Pratchett, M., Waycott, M., 2011. Vulnerability of Tropical Pacific Fisheries and Aquaculture to Climate Change: Summary for Pacific Island Countries and Territories. Secretariat of the Pacific Community, Noumea, New Caledonia.

Benns, M., 2011. Tuvalu to run out of water by Tuesday [WWW Document]. Dly. Telegr. URL www.telegraph.co.uk/news/worldnews/australiaandthepacific/tuvalu/8804093/Tuvalu-to-run-out-of-water-by-Tuesday.html (accessed 2.26.15).

Campbell, J.R., 2014. Climate-Change Migration in the Pacific. Contemp. Pac. 26, 1–28.

Christidis, N., Stott, P.A., Brown, S., Hegerl, G.C., Caesar, J., 2005. Detection of changes in temperature extremes during the second half of the 20th century. Geophys. Res. Lett. 32. https://doi.org/10.1029/2005GL023885

Dai, A., 2013. Increasing drought under global warming in observations and models. Nat. Clim. Chang. 3, 52–58.

Donat, M.G., Alexander, L. V, Herold, N., Dittus, A.J., 2016. Temperature and precipitation extremes in century-long gridded observations, reanalyses, and atmospheric model simulations. J. Geophys. Res. Atmos. 121, 11,111-174,189. https://doi.org/10.1002/2016JD025480

Donat, M.G., Sillmann, J., Fischer, E.M., 2020. Chapter 3 – Changes in climate extremes in observations and climate model simulations. From the past to the future, in: Sillmann, J., Sippel, S., Russo, S.B.T.-C.E. and T.I. for I. and R.A. (Eds.), . Elsevier, pp. 31–57. https://doi.org/https://doi.org/10.1016/B978-0-12-814895-2.00003-3

Dunn, R.J.H., Alexander, L. V, Donat, M.G., Zhang, X., Bador, M., Herold, N., Lippmann, T., Allan, R., Aguilar, E., Barry, A.A., Brunet, M., Caesar, J., Chagnaud, G., Cheng, V., Cinco, T., Durre, I., de Guzman, R., Htay, T.M., Ibadullah, W.M.W., Ibrahim, M.K.I. Bin, Khoshkam, M., Kruger, A., Kubota, H., Leng, T.W., Lim, G., Li-Sha, L., Marengo, J., Mbatha, S., McGree, S., Menne, M., Skansi, M. de los M., Ngwenya, S., Nkrumah, F., Oonariya, C., Pabon-Caicedo, J.D., Panthou, G., Pham, C., Rahimzadeh, F., Ramos, A., Salgado, E., Salinger, J., Sané, Y., Sopaheluwakan, A., Srivastava, A., Sun, Y., Timbal, B., Trachow, N., Trewin, B., van der Schrier, G., Vazquez-Aguirre, J., Vasquez, R., Villarroel, C., Vincent, L., Vischel, T., Vose, R., Yussof, M.N.A.B.H., 2020. Development of an updated global land in-situ-based dataset of temperature and precipitation extremes: HadEX3. J. Geophys. Res. Atmos. n/a, e2019JD032263. https://doi.org/10.1029/2019JD032263

Emori, S., Brown, S.J., 2005. Dynamic and thermodynamic changes in mean and extreme precipitation under changed climate. Geophys. Res. Lett. 32. https://doi.org/10.1029/2005GL023272

Fischer, E.M., Knutti, R., 2014. Detection of spatially aggregated changes in temperature and precipitation extremes. Geophys. Res. Lett. 41, 547–554. https://doi.org/10.1002/2013GL058499

Folland, C.K., Renwick, J.A., Salinger, M.J., Mullan, A.B., 2002. Relative influences of the Interdecadal Pacific Oscillation and ENSO on the South Pacific Convergence Zone. Geophys. Res. Lett. 29, 21–24. https://doi.org/10.1029/2001GL014201

Hay, J.E., Duvat, V., Magnan, A.K., 2019. Trends in Vulnerability to Climate-related Hazards in the Pacific: Research, Understanding and Implications, in: Pfeffer, W.T., Smith, J.B., and Kristie L. E (Eds.), The Oxford Handbook of Planning for Climate Change Hazards. https://doi.org/10.1093/oxfordhb/9780190455811.013.4

IPCC, 2018. Summary for policymakers, in: Masson-Delmotte, V., Zhai, P., Pörtner, H.O., Roberts, D., Skea, J., Shukla, P.R., Pirani, A., Moufouma-Okia, W., Péan, C., Pidcock, R., Connors, S., Matthews, J.B.R., Chen, Y., Zhou, X., Gomis, M.I., Lonnoy, E., Maycock, T., Tignor, M., Waterfield, T. (Eds.), Global Warming of 1.5°C. An IPCC Special Report on the Impacts of Global Warming of 1.5°C above Pre-Industrial Levels and Related Global Greenhouse Gas Emission Pathways, in the Context of Strengthening the Global Response to the Threat of Climate Change. World Meteorological Organization, Geneva, Switzerland, p. 32.

IPCC, 2014a. Climate Change 2014: Synthesis Report. Contribution of Working Groups I, II and III to the Fifth Assessment Report of the Intergovernmental Panel on Climate Change. IPCC, Geneva, Switzerland.

IPCC, 2014b. Climate Change 2014: Impacts, Adaptation and Vulnerability. Part B Regional Aspects. Contribution of Working Group II to the Fifth Assessment Report of the Intergovernmental Panel on Climate Change., in: Barros, V.., Field, C.., Dokken, D.., Mastrandrea, M.., Mach, K.., Bilir, T.., Chatterjee, S., Mastrandrea, P.., White, L.. (Eds.), . Cambridge University Press, Cambridge, United Kingdom and New York, NY, USA, p. 688.

IPCC, 2013. Climate Change 2013: The Physical Science Basis. Contribution of Working Group I to the Fifth Assessment Report of the Intergovernmental Panel on Climate Change, in: Stocker, T.., Qin, D., Plattner, G.-K., Tignor, M., Allen, S.., Boschung, J., Nauels, A., Xia, Y., Bex, V., Midgley, P.. (Eds.), . Cambridge University Press, Cambridge, United Kingdom and New York, NY, USA, p. 1535.

IPCC, 2012. Managing the Risks of Extreme Events and Disasters to Advance

Climate Change Adaptation. A Special Report of Working Groups I and II of the Intergovernmental Panel on Climate Change. Cambridge University Press, Cambridge, United Kingdom and New York, NY, USA.
IPCC, 2007. Climate Change 2007: The Physical Science Basis. Contribution of Working Group I to the Fourth Assessment Report of the Intergovernmental Panel on Climate Change, in: Solomon, S., Qin, D., Manning, M., Chen, Z., Marquis, M., Averyt, K.., Tignor, M., Miller, H.. (Eds.), . Cambridge University Press, Cambridge, United Kingdom and New York, NY, USA.
Kaufman, D., and Coauthors, 2020: A global database of Holocene paleotemperature records. Sci. Data, 7, 115, https://doi.org/10.1038/s41597-020-0445-3.
Knutson, T.R., Sirutis, J.J., Zhao, M., Tuleya, R.E., Bender, M., Vecchi, G.A., Villarini, G., Chavas, D., 2015. Global Projections of Intense Tropical Cyclone Activity for the Late Twenty-First Century from Dynamical Downscaling of CMIP5/RCP4.5 Scenarios. J. Clim. 28, 7203–7224. https://doi.org/10.1175/JCLI-D-15-0129.1
Knutson, T.R., McBride, J.L., Chan, J., Emanuel, K., Holland, G., Landsea, C., Held, I., Kossin, J.P., Srivastava, A.K., Sugi, M., 2010. Tropical cyclones and climate change. Nat. Geosci. 3, 157–163. https://doi.org/10.1038/ngeo779
Lough, J.M., Meehl, G.A., Salinger, M.J., 2011. Observed and projected changes in surface climate of the tropical Pacific, in: Bell, J.D., Johnson, J.E., Hobday, A.J. (Eds.), Vulnerability of the Tropical Pacific Fisheries and Aquaculture to Climate Change. Secretariat of the Pacific Community, Noumea, New Caledonia.
Manhire, T., 2011. Tuvalu drought could be dry run for dealing with climate change [WWW Document]. Guard. URL http://www.theguardian.com/world/2011/oct/17/tuvalu-drought-climate-change (accessed 2.23.15).
McCubbin, S., Smit, B., Pearce, T., 2015. Where does climate fit? Vulnerability to climate change in the context of multiple stressors in Funafuti, Tuvalu. Glob. Environ. Chang. 30, 43–55. https://doi.org/https://doi.org/10.1016/j.gloenvcha.2014.10.007
McMichael, A., Woodruff, R., Whetton, P., Hennessy, K., Nicholls, N., Hales, S., Woodward, A., Kjellstrom, T., 2003. Human Health and Climate Change in Oceania: A Risk Assessment. Canberra, Australia.
Min, S.K.-., Zhang, X., Zwiers, F.W., Hegerl, G.C., 2011. Human contribution to more-intense precipitation extremes. Nature 470, 378–381. https://doi.org/10.1038/nature09763
Nicholls, N., 1996. Long-Term Climate Monitoring and Extreme Events BT – Long-Term Climate Monitoring by the Global Climate Observing System: International Meeting of Experts, Asheville, North Carolina, USA, in: Karl, T.R. (Ed.), . Springer Netherlands, Dordrecht, pp. 101–115. https://doi.org/10.1007/978-94-011-0323-7_8
Nicholls, N., Baek, H.J., Gosai, A., Chambers, L.E., Choi, Y., Collins, D., Della-Marta, P.M., Griffiths, G.M., Haylock, M.R., Iga, N., Lata, R., Maitrepierre, L., Manton, M.J., Nakamigawa, H., Ouprasitwong, N., Solofa, D., Tahani, L., Thuy, D.T., Tibig, L., Trewin, B., Vediapan, K., Zhai, P., 2005. The El Niño-Southern Oscillation and daily temperature extremes in east Asia and the west Pacific. Geophys. Res. Lett. 32, 1–4.

https://doi.org/10.1029/2005GL022621
Nurse, N.L., McLean, R.F., Agard, J., Briguglio, L., Lefale, P., Payet, R., G, S., 2007. Small Islands, in: Parry, M.., Canziani, O.., Palutikof, J.., Van Der Linde, P.J., Hanso, C.. (Eds.), Climate Change 2007. Impacts, Adaptation and Vulnerability. Contribution of Working Group II to the Fourth Assessment Report of the Intergovernmental Panel on Climate Change. Cambridge University Press, Cambridge, United Kingdom, pp. 687–716.
Pall, P., Allen, M.R., Stone, D.A., 2007. Testing the Clausius–Clapeyron constraint on changes in extreme precipitation under CO2 warming. Clim. Dyn. 28, 351–363. https://doi.org/10.1007/s00382-006-0180-2
Pelling, M., Uitto, J.I., 2001. Small island developing states: natural disaster vulnerability and global change. Glob. Environ. Chang. Part B Environ. Hazards 3, 49–62. https://doi.org/https://doi.org/10.1016/S1464-2867(01)00018-3
RNZ, 2011. Tuvalu: state of emergency declared over water shortages.
Salmon, C., Duvat, V.K.E., Laurent, V., 2019. Human- and climate-driven shoreline changes on a remote mountainous tropical Pacific Island: Tubuai, French Polynesia. Anthropocene 25, 100191. https://doi.org/https://doi.org/10.1016/j.ancene.2019.100191
Santer, B.D., Mears, C., Wentz, F.J., Taylor, K.E., Gleckler, P.J., Wigley, T.M.L., Barnett, T.P., Boyle, J.S., Brüggemann, W., Gillett, N.P., Klein, S.A., Meehl, G.A., Nozawa, T., Pierce, D.W., Stott, P.A., Washington, W.M., Wehner, M.F., 2007. Identification of human-induced changes in atmospheric moisture content. Proc. Natl. Acad. Sci. 104, 15248 LP – 15253. https://doi.org/10.1073/pnas.0702872104
Sheffield, J., Wood, E.F., Roderick, M.L., 2012. Little change in global drought over the past 60 years. Nature 491, 435–438. https://doi.org/10.1038/nature11575
Singh, R.B.K., Hales, S., Wet, N. de, Raj, R., Hearnden, M., Weinstein, P., 2001. The Influence of Climate Variation and Change on Diarrheal Disease in the Pacific Islands. Environ. Health Perspect. 109, 155–159. https://doi.org/10.2307/3434769
Stott, P.A., Gillett, N.P., Hegerl, G.C., Karoly, D.J., Stone, D.A., Zhang, X., Zwiers, F., 2010. Detection and attribution of climate change: a regional perspective. WIREs Clim. Chang. 1, 192–211. https://doi.org/10.1002/wcc.34
Trenberth, K.E., 2011. Attribution of climate variations and trends to human influences and natural variability. WIREs Clim. Chang. 2, 925–930. https://doi.org/10.1002/wcc.142
Trenberth, K.E., Dai, A., van der Schrier, G., Jones, P.D., Barichivich, J., Briffa, K.R., Sheffield, J., 2014. Global warming and changes in drought. Nat. Clim. Chang. 4, 17–22. https://doi.org/10.1038/nclimate2067
UNISDR, 2005. Framework for Action 2005-2015. Building the Resilience of Nationsand Communities to Disasters. Geneva, Switzerland.
Veron, S., Mouchet, M., Govaerts, R., Haevermans, T., Pellens, R., 2019. Vulnerability to climate change of islands worldwide and its impact on the tree of life. Sci. Rep. 9, 14471. https://doi.org/10.1038/s41598-019-51107-x
Wang, G., Power, S.B., McGree, S., 2016. Unambiguous warming in the western tropical Pacific primarily caused by anthropogenic forcing. Int. J. Climatol. 36. https://doi.org/10.1002/joc.4395

Whan, K., Alexander, L.V., Imielska, A., Mcgree, S., Jones, D., Ene, E., Finaulahi, S., Inape, K., Jacklick, L., Kumar, R., Laurent, V., Malala, H., Malsale, P., Pulehetoa-Mitiepo, R., Ngemaes, M., Peltier, A., Porteous, A., Seuseu, S., Skilling, E., Tahani, L., Toorua, U., Vaiimene, M., 2014. Trends and variability of temperature extremes in the tropical Western Pacific. Int. J. Climatol. 34. https://doi.org/10.1002/joc.3861
Zwiers, F.W., Zhang, X., Feng, Y., 2011. Anthropogenic Influence on Long Return Period Daily Temperature Extremes at Regional Scales. J. Clim. 24, 881–892. https://doi.org/10.1175/2010JCLI3908.1

# 2 Trends and Variability in Droughts in the Pacific Islands and Northeast Australia

Precipitation records for eastern Australia, Hawaii and the Pacific Islands are examined to identify trends in drought occurrence, duration and magnitude. The strength of the relationship between the main climate drivers of variability and precipitation is also examined. Drought trends are largely positive but the majority are statistically non-significant. A significant relationship between the oceanic component of El Niño-Southern Oscillation and precipitation is confirmed for a large part of the study region with a strong lagged relationship in the year after the El Niño onset at locations southwest of the South Pacific Convergence Zone (SPCZ) and north of the Intertropical Convergence Zone (ITCZ). Similarly, a strong relationship is identified with the Interdecadal Pacific Oscillation (IPO) and Pacific Decadal Oscillation (PDO) at most locations. Droughts are longer and more severe southwest of the SPCZ and north of the ITCZ during the positive phase of IPO and PDO.

The contents of this chapter have been published in the following peer-reviewed journal. I confirm the first author has produced >95% of the work presented:

McGree, S., S. Schreider, and Y. Kuleshov, 2016: Trends and Variability in Droughts in the Pacific Islands and Northeast Australia. *J. Climate*, **29**, 8377–8397, https://doi.org/10.1175/JCLI-D-16-0332.1

## 2.1 Introduction

Drought is a recurrent climate feature of the Pacific Islands (Giambelluca et al. 1991; d’Aubert and Nunn 2012) and northeast Australia (Tapper and Hurry 1993; Anderson 2014) with meteorological and socio-economic impacts documented from early European settlement. Paleoclimate research also points to periods of low precipitation over the last millennium with some events of greater magnitude and duration than those observed in the last century (Nunn 2007; Vance et al. 2014). While drought affects agriculture productivity on all of the Pacific Islands, it is a particular problem on atolls because they have a fragile freshwater resource base which can be quickly depleted when precipitation drops (Barnett and Campbell 2010). Drought also affects the high islands and often causes serious losses in agricultural productivity (Barnett 2011), decreased electricity production (Sawlani 2015), disease (Singh et al. 2001) and nutritional deficiencies (World-Bank 2000).

Recent severe and prolonged droughts have highlighted the Pacific Islands' and Australia's vulnerability to prolonged periods of suppressed precipitation and their persistence and intensity have alerted the general public and governments to the many socio-economic problems accompanying water storage and the need for drought mitigation measures. In mid-2011, the south Pacific nation of Tuvalu (population about 10,500) experienced a major water availability crisis. A drought that began in March 2009 on Funafuti atoll became the worst (both duration and magnitude) in almost a century (Kuleshov et al. 2014). A state of emergency was declared in late September 2011 due to severe water shortages resulting in households on the islands of Funafuti and Nukulaelae rationed to about 40L of fresh-water a day. To exacerbate the situation Tuvaluans paid higher costs for imported food as local agricultural crops failed (Manhire 2011). The precipitation deficit caused contamination of the remaining ground water supplies with the Red Cross declaring the water unsafe for human consumption (Benns 2011).

The drought in Tuvalu was associated with the 2010–12 La Niña, one of the strongest on record (Kuleshov et al. 2014), comparable in strength to the La Niña events of 1917–18, 1955–56 and 1975–76. The Southern Oscillation Index (SOI) values in October and December 2010, and February and March 2011, were the highest for each month since records began (Australian Bureau of Meteorology 2012).

El Niño–Southern Oscillation (ENSO) is the largest source of climate variability in the Pacific on interannual timescales (McPhaden et al. 2006; Australian Bureau of Meteorology and CSIRO 2011). Its opposite phases, El Niño and La Niña are accompanied by major changes in tropical sea surface temperatures (SST) and atmospheric pressure, thereby producing shifts and changes in wind patterns, convection (Folland et al. 2002; Chu and Chen 2005; Murphy et al. 2014; Salinger et al. 2014) and air temperatures (Power et al. 1998). There are also climate teleconnections beyond the Pacific region, for example, suppressed convection over southern Africa and northern South America, and excess convection in southeastern South America, eastern equatorial Africa, and the southern US (Ropelewski and Halpert, 1989; Allan et al. 1996).

Global-scale studies on trends in drought to date, e.g., Spinoni et al. (2014) present little information on the Pacific as the islands have little visibility at a global scale and Pacific data in global datasets are limited. Australia-Pacific studies on a regional scale are non-existent with most work at national or subnational scales, e.g., Hennessy et al. (2008) and Gallant et al. (2013). Results vary depending on the drought indicator and the time-scale of drought considered. There is however, broad usage of the WMO/CLIVAR annual consecutive dry days (CDD) index in extreme precipitation studies across Australia and the Pacific. The CDD index is the maximum number of consecutive days in a calendar with precipitation < 1mm. As this typically occurs in the dry season, the index provides limited information on precipitation deficiency in the wetter months of the year when deficiencies are typically of greater importance. Nevertheless, these results are presented in the absence of an alternative.

For the 1950–2014 period, negative CDD trends exist across northern Australia with positive trends through the southern half of Queensland (QLD). Trends are smaller and mixed in New South Wales (NSW) and Victoria (Australian Bureau of Meteorology 2015). Similar patterns are presented in the Climate Change 2013 Working Group I report for the 1950–2010 period (IPCC 2013) and in Spinoni et al. (2014) using the 12-month Standardised Precipitation Index (SPI). The SPI is a normalised index representing the probability of occurrence of an observed precipitation amount when compared with the precipitation climatology at a certain geographical location. Negative SPI values represent precipitation deficit, whereas positive SPI values indicate precipitation surplus (McKee et al. 1993, 1995). CDD trends are largely positive and statistically significant for the Hawaiian Islands between 1950 and 2007 on all major islands (Chu et al. 2010). For the western Pacific, subregional CDD trends over 1951–2011 are non-significant with only two stations showing significant trends in the Federated States of Micronesia (FSM) and French Polynesia (McGree et al. 2014).

There is a general perception amongst Pacific Island residents that the frequency and magnitude of drought has increased, particularly in the last couple of decades (Australian Bureau of Meteorology and CSIRO 2011). This would be of significant concern as agriculture and water storages on most Pacific Islands are particularly sensitive to drought.

Considering the dearth of information on historical trends in drought and the importance of this subject, the objectives of this study are (i) to determine if there has been a statistically significant change in droughts occurrence, duration and magnitude, and (ii) examine the strength of the relationship between the main climate drivers and Pacific and northeast Australia precipitation on regional/subregional scales.

Our study region covers the Pacific from 127°E to 130°W and 23°N to 32°S, excluding Indonesia and most of western and southern Australia. The paper is organised as follows. Section 2.2 provides a description of the data used and outlines the research methods. Section 2.3 presents the results of our research into drought trends and variability in the western Pacific and northeast Australia. The discussion of the results presented in Section 2.4 and conclusions in Section 2.5.

## 2.2 Data and Indices

### 2.2.1 Precipitation

Data for Australia (36 station records) were obtained from the Bureau of Meteorology Climate Change and Variability pages www.bom.gov.au/climate/change/index.shtml#tabs=Tracker&tracker=site-networks and are part of the Lavery et al. (1997) high-quality dataset. Data for the Hawaiian Islands (24 station records) were obtained from NOAA Climate Data Online www.ncdc.noaa.gov/cdo-web/search#t=secondTabLink with station selection largely based on the work of Chen and Chu (2014) and Kruk et al. (2015). The Australian and Hawaiian stations are subsets of much larger precipitation observation networks. While additional Australian and Hawaiian stations could have been included, the authors chose not to overwhelm the limited records from the remaining Pacific Islands. The latter is comprised of 53 station records for the Australian islands in the Pacific, Cook Islands, FSM, Fiji, French Polynesia, Kiribati, Republic of the Marshall Islands (RMI), Nauru, New Caledonia, New Zealand, Niue, Palau, Papua New Guinea, Pitcairn Islands, Samoa, Solomon Islands, Tonga, Tuvalu and Vanuatu. Details on the quality control and homogenisation of these data are provided by McGree et al. (2014). Additional data were obtained for Fiji, French Polynesia, New Caledonia, Commonwealth of the Northern Mariana Islands (CNMI) and Tuvalu to fill gaps in the historical record. The Pacific Islands data has been obtained from the respective national meteorological services.

Data for the period 1951–2010 are used in this study. While longer timeseries are available, the selected period provides the best temporal and spatial representation. Data quality requirements include no more than 10% missing data overall and no more than 5% missing data in the first and last decades. It is essential the amount of missing data be minimised as data gaps increase the uncertainty of the trend calculated upon the timeseries. Overall, 113 station records are used in this study. The station names are presented in Appendix 2.1 and locations in Figure 2.1.

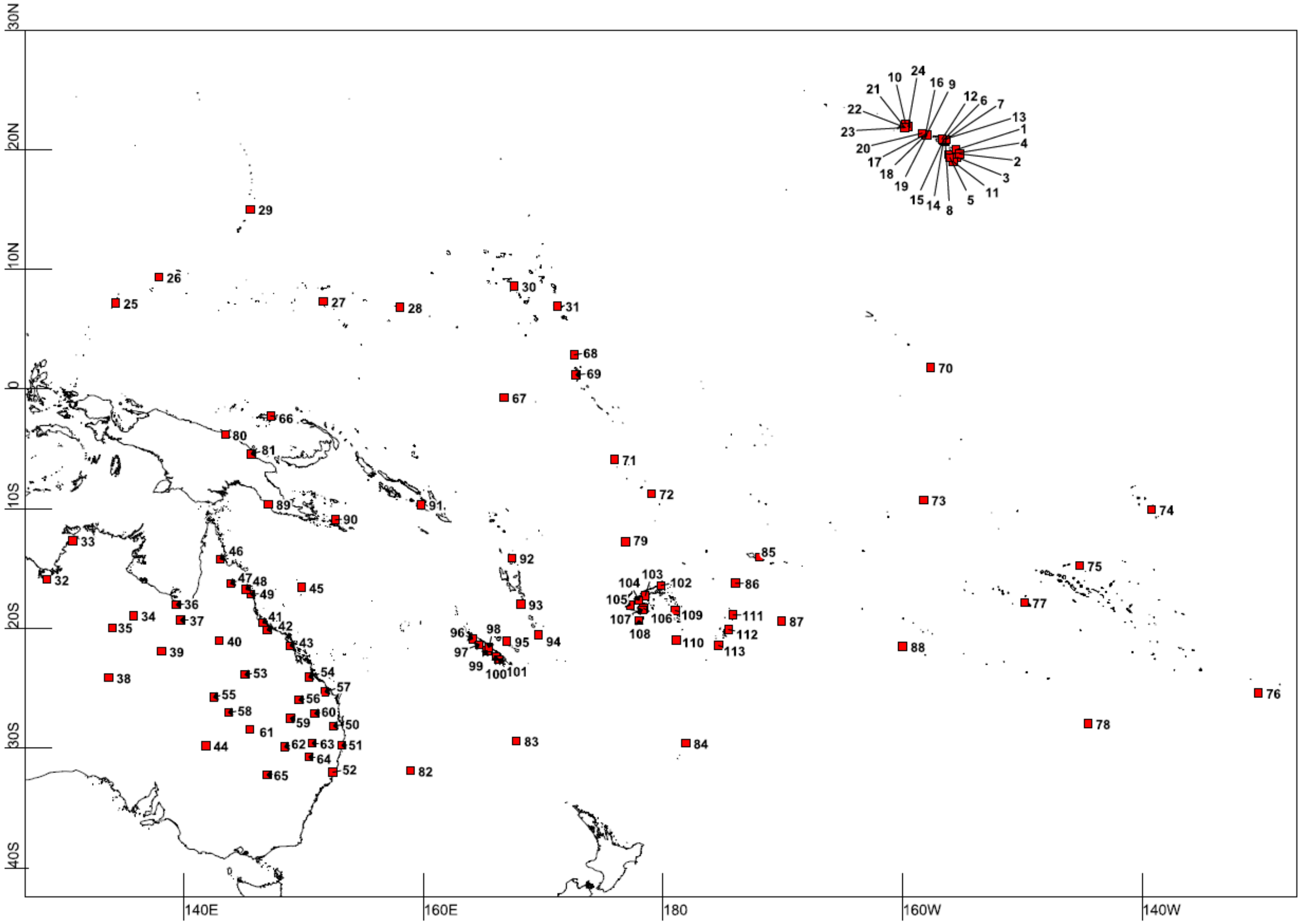


Figure 2.1 Map of the Pacific and northeast Australia region showing the study region and station locations. Station numbers are associated with station names in Appendix 2.1

### 2.2.2 ENSO index

Monthly NINO3.4 sea surface temperature (SST) anomalies are used as a representative indicator of ENSO behaviour, in line with findings of Barnston et al. (1997). We have used the monthly ERSSTv4 dataset with a base period of 1981–2010. Data were obtained from www.cpc.ncep.noaa.gov/data/indices/ersst4.nino.mth.81-10.ascii

### 2.2.3 IPO index

The Tripole Index (TPI) for the Interdecadal Pacific Oscillation (IPOHenley et al. 2015) is used as the primary method for characterising north Pacific and south Pacific low frequency variability. We use the monthly HadISST2.1 unfiltered, composite of 10 realisations version of the TPI with data from 1870 to 2010 (www.esrl.noaa.gov/psd/data/timeseries/IPOTPI). The TPI is based on the difference between the SST Anomaly (SSTA) averaged over the central equatorial Pacific and the average of the SSTA in the Northwest and Southwest Pacific. The regions used to calculate the index are: Region 1: 25°N–45°N, 140°E–145°W; Region 2: 10°S–10°N, 170°E–90°W; Region 3: 50°S–15°S, 150°E–160°W. The base period is 1971–2000.

Interannual variability of ENSO and the strength of its climate teleconnections are modulated on decadal timescales (Power et al. 1999). The IPO is described as a natural ENSO-like pattern of Pacific SST anomalies that operates at decadal and interdecadal timescales. Changes in the phase of the IPO have been linked to significant changes in climate regimes across the Pacific. In the IPO negative phase, La Niña intensity is more strongly related to precipitation extremes in Australia than during IPO positive phases (Power et al. 1998; Cai and van Rensch 2012). The IPO also influences the SPCZ intensity and location (Folland et al. 2002; Salinger et al. 2001, 2014). The IPO and ENSO have fairly similar (but independent) influences on the SPCZ with the location of the SPCZ convergence maximum shifting southwest during negative IPO and La Niña episodes and northeast during positive IPO and El Niño episodes (Figure 2.2). Positive IPO phases characterised the periods 1924–44

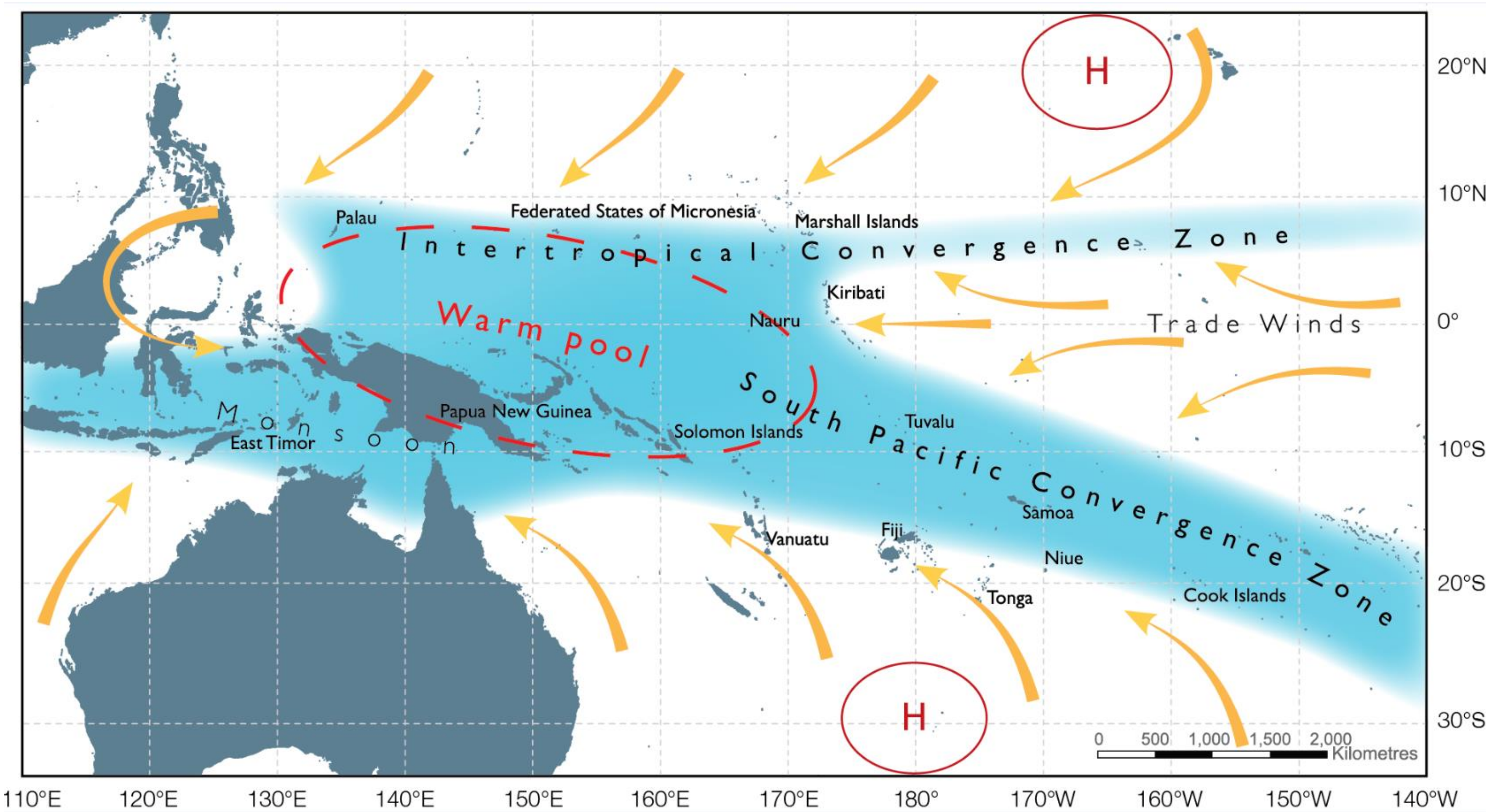


Figure 2.2 Schematic of circulation in the Pacific. The red broken line represents the bounds of the West Pacific Warm Pool. From Australian Bureau of Meteorology and CSIRO (2011).

and 1977–98. These phases were separated by negative IPO phases from 1945–76 and 1999 to present.

### 2.2.4 PDO index

The more widely known Pacific Decadal Oscillation (PDO) index of Mantua et al. (1997) is used as a secondary method for characterising low frequency variability (http://research.jisao.washington.edu/pdo/PDO.latest). This is the north Pacific manifestation of a Pacific-wide pattern encompassed by the IPO (Folland et al. 2002). The PDO is defined as the leading principal component of the monthly SSTA residuals (poleward of 20°N), whereas residuals are understood as the grid-point anomalies after the global mean monthly SST is removed from every location (Zhang et al. 1997). Positive values of this index describe anomalously cold SSTAs around 45°N. Positive PDO phase prevailed from 1926 to 1946 and 1977 to 1998 and negative phases from 1947 to 1976 and over the decade from 1999.

While the TPI and PDO indices cover near-identical sets of years their relationship with precipitation is expected to be different as the PDO index is based on north Pacific SSTAs whereas the TPI encompasses both hemispheres.

### 2.2.5 Standardized Precipitation Index

Drought can be defined as meteorological, hydrological, agricultural and socio-economical. As a result there are numerous drought index parameters in the literature (Dracup et al. 1980; Wilhite and Glantz 1985; Lloyd-Hughes and Saunders 2002). While a study of drought using evapotranspiration and hydrological data would have been preferred, limited data availability constrains this study to a precipitation only analysis of drought. Fortunately, indices based solely on precipitation data perform well when compared to more complex hydrological indices (Oladipo 1985).

The SPI ranks in the top positions among drought indicators for robustness and reliability (Heim 2002; Keyantash and Dracup 2002). The SPI is also recommended by the World Meteorological Organization and is likely to be the most frequently used drought indicator worldwide. The SPI is currently employed in more than 70 countries (WMO 2012).

The SPI is a statistical monthly indicator that compares the accumulated precipitation during a period of N months with the long-term accumulated precipitation distribution for the same location and accumulation period. This long-term record is fitted to a probability distribution e.g. gamma distribution, which is then transformed into a normal distribution so that the mean SPI for the location and desired period is zero (Edwards and McKee 1997).

McKee et al. (1993) used the classification system shown in Table 2.1 to define drought and wet period intensities. A drought occurs when SPI-N is continuously negative and reaches an intensity of -1.0 or less. The event ends when the respective SPI-N becomes positive. The positive sum of the SPI for all the months within a drought or wet period event is defined as the magnitude. Each event, therefore, has a duration defined by its beginning and end, and intensity for each month that the event continues.

Table 2.1 Classification used for the SPI

| **SPI value** | **Class** | **Probability %** |
|---|---|---|
| SPI ≥ 2.0 | Extremely wet | 2.3 |
| 1.5 ≤ SPI < 2.0 | Severely wet | 4.4 |
| 1.0 ≤ SPI < 1.5 | Seriously wet | 9.2 |
| −1.0 < SPI < 1.0 | Near normal | 68.2 |
| −1.5 < SPI ≤ −1.0 | Seriously dry | 9.2 |
| −2.0 < SPI ≤ −1.5 | Severely dry | 4.4 |
| SPI ≤ −2.0 | Extremely dry | 2.3 |

The standardisation of the SPI also allows the user to compare historical and current droughts between different climatic and geographic locations when assessing how rare, or frequent, a given drought event is.

### 2.2.6 Defining drought and wet period events, their frequency, duration and magnitude

To allow the comparison of the results from this study with those of Spinoni et al. (2014) we have selected the SPI-12 timescale and 1951–2010 study period. Spinoni et al. (2014) found that a medium term accumulation period is more suitable to depict the various precipitation regimes than shorter (SPI-3, SPI-6) or longer periods (SPI-24, SPI-48) which may be too sensitive to extremes or miss relevant drought events. They also found comparable drought patterns on a spatial basis, both on global and continental scales using SPI-6, SPI-12 and SPI-24.

Drought frequency (DF), total drought duration (TDD), and total drought magnitude (TDM) have been calculated for each station for 10 year intervals between 1951 and 2010. TDD and TDM represent the sum of the durations and magnitudes of drought events occurred in the considered period and they are expressed in the number of months for duration and in a dimensionless severity score for magnitude.

## 2.3 Methodology

### 2.3.1 Linear drought trends

Linear drought trends (DF, TDD and TDM) are calculated over the six decades and the statistical significance of each trend tested using the Student's T-test with a confidence level of 95%. While this methodology is limited in that the trends have been computed using only six points, this method is preferred to the alternative, which is to calculate trends using the actual SPI values. For example, an annual trend for 1951–2010 would involve a regression calculation using the December SPI-12 values for 1951–2010 (December SPI-12 covers the period January to December). The authors argue that the latter is a trend in standardised precipitation rather than drought.

### 2.3.2 Drought occurrence differences between individual decades and two 30-year periods

The Kruskal–Wallis test (Kruskal and Wallis 1952) is a non-parametric alternative to a one-way analysis of variance (ANOVA) where ANOVA is used to determine if there are statistically significant differences between the means of two or more independent (unrelated) groups. The test does not require the data to be normal, but instead uses the rank instead of the actual data values for the analysis. The Kruskal–Wallis test is used to determine if the differences in the DF, TDD and TDM medians of respective six decades are statistically significant. The null hypothesis is: $H_0$: the population medians are all equal.

The Mann–Whitney rank sum test (Mann and Whitney 1947) is used to determine if there is a difference in the medians between the two 30-year periods (first three decades and latter three decades). Like the Kruskal–Wallis test, the Mann–Whitney test uses the ranks of the sample data, instead of their specific values, to detect statistical significance. The null hypotheses is: $H_0$: $\eta_1 = \eta_2$, the median of the first population (η1) equals the median of the second population (η2) (Lattin et al. 2003).

### 2.3.3 Determining regions with homogeneous precipitation variability

Cluster analysis is widely used in climatology to divide precipitation for a single large region into homogeneous smaller regions of precipitation variability. Annual precipitation is scaled to a mean of zero and standard deviation of one. A hierarchical agglomerative clustering method is used to define clusters of precipitation stations. Each precipitation station is initially considered a separate cluster and, at each successive step, clusters are compared and the clusters with the smallest between cluster dissimilarities (a measure of the 'difference' between clusters) merged until the desired numbers of clusters is reached. The average linkage method with a Euclidean distance measure has been found to be the most desirable and has been used in the analysis of Australian district precipitation variability on seasonal timescales by Drosdowsky (1993). Ward's method has also been used to identify the main seasonal precipitation regimes in Australia (Chambers 2001, 2003) and Hawaii (Diaz et al. 2005) but has a tendency to produce clusters of similar numbers of observations which is undesirable in this study as most of the precipitation stations are southwest of the SPCZ, therefore likely to be part of the same cluster. Salinger et al. (1995) applied a hierarchical agglomerative clustering methodology (Willmott, 1978) to annual Pacific temperature and precipitation (1951-1990) correlation matrixes. Salinger et al. (1995) do not specify the agglomeration method but the Willmott (1978) reference suggests Ward's method was employed. Salinger et al. (1995) then use rotated (varimax criterion) principal component analysis to confirmation the cluster methodology groupings. A dendrogram delineates the level of association at which stations are grouped. The selection of the optimum number of clusters is complex, with no single criterion available to make an objective decision. A subjective choice of 10% of the total number of stations is suggested by Torok (1996). We have also considered the method of Lattin et al.

(2003), which looks for a relatively wide range of distances over which the number of clusters in the solution do not change.

To confirm these groupings, Year-0 and Year +1 (lagged) annual precipitation and NINO3.4 SSTA correlation coefficients are calculated and compared. A relationship is deemed to exist if the correlation coefficients are significant at the 95% level. Non-significant *p*-values are > 0.05.

### 2.3.4 Interdecadal variability

To detect low frequency variability, a 13-year running mean is applied to SPI-12 precipitation at a cluster level to remove interannual fluctuations and those on ENSO timescales. This method has been used previously by Power et al. (1999) to examine the strength of the relationship between Australian precipitation, temperature, river flow and crop yield and the IPO and SOI on decadal timescales.

Firstly, an annual timeseries of December SPI values over 1951–2010 is calculated as these are cumulative standardised totals of precipitation for the 11 preceding months including December. Cluster scale annual timeseries are then calculated by averaging the station annual timeseries. Regional 13-year running mean timeseries are produced from the cluster scale annual timeseries. TPI and PDO 13-year running means are also produced from the monthly TPI and PDO timeseries. Finally, correlation coefficients are calculated using the Spearman rank-order method. A relationship is deemed to exist if the correlation coefficients are significant at the 95% level.

It is possible the duration and magnitude of droughts differ between positive and negative phases of the IPO/PDO. If so, greater attention should be placed on drought during the IPO/PDO phase associated with longer and more intense droughts. We use the Mann–Whitney test to determine if the differences in median duration and magnitude occurrence are statistically significant. Drought magnitude at a station level (for each region) are aggregated over the 1951–77, 1999–2010 and 1978–98 periods then compared. This also applies to drought duration.

## 2.4 Results

### 2.4.1 Trends in drought DF, TDD and TDM on a station scale

The DF trends over 1951–2010 (Figure 2.3a) are generally positive indicating more frequent drought occurrence in recent decades, but mixed spatially and largely statistically non-significant at the 95% level (102 of 113 stations). There

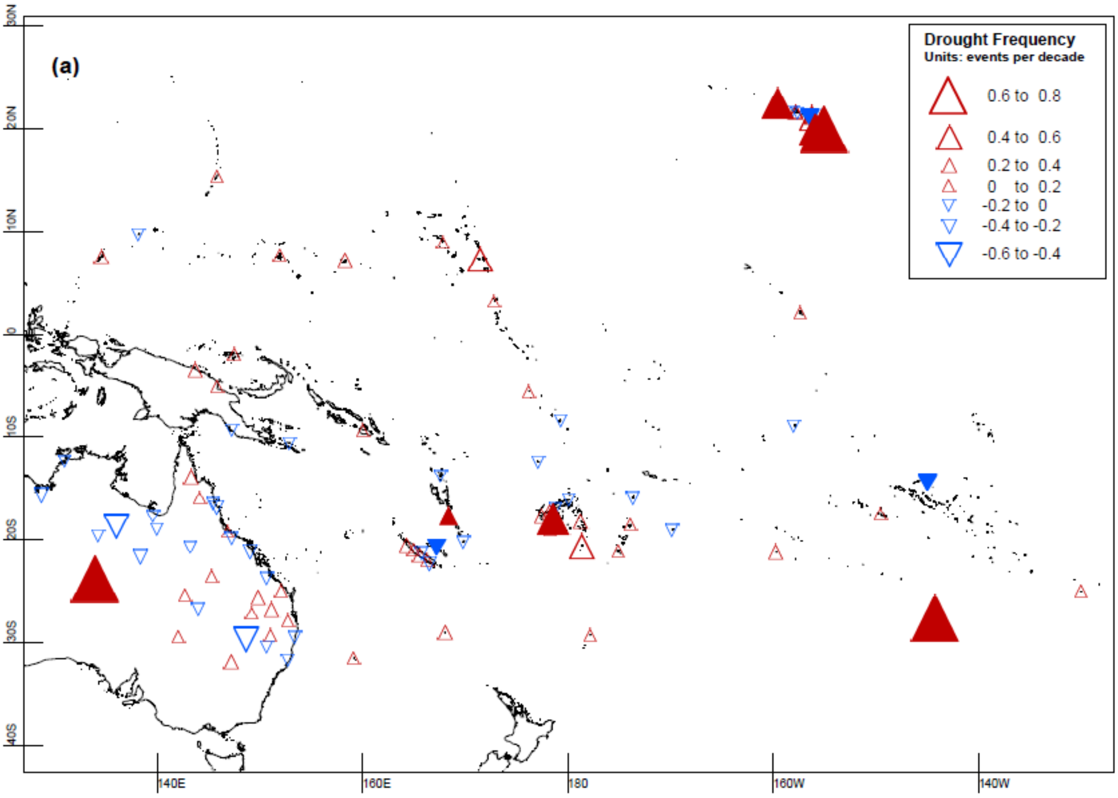

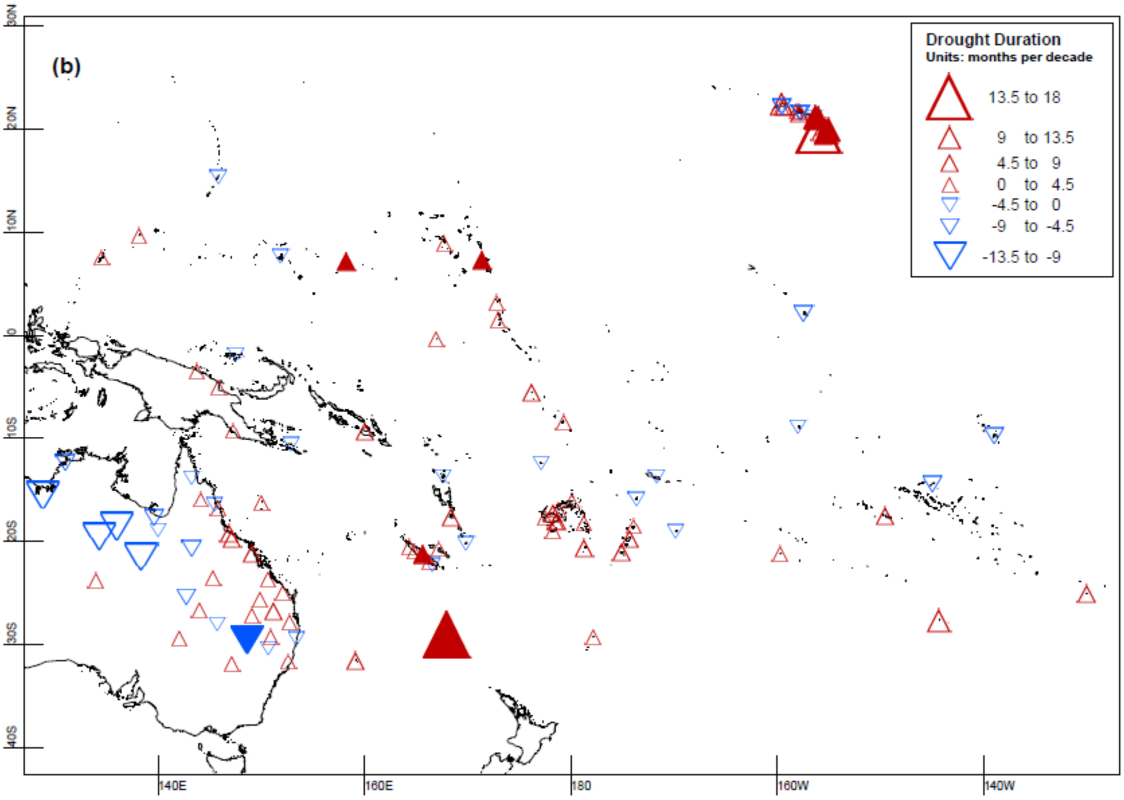
(b)
Drought Duration
Units: months per decade
13.5 to 18
9 to 13.5
4.5 to 9
0 to 4.5
-4.5 to 0
-9 to -4.5
-13.5 to -9
30N
20N
10N
0
10S
20S
30S
40S
140E
160E
180
160W
140W

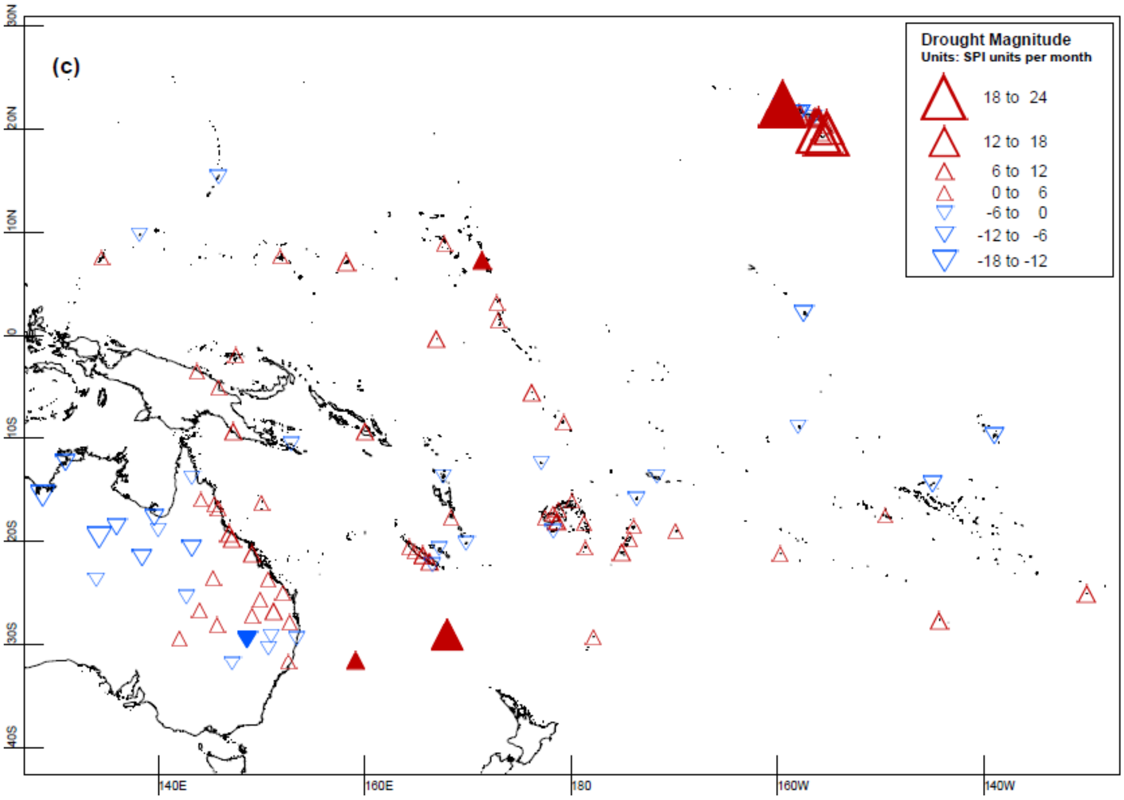

Figure 2.3 Linear drought trends for the period 1951–2010 (a) drought frequency, (b) total drought duration, and (c) total drought magnitude. Filled triangles represent trends significant at the 95% level

is some spatial consistency in parts of the study region for example in the Hawaiian Islands region where the DF trends are largely positive. Positive DF trends are also by large present, but smaller in size in the northwest Pacific, equatorial Pacific and in the south Pacific subtropics.

The results are similar for TDD (Figure 2.3b) and TDM (Figure 2.3c) in that a majority of the trends are positive, spatially mixed and largely non-significant. Sub-regionally, spatial patterns are similar to that of DF with the addition of generally negative trends in north-central Australia and smaller negative trends in the eastern Australia. Figure 2.4a and Figure 2.4b show mean TDD and TDM respectively for the Hawaiian stations. On a state scale the TDD and TDM trends over the six decades are positive but not significant.

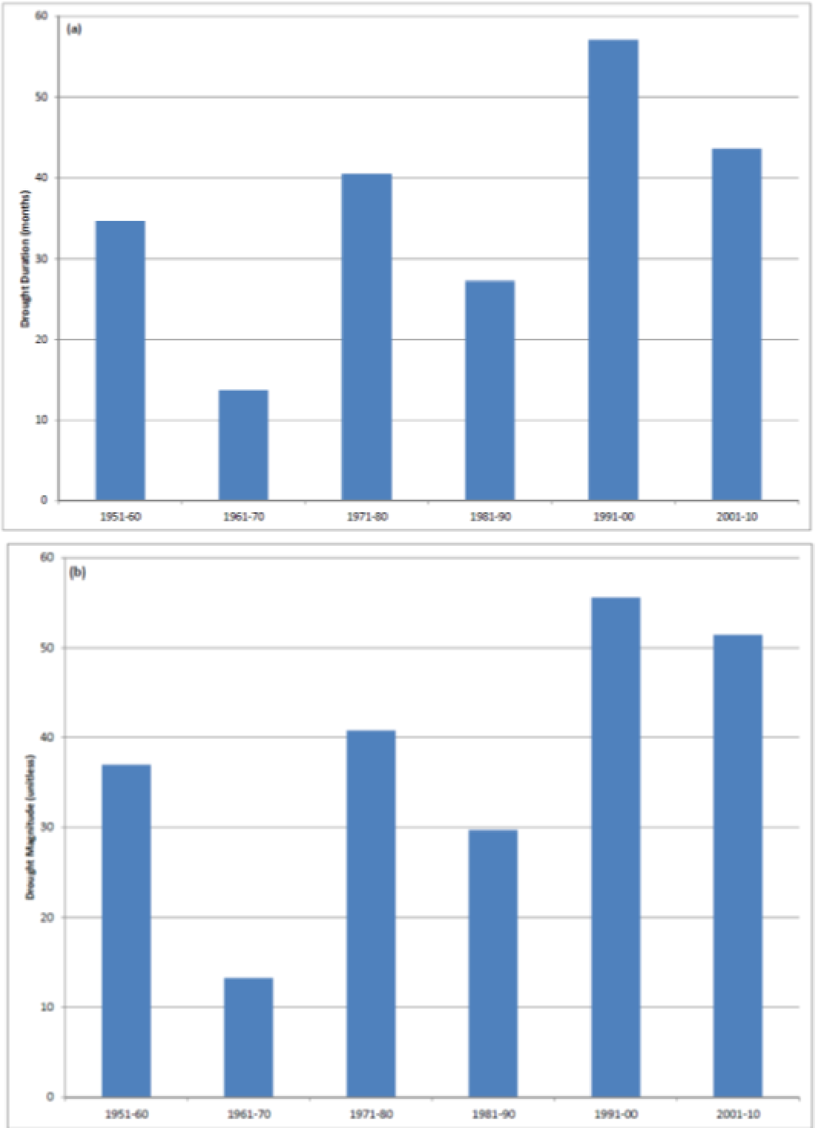


Figure 2.4 Mean decadal total drought duration and total drought magnitude 1951–2010 for the selected Hawaiian stations: (a) TDD and (b) TDM

Drought patterns in this study are comparable with those of Spinoni et al. (2014) for Australia. Both efforts show a decrease in TDD and TDM in the northern part of the Northern Territory (NT) and from northwest QLD southeast to NSW and an increase in TDD and TDM along the eastern Australia coast. Our results indicate largely non-significant trends for Australia whereas Spinoni et al. (2014) found significant trends for both TDD and TDM in the northern part of the NT. The differences may be due to station selection and/or the gridding technique used by Spinoni et al. (2014).

### 2.4.2 Difference in DF, TDD and TDM medians

DF, TDD and TDM medians for 1951–80 and 1981–2010 are presented in Table 2.2 then compared using the Mann–Whitney test. The 1981–2010 DF, TDD and TDM medians are larger than those for 1951–80 with the differences highly significant as shown by the *p*-values.

Table 2.2 Median DF, TDD and TDM over 1951–80 and 1981–2010

| | **1951–80** | **1981–2010** | ***p*-value** |
|---|---|---|---|
| **DF** | 5 | 6 | 0.0022 |
| **TDD** | 92 | 116 | 0.0000 |
| **TDM** | 96.9 | 121.8 | 0.0000 |

The above results show droughts have been more frequent, longer and more intense since 1981. In order to determine if the trend is linear, the six decade medians from 1951 are computed then compared using the Kruskal–Wallis test. The *p*-values at the bottom of Table 2.3 point to at least one of the decade medians being greater than the others with the difference significant at

Table 2.3 Median DF, TDD and TDM over individual decades between 1951 and 2010

| | **DF** Median (Ave rank) | **TDD** Median | **TDM** Median |
|---|---|---|---|
| **1951–60** | 2 (298.4) | 27 | 26.9 |
| **1961–70** | 2 (337.3) | 30 | 29.5 |
| **1971–80** | 2 (318.6) | 28 | 29.5 |
| **1981–90** | 2 (357.2) | 33 | 34.0 |
| **1991–00** | 2 (375.8) | 47 | 54.5 |
| **2001–10** | 2 (349.6) | 34 | 35.0 |
| ***p*-value** | 0.044 | 0.000 | 0.000 |

the 95% level. In the case of TDD and TDM, the 1991–2000 median is greater than all the other decade medians (as determined by the Mann–Whitney test) with the difference significant at the 95% level. For DF the 1981–90, 1991–2000 and 2001–2010 decade, the medians are larger than that for 1951–60 and the 1991–2000 median is also greater than the median for 1971–80.

To display the occurrence of drought in the 1990s in comparison to the occurrence of drought in the remaining decades, drought hot spots are calculated and presented in Figure 2.5.

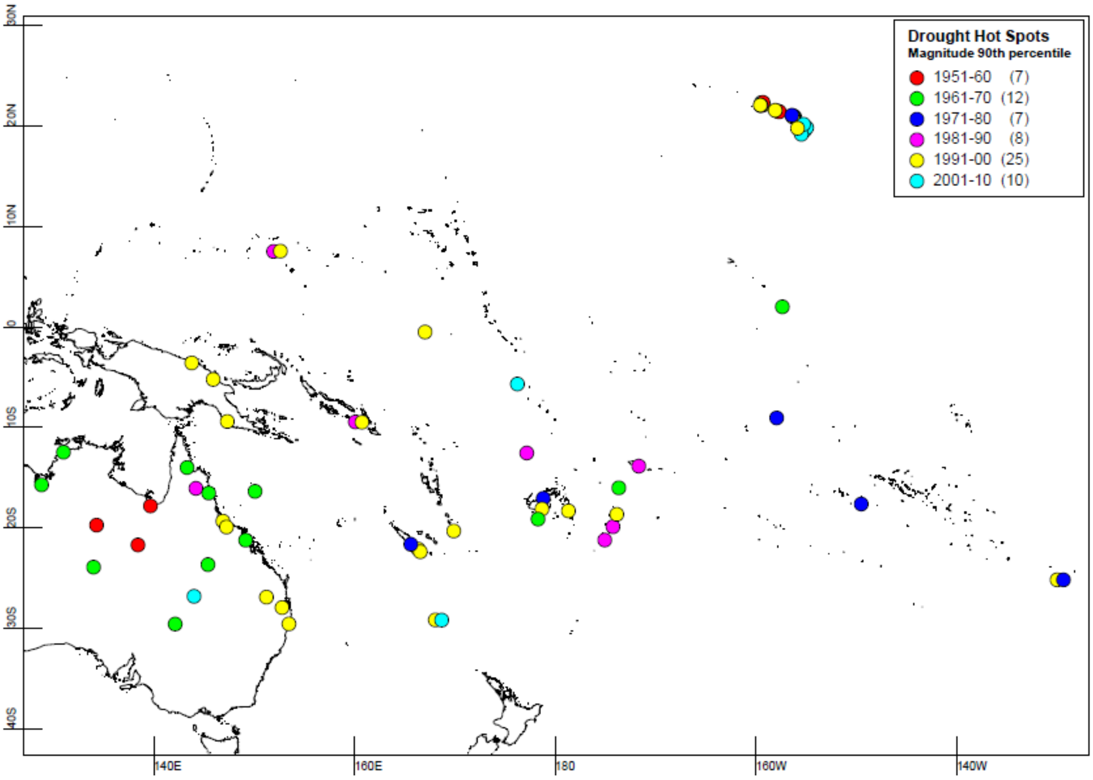


Figure 2.5 Drought hot spots on decadal timescales 1951–2010. Numbers in parentheses refer to the number of stations for the respective decade

These are locations where decade TDM is ≥ 70.3 (the 90th percentile for the entire region and study period). As expected, TDM for the 1990s dominate (25 of 69 station markers, next highest decade has 12 markers). Most of the 1990s hot spot locations experience droughts during El Niño events.

Eleven coherent precipitation regions were found using cluster analysis – three in the north Pacific, six in the south Pacific and two in northeast Australia (Figure 2.6). From this point forward, we focus on results of the cluster analysis and annual precipitation correlations with NINO3.4 SSTA.

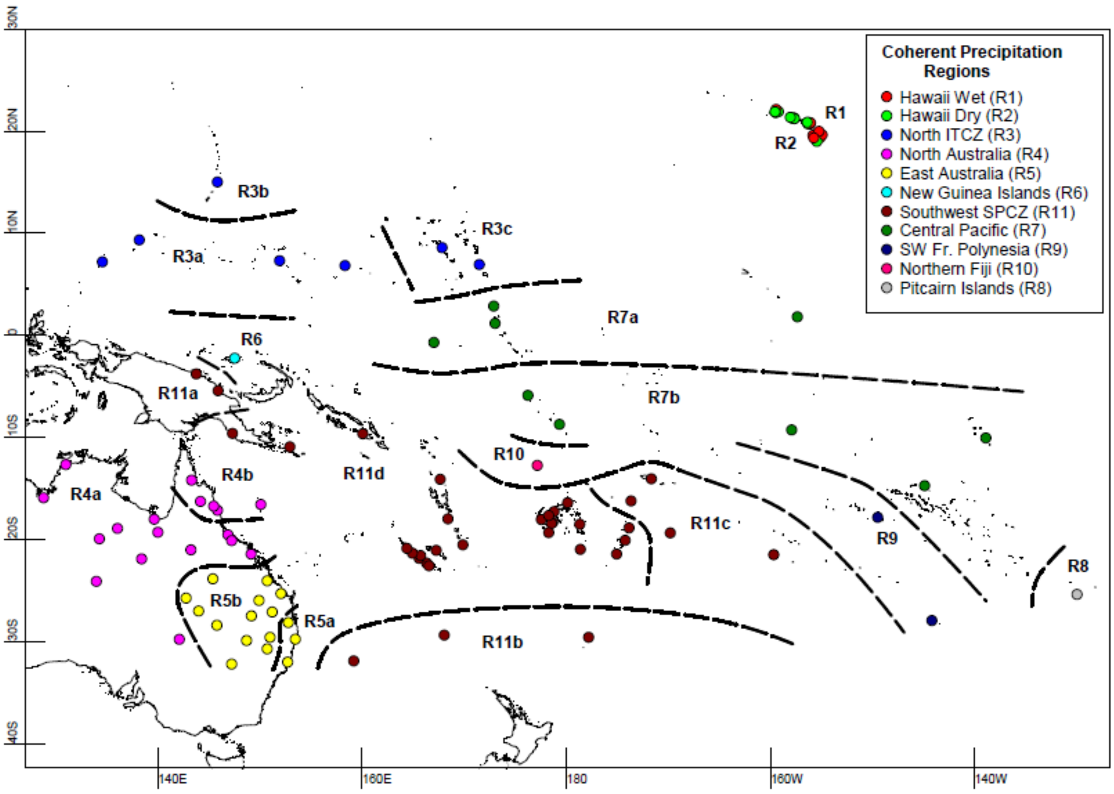


Figure 2.6 Pacific Islands and northeast Australian coherent annual precipitation subregions as defined by cluster analysis

*Region 1 (Hawaii Wet).* Cluster analysis divides the Hawaiian Islands into two regions defined as R1(Hawaii Wet) and R2 (Hawaii Dry), respectively. This division is based on high (low) annual precipitation associated with the windward (leeward) sides of the islands.

An examination of the lag-0 relationship between annual precipitation in R1 and NINO3.4 SSTA (Appendix 2.1) reveals a largely non-significant precipitation relationship with ENSO, as only the correlation coefficient between NINO3.4 SSTA and annual precipitation at Paauilo 221 is statistically significant. When annual precipitation is lagged by a year, there is an inclination towards negative and stronger relationships, however, the *p*-values remain largely non-significant. This relationship is also reflected in the SPI-12 drought record for Hawaii Wet, where at least 50% of the droughts events between 1951 and 2010 are associated with El Niño events. Four DF trends in this cluster are positive with a fifth at Pauoa Flats also positive but only significant at the 90% level. For TDD, two on the Big Island and one on Maui show positive trends. The Haleakala Ranger Station on Maui and PH Wainiha on Kaua’i display positive trends but only at the 90% level. For TDM, there is a positive trend at PH Wainiha. Two stations on the Big Island and one on Maui also show positive trends, significant at the 90% level. DF, TDD and TDM over 1951–80 and 1981–2010 are presented in Table 2.4.

Table 2.4 Station median DF, TDD and TDM for 1951–1980 and 1981–2010

| Cluster | DF (No. of events) | | TDD (months) | | TDM (SPI units) | |
|---|---|---|---|---|---|---|
| | 1951–80 | 1981–2010 | 1951–80 | 1981–2010 | 1951–80 | 1981–2010 |
| **1. Hawaii Wet** | 5 | 7 | 71 | 153 | 71.4 | 152.8 |
| **2. Hawaii Dry** | 5 | 6 | 104 | 115 | 113.8 | 116.0 |
| **3. North ITCZ** | 6 | 7 | 71 | 116 | 68.8 | 139.1 |
| **4. North Australia** | 6 | 6 | 107 | 106 | 113.1 | 109.7 |
| **5. East Australia** | 7 | 7 | 107 | 116 | 107.3 | 117.9 |
| **6. New Guinea Islands** | 6 | 6 | 100 | 82 | 106.3 | 113.5 |
| **7. Central Pacific** | 5 | 5 | 117 | 89 | 124.3 | 116.9 |
| **8. Pitcairn** | 2 | 2 | 58 | 84 | 95.9 | 114.1 |
| **9. SW French Polynesia** | 5 | 8 | 80 | 117 | 88.2 | 110.8 |
| **10. Northern Fiji** | 8 | 8 | 97 | 102 | 87.1 | 115.1 |
| **11. South SPCZ** | 5 | 7 | 83 | 120 | 88.1 | 138.8 |

*Region 2 (Hawaii Dry).* As for Hawaii Wet, the lag-0 relationships between annual precipitation in R2 and NINO3.4 SSTA are weak and non-significant. Lagged relationships produce stronger coefficient values that are statistically significant at five (on Kauai and Oahu) of 14 stations. The only significant drought trend is a DF negative trend at Puunene 396. This is supported by the small change in R2 DF, TDD and TDM over the first and second 30 year periods as shown in Table 2.4.

*Region 3 (North ITCZ)*. This region is made up of the CNMI, Palau, FSM and the RMI. Cluster analysis suggests this region can be divided into three subregions; Palau and FSM (R3a), CNMI (R3b), and the RMI (R3c). The lag-0 relationships between annual precipitation and NINO3.4 SSTA are significant at three of four stations in R3a and at Majuro in R3c. The relationship becomes statistically significant at all the R3 stations when annual precipitation is lagged by a year. Most SPI-12 droughts are associated with El Niño. Only the following drought trends were statistically significant: R3a, the Majuro positive TDD and TDM trends and R3c, the Pohnpei positive TDD trend. This is supported by larger R3 TDD and TDM medians over 1981–2010 when compared with 1951–80.

*Region 4 (North Australia).* This region includes the Kimberley Research Station in Western Australia (WA), five NT stations; Tibooburra Post Office (P.O.) in NSW, Willis Is., and the QLD stations with the exception of the group between Rockley, south to the Harrisville P.O. near Brisbane and west to the Cunnamulla P.O. Cluster analysis suggests R4 can be divided into two subregions. R4a comprises most of R4, except Willis Is., Palmerville, Mossman South, Coen P.O. and Cairns Aero in northeast QLD which form R4b. The relationship between the annual precipitation and NINO3.4 SSTA is largely non-significant in the western part of the R4 and largely negatively correlated and significant to the east. Drought trends are largely non-significant in this part of Australia with the exception of the positive DF trend at the Alice Springs Airport. At the 90% level only the negative TDD trend at the Windorah P.O. and negative TDM trend at Brunette Downs are significant. Unlike Spinoni et al. (2014) we do not find significant negative TDD and TDM trends in the northern part of the NT, however we do find large negative non-significant trends in this region.

*Region 5 (East Australia).* This region includes the QLD stations excluded in R4 and Collarenebri, Wallangra, Nyngan, Barraba P.O., Lorne and Yamba Pilot Station in New South Wales. Cluster analysis suggests there are two subregions in R5; Lorne, Harrisville P.O. and Yamba Pilot Station in R5a with the remaining R5 QLD and NSW stations in R5b. Annual precipitation is negatively correlated with NINO3.4 SSTA and statistically significant for most of the R5 stations. Unlike the north Pacific, lagged correlations by large do not produce stronger relationships with the NINO3.4 SSTA in Australia. Significant negative TDD and TDM trends are only present at Collarenebri in R5b.

*Region 6 (New Guinea Islands).* This cluster is made up of Momote W.O. only, located on Manus Island north of the New Guinea mainland. The correlation coefficient between Momote annual precipitation and NINO3.4 SSTA is non-significant for both the concurrent and lagged relationships. Equal numbers of droughts for SPI-12 occur during El Niño and La Niña. DF, TDD and

TDM trends are non-significant. Kavieng precipitation on New Ireland shows a similar relationship with NINO3.4 SSTA. Limited data prevents Kavieng from being included in this study.

*Region 7 (Central Pacific).* This region includes Nauru, Kiribati, Tuvalu, the northern Cook Islands, and the French Polynesia Tuamotu and Marquesas Groups. These islands lie between the ITCZ to the north and SPCZ to the southwest. Annual precipitation is strongly related to the phase of ENSO and most droughts occur during La Niña. Cluster analysis suggests there are two subregions in R7 which are made up of Nauru and Kiribati (R7a) and Tuvalu, northern Cook Islands and northeast French Polynesia (R7b). Annual precipitation is strongly positively correlated with NINO3.4 SSTs in R7a and to a lesser extent in R7b with the exception of the northernmost station in Tuvalu which has a correlation coefficient more related to R7a. R7b stations have strong significant lagged relationships with the NINO3.4 SSTA which is not the case for R7a. With regards to drought trends in this region only the negative DF trend at Takaroa in R7b is statistically significant.

*Region 8 (Pitcairn Islands).* This region is composed solely of the Pitcairn Islands. Pitcairn has little seasonality in precipitation as it lies to the east of the SPCZ. Neither the concurrent nor lagged relationship between annual precipitation and NINO3.4 SSTA are statistically significant. Two of the four SPI-12 droughts between 1954 and 2010 cover a total period of 122 months. Drought trends are not significant.

*Region 9 (Southwest French Polynesia).* This region is made up of Tahiti (Society Islands) and Rapa (Austral Islands) in French Polynesia at the eastern end of the diagonal portion of the SPCZ. Unlike R8, the presence of the SPCZ results in seasonality, but like Pitcairn the lag-0 annual precipitation and NINO3.4 SSTA relationships are weak. La Niña marginally dominate the drought record for Tahiti and El Niño for Rapa. This is perhaps associated with stronger but non-significant lagged correlations with NINO3.4 SSTA. Only the negative DF trend at Rapa is significant.

*Region 10 (Northern Fiji).* This region comprises of Rotuma only, the northernmost Fiji Island which is located under SPCZ for a large part of the year. Both the lag-0 and lag-1 relationships between Rotuma precipitation and NINO3.4 SSTA are non-significant. The climate of Rotuma is unique as droughts occur during El Niño and La Niña. La Niña results in SPCZ displacement towards Fiji but extreme southwest displacement leads to drought. Drought trends are not statistically significant. Supporting these results are data for Niulakita (not included in this study), the southernmost Tuvalu Island, located about 330km to the northeast. Niulakita displays similar non-significant relationships with NINO3.4 SSTA.

*Region 11 (Southwest SPCZ).* This region occupies the largest part of the study area; PNG mainland, Solomon Islands, Vanuatu, New Caledonia, main islands of Fiji, Tonga, Niue, southern Cook Islands and the Australian and NZ subtropical islands. With the exception of the stations on the northern coast of PNG, the remaining stations lie to the southwest of the SPCZ and are affected by the subtropical high pressure belt. Cluster analysis suggests there are four subregions which are Madang and Wewak in PNG (R11a), Lord Howe, Norfolk and Raoul Islands in the subtropics (R11b), northern Tonga, Niue, Samoa and the southern Cook Islands (R11c) and the remaining stations between southern PNG and Tonga (R11d). There are significant lag-0 negative relationships between annual precipitation and NINO3.4 SSTA at all 34 R11 stations. Stations in R11a, R11b and R11c have non-significant lagged relationships with NINO3.4 SSTA while most stations in R11d do have significant lagged relationships. Most droughts are associated with El Niño in R11.

In R11b, the Norfolk Island TDD and TDM trends are positive and significant. The DF trend is also positive and significant but only at the 90% level. The Lord Howe Island TDM trend is positive. Drought trends are mixed in the R11d. At Nausori Airport in Fiji and Port Vila-Bauerfield Airport in Vanuatu the DF trends are positive. The DF trend is negative at Chepenehe on Lifou Island in New Caledonia. At Houailou P. the TDD trend is positive and the TDM trends at Houailou P. and Kone are significant at the 90% level. Overall, for R11, TDD and TDM are notably larger over 1981–2010 when compared with TDD and TDM for 1951–80.

### 2.4.3 Drought variability on decadal timescales

There is a negative relationship between 13-year running average annual standardized precipitation and TPI/PDO in the Hawaii Wet, North ITCZ, North Australia (TPI only), New Guinea Islands, Pitcairn Is. (PDO only), Rotuma (PDO only) and Southwest Pacific regions and a strong positive relationship in the Central Pacific (Table 2.5). These results show there is decadal scale variability in annual precipitation at these locations in phase with the IPO/PDO. On a Hawaiian Islands scale and PDO-precipitation relationship is statistically significant. The TPI – East Australia relationship is also significant but only at the 90% level.

Table 2.5 Correlation coefficients for TPI/PDO and annual standardised precipitation (columns 2–3). Median drought duration and drought magnitude for the TPI/PDO negative phases (1951–77, 1999–2010) and TPI/PDO positive phase (1978–98, columns 4–7). Correlation coefficients and medians differences statistically significant at the 95% level are presented in italics.

| **Cluster** | **TPI** | **PDO** | **DD IPO -ve** | **DD IPO +ve** | **DM IPO -ve** | **DM IPO +ve** |
|---|---|---|---|---|---|---|
| 1 | 2 | 3 | 4 | 5 | 6 | 7 |
| **1. Hawaii Wet** | *-0.39* | *-0.58* | *15* | *12* | *15.8* | *10.8* |
| **2. Hawaii Dry** | -0.04 | -0.23 | 14 | 16 | 14.6 | 14.7 |
| **3. North ITCZ** | *-0.72* | *-0.81* | *11* | *16* | *12.2* | *21.7* |
| **4. North Australia** | *-0.35* | -0.08 | 14 | 13 | 16.9 | 12.9 |
| **5. East Australia** | -0.26 | -0.08 | 13 | 12 | 13.4 | 11.9 |
| **6. New Guinea Islands** | *-0.32* | *-0.30* | 13 | 14 | 16.5 | 22.7 |
| **7. Central Pacific** | *+0.96* | *+0.92* | 19 | 15 | 21.7 | 16.5 |
| **8. Pitcairn Islands** | -0.22 | *-0.44* | 29 | 42 | 47.9 | 57.0 |
| **9. SW Fr. Polynesia** | +0.10 | -0.15 | 19 | 9 | 16.0 | 9.2 |
| **10. Northern Fiji** | -0.22 | *-0.37* | 9 | 13 | 9.2 | 17.6 |
| **11. South SPCZ** | *-0.95* | *-0.85* | *11* | *13* | *12.0* | *19.5* |

Drought duration was longer and drought magnitude larger during the TPI/PDO negative phases in the Hawaii Wet region. Conversely droughts were longer and more intense in the North ITCZ and Southwest SPCZ regions during the TPI/PDO positive phase from 1978–98 (Table 2.4).

## 2.5 Summary of Regional Findings

In this study we use the Standardized Precipitation Index (SPI-12 timescale) to examine the historical precipitation record for trends in drought frequency, duration and magnitude over 1951–2010 using 113 station records for 21 countries and territories in western Pacific. This is followed by analyses to determine the strength of the relationship between precipitation and drivers of Pacific climate namely ENSO and the IPO/PDO.

Station scale trends in drought are largely positive but non-significant (>90%) and spatially heterogeneous trends over 1951–2010 implying that there has been little change in meteorological drought occurrence for most of the study region over the last 60 years. Where trends are significant, they are also largely positive and located in the subtropics.

In the Hawaiian region, the positive drought trends complement earlier work that found an increase in CDD across the State over 1950–2007 (Chu et al., 2010). According to Chu and Chen (2005) the drying trends are associated with anomalous surface westerlies to the north of Hawaii, anomalously stronger and deeper sinking motions and anomalously vertically integrated moisture flux divergence over Hawaii. These together with weakened northeast trade winds since the mid-1970s (Garza et al. 2012) provide unfavourable conditions for convection especially during the winter period. There are also a number of studies that suggest the width of the tropical belt has changed (Seidel et al. 2008; Lu et al. 2007, 2009). Further, Li et al. (2011) show significant heat flux changes in the Pacific and suggest that the changes are closely linked to global warming forcing. In particular, Figure 5 of the Li et al. (2011) paper suggests lower latent heat fluxes, particularly post 1990 in a broad region around and northeast of Hawaii, which may be associated with reduced precipitation in the Hawaiian Islands in recent decades (Diaz and Giambelluca 2012).

In the south Pacific subtropics, the significant positive TDD and TDM trends are supported by negative trends in total annual precipitation and annual days with precipitation > 1mm and > 10mm since 1951 (Jovanovic et al. 2012; McGree et al. 2014). Increasing trends in droughts in subtropical southern Australia (CSIRO 2012) and the Altiplano in South America (Morales et al. 2011), have previously been linked to changes in the Hadley Circulation. As the Norfolk and Lord Howe Islands are adjacent to southern Australia it is likely the intensification of the Hadley Circulation and poleward shift of the subtropical dry zone are also responsible for the drying trends. The reason for the intensification is the subject of considerable debate with some studies attributing the change to stratospheric ozone depletion (Min and Son 2013), while others favour increased surface global warming (Nguyen et al. 2015) or a combination of the two (Allen et al. 2014).

An alternative method of examining drought change over time is to compare the DF, TDD and TDM medians for 1951–80 and 1981–2010. The 1981–2010 DF, TDD and TDM medians are larger than those for 1951–80 with the differences in the median values highly significant. However, the change is non-linear as discovered by comparing the six decade medians from 1951. For all three measures of drought one of the decade medians is greater than the others with the difference statistically significant. In the case of TDD and TDM, the 1991–2000 median is greater than all the other decade medians. This feature is notable in Figure 2.6, which shows drought hot spots (TDM) for the study region. Station markers for the 1991–2000 period are in the majority (~35%). A period when a number of very strong El Niño events occurred, most notably the 1982–83 and 1997–98 events. The results of the study to this point suggest ENSO and possibly IPO influence drought frequency, duration and magnitude which leads to the second part of the study where the aim is to investigate the strength of the relationship between precipitation and drivers of Pacific climate especially in the tropical Pacific.

In the central north Pacific, El Niño events are associated with the upper-tropospheric jet stream extending eastward during the boreal winter. The Hawaiian Islands are located in the right exit region of the jet stream, in an area of upper-level convergence. The expected anomalous sinking motion resulting from upper-level convergence tends to hinder the development of subtropical cyclones, upper-level lows, and the passage of mid-latitude frontal systems to the Hawaiian Islands. These features, together with reduced north-easterly trade winds result in low wet season precipitation (Chu 1995; Chu and Chen 2005; Cao et al. 2007; Garza et al. 2012). In the northwestern tropical Pacific in the vicinity of the ITCZ, El Niño is associated with weakened trade winds (Lander 2004) and the ITCZ displaced on average closer to the equator and more intense between 160°E–120°W, 0°–15°N (Australian Bureau of Meteorology and CSIRO 2011) resulting in droughts in the islands immediately to the north (Figure 2.2).

In the southwest Pacific, ENSO has a notable influence on the SPCZ and therefore on precipitation received in the countries nearby (Trenberth 1976; Vincent 1994; Folland et al. 2002; Vincent et al. 2009). Trenberth (1976) described the movement of the SPCZ as north and east during El Niño and south and west during La Niña. Asymmetric orientations of the SPCZ resulted in a near-parallel alignment with the equator (and in large displacement) for the very strong El Niño events of 1982–83 and 1997–98. There is also evidence that meridional Hadley Circulation strengthens during El Niño (Chu and Chen 2005; Lough et al. 2011) resulting in cooler, drier tradewinds in the south Pacific.

In the PNG and northeast Australian region the West Pacific Monsoon (WPM) (Figure 2.2) is associated with a seasonal reversal of wind direction that brings heavy precipitation to northern Australia, and western tropical Pacific Islands. Variations in the timing, position, intensity, longevity and extent of the monsoon account for much of the precipitation variability in this region. ENSO causes some variability in the WPM. The two most extreme maximum eastern extents of the monsoon domain occurred during the strong El Niño events of 1982–83 and 1997–98 (Australian Bureau of Meteorology and CSIRO 2011). Although Australia is influenced by many climate drivers, El Niño and La Niña have perhaps the strongest influence on interannual precipitation variability. The shift in precipitation away from the western Pacific, associated with El Niño, means that Australian precipitation is usually reduced through winter–spring, particularly across the eastern and northern parts of the continent. The date of the monsoon onset in tropical Australia is generally 2–6 weeks later during El Niño years than in La Niña years. This means that precipitation in the northern tropics is typically well-below-average during the early part of the wet season for El Niño years (Nicholls 1984; Lo et al. 2007; Timbal and Drosdowsky 2013).

The literature survey demonstrates precipitation variability is dissimilar across the study region and as such a simple region averaged precipitation timeseries would not be appropriate. In an effort to reduce the number of variables and reduce noise at a station level, multivariate analyses is applied to group the precipitation timeseries into coherent regions of variability. Eleven coherent precipitation regions of variability were found using cluster analysis – three in the north Pacific, two in northeast Australia and six in the south Pacific. We confirm the cluster groupings and derive additional information by computing the strength of the ENSO (using NINO3.4 SSTA) and precipitation relationship using correlation coefficients.

Cluster analysis divides the Hawaiian Islands into two regions based on high (low) annual precipitation largely associated with the windward (leeward) sides of the islands. Our investigation of the strength of the relationship between annual precipitation and NINO3.4 SSTA finds a non-significant relationship at lag-0 across the State but a negative relationship at lag-1 at almost 50% of the stations on the leeward side of the islands and at one of 10 stations on the windward side.

Numerous studies have documented the negative correlation between equatorial Pacific SSTs and precipitation across most of Australia, including QLD e.g. McBride and Nicholls (1983); Allan (1988); Lough (1991); Murphy and Ribbe (2004). There have also been a number of attempts to group northeast Australia precipitation into coherent regions of variability e.g. Drosdowsky (1993). Results vary depending on time-period and data selected. Our results show two main clusters with the first covering the northeast WA, the NT, QLD with exception of the stations to the southeast, the northwest portion of NSW and Willis Island off the coast of QLD. The second cluster covers the remaining portion of QLD and NSW. The annual precipitation relationship with NINO3.4 SSTA is by large non-significant in the monsoon dominated portion of northern Australia but largely significant to the east. Unlike the North ITCZ and Southwest SPCZ clusters NINO3.4 SSTA does not have a lagged relationship with northeast Australia precipitation.

We are only aware of one previous study (Salinger et al. 1995) beyond Australia and Hawaii that groups Pacific Islands precipitation timeseries into coherent regions of variability using statistical techniques. There are noteworthy differences between results of Salinger et al. (1995) and this study. The Northern Fiji cluster in this study does not include Samoa and the southern Cook Islands, partly due to there being a significant inverse relationship between stations at these locations and NINO3.4 SSTA whereas there is a weak relationship between the Northern Fiji cluster precipitation and NINO3.4 SSTA. In Salinger et al. (1995) the Southwest SPCZ region is labelled 'Subtropical region'. With a larger dataset the 'Subtropical region' is expanded in this study to include the PNG mainland, Solomon Islands, Australian Pacific subtropical islands, Samoa and the southern Cook Islands.

Further, we present a lagged relationship between annual precipitation and NINO3.4 SSTA for most of the stations between southern PNG and southern Tonga (southwest of the zonal portion of the SPCZ (Folland et al. 2002)) which does not include the northern Tonga to southern Cook Islands portion (southwest of the diagonal portion of the SPCZ) of the Southwest SPCZ cluster. Grouping precipitation timeseries into coherent regions of variability has not been attempted for the north tropical Pacific. We have found a North ITCZ cluster that covers the CNMI, Palau, FSM and the RMI region. El Niño events correspond closely with increased risk of drought in the following year in this Micronesia region with drought tending to be most extreme during the northern hemisphere winter and spring following an El Niño (Keener et al. 2012). We have found lag-0 relationships between annual precipitation and NINO3.4 SSTA significant at four of six stations in the Palau-FSM and RMI sub-clusters. This relationship becomes statistically significant at all seven stations in the North ITCZ cluster when the precipitation is lagged by a year.

Finally, we determine the strength of the relationship between the precipitation clusters and IPO/PDO as well as determine whether droughts are longer and/or more severe during a particular phase of IPO/PDO. The results show that during the IPO/PDO positive (negative) phase the Hawaii Wet, North ITCZ, North Australia (IPO only), New Guinea Islands, Pitcairn Is. (PDO only), Northern Fiji (PDO only) and Southwest SPCZ clusters were ‘drier’ (‘wetter’) with the reverse applying for the Central Pacific cluster. When the Hawaii Wet and Hawaii Dry clusters are merged, the 13-year running average Hawaiian standardised precipitation and PDO relationship is found to be highly significant ($\rho$ = -0.369, p = 0.010) in line with previous conclusions on the PDO and Hawaiian precipitation relationship (Mantua et al. 1997; Chu and Chen 2005). The above result for Hawaii Dry suggests PDO's influence on Hawaiian precipitation is stronger on the windward side of the islands.

For the North ITCZ and Southwest SPCZ clusters ‘drier’ periods are associated with longer and more severe droughts. In the Central Pacific and where the precipitation clusters and IPO/PDO relationships were weaker (North Australia, New Guinea Islands, Pitcairn Is., Northern Fiji) there was no significant difference in median drought duration or magnitude. For Australia, this finding correlates with earlier studies that found that during the earlier IPO positive phase ENSO and QLD precipitation became uncorrelated. During these years, QLD precipitation became less variable on interannual scales, presumably due to the lack of a large-scale climate driver (Lough 1991). Further, Power et al. (1999) found that the positive IPO phase resulted in a weakening of ENSO–Australian–precipitation teleconnection. Unexpectedly, drought duration and magnitude were found to be greater during Hawaii Wet ‘wet’ phases. However, on a state scale the median differences are not statistically significant. It is possible the longer and more severe droughts in the Hawaii Wet cluster during PDO negative periods are the result of positive trends in drought at a number of stations in this cluster. This is supported by Frazier et al. (2011) and Diaz and Giambelluca (2012) who show some degree of negative correlation between PDO and Hawaiian winter precipitation prior to the late 1970s climate shift in the Pacific. However, since about 1980 the precipitation association with the PDO index has become much weaker or non-existent.

There is a notable difference between PDO and IPO (as defined by the TPI) their relationship with precipitation as shown in Table 2.5. This is in contract to the findings of Folland et al. (2002) who found PDO and IPO to be essentially equivalent in describing Pacific-wide variations in ocean climate. The relationship between the PDO and north Pacific precipitation (Hawaii Wet, Hawaii Dry and North ITCZ clusters) is stronger than that of the TPI and Hawaiian precipitation while the reverse applies in the south Pacific (North Australia, East Australia and Southwest SPCZ clusters). In the near-equatorial Pacific the relationships between the decadal indices and precipitation are near equivalent (Central Pacific and New Guinea Islands cluster). The weaker (as compared with the PDO) Northern Fiji and Pitcairn Islands cluster relationships with TPI are unexpected. This may be associated with weak to non-existent relationships between precipitation and ENSO at these locations.

## 2.6 Conclusions

In response to the general perception amongst Pacific Islanders that the frequency of drought has increased, particularly in the last couple of decades, the results of this study show from a meteorological perspective, drought frequency, duration and magnitude for Pacific Islands and northeast Australia were greater over 1981–2010 as compared with 1951–80. The increase was not linear and was in a large part due to low frequency variability namely the positive phase of the IPO from 1977–98. The switch to the negative phase of IPO from 1999 resulted in a decade from 2000 with reduced drought activity. The subtropics of both hemispheres are notable exceptions. Here changes in the Hadley Circulation resulted in a number of locations displaying positive drought trends that are statistically significant.

Overall, IPO and ENSO were the dominant drivers of drought occurrence over the period 1951–2010 with the exception of the Pacific Ocean subtropics in recent decades.

*Acknowledgements.* The authors thank Dr John Marra, Dr Michael Kruk and Dr Blair Trewin for their assistance with selecting the Hawaiian and Australian stations for this study. Valuable comments from Dr Blair Trewin, Ms Janita Pahalad and Mr Neil Plummer helped improve quality of the manuscript. Approval from the respective heads of the Pacific Island National Meteorological & Hydrological Services for the use of their meteorological data is greatly appreciated.

## Appendix 2.1

Spearman rank correlation coefficients demonstrating the strength of the relationship between annual NINO3.4 SSTA and annual precipitation (lag-0) and NINO3.4 SSTA and annual precipitation lagged by a year (lag-1) on a station scale. Values in italics show correlation coefficients significant at the 95% level.

| No. | Name | Longitude | Latitude | Cluster | Lag-0 | Lag-1 |
|---|---|---|---|---|---|---|
| **1** | Paauilo 221 | 20.1°N | 155.4°W | 1 | *0.36* | 0.13 |
| **2** | Hilo Int. Apt. | 19.7°N | 155.1°W | 1 | 0.11 | -0.23 |
| **3** | Hawaii Vol. Nat. Park. HQ. | 19.4°N | 155.3°W | 1 | -0.13 | *-0.35* |
| **4** | Lanihau 68.2 | 19.7°N | 156.0°W | 1 | -0.16 | *-0.48* |
| **5** | Honaunau 27 | 19.4°N | 155.9°W | 1 | -0.07 | -0.19 |
| **6** | Hamakuapoko 485 | 20.9°N | 156.4°W | 1 | 0.17 | -0.08 |
| **7** | Kailua 446 | 20.9°N | 156.2°W | 1 | -0.06 | -0.19 |
| **8** | Haleakala Ranger Stat. 338 | 20.8°N | 156.3°W | 1 | 0.10 | -0.23 |
| **9** | Pauoa Flats 784 | 21.4°N | 157.8°W | 1 | 0.10 | -0.09 |
| **10** | PH Wainiha 1115 | 22.2°N | 159.6°W | 1 | -0.02 | -0.21 |
| **11** | Naalehu 14 | 19.1°N | 155.6°W | 2 | -0.14 | -0.15 |
| **12** | Waihee Valley 482 | 20.9°N | 156.5°W | 2 | 0.15 | -0.18 |
| **13** | Puunene 396 | 20.9°N | 156.5°W | 2 | 0.12 | -0.20 |
| **14** | Keahua 410 | 20.9°N | 156.4°W | 2 | 0.28 | -0.08 |
| **15** | Kihei 311 | 20.8°N | 156.4°W | 2 | 0.05 | -0.24 |
| **16** | Moanalua 770 | 21.4°N | 157.9°W | 2 | 0.10 | *-0.30* |
| **17** | Honolulu Int. Apt. | 21.3°N | 157.9°W | 2 | 0.05 | *-0.34* |
| **18** | Punchbowl Crater 709 | 21.3°N | 157.9°W | 2 | 0.04 | 0.07 |
| **19** | Wilhelmina Rise 721 | 21.3°N | 157.8°W | 2 | 0.28 | -0.16 |
| **20** | Waianae 798 | 21.4°N | 158.2°W | 2 | -0.08 | *-0.31* |
| **21** | Waimea 947 | 22.0°N | 159.7°W | 2 | 0.05 | *-0.44* |
| **22** | Makaweli 945 | 21.9°N | 159.6°W | 2 | 0.03 | *-0.40* |

| **No.** | **Name** | **Longitude** | **Latitude** | **Cluster** | **Lag-0** | **Lag-1** |
|---|---|---|---|---|---|---|
| **23** | Eleele 927 | 21.9°N | 159.6°W | 2 | -0.07 | -0.27 |
| **24** | Lihue WSO Apt. | 22.0°N | 159.4°W | 2 | -0.02 | -0.28 |
| **25** | Koror | 7.3°N | 134.5°E | 3a | *-0.32* | *-0.34* |
| **26** | Yap | 9.5°N | 138.1°E | 3a | *-0.48* | *-0.50* |
| **27** | Chuuk | 7.5°N | 151.8°E | 3a | *-0.40* | *-0.38* |
| **28** | Pohnpei | 7.0°N | 158.2°E | 3a | -0.17 | *-0.54* |
| **29** | Saipan Int. Apt. | 15.1°N | 145.7°E | 3b | -0.15 | *-0.35* |
| **30** | Kwajalein | 8.7°N | 167.7°E | 3c | -0.04 | *-0.37* |
| **31** | Majuro | 7.1°N | 171.4°E | 3c | *-0.29* | *-0.48* |
| **32** | Kimberley Res. Stat. | 15.7°S | 128.7°E | 4a | -0.21 | -0.07 |
| **33** | Darwin Apt. | 12.4°S | 130.9°E | 4a | -0.11 | 0.01 |
| **34** | Brunette Downs | 18.6°S | 136.0°E | 4a | *-0.36* | *-0.27* |
| **35** | Tennant Creek Apt. | 19.6°S | 134.2°E | 4a | -0.05 | -0.20 |
| **36** | Burketown P.O. | 17.7°S | 139.6°E | 4a | *-0.37* | -0.10 |
| **37** | Lorraine | 19.0°S | 139.9°E | 4a | -0.20 | -0.22 |
| **38** | Alice Springs Apt. | 23.8°S | 133.9°E | 4a | -0.19 | -0.15 |
| **39** | Urandangi | 21.6°S | 138.3°E | 4a | -0.26 | -0.24 |
| **40** | Richmond P.O. | 20.7°S | 143.1°E | 4a | *-0.46* | *-0.30* |
| **41** | Townsville Aero | 19.3°S | 146.8°E | 4a | *-0.31* | *-0.31* |
| **42** | Woodhouse | 19.8°S | 147.1°E | 4a | *-0.29* | *-0.33* |
| **43** | Pleystowe Sugar Mill | 21.1°S | 149.0°E | 4a | *-0.39* | -0.28 |
| **44** | Tibooburra P.O. | 29.4°S | 142.0°E | 4a | *-0.39* | -0.17 |
| **45** | Willis Is. | 16.3°S | 150.0°E | 4b | -0.17 | -0.12 |
| **46** | Coen P.O. | 13.9°S | 143.2°E | 4b | *-0.35* | -0.08 |
| **47** | Palmerville | 16.0°S | 144.1°E | 4b | *-0.45* | -0.18 |
| **48** | Mossman South | 16.5°S | 145.4°E | 4b | -0.25 | -0.18 |
| **49** | Cairns Aero. | 16.9°S | 145.8°E | 4b | *-0.29* | -0.27 |
| **50** | Harrisville P.O. | 27.8°S | 152.7°E | 5a | *-0.48* | -0.02 |

| No. | Name | Longitude | Latitude | Cluster | Lag-0 | Lag-1 |
|---|---|---|---|---|---|---|
| **51** | Yamba Pilot Stat. | 29.4°S | 153.4°E | 5a | -0.26 | -0.01 |
| **52** | Lorne (Lorne Rd.) | 31.7°S | 152.6°E | 5a | *-0.41* | -0.20 |
| **53** | Barcaldine P.O. | 23.6°S | 145.3°E | 5b | *-0.34* | -0.13 |
| **54** | Rockley | 23.8°S | 150.6°E | 5b | *-0.45* | -0.13 |
| **55** | Windorah P.O. | 25.4°S | 142.7°E | 5b | *-0.33* | -0.21 |
| **56** | Taroom P.O. | 25.7°S | 149.8°E | 5b | *-0.38* | 0.16 |
| **57** | Gin P.O. | 25.0°S | 152.0°E | 5b | *-0.45* | 0.05 |
| **58** | Whynot | 26.7°S | 143.9°E | 5b | *-0.54* | -0.28 |
| **59** | Surat | 27.2°S | 149.1°E | 5b | *-0.43* | 0.25 |
| **60** | Jandowae P.O. | 26.8°S | 151.1°E | 5b | *-0.32* | 0.13 |
| **61** | Cunnamulla P.O. | 28.1°S | 145.7°E | 5b | *-0.42* | -0.03 |
| **62** | Collarenebri | 29.6°S | 148.6°E | 5b | *-0.32* | 0.06 |
| **63** | Wallangra Stat. | 29.2°S | 150.9°E | 5b | *-0.33* | 0.20 |
| **64** | Barraba P.O. | 30.4°S | 150.6°E | 5b | *-0.40* | 0.08 |
| **65** | Nyngan | 31.9°S | 147.1°E | 5b | *-0.41* | 0.06 |
| **66** | Momote W.O. | 2.1°S | 147.4°E | 6 | 0.01 | 0.19 |
| **67** | Nauru Arc-2 | 0.5°S | 166.9°E | 7a | *0.78* | -0.06 |
| **68** | Butaritari | 3.0°N | 172.8°E | 7a | *0.68* | -0.04 |
| **69** | Tarawa | 1.4°N | 172.9°E | 7a | *0.82* | 0.01 |
| **70** | Kiritimati | 2.0°N | 157.5°W | 7a | *0.70* | 0.07 |
| **71** | Nanumea | 5.7°S | 176.1°E | 7b | *0.71* | *0.52* |
| **72** | Funafuti | 8.5°S | 179.2°E | 7b | *0.38* | *0.58* |
| **73** | Penrhyn | 9.0°S | 158.1°W | 7b | *0.53* | *0.60* |
| **74** | Atuona | 9.8°S | 139.0°W | 7b | *0.33* | *0.49* |
| **75** | Takaroa | 14.5°S | 145.0°W | 7b | *0.43* | *0.41* |
| **76** | Pitcairn | 25.1°S | 130.1°W | 8 | 0.07 | -0.04 |
| **77** | Tahitii-Faaa | 17.6°S | 149.6°W | 9 | -0.05 | 0.12 |
| **78** | Rapa | 27.6°S | 144.3°W | 9 | -0.07 | -0.11 |

| No. | Name | Longitude | Latitude | Cluster | Lag-0 | Lag-1 |
|---|---|---|---|---|---|---|
| **79** | Rotuma | 12.5°S | 177.1°E | 10 | 0.09 | 0.10 |
| **80** | Wewak W.O. | 3.6°S | 143.7°E | 11a | *-0.64* | 0.05 |
| **81** | Madang W.O. | 5.2°S | 145.8°E | 11a | *-0.59* | -0.11 |
| **82** | Lord Howe Is. Aero | 31.5°S | 159.1°E | 11b | *-0.42* | 0.10 |
| **83** | Norfolk Is. Aero | 29°S | 167.9°E | 11b | *-0.52* | 0.18 |
| **84** | Raoul Is. | 29.3°S | 177.9°W | 11b | *-0.57* | -0.12 |
| **85** | Apia | 13.8°S | 171.8°W | 11c | *-0.50* | -0.09 |
| **86** | Keppel | 16.0°S | 173.8°W | 11c | *-0.31* | -0.01 |
| **87** | Hanan Airport | 19.1°S | 169.9°W | 11c | *-0.33* | -0.16 |
| **88** | Rarotonga | 21.2°S | 159.8°W | 11c | *-0.60* | -0.02 |
| **89** | Port Moresby | 9.4°S | 147.2°E | 11d | *-0.54* | *-0.37* |
| **90** | Misima W.O. | 10.7°S | 152.8°E | 11d | *-0.61* | *-0.43* |
| **91** | Honiara | 9.4°S | 160.0°E | 11d | *-0.29* | -0.26 |
| **92** | Sola (Vanua Lava) | 13.9°S | 167.6°E | 11d | *-0.42* | *-0.36* |
| **93** | Bauerfield (Efate) | 17.7°S | 168.3°E | 11d | *-0.62* | *-0.33* |
| **94** | Aneityum | 20.2°S | 169.8°E | 11d | *-0.62* | *-0.37* |
| **95** | Chepenehe | 20.8°S | 167.2°E | 11d | *-0.54* | -0.15 |
| **96** | Koumac | 20.6°S | 164.3°E | 11d | *-0.44* | *-0.39* |
| **97** | Kone | 21.1°S | 164.8°E | 11d | *-0.61* | *-0.31* |
| **98** | Houailou P. | 21.3°S | 165.6°E | 11d | *-0.45* | -0.15 |
| **99** | Bourail | 21.6°S | 165.5°E | 11d | *-0.54* | -0.25 |
| **100** | La Tontouta | 22.0°S | 166.2°E | 11d | *-0.62* | -0.25 |
| **101** | Noumea | 22.3°S | 166.5°E | 11d | *-0.46* | *-0.35* |
| **102** | Udu Point | 16.1°S | 180.0 | 11d | *-0.52* | *-0.43* |
| **103** | Nabouwalu | 17.0°S | 178.7°E | 11d | *-0.63* | *-0.54* |
| **104** | Penang Mill | 17.4°S | 178.2°E | 11d | *-0.56* | *-0.51* |
| **105** | Nadi Apt. | 17.8°S | 177.5°E | 11d | *-0.59* | *-0.43* |
| **106** | Nausori Apt. | 18.1°S | 178.6°E | 11d | *-0.48* | -0.23 |

| No. | Name | Longitude | Latitude | Cluster | Lag-0 | Lag-1 |
|---|---|---|---|---|---|---|
| **107** | Suva | 18.2°S | 178.5°E | 11d | *-0.41* | *-0.39* |
| **108** | Vunisea | 19.1°S | 178.2°E | 11d | *-0.59* | *-0.36* |
| **109** | Lakeba | 18.2°S | 178.8°W | 11d | *-0.48* | *-0.60* |
| **110** | Ono-i-Lau | 20.7°S | 178.7°W | 11d | *-0.52* | *-0.45* |
| **111** | Lupepau‘u | 18.6°S | 174.0°W | 11d | *-0.55* | *-0.39* |
| **112** | Haapai | 19.8°S | 174.4°W | 11d | *-0.46* | *-0.53* |
| **113** | Nuku‘alofa | 21.1°S | 175.2°W | 11d | *-0.50* | *-0.46* |

## References

Allan, R. J., 1988: El Niño Southern Oscillation influences in the Australasian region. *Prog. Phys. Geogr.*, **12**, 313–348, doi:10.1177/030913338801200301.
Allan, R. J., R. Lindesay, and D. Parker, 1996: *El Nino Southern Oscillation and Climatic Variability*. CSIRO, 402 pp.
Allen, R. J., J. R. Norris, and M. Kovilakam, 2014: Influence of anthropogenic aerosols and the Pacific Decadal Oscillation on tropical belt width. *Nat. Geosci*, **7**, 270–274.
Anderson, D., 2014: *Endurance Australian Stories of Drought*. CSIRO Publishing, Collingwood, Victoria, Australia, 237 pp.
Australian Bureau of Meteorology, 2012: Record-breaking La Niña events. An analysis of the La Niña life cycle and the impacts and significance of the 2010–11 and 2011–12 La Niña events in Australia. http://www.bom.gov.au/climate/enso/history/La-Nina-2010-12.pdf (Accessed January 15, 2015).
——, 2015: Australian climate extremes – Trend maps, Consecutive Dry Days, 1950-present. http://www.bom.gov.au/climate/change/#tabs=Tracker&tracker=extremes-trend-maps&tQ[map]=CDDs&tQ[period]=1950 (Accessed March 13, 2015).
——, and CSIRO, 2011: *Climate Change in the Pacific: Scientific Assessment and New Research. Volume 1: Regional Review. Volume 2: Country Reports.* Melbourne, Australia, http://www.pacificclimatechangescience.org/publications/reports/report-climate-change-in-the-pacific-scientific-assessment-and-new-research/.
Barnett, J., 2011: Dangerous climate change in the Pacific Islands: food production and food security. *Reg. Environ. Chang.*, **11**, 229–237, doi:10.1007/s10113-010-0160-2.
Barnett, J., and J. Campbell, 2010: *Climate Change and Small Island States: Power, Knowledge, and the south Pacific*. Earthscan, 218 pp.
Barnston, A. G., M. Chelliah, and S. B. Goldenberg, 1997: Documentation of a highly ENSO-related sst region in the equatorial pacific: Research note. *Atmosphere-Ocean*, **35**, 367–383, doi:10.1080/07055900.1997.9649597.
Benns, M., 2011: Tuvalu to run out of water by Tuesday. *Dly. Telegr.*,. www.telegraph.co.uk/news/worldnews/australiaandthepacific/tuvalu/8804093/Tuvalu-to-run-out-of-water-by-Tuesday.html (Accessed February 26, 2015).
Cai, W., and P. van Rensch, 2012: The 2011 southeast Queensland extreme summer rainfall: A confirmation of a negative Pacific Decadal Oscillation phase? *Geophys. Res. Lett.*, **39**, L08702, doi:10.1029/2011GL050820.
Cao, G., T. W. Giambelluca, D. E. Stevens, and T. A. Schroeder, 2007: Inversion Variability in the Hawaiian Trade Wind Regime. *J. Clim.*, **20**, 1145–1160, doi:10.1175/JCLI4033.1.
Chambers, L. E., 2001: Classifying rainfall districts: A south western Australian study. *Aust. Meteorol. Mag.*, **50**, 91–103.
——, 2003: *South Australian rainfall variability and trends*. Australian Bureau of Meteorology Research Centre (BMRC) Report, Melbourne, 40 pp.
Chen, Y. R., and P.-S. Chu, 2014: Trends in precipitation extremes and return

levels in the Hawaiian Islands under a changing climate. *Int. J. Climatol.*, **29**, 3913–3925, doi:10.1002/joc.3950.
Chu, P.-S., 1995: Hawaii Rainfall Anomalies and El Niño. *J. Clim.*, **8**, 1697–1703, doi:http://dx.doi.org/10.1175/1520-0442(1995)008<1697:HRAAEN>2.0.CO;2.
——, and H. Chen, 2005: Interannual and Interdecadal Rainfall Variations in the Hawaiian Islands. *J. Clim.*, **18**, 4796–4813, doi:10.1175/JCLI3578.1.
——, Y. R. Chen, and T. A. Schroeder, 2010: Changes in Precipitation Extremes in the Hawaiian Islands in a Warming Climate. *J. Clim.*, **23**, 4881–4900, doi:10.1175/2010JCLI3484.1.
CSIRO, 2012: *Climate and water availability in south-eastern Australia: A synthesis of findings from Phase 2 of the South Eastern Australian Climate Initiative (SEACI).* 41 pp.
d'Aubert, A., and P. D. Nunn, 2012: *Furious Winds and Parched Islands: Tropical Cyclones (1558-1970) and Droughts (1722-1987) in the Pacific*. Xlibris Corporation, Australia, 360 pp.
Diaz, H. F., and T. W. Giambelluca, 2012: Changes in atmospheric circulation patterns associated with high and low rainfall regimes in the Hawaiian Islands region on multiple time scales. *Glob. Planet. Change*, **98–99**, 97–108, doi:http://dx.doi.org/10.1016/j.gloplacha.2012.08.011.
Diaz, H. F., P. S. Chu, and J. K. Eischeid, 2005: Rainfall changes in Hawaii during the last century. *16th Conference on Climate Variability and Change*, San Diego, CA.
Dracup, J. A., K. S. Lee, and E. G. Paulson, 1980: On the definition of droughts. *Water Resour. Res.*, **16**, 297–302, doi:10.1029/WR016i002p00297.
Drosdowsky, W., 1993: An analysis of Australian seasonal rainfall anomalies: 1950–1987. I: Spatial patterns. *Int. J. Climatol.*, **13**, 1–30, doi:10.1002/joc.3370130102.
Edwards, D. C., and T. B. McKee, 1997: *Characteristics of 20th century drought in the United States at multiple scales*. Climatological Report No.97-2, Colorado State University: Fort Collins,.
Folland, C. K., J. A. Renwick, M. J. Salinger, and A. B. Mullan, 2002: Relative influences of the Interdecadal Pacific Oscillation and ENSO on the South Pacific Convergence Zone. *Geophys. Res. Lett.*, **29**, 21–24, doi:10.1029/2001GL014201.
Frazier, A. G., H. F. Diaz, and T. W. Giambelluca, 2011: Rainfall in Hawai'i: Spatial and temporal changes since 1920 (Abstract #GC21B-0900). *Poster presented at the American Geophysical Union Fall Meeting, San Francisco, CA.*
Gallant, A. J. E., M. J. Reeder, J. S. Risbey, and K. J. Hennessy, 2013: The characteristics of seasonal-scale droughts in Australia, 1911–2009. *Int. J. Climatol.*, **33**, 1658–1672, doi:10.1002/joc.3540.
Garza, J. A., P.-S. Chu, C. W. Norton, and T. A. Schroeder, 2012: Changes of the prevailing trade winds over the islands of Hawaii and the North Pacific. *J. Geophys. Res. Atmos.*, **117**, D11109, doi:10.1029/2011JD016888.
Giambelluca, T. W., D. Nullet, M. A. Ridgley, P. R. Eyre, J. E. T. Moncur, and S. Price, 1991: *Drought in Hawai'i, Report R88*. Commission on Water Resources Management, State of Hawai'i, Honolulu., 232 pp.
Heim, R. R., 2002: A Review of Twentieth-Century Drought Indices Used in the United States. *Bull. Am. Meteorol. Soc.*, **83**, 1149–1165, doi:10.1175/1520-

0477(2002)083<1149:AROTDI>2.3.CO;2.
Henley, B., J. Gergis, D. Karoly, S. Power, J. Kennedy, and C. Folland, 2015: A Tripole Index for the Interdecadal Pacific Oscillation. *Clim. Dyn.*, 1–14, doi:10.1007/s00382-015-2525-1.
Hennessy, K., and Coauthors, 2008: *An assessment of the impact of climate change on the nature of frequency of exceptional climatic events. A consultancy report by CSIRO and the Australian Bureau of Meteorology for the Australian Bureau of Rural Sciences*. 33 pp. http://www.bom.gov.au/climate/droughtec/download.shtml.
IPCC, 2013: *Climate Change 2013: The Physical Science Basis. Contribution of Working Group I to the Fifth Assessment Report of the Intergovernmental Panel on Climate Change*. T.F. Stocker et al., Eds. Cambridge University Press, Cambridge, United Kingdom and New York, NY, USA, 1535 pp.
Jovanovic, B., K. Braganza, D. Collins, and D. Jones, 2012: Climate variations and change evident in high-quality climate data for Australia’s Antarctic and remote island weather stations. *Aust. Meteorol. Ocean. J.*, **62**, 247–261.
Keener, V. W., J. J. Maara, M. L. Finucane, D. Spooner, and M. H. Smith, 2012: *Climate Change and Pacific Islands: Indicators and Impacts. Report for the 2012 Pacific Islands Regional Climate Assessment*. Island Press, Washington D.C, 170 pp.
Keyantash, J., and J. A. Dracup, 2002: The Quantification of Drought: An Evaluation of Drought Indices. *Bull. Am. Meteorol. Soc.*, **83**, 1167–1180, doi:10.1175/1520-0477(2002)083<1191:TQODAE>2.3.CO;2.
Kruk, M. C., A. M. Lorrey, G. M. Griffiths, M. Lander, E. J. Gibney, H. J. Diamond, and J. J. Marra, 2015: On the state of the knowledge of rainfall extremes in the western and northern Pacific basin. *Int. J. Climatol.*, **35**, 321–336, doi:10.1002/joc.3990.
Kruskal, W. H., and W. A. Wallis, 1952: Use of Ranks in One-Criterion Variance Analysis. *J. Am. Stat. Assoc.*, **47**, 583–621, doi:10.1080/01621459.1952.10483441.
Kuleshov, Y., and Coauthors, 2014: Extreme weather and climate events and their impacts on island countries in the Western Pacific: Cyclones, Floods and Droughts. *Atmos. Clim. Sci.*, **4**, 803–818, doi:10.4236/acs/2014.45071.
Lander, M. A., 2004: *Rainfall climatology for Saipan: Distribution, return-periods, El Niño, tropical cyclones and long term variations*. Water and Environmental Research Institute of the Western Pacific, University of Guam, 54 pp. http://www.weriguam.org/docs/reports/103.pdf.
Lattin, J. M., J. D. Carroll, and P. E. Green, 2003: *Analyzing Multivariate Data*. Brooks/Cole Cengage Learning, Belmont, CA., 556 pp.
Lavery, B., G. Joung, and N. Nicholls, 1997: An extended high-quality historical rainfall dataset for Australia. *Aust. Meteorol. Mag.*, **46**, 27–38.
Li, J., S.-P. Xie, E. R. Cook, G. Huang, R. D’Arrigo, F. Liu, J. Ma, and X.-T. Zheng, 2011: Interdecadal modulation of El Nino amplitude during the past millennium. *Nat. Clim. Chang.*, **1**, 114–118.
Lloyd-Hughes, B., and M. A. Saunders, 2002: A drought climatology for Europe. *Int. J. Climatol.*, **22**, 1571–1592, doi:10.1002/joc.846.
Lo, F., M. C. Wheeler, H. Meinke, and A. Donald, 2007: Probabilistic Forecasts of the Onset of the North Australian Wet Season. *Mon. Weather Rev.*, **135**, 3506–3520, doi:10.1175/MWR3473.1.
Lough, J. M., 1991: Rainfall variations in Queensland, Australia: 1891–1986. *Int.*

*J. Climatol.*, **11**, 745–768, doi:10.1002/joc.3370110704.
——, G. A. Meehl, and M. J. Salinger, 2011: Observed and projected changes in surface climate of the tropical Pacific. *Vulnerability of the tropical Pacific fisheries and aquaculture to climate change*, J.D. Bell, J.E. Johnson, and A.J. Hobday, Eds., Secretariat of the Pacific Community, Noumea, New Caledonia.
Lu, J., G. A. Vecchi, and T. Reichler, 2007: Expansion of the Hadley cell under global warming. *Geophys. Res. Lett.*, **34**, doi:10.1029/2006GL028443.
——, C. Deser, and T. Reichler, 2009: Cause of the widening of the tropical belt since 1958. *Geophys. Res. Lett.*, **36**, doi:10.1029/2008GL036076.
Manhire, T., 2011: Tuvalu drought could be dry run for dealing with climate change. *Guard.*,. http://www.theguardian.com/world/2011/oct/17/tuvalu-drought-climate-change (Accessed February 23, 2015).
Mann, H. B., and D. R. Whitney, 1947: On a Test of Whether one of Two Random Variables is Stochastically Larger than the Other. *Ann. Math. Stat.*, **18**, 50–60, doi:10.1214/aoms/1177730491.
Mantua, N. J., S. R. Hare, Y. Zhang, J. M. Wallace, and R. C. Francis, 1997: A Pacific Interdecadal Climate Oscillation with Impacts on Salmon Production. *Bull. Am. Meteorol. Soc.*, **78**, 1069–1079, doi:10.1175/1520-0477(1997)078<1069:APICOW>2.0.CO;2.
McBride, J. L., and N. Nicholls, 1983: Seasonal Relationships between Australian Rainfall and the Southern Oscillation. *Mon. Weather Rev.*, **111**, 1998–2004, doi:10.1175/1520-0493(1983)111<1998:SRBARA>2.0.CO;2.
McGree, S., and Coauthors, 2014: An updated assessment of trends and variability in total and extreme rainfall in the western Pacific. *Int. J. Climatol.*, **34**, 2775–2791, doi:10.1002/joc.3874.
McKee, T. B., N. J. Doeskin, and J. Kleist, 1993: The relationship of drought frequency and duration to time scales. *8th Conf. on Applied Climatology*, Anaheim, Canada, 179–184.
McKee, T. B., N. J. Doesken, and J. Kleist, 1995: Drought monitoring with multiple time scales. *Proceedings of the Ninth Conference on Applied Climatology*, Boston, American Meteorological Society, 233–236.
McPhaden, M. J., S. E. Zebiak, and M. H. Glantz, 2006: ENSO as an Integrating Concept in Earth Science. *Science (80-. ).*, **314**, 1740–1745, doi:10.1126/science.1132588.
Min, S.-K., and S.-W. Son, 2013: Multimodel attribution of the Southern Hemisphere Hadley cell widening: Major role of ozone depletion. *J. Geophys. Res. Atmos.*, **118**, 3007–3015, doi:10.1002/jgrd.50232.
Morales, M. S., and Coauthors, 2011: Precipitation changes in the South American Altiplano since 1300 AD reconstructed by tree-rings. *Clim. Past*, **8**, 653–666, doi:10.5194/cp-8-653-2012.
Murphy, B. F., and J. Ribbe, 2004: Variability of southeastern Queensland rainfall and climate indices. *Int. J. Climatol.*, **24**, 703–721, doi:10.1002/joc.1018.
——, S. B. Power, and S. McGree, 2014: The Varied Impacts of El Niño–Southern Oscillation on Pacific Island Climates. *J. Clim.*, **27**, 4015–4036, doi:10.1175/JCLI-D-13-00130.1.
Nguyen, H., C. Lucas, A. Evans, B. Timbal, and L. Hanson, 2015: Expansion of the Southern Hemisphere Hadley Cell in Response to Greenhouse Gas Forcing. *J. Clim.*, **28**, 8067–8077, doi:10.1175/JCLI-D-15-0139.1.

Nicholls, N., 1984: A system for predicting the onset of the north Australian wet-season. *J. Climatol.*, **4**, 425–435, doi:10.1002/joc.3370040407.
Nunn, P. D., 2007: *Climate, Environment, and Society in the Pacific during the Last Millennium*. Elsevier Science, 316 pp.
Olukayode Oladipo, E., 1985: A comparative performance analysis of three meteorological drought indices. *J. Climatol.*, **5**, 655–664, doi:10.1002/joc.3370050607.
Power, S., F. Tseitkin, S. Torok, B. Lavery, R. Dahni, and B. McAvaney, 1998: Australian temperature, Australian rainfall and the Southern Oscillation, 1910-1992: coherent variability and recent changes. *Aust. Meteorol. Mag.*, **47**, 85–101.
Power, S., T. Casey, C. Folland, A. Colman, and V. Mehta, 1999: Inter-decadal modulation of the impact of ENSO on Australia. *Clim. Dyn.*, **15**, 319–324.
Ropelewski, C. F., and M. S. Halpert, 1989: Precipitation Patterns Associated with the High Index Phase of the Southern Oscillation. *J. Clim.*, **2**, 268–284, doi:10.1175/1520-0442(1989)002<0268:PPAWTH>2.0.CO;2.
Salinger, M. J., R. E. Basher, B. B. Fitzharris, J. E. Hay, P. D. Jones, J. P. Macveigh, and I. Schmidely-Leleu, 1995: Climate trends in the South-west Pacific. *Int. J. Climatol.*, **15**, 285–302, doi:10.1002/joc.3370150305.
——, J. A. Renwick, and A. B. Mullan, 2001: Interdecadal Pacific Oscillation and South Pacific climate. *Int. J. Climatol.*, **21**, 1705–1721, doi:10.1002/joc.691.
——, S. McGree, F. Beucher, S. B. Power, and F. Delage, 2014: A new index for variations in the position of the South Pacific convergence zone 1910/11–2011/2012. *Clim. Dyn.*, 1–12, doi:10.1007/s00382-013-2035-y.
Sawlani, G., 2015: PNG’s drought disaster impacting on Port Moresby's power supply. *Aust. Broadcast. Comm. Pacific Beat*,. http://www.abc.net.au/news/2015-09-08/pngs-drought-disaster-impacting-on-port-moresbys/6759266 (Accessed January 2, 2015).
Seidel, D. J., Q. Fu, W. J. Randel, and T. J. Reichler, 2008: Widening of the tropical belt in a changing climate. *Nat. Geosci*, **1**, 21–24. http://dx.doi.org/10.1038/ngeo.2007.38.
Singh, R. B. K., S. Hales, N. de Wet, R. Raj, M. Hearnden, and P. Weinstein, 2001: The Influence of Climate Variation and Change on Diarrheal Disease in the Pacific Islands. *Environ. Health Perspect.*, **109**, 155–159, doi:10.2307/3434769.
Spinoni, J., G. Naumann, H. Carrao, P. Barbosa, and J. Vogt, 2014: World drought frequency, duration, and severity for 1951–2010. *Int. J. Climatol.*, **34**, 2792–2804, doi:10.1002/joc.3875.
Tapper, N., and L. Hurry, 1993: *Australia’s Weather Patterns: An Introductory Guide*. Dellasta, 130 pp.
Timbal, B., and W. Drosdowsky, 2013: The relationship between the decline of Southeastern Australian rainfall and the strengthening of the subtropical ridge. *Int. J. Climatol.*, **33**, 1021–1034, doi:10.1002/joc.3492.
Torok, S. J., 1996: The development of a high quality historical temperature database for Australia. Unpublished Ph.D. Thesis, University of Melbourne, Australia, .
Trenberth, K. E., 1976: Spatial and temporal variations of the Southern Oscillation. *Q. J. R. Meteorol. Soc.*, **102**, 639–653, doi:10.1002/qj.49710243310.
Vance, T. R., J. L. Roberts, C. T. Plummer, a S. Kiem, and T. D. van Ommen,

2014: Interdecadal Pacific variability and eastern Australian mega-droughts over the last millennium. *Geophys. Res. Lett.*, 2014GL062447, doi:10.1002/2014GL062447.

Vincent, D. G., 1994: The South Pacific Convergence Zone (SPCZ): A Review. *Mon. Weather Rev.*, **122**, 1949–1970, doi:10.1175/1520-0493(1994)122<1949:TSPCZA>2.0.CO;2.

Vincent, E., M. Lengaigne, C. Menkes, N. Jourdain, P. Marchesiello, and G. Madec, 2009: Interannual variability of the South Pacific Convergence Zone and implications for tropical cyclone genesis. *Clim. Dyn.*, **36**, 1881–1896, doi:10.1007/s00382-009-0716-3.

Wilhite, D. A., and M. H. Glantz, 1985: Understanding: the Drought Phenomenon: The Role of Definitions. *Water Int.*, **10**, 111–120, doi:10.1080/02508068508686328.

Willmott, C.J., 1978. P-mode principal components analysis, grouping and precipitation regions in California. Arch. für Meteorol. Geophys. und Bioklimatologie, Ser. B 26, 277–295. https://doi.org/10.1007/BF02243232.

WMO, 2012: *Standardized Precipitation Index User Guide (M. Svoboda, M. Hayes and D. Wood) WMO-No.1090*. Geneva, 24 pp. http://www.wamis.org/agm/pubs/SPI/WMO_1090_EN.pdf.

World-Bank, 2000: *Cities, Seas, Storms. Managing Change in Pacific Island Economies. Summary Report*. The International Bank for Reconstruction and Development/The World Bank, Washington D.C., USA,.

Zhang, Y., J. M. Wallace, and D. S. Battisti, 1997: ENSO-like Interdecadal Variability: 1900–93. *J. Clim.*, **10**, 1004–1020, doi:10.1175/1520-0442(1997)010<1004:ELIV>2.0.CO;2.

# 3 Trends and Variability in Mean and Extreme Temperature and Precipitation in the Western Pacific Islands

Trends in mean and extreme annual and seasonal temperature and precipitation are calculated for 20 western Pacific Island countries and territories. The extremes indices are those of the World Meteorological Organization Expert Team on Sector-specific Climate Indices. A rise in mean temperature is found at most stations, in all seasons and in both halves of the study period. The temperature indices also showed strong warming. While changes in precipitation are less consistent and trends generally weak at most locations, declines in both total and extreme precipitation are found in Southwest French Polynesia and the Southern subtropics. The relationship between total and extreme precipitation and Pacific basin sea surface temperatures are investigated with a focus on the influence of the ENSO. A strong relationship between ENSO and total precipitation is confirmed and a similar relationship for the threshold extreme indices is established. The percentile-based and absolute extreme indices are influenced by ENSO to a lesser extent and in some cases the influence is marginal.

The contents of this chapter have been published in the following peer-reviewed journals. The first author has produced >95% of the work presented:

McGree, S., N. Herold, L. Alexander, S. Schreider, Y. Kuleshov, E. Ene, S. Finaulahi, K. Inape, B. Mackenzie, H. Malala, A. Ngari, B. Prakash, and L. Tahani, 2019: Recent Changes in Mean and Extreme Temperature and Precipitation in the Western Pacific Islands. *J. Climate*, **32**, 4919–4941, https://doi.org/10.1175/JCLI-D-18-0748.1

McGree, S., and Coauthors, 2014: An updated assessment of trends and variability in total and extreme rainfall in the western Pacific. *Int. J. Climatol.*, **34**, 2775–2791, https://doi.org/10.1002/joc.3874

## 3.1 Introduction

The character and severity of impacts from climate extremes depend not only on the extremes themselves but also on society's exposure and vulnerability (IPCC 2012). While Small Island Developing States vary in their geography, climate, culture and stage of economic development, they have many common characteristics which highlight their exposure and vulnerability, particularly as it relates to sustainable development and climatic change. These characteristics include: limited physical size, generally limited natural resources, high susceptibility to natural hazards, relatively thin water lenses, extreme openness of small economies, high sensitivity to external market shocks, and in some cases high population densities, high population growth rates, and frequently poorly developed infrastructure (IPCC 2001). Therefore, it is imperative that a sound understanding of past, recent and likely future changes in western Pacific climate is attained, so as to inform decision making, and to stand the best chance of sustaining life on these islands in the coming century and beyond.

Trends and variability in western Pacific observed total precipitation and mean temperature have been studied on several occasions in the past (e.g. Salinger et al. 1995; Folland et al. 2003; Salinger and Lefale 2005), Australian Bureau of Meteorology and CSIRO 2011; Lough et al. 2011; Jones et al. 2013). The first attempt at examining changes in precipitation and temperature extremes was through a series of five workshops, from 1998 to 2004, funded by the Asia-Pacific Network (APN) for Global Change Research (Manton et al. 2001; Page et al. 2004; Griffiths et al. 2003, 2005). The initial workshop led to a series of climate change workshops across the globe under the guidance of the former World Meteorological Organization (WMO) Commission for Climatology (CCl), World Climate Research Programme, and the WMO/Intergovernmental Oceanographic Commission Joint Technical Commission for Oceanography and Marine Meteorology Expert Team on Climate Change Detection and Indices (ETCCDI) (Peterson and Manton 2008; Zhang et al. 2011). The ETCCDI, which was formed in 1999, developed a set of core indices consisting of 27 descriptive indices aimed at detecting changes in ‘moderate extremes’. These internationally agreed standard definitions and procedures allow results to be compared consistently across different regions and countries (Peterson and Manton 2008; Zhang et al. 2011; Alexander 2016). In the western Pacific, the ETCCDI indices were used at a WMO World Climate Data and Monitoring Programme workshop in Hanoi, Vietnam in December 2007 (Caesar et al. 2011) and at an APN workshop in Seoul, South Korea in February 2008 (Choi et al. 2009). These workshops were largely focused on Asia-Australia, with minimal inclusion of the Pacific Islands (Fiji at the Hanoi workshop, and Australia and New Zealand subtropical Pacific Islands at the Seoul workshop). The most recent work on changes in Pacific Islands temperature and precipitation extremes (Australian Bureau of Meteorology and CSIRO 2014; Whan et al. 2014a) was conducted through the Australian Aid funded Pacific-Australia Climate Change Science and Adaptation Planning (PACCSAP) Program; it also used the ETCCDI methodology and recommended software. The Pacific Climate Change Data Portal www.bom.gov.au/climate/pccsp, which presents trends in the mean and extreme temperature and precipitation for the western Pacific Islands, is an outcome of the PACCSAP Program.

While some of the ETCCDI indices are potentially useful for sector applications (e.g., number of days with frost for agricultural applications, heatwaves for health applications), many of the others have no obvious sector-relevance. As a result, the WMO CCl set up the Expert Team on Sector-specific Climate Indices (ET-SCI, www.wmo.int/pages/prog/wcp/ccl/opace/ opace4/ET-SCI-4-1.php). In cooperation with sectoral experts in agricultural meteorology, water resources and health, the ET-SCI is working to identify and evaluate additional sector-specific indices, both single- and multi-variable types, to define both simple and complex climate risks of interest to user groups. Relying on the principles of ETCCDI, this work focuses on systematic and globally consistent approaches using high-quality data and appropriate statistical methods to help characterise the susceptibility of various sectors to climate variability and change in an authoritative manner (Alexander 2016). The first proof of concept ET-SCI workshop for six South American countries was held in Ecuador in June 2013.

As part of the Programme of Implementing the Global Framework on Climate Services on Regional and National Scales funded by Environment Canada, the ET-SCI organised a second workshop on Enhancing Climate Indices for Sector-Specific Applications in the Pacific Island Region, in Nadi, Fiji from 7 to11 December 2015. This research presents results from and further analyses associated with this workshop. Much like the earlier APN and PACCSAP Program workshops, the ET-SCI Pacific workshop's objectives were to build and develop capacity in the quality control and homogenisation of climate data, calculate core ET-SCI indices using standardised software (ClimPACT2), and conduct the first stage of analysis of sectoral data. The workshop brought together experts from national meteorological and hydrological services of American Samoa, Cook Islands, Federated States of Micronesia, Fiji, Papua New Guinea (PNG), Samoa, Solomon Islands, Tonga, Tuvalu and Vanuatu, along with national representatives from agriculture and food security, water and health. The WMO, University of New South Wales (Sydney, Australia), Australian Bureau of Meteorology, New Zealand Institute for Water and Atmosphere, Pacific Regional Environmental Programme (SPREP) and Caribbean Institute for Meteorology and Hydrology were also represented.

Regional scale studies on trends in total and extreme precipitation for the western Pacific Islands (e.g., Manton et al. 2001; Salinger et al. 2001; Griffiths et al. 2003) were limited spatially and temporally. Recent work has largely been on national or subnational scales (e.g., Mataki et al. 2006; Cavarero et al. 2012; Jovanovic et al. 2012) or part of neighbouring regional analyses (e.g., Choi et al. 2009; Caesar et al. 2011), often with dissimilar methodology and study periods. The regional scale studies have focused mainly on the south Pacific where the effects of the South Pacific Convergence Zone (SPCZ; Figure 3.1) on mean precipitation regimes have been large in the past. Much of this variability is linked to the El Niño–Southern Oscillation (ENSO) or the Interdecadal Pacific Oscillation (IPO; Salinger et al. 2001) and is directly attributable to shifts in the SPCZ (Folland et al. 2002).

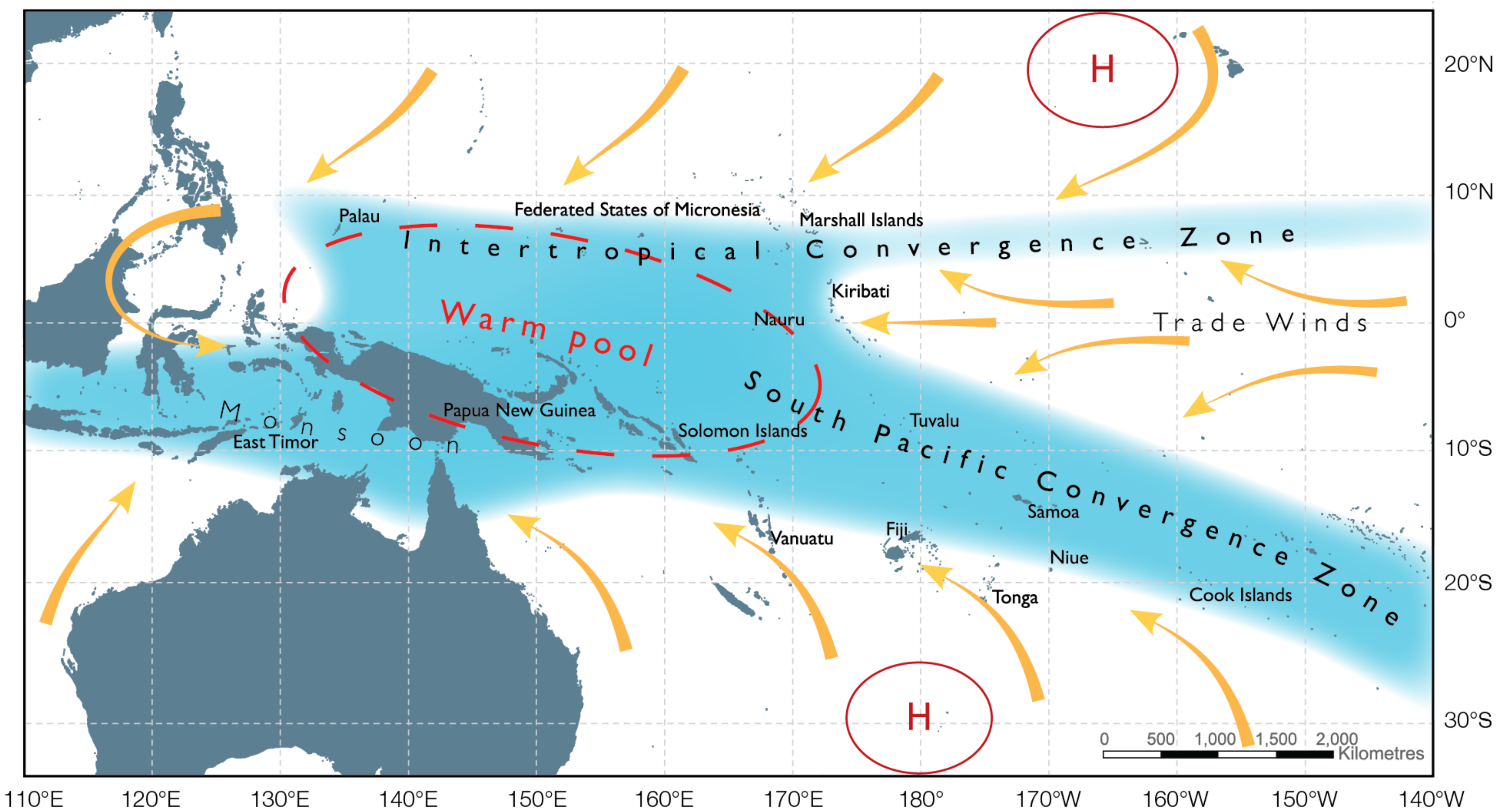


Figure 3.1 Schematic of circulation in the Pacific. From Australian Bureau of Meteorology, and CSIRO, 2011

The mean position of the SPCZ extends from the Solomon Islands to southern French Polynesia and is composed of two parts which include a ‘zonal’ portion, normally located over the western Pacific ‘warm pool’ and a ‘diagonal’ portion orientated northwest-southeast lying east of the Date Line (Vincent 1994). There is significant movement around the SPCZ mean position seasonally, annually and on longer timescales. Trenberth (1976) described the movement of the SPCZ as north and east during El Niño events and south and west during La Niña events.

The IPO is a natural Pacific-wide interdecadal signature with sea surface temperatures (SSTs) similar to those seen during ENSO events. When the IPO is in its positive (negative) phase, the mean SPCZ position is displaced north-east (southwest; Folland et al. 2002), consistent with the changes associated with ENSO. Folland et al. (2002) found that shifts in the position of the SPCZ were related to variability of ENSO on interannual timescales, and the IPO on decadal timescales. These shifts appeared to be of similar magnitude and were largely linearly independent. Therefore, the SPCZ is located furthest northeast during El Niño events with a positive IPO, and furthest southwest during La Niña events with a negative IPO. The position of the SPCZ varies most strongly in the diagonal section of the SPCZ, between about 180° and 130°W, with the zonal section of the SPCZ showing slightly less latitude change under the effects of ENSO and the IPO (Folland et al. 2002). Since the late 1990s, the IPO has switched to a negative phase, and the SPCZ is currently displaced southwest of its mean position on a decadal timescale (Australian Bureau of Meteorology and CSIRO 2011; Salinger et al. 2014).

Trends in precipitation have previously been examined for the period 1961–98 and 1961–2000 for a number of stations in the south Pacific (Manton et al. 2001; Griffiths et al. 2003). Total annual precipitation showed a general decrease at locations to the southwest of the SPCZ and a general increase to the northeast of the SPCZ with the largest trends east of 160°W. Significant increases in total precipitation occurred at Penrhyn (Northern Cook Islands, about 500mm per decade) and at Atuona (northern French Polynesia, about 250mm per decade). Small but not statistically significant decreases occurred at Aitutaki (Southern Cook Islands), Rapa (southern French Polynesia), Apia (Samoa), Nuku‘alofa (Tonga) and Raoul Island (New Zealand), but there was a statistically significant decline of 180mm per decade at Pitcairn Island. West of the Date Line, trends were small and there were no obvious spatial patterns within the island groups of Tonga, Fiji, New Caledonia and Tuvalu. Here trends were incoherent and non-significant (Griffiths et al. 2003). The trends at this point in time were associated with northeast movement of the diagonal SPCZ since the late 1970s through to the 1990s, associated with a shift to a positive IPO phase (Folland et al. 2002; Salinger et al. 2014; Henley et al. 2015).

For the subtropical south Pacific, Jovanovic et al. (2012) found non-significant negative trends in total precipitation at Norfolk Island (since 1915) and Lord Howe Island (since 1950) with stronger negative trends over the more recent 1970–2009 period. Little change was observed at Willis Island, in the Coral Sea, over 1924–2009.

Past changes in extreme precipitation in the Pacific have been analysed by frequency of extremes, intensity, proportion of total precipitation and dry spell length indices. Trends in the number of rain days were generally similar to those of total precipitation, with more (less) days typically associated with more (less) total precipitation (Manton et al. 2001; Griffiths et al. 2003) and thus consistent with the diagonal SPCZ displacement (Folland et al. 2002). These studies have also found a strong relationship between ENSO and total precipitation and between ENSO and the threshold ETCCDI indices. Generally, in the western Pacific tropics, wetter years receive rain on more days, with higher extreme precipitation intensities, and more frequent extreme events. More extreme total precipitation is also significantly correlated to more extreme extended-duration precipitation events (Griffiths et al. 2003).

There is little information available on the general climate and trends in total and extreme precipitation for PNG, Nauru and the Pacific Islands north of the equator. In addition to ENSO, the major climate features that influence precipitation in these regions are the West Pacific Monsoon (WPM) and the Intertropical Convergence Zone (ITCZ; Figure 3.1). The WPM is the southern extension of the larger Asian-Australian Monsoon system that moves seasonally from the northern hemisphere into the tropical regions of the southern hemisphere during December to February (Australian Bureau of Meteorology and CSIRO 2011). The WPM can be characterised as the seasonal reversal of prevailing winds (Kim et al. 2008) that brings heavy precipitation to the region north of Australia, extending from East Timor to the Solomon Islands. Much of the precipitation variability in this region can be attributed to variations in the timing, position, intensity, longevity and extent of the monsoon. Year-to-year variability is somewhat associated with ENSO (with the most extreme eastward extents occurring during the 1982–83 and 1997–98 El Niño events) and the extent of the monsoon-affected region is substantial, especially on the eastern edge, where it varies by more than 5000km between maximum and minimum extent. The north-south variability of the western wind domain is much less pronounced (Australian Bureau of Meteorology and CSIRO 2011).

The ITCZ is located close to the equator and extends longitudinally across the tropical north Pacific for much of the year (Barry and Chorely 1992). The ITCZ is one of the major features determining the climate of the tropical north Pacific, marked by the presence of a surface pressure trough, and formed by the convergence of moisture and heat-laden Northern and southern hemisphere trade winds. The upward branch of the Hadley Circulation cell in the Pacific sits over the ITCZ (Australian Bureau of Meteorology and CSIRO 2011). In the central and eastern Pacific, the ITCZ is narrow, whereas in the west the ITCZ becomes broad, due to strong monsoon flows, and the breadth of the ‘warm pool’ to the north and south. The position of the ITCZ in the central and eastern Pacific varies seasonally by approximately 5°. The ITCZ is closest to the equator from March to May, and furthest north from September to November, when it becomes broader, expanding both to the north and south (Waliser and Gautier 1993). Precipitation totals in the ITCZ region peak in September to November at values around 50% higher than those of the (late) southern summer, January to March (Australian Bureau of Meteorology and CSIRO 2011).

Previous studies have found mean air temperature trends were spatially homogenous across the region with mean warming of 0.18°C per decade over 1961–2011 (Whan et al. 2014a). This trend is consistent with the 0.16°C per decade from Jones et al. (2013), albeit for a slightly different set of stations for 1961–2010. Spatially coherent warming trends in the maximum and minimum air temperature extremes were also found over 1951–2011 on a regional and subregional level (Whan et al. 2014a). Where comparison is possible these works were largely consistent with results from earlier studies (Manton et al. 2001; Griffiths et al. 2005).

Larger warming trends were generally found in the hottest day and hottest night of the year compared with the coolest day and coolest night of the year. Warming trends were also found for all the percentile indices, although there were fewer differences between the number of days and nights per year where maximum or minimum exceeded percentile thresholds (Whan et al. 2014a).

Statistically significant relationships between ENSO and indices of extreme temperature have been found in the east Asia–west Pacific region (Nicholls et al. 2005; Whan et al. 2014a). Nicholls et al. (2005) found an increase in the number of warm nights and hot days during an El Niño event, with the number of cool days and nights tending to decrease. The Whan et al. (2014a) study also highlighted the role of decadal variability in the trends of the percentile indices: steady increases in the value of extreme temperatures are combined with considerable variability in the number of days per year that exceed extreme temperature thresholds. This showed the complex nature of temperature extremes in a region with low temperature variability.

None of these studies, however, present results that are explicitly sector-relevant. They examined trends on a subregional scale from 1951 and did not examine trends on a seasonal scale. The objectives of this study, therefore, are to examine trends in the mean and extremes for the ET-SCI sector-relevant indices from 1951–2015, using quality-controlled and homogenised daily temperature and precipitation data from the western Pacific.

The study region covers the Pacific from about 134°E to 135°W and 15°N to 32°S, excluding Indonesia and the Australian mainland. The paper is organised as follows: Section 2 provides a description of the data used and outlines the research methods; Section 3 examines the linear trends in the indices and relationship with ENSO; the discussion of the results and conclusions are presented in Section 4.

## 3.2 Data and Methodology

### 3.2.1 Data

Station data were collated from multiple sources. Data from 1951 to about 2013 were obtained from the Pacific Climate Change Data Portal (www.bom.gov.au/climate/pccsp) which has previously been used by Jones et al. (2013); Whan et al. (2014b). Prior to the ET-SCI workshop, participants representing 10 countries, were asked to update their data to 2015. Data for 11 additional countries and territories (French Polynesia, Guam, Kiribati, Marshall Islands, Nauru, New Caledonia, Niue, Northern Mariana Islands, Palau, Pitcairn Islands and Wallis & Futuna) not represented at the workshop were obtained from the respective national agencies following the workshop. Only station records from 1951–2015 that were at least 80% complete were retained to ensure a robust analysis of Pacific trends was undertaken. All the data obtained was archived in the Pacific Climate Change Data Portal.

To determine if there is a relationship between IPO and mean and extreme temperature and precipitation the Tripole Index (TPI, NOAA ERSST V5, unfiltered) (Henley et al. 2015) for the period 1951–2015 was obtained from www.esrl.noaa.gov/psd/data/timeseries/IPOTPI.

### 3.2.2 Data quality and homogeneity

Before undertaking any analyses of extremes, whether it is at a regional or global level, it is important to ensure that the input data are of high quality and free from artificial inconsistencies (Alexander 2016).

Basic quality control of all the data was undertaken at the data source. Further quality control was performed at and following the Nadi workshop using the freely available RClimDex v1.1 software package (Zhang and Yang 2004), and the ‘extraQC’ version of RClimDex (Aguilar and Prohom 2011). The latter performs an additional series of tests to further ensure internal consistency (e.g., identifies consecutive identical values and rounded values) and temporal coherency (locates large inter-daily differences), in addition to the usual gross-error and tolerance tests.

Errors in station records such as negative daily precipitation values and daily minimum temperature values greater than daily maximum temperature were identified using RClimDex. Outliers in precipitation, maximum and minimum temperature based on user-defined thresholds were also identified. A daily precipitation upper threshold of 200mm was defined, however, as tropical disturbances are common in the tropical Pacific and not all of these events documented, it is near impossible to identify suspicious values during the tropical cyclone/typhoon season. Confirmation that precipitation events ≥ 200mm were related to real meteorological events, rather than being erroneous, was undertaken where possible.

For maximum and minimum temperature, a threshold of five standard deviations was defined. On occasion, it was apparent the maximum temperature value was the correct minimum temperature value or vice versa; a data-entry error had occurred, e.g., swapping the two digits before the decimal point, or the decimal point was misplaced or not added (also applied to precipitation). In such cases, the erroneous value was replaced with a realistic value and where possible confirmation with the original observation field book was undertaken. Outliers identified as very likely erroneous were removed. Overall, less than 1% of the daily temperature and daily precipitation records were corrected for errors and outliers.

To reliably determine long-term change in climate it is important to have data whose changes reflect changes in the climate and not changes due to circumstances under which the observations were taken. There are numerous factors that can affect observation records. Among the most common are changes in instrumentation, changes in the surrounding environment, site relocations, and changes in observing practices (Trewin 2010; Vincent et al. 2012). To homogenise a station record, detailed metadata of the station in question is required, ideally along with the complete records of the station and its closest neighbours. Homogenisation of Pacific Islands meteorological data is difficult as most stations are isolated and often belong to different climate regimes from their neighbours. In addition, metadata are often sparse or non-existent (Jones et al. 2013).

While removing inhomogeneous stations has generally been the approach taken by the ETCCDI at most of their regional workshops (Peterson and Manton 2008), this practice would severely restrict the number of western Pacific temperature records available for analyses. Clearly data homogenisation is acceptable, as many regions, e.g., the Caribbean (Stephenson et al. 2014), and countries, e.g., Australia (Trewin 2013), have adjusted daily and/or monthly timeseries in their high-quality datasets.

Each series was assessed for potential inhomogeneities using subjective and objective tests. This involved a combination of visual examinations, neighbour comparisons and the application of the RHtestsV4 software package (Wang and Feng 2013). Step changes were identified using monthly timeseries (precipitation was log-transformed), so as to avoid the challenge of additional noise present in the daily series. In addition, data was at times more complete at the monthly than at daily timescales. Using the changepoints detected in the monthly timeseries the daily timeseries were adjusted as required.

Step changes were detected using multiple tests to increase confidence in the adjustments. The first test involved using the RHtestsV4 penalized maximal *F*-test (Wang 2008a,b) to locate step changes in the record that were significant at the 99% confidence level. The second test involved using the RHtestsV4 penalized maximal *t*-test (Wang et al. 2007; Wang 2008a) where the closest neighbouring homogenous station was used as a reference series, where available, to identify step changes in the base series. The third test was based upon the strong relationship between island coastal temperatures and local SSTs (Kenyon and Hegerl 2008; Alexander et al. 2009; Jones et al. 2013; Whan et al. 2014a). SSTs (1951–2015) from the HadISST1 1º reconstruction dataset (Rayner et al. 2003) were used to create a local time series (10º × 10º area-averaged SST series centred over each station) which was tested, and if found homogeneous, used as a reference series. For the fourth test, step changes (99% confidence level) in the diurnal temperature range were assessed, as changes in measurement practice can preferentially alter either maximum or minimum temperature (Zhou and Ren 2011; Jones et al. 2013).

Even with the log-transformation of precipitation, detection of precipitation inhomogeneities using the penalized maximal *F*-test was difficult due to high variability in the data series and large distances between neighbouring stations. In most cases where an inhomogeneity was detected, the discontinuity was not consistent between tests; therefore no action was taken. In most cases only the maximal *F*-test was applied to the precipitation records as almost all the precipitation stations were too isolated to apply the penalized maximal *t*-test and tests three and four only apply to temperature. Precipitation records were excluded from further analyses where consistent inhomogeneities were found. Excluded records include Nanumea and Niulakita from Tuvalu, La Tontouta from New Caledonia and Pitcairn Island.

Temperature timeseries were adjusted where metadata or most of the detection tests provided good reason for the modification. Greatest confidence was gained from metadata. However, we note that metadata is most likely incomplete or lacking detail as record keeping tends to focus on the observation enclosure, at times omitting changes in the surrounding environment. Detected discontinuities were often inconsistent between each of the inhomogeneity tests. Without metadata support, temperature records were only adjusted if at least three of the four tests identified a discontinuity at a particular point in time. For stations with little metadata there is a greater reliance on the statistical tests.

While reference series were used to detect discontinuities, the quantile-matching ‘without a reference series’ method in RHtestsV4 was used to adjust (only for discontinuities identified by three of the four tests) both the daily and monthly temperature timeseries (Appendix A). The sparse data network inhibited the use of reference series in most cases when it came to adjustments. As for Whan et al. (2014a), SSTs have not been used as reference series so as not to bias the air temperature records with long-term change at the sea surface. It is possible air temperature is changing more or less than the ocean.

Fifty-five monthly precipitation, 31 monthly temperature, 52 daily precipitation and 29 daily temperature stations were available for analysis with >80% of data available over the 1951–2015 period (Table 3.1; Figure 3.2).

Table 3.1 List of stations, their location and period of record

| Country | Station | Longitude | Latitude | Period daily precipitation (period of monthly record if different)* | Period daily temperature (period of monthly record if different)* |
|---|---|---|---|---|---|
| **American Samoa** | Pagopago | 170.71°E | 14.33°S | 1956–2015 | 1957–2015 |
| **Australia** | Willis Island | 149.98°E | 16.30°S | 1951–2015 | 1951–2015 |
| | Norfolk Island Aero | 167.94°E | 29.04°S | 1951–2015 | 1951–2015 |
| | Lord Howe Island Aero | 159.08°E | 31.54°S | 1951–2015 | 1951–2015 |
| **Cook Islands** | Penrhyn | 158.05°W | 9.03°S | 1951–2015 | – |
| | Rarotonga | 159.80°W | 21.20°S | 1951–2015 | 1951–2015 |
| **Federated States of Micronesia** | Pohnpei | 158.22°E | 6.97°N | 1951–2015 | 1951–2015 |
| | Yap | 138.08°E | 9.48°N | 1951–2015 | (1951–2015) |
| | Chuuk | 151.83°E | 7.45°N | 1951–2015 | 1951–2015 |
| **Fiji** | Rotuma | 177.05°E | 12.50°S | 1951–2015 | – |
| | Penang Mill | 178.17°E | 17.37°S | 1951–2015 | – |
| | Lautoka Mill | 177.45°E | 17.60°S | 1951–2015 | 1951–2015 |
| | Nadi Airport | 177.45°E | 17.77°S | 1951–2015 | 1951–2015 |
| | Nausori Airport | 178.57°E | 18.05°S | 1956–2015 | 1957–2015 |
| | Laucala Bay, Suva | 178.45°E | 18.15°S | 1951–2015 | 1951–2015 |
| | Nabouwalu | 178.70°E | 17.00°S | 1951–2015 | 1952–2015 |
| | Lakeba | 178.80°W | 18.23°S | 1951–2015 | – |
| **French Polynesia** | Atuona (Hiva Oa, Marquesas Islands) | 139.03°W | 9.82°S | 1951–2015 | – |
| | Takaroa (Tuamotu Group) | 145.03°W | 14.48°S | 1951–2015 | 1951–2015 |

| Country | Station | Longitude | Latitude | Period daily precipitation (period of monthly record if different)* | Period daily temperature (period of monthly record if different)* |
|---|---|---|---|---|---|
| | Tahiti-Faaa (Society Islands) | 149.61°W | 17.55°S | 1957–2015 (1951–1956) | 1957–2015 |
| | Mataura (Tubuai, Austral Islands) | 149.48°W | 23.35°S | 1951–2015 | – |
| | Rapa (Austral Islands) | 144.33°W | 27.62°S | 1951–2015 | 1951–2015 |
| **Guam** | Agana (Guam Int. Airport) | 144.80°E | 13.48°N | 1957–2015 | – |
| **Kiribati** | Butaritari | 172.78°E | 3.03°N | (1951–2015) | – |
| | Kiritimati | 157.48°W | 1.98°N | 1951–2015 | – |
| | Tarawa | 172.92°E | 1.35°N | 1951–2015 | 1951–2015 |
| **Marshall Islands** | Kwajalein/Bucholz Aaf | 167.73°E | 8.73°N | 1951–2015 | 1951–2015 |
| | Majuro | 171.38°E | 7.08°N | 1951–2015 | 1951–2015 |
| **Nauru** | Nauru Arc-2 | 166.92°E | 0.52°N | (1951–2015) | – |
| **New Caledonia** | Koumac | 164.28°E | 20.56°S | 1951–2015 | 1951–2015 |
| | Touho Gend | 165.23°E | 20.78°S | 1952–2015 | – |
| | La Foa | 165.81°E | 21.70°S | 1951–2015 | 1952–2015 |
| | Kone | 164.83°E | 21.05°S | 1951–2015 | – |
| | Ponerihouen | 165.40°E | 21.08°S | 1952–2015 | – |
| | Houailou P | 165.63°E | 21.28°S | 1952–2015 | – |
| | Noumea | 166.45°E | 22.28°S | 1951–2015 | 1951–2015 |
| **New Zealand** | Raoul Island | 177.92°W | 29.25°S | 1951–2015 | 1951–2015 |
| **Niue** | Hanan Airport | 169.93°W | 19.08°S | 1951–2015 | 1951–2015 |
| **Northern Mariana Islands** | Saipan International Airport | 145.73°E | 15.12°N | 1954–2015 | – |
| **Palau** | Koror | 134.48°E | 7.33°N | 1951–2015 | 1951–2015 |

| Country | Station | Longitude | Latitude | Period daily precipitation (period of monthly record if different)* | Period daily temperature (period of monthly record if different)* |
|---|---|---|---|---|---|
| **Papua New Guinea** | Momote | 147.42°E | 2.05°S | 1951–2015 | – |
| | Kavieng | 150.82°E | 2.57°S | 1951–2014 | – |
| | Wewak | 143.67°E | 3.58°S | 1951–2015 | – |
| | Madang | 145.80°E | 5.22°S | 1951–2015 | – |
| | Port Moresby | 147.22°E | 9.38°S | 1951–2015 | 1951–2015 |
| | Misima | 152.83°E | 10.68°S | 1951–2015 | – |
| **Solomon Islands** | Honiara | 159.97°E | 9.42°S | 1951–2015 | – |
| | Honiara_Henderson | 160.05°E | 9.42°S | – | 1951–2015 |
| **Tonga** | Keppel | 173.77°W | 15.95°S | 1951–2015 | – |
| | Lupepau‘u (Vava‘u) | 173.97°W | 18.58°S | 1951–2015 | 1956–2015 |
| | Haapai | 174.35°W | 19.80°S | 1951–2015 | – |
| | Nuku‘alofa | 175.18°W | 21.13°S | (1951–2015) | (1951–2015) |
| **Tuvalu** | Funafuti | 179.22°E | 8.50°S | 1951–2015 | 1951–2015 |
| **Vanuatu** | Sola | 167.55°E | 13.85°S | 1951–2015 | – |
| | Port Vila_Bauerfield | 168.30°E | 17.70°S | – | 1951–2015 |
| | Port Vila | 168.32°E | 17.74°S | 1951–2015 | – |
| | Aneityum | 169.77°E | 20.23°S | 1951–2015 | – |

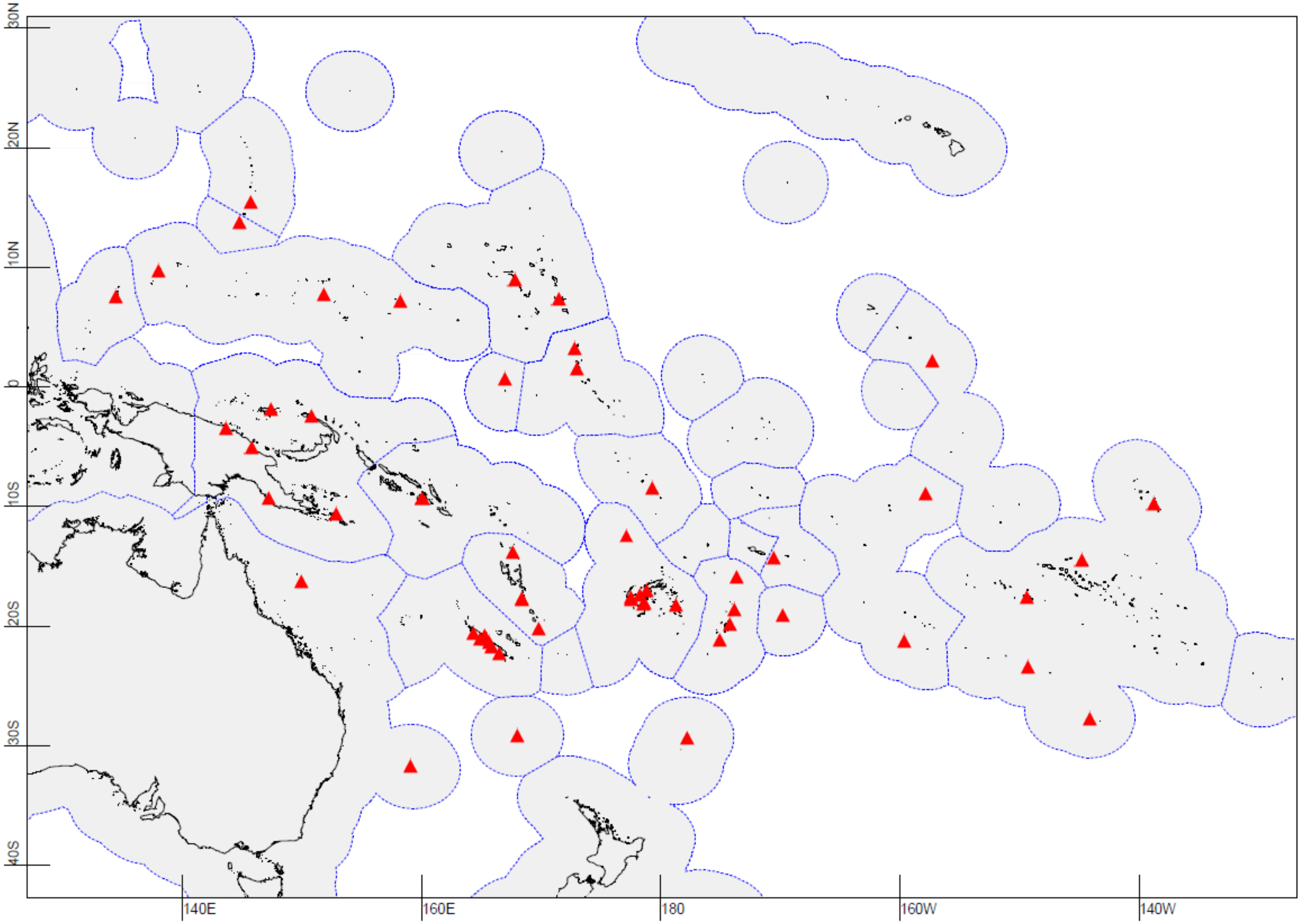


Figure 3.2 Locations of the 57 stations. Station names and locations are presented in Table 3.1

While it is possible that several inhomogeneities have escaped detection, these data are believed to be largely homogeneous.

### 3.2.3 Calculation of ET-SCI indices

The ET-SCI indices were then calculated by applying ClimPACTv2 to the homogenised series (Alexander and Herold 2015). ClimPACTv2 facilitates the calculation of over 60 ET-SCI sector-specific (including the ETCCDI) indices. The 'core set' is made up of 34 indices (including four user-defined indices), while the remaining 30 are defined as 'additional indices'. These include five heatwave indices, three additional extreme temperature indices and 14 ETCCDI indices. The full list of ET-SCI indices is presented in Table 3.2.

There are several user-defined indices: for WSDId and CSDId, three days has been selected; for Rnnmm, 1mm has been selected; and for RXdday 2 days was used.

The annual and seasonal trends in total precipitation, mean, maximum and minimum temperature were calculated from monthly values rather than the corresponding indices, as there are fewer gaps in the monthly records.

Monthly indices were calculated if no more than three days were missing in a month, while annual values were calculated if no more than 15 days were missing in a year. In the case of monthly totals and averages only, annual values were not calculated if one or more months of data were missing. For threshold indices, a threshold was calculated if at least 75% of the data was present. It is essential the amount of missing data be minimised as data gaps increase the uncertainty of the trend calculated upon the timeseries. For spell duration indicators, a spell can continue into the next year and was counted against the year in which the spell ended. Percentiles were calculated if no more than 20% of the values were missing over 1971–2000.

Table 3.2 Core and additional ET-SCI indices. Index codes in bold refer to those that are solely ET-SCI indices (not also ETCCDI indices). TM = mean temperature, TN = minimum temperature, TX = maximum temperature, PR = precipitation. Indices in italics have not been used in this study

| Index codes | Indicator name | Definition | Units |
|---|---|---|---|
| **Core indices** | | | |
| *FD* | *Frost days* | *Number of days when TN < 0ºC. Not used in this study* | *days* |
| ***TNlt2*** | *TN below 2ºC* | *Number of days when TN < 2ºC. Not used in this study* | *days* |
| ***TNltm2*** | *TN below -2ºC* | *Number of days when TN < -2ºC. Not used in this study* | *days* |
| ***TNltm20*** | *TN below -20ºC* | *Number of days when TN < -20ºC. Not used in this study* | *days* |
| *ID* | *Ice days* | *Number of days when TX < 0ºC. Not used in this study* | *days* |
| SU | Summer days | No. of days when TX > 25ºC | days |
| TR | Tropical nights | No. of days when TN > 20ºC | days |
| *GSL* | *Growing season length* | *Annual number of days between the first occurrence of six consecutive days with TM > 5ºC and the first occurrence of six consecutive days with TM < 5ºC. Not used in this study* | *days* |
| TXx | Max TX | Warmest daily TX | ºC |
| TNn | Min TN | Coldest daily TN | ºC |
| *WSDI* | *Warm spell duration indicator* | *Annual number of days contributing to events where 6 or more consecutive days* | *days* |

| | | | |
|---|---|---|---|
| | | *experience TX > 90th percentile* | |
| **WSDId** | User-defined WSDI | Annual number of days contributing to events where *d* or more consecutive days experience TX > 90th percentile. We used d = 3 | days |
| *CSDI* | *Cold spell duration indicator* | *Annual number of days contributing to events where 6 or more consecutive days experience TN < 10th percentile* | *days* |
| **CSDId** | User-defined CSDI | Annual number of days contributing to events where *d* or more consecutive days experience TN < 10th percentile. We used d = 3 | days |
| **TXgt50p** | Fraction of days with above average temperature | Percentage of days where TX > 50th percentile | % |
| **TX95t** | Very warm day threshold | Value of 95th percentile of TX | °C |
| ***TMge5*** | *TM of at least 5ºC* | *Number of days when TM ≥ 5ºC. Not used in this study* | *days* |
| ***TMlt5*** | *TM below 5ºC* | *Number of days when TM < 5ºC. Not used in this study* | *days* |
| ***TMge10*** | *TM of at least 10ºC* | *Number of days when TM ≥ 10ºC. Not used in this study* | *days* |
| ***TMlt10*** | *TM below 10ºC* | *Number of days when TM < 10ºC. Not used in this study* | *days* |
| **TXge30** | TX of at least 30ºC | Number of days when TX ≥ 30ºC | days |

| | | | |
|---|---|---|---|
| ***TXge35*** | *TX of at least 35ºC* | *Number of days when TX ≥ 35ºC. Not used in this study* | *days* |
| ***TXdTNd*** | *User-defined consecutive number of hot days and nights* | *Annual count of d consecutive days when both TX > 95th percentile and TN > 95th percentile, where 10 ≥ d ≥ 2. Not used in this study* | *events* |
| ***HDDheatn*** | *Heating degree days* | *Annual sum of n - TM (where n is a user-defined location-specific base temperature and TM < n). Not used in this study* | *degree-days* |
| **CDDcoldn** | Cooling degree days | Annual sum of TM - *n* (where *n* is a user-defined location-specific base temperature and TM > *n*). We used n = 18 | degree-days |
| ***GDDgrown*** | *Growing degree days* | *Annual sum of TM - n (where n is a user-defined location-specific base temperature and TM > n). Not used in this study* | *degree-days* |
| CDD | Consecutive dry days | Maximum number of consecutive dry days (when PR < 1.0mm) | days |
| R20mm | Number of very heavy rain days | Number of days when PR ≥ 20mm | days |
| R95pTOT | Contribution from very wet days | 100*R95p / PRCPTOT | % |
| R99pTOT | Contribution from extremely wet days | 100*R99p / PRCPTOT | % |
| **RXdday** | User-defined consecutive days PR amount | Maximum *d*-day PR total. We used d = 2 | mm |
| **SPI** | Standardised Precipitation Index (SPI) | Measure of 'drought' using the SPI on timescales of 3, 6 and 12 | unitless |

| | | | |
|---|---|---|---|
| | | months. See McKee et al. (1993); WMO (2012) for further details | |
| **SPEI** | Standardised Precipitation Evapotranspiration Index (SPEI) | Measure of ‘drought’ using the SPEI on timescales of 3, 6 and 12 months. See Vicente-Serrano et al. (2010) for further details | unitless |
| **Additional indices** | | | |
| ***TXbdTNbd*** | *User-defined consecutive number of cold days and nights* | *Annual number of d consecutive days when both TX < 5th percentile and TN < 5th percentile, where 10 ≥ d ≥ 2. Not used in this study* | *events* |
| DTR | Daily Temperature Range | Mean difference between daily TX and daily TN | ºC |
| TNx | Max TN | Warmest daily TN | ºC |
| TXn | Min TX | Coldest daily TX | ºC |
| **TMm** | Mean TM | Mean daily mean temperature | ºC |
| **TXm** | Mean TX | Mean daily maximum temperature | ºC |
| **TNm** | Mean TN | Mean daily minimum temperature | ºC |
| TX10p | Amount of cool days | Percentage of time when TX < 10th percentile | % |
| TX90p | Amount of hot days | Percentage of time when TX > 90th percentile | % |
| TN10p | Amount of cold nights | Percentage of time when TN < 10th percentile | % |
| TN90p | Amount of warm nights | Percentage of time when TN > 90th percentile | % |

| | | | |
|---|---|---|---|
| CWD | Consecutive Wet Days | Maximum annual number of consecutive wet days (when PR ≥ 1.0mm) | days |
| R10mm | Number of heavy rain days | Number of days when PR ≥ 10mm | days |
| Rnnmm | Number of customised rain days | Number of days when PR ≥ *nn.* We used nn = 1mm | days |
| SDII | Simple daily PR intensity | Annual total PR divided by the number of wet days (when total PR ≥ 1.0mm) | mm per day |
| R95p | Total annual PR from heavy rain days | Annual sum of daily PR > 95th percentile | mm |
| R99p | Total annual PR from very heavy rain days | Annual sum of daily PR > 99th percentile | mm |
| Rx1day | Max 1-day PR | Maximum 1-day precipitation total | mm |
| Rx5day | Max 5-day PR | Maximum 5-day precipitation total | mm |
| ***HWN(EHF/Tx90/Tn90)*** | *Heatwave number (HWN) as defined by either the Excess Heat Factor (EHF), 90th percentile of TX or the 90th percentile of TN* | *The number of individual heatwaves that occur each summer (Nov–Mar in southern hemisphere and May to Sepember in northern hemisphere). A heatwave is defined as three or more days where either the EHF is positive, TX > 90th percentile of TX or where TN > 90th percentile of TN. Where percentiles are calculated from base period specified by user. See Perkins and* | *events* |

| | | | |
|---|---|---|---|
| | | *Alexander (2013) for more details on the HWN, HWF, HWD, HWM and HWA indices. Not used in this study* | |
| ***HWF(EHF/Tx90/Tn90)*** | *Heatwave frequency (HWF) as defined by either the Excess Heat Factor (EHF), 90th percentile of TX or the 90th percentile of TN* | *The number of days that contribute to heatwaves as identified by HWN. Not used in this study* | *days* |
| ***HWD(EHF/Tx90/Tn90)*** | *Heatwave duration (HWD) as defined by either the Excess Heat Factor (EHF), 90th percentile of TX or the 90th percentile of TN* | *The length of the longest heatwave identified by HWN. Not used in this study* | *days* |
| ***HWM(EHF/Tx90/Tn90)*** | *Heatwave magnitude (HWM) as defined by either the Excess Heat Factor (EHF), 90th percentile of TX or the 90th percentile of TN* | *The mean temperature of all heatwaves identified by HWN. Not used in this study* | *ºC (ºC$^2$ for EHF)* |
| ***HWA(EHF/Tx90/Tn90)*** | *Heatwave amplitude (HWA) as defined by either the Excess Heat Factor (EHF), 90th percentile of TX or the 90th percentile of TN* | *The peak daily value in the hottest heatwave (defined as the heatwave with highest HWM). Not used in this study* | *ºC (°C$^2$ for EHF)* |
| ***CWN_ECF*** | *Coldwave number (CWN) as defined by the Excess Cold Factor (ECF).* | *The number of individual ‘coldwaves’ that occur each year. See Nairn and Fawcett (2015) for more details on CWN, CWF, CWD, CWM and CWA. Not used in this study* | *events* |
| ***CWF_ECF*** | *Coldwave frequency (CWF) as defined by* | *The number of days that* | *days* |

| | | | |
|---|---|---|---|
| | *the Excess Cold Factor (ECF).* | *contribute to 'coldwaves' as identified by ECF_HWN. Not used in this study* | |
| ***CWD_ECF*** | *Coldwave duration (CWD) as defined by the Excess Cold Factor (ECF).* | *The length of the longest 'coldwave' identified by ECF_HWN. Not used in this study* | *days* |
| ***CWM_ECF*** | *Coldwave magnitude (CWM) as defined by the Excess Cold Factor (ECF).* | *The mean temperature of all 'coldwaves' identified by ECF_HWN. Not used in this study* | *ºC$^2$* |
| ***CWA_ECF*** | *Coldwave amplitude (CWA) as defined by the Excess Cold Factor (ECF).* | *The minimum daily value in the coldest 'coldwave' (defined as the coldwave with lowest ECF_HWM). Not used in this study* | *ºC$^2$* |

### 3.2.4 Trend calculations and regional series

Linear annual and seasonal trends were calculated using the non-parametric Kendall's tau based slope estimator (Sen 1968). This method has notable advantages over the more commonly used least squares estimate. It is non-parametric and is less affected by outliers, making it well-suited to meteorological and hydrological timeseries. The significance of the trend is determined using Kendall's test. This test does not assume an underlying probability distribution of the data series. Calculations were performed using an 'autotrend' R script developed by Environment Canada (Zhang et al. 2000). 'Autotrend' also accounts for autocorrelation also known as serial correlation. This is defined as the correlation of a variable with itself over successive time intervals. Autocorrelation increases the chances of finding significant trends even if they are absent and vice versa. Autocorrelation adjustments were incorporated in the Zhang et al. (2000) study and a number of ETCCDI associated publications (e.g. Zhang et al. 2005; Aguilar et al. 2009; Choi et al. 2009; Whan et al. 2014a).

Throughout this paper, we use the 5% level to define statistically significant trends. Only significant trends from this point forward are referred to as positive or negative.

As the stations are located over a large geographical area and unique relationships exist, especially for precipitation, with the major modes of variability including ENSO, precipitation analyses are conducted on a subregional basis (eight subregions) largely as defined by McGree et al. (2016). The exceptions are: Willis Island included in the Southwest SPCZ subregion and Rotuma included in the southeast SPCZ subregion. The Southwest SPCZ subregion was divided into three subcomponents, namely North Papua New Guinea (PNG), Southwest SPCZ and southern subtropics (Figure 3.3). The reclassification is based on an extension of the cluster analysis initially undertaken by McGree et al. (2016).

To account for the spatial distribution of the stations, anomalies were first calculated for each station (base period 1971–2000), and then averaged over the entire region for temperature and eight subregions for precipitation. Regional averages for individual years were calculated where less than 30% of

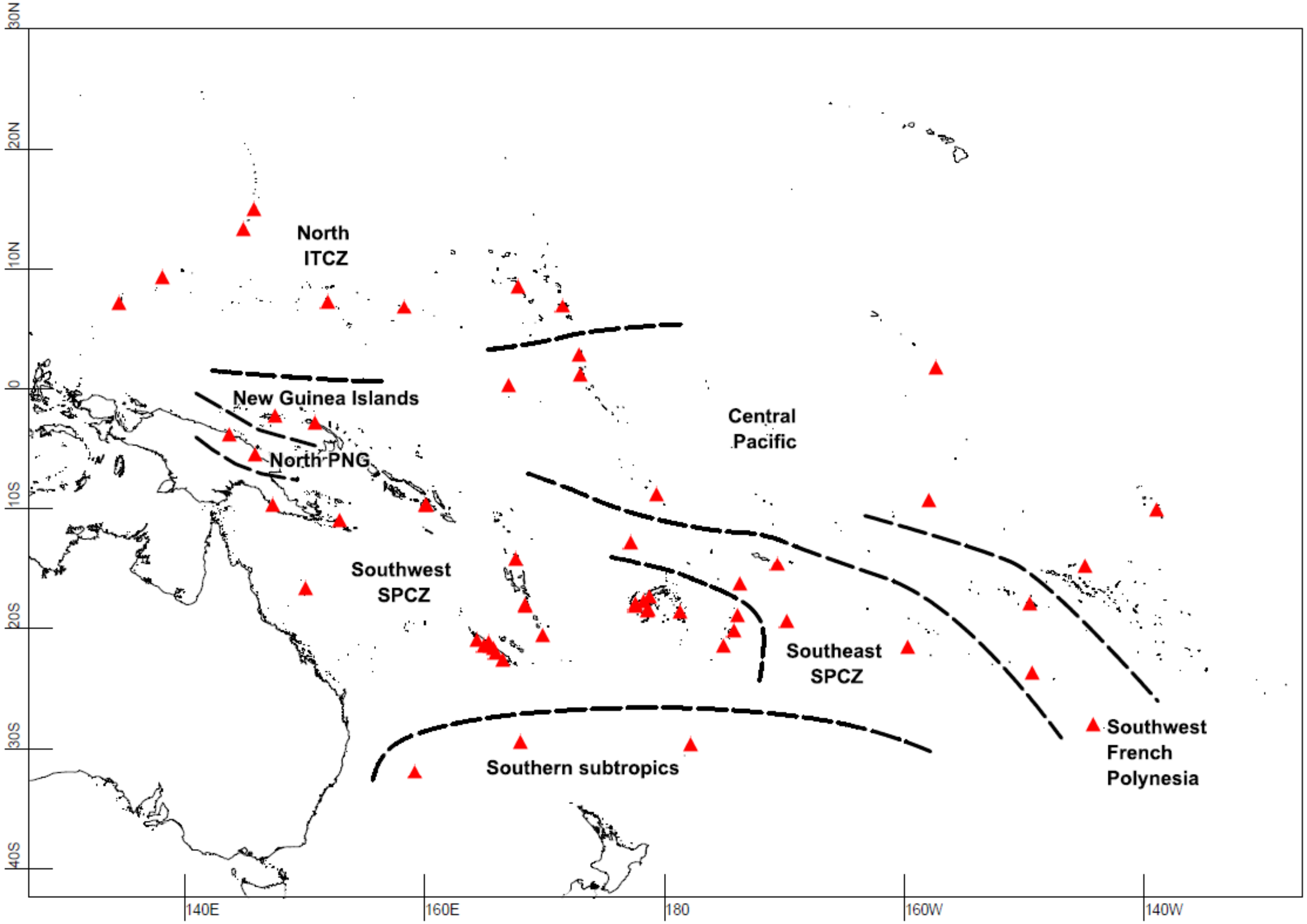


Figure 3.3 Western Pacific Islands coherent annual precipitation subregions as defined by cluster analysis

the stations making up the region or subregion were missing**.** While variance adjustment has been used in similar studies in the past, this method was found during the Whan et al. (2014a) analysis to remove interannual variability, which is undesirable. As most of the stations have a common start and end date and the timeseries are relatively complete, the use of the variance adjustment method is unnecessary.

To determine if the IPO influences trends in total and extreme temperature and precipitation, trends in the ET-SCI index with and without IPO present were compared. Trends with IPO removed that were within the 95% confidence interval of trends with IPO present were deemed not 'significantly' different. To calculate the trend in the ET-SCI index with IPO removed, the strength of the relationship between 13-year running mean TPI and the 13-year running mean ET-SCI index was calculated using the Kendall's tau correlation method. If significant at the 5% level, the trend in the residual of TPI and the ET-SCI index was calculated using previously described methods. Finally, based on the method of Guerreiro et al. (2018) we assess changes in the magnitude of daily precipitation between 1951–82 and 1983–2015 to determine if the most extreme precipitation events, especially those associated with typhoons/tropical cyclones have increased in recent decades. In this case, we are not interested in event attribution, only whether a statistically significant change has taken place.

Daily precipitation was ranked from highest to lowest for the complete record for each station. The largest value for the purposes of this exercise was labelled K1, the second largest value K2 and so on. K1–K20 values were assigned to Bin 1, K21–K40 to Bin 2 until seven bins were created. The median value was then calculated for each bin. The station difference value is the median for 1983–2015 minus the median for 1951–82 for the same bin. Each station therefore had station difference values for Bin 1 to Bin 7. As we were particularly interested in change associated with the highest 20 values we used the Mann–Whitney rank sum test (Mann and Whitney 1947) to determine if the station difference value for Bin 1 was statistically significant. The Mann–Whitney rank sum test is a non-parametric test that uses the ranks of the sample data, instead of their specific values, to detect statistical significance. The null hypothesis is: H0: $\eta 1 = \eta 2$, the median of the first population ($\eta 1$) equals the median of the second population ($\eta 2$).

Further, we calculated the regional change in magnitude for each bin by averaging (mean) the station differences across the 52 stations. The Mann–Whitney rank sum test was used again to determine if the difference in the regional medians for Bin 1 (1951–82) and Bin 1 (1983–2015) was statistically significant. This was repeated for Bins 2–7.

## 3.3 Results

### 3.3.1 Annual and seasonal changes in mean and extreme temperatures

#### 3.3.1.1 Mean temperature

Annual mean temperature (TM) increased at all, but two locations (Lautoka Mill and Raoul Island) in the western Pacific Islands (Figure 3.4). On a regional scale, annual TM warmed 0.14ºC per decade over 1951–2015 (Table 3.3, 0.91ºC over 65 years). Rates of warming were the same for December to February (DJF), March to May (MAM) and September to November (SON, 0.14ºC per decade). Warming also occurs in June to August (JJA) but at a slower rate (0.11ºC per decade). The TM trend over 1961–2011 (0.15ºC per decade) was also calculated and compared with that for Whan et al. (2014a, 0.18ºC per decade, 1961–2011) and Jones et al. (2013, 0.16ºC per decade, 1961–2010). The warmest five years (2010, 1998, 2007, 2013 and 2002 in descending order of TM) occurred in the last 18 of the 65-year study period (Figure 3.4).

Warming of annual TM occurred in both halves of the study period with warming over 1983–2015 (0.12ºC per decade) stronger than over 1951–82 (0.09ºC per decade). For DJF, JJA and SON warming was stronger in the first half of the study period while the opposite applies to MAM (not shown).

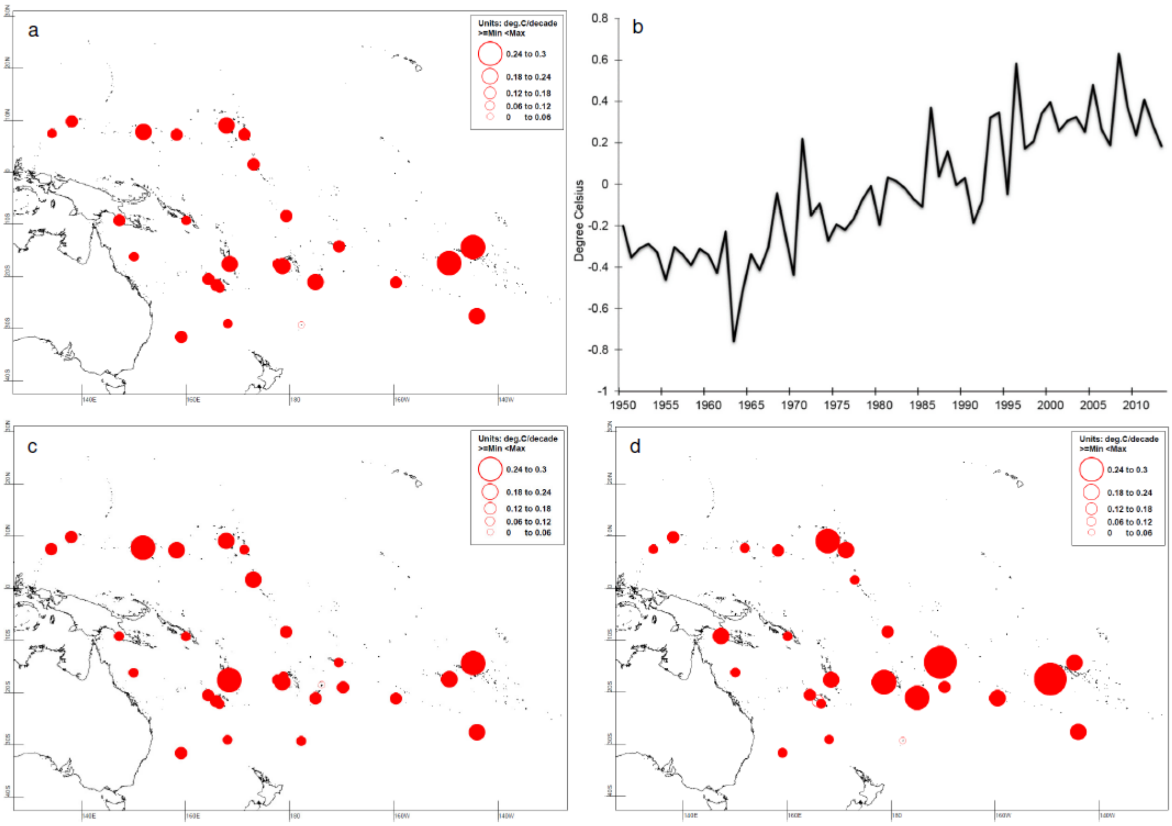


Figure 3.4 Trends in annual temperature over 1951–2015 for (a) mean temperature, (b) regional mean temperature anomalies relative to 1971–2000 climatology, (c) maximum temperature, and (d) minimum temperature. Solid circles represent trends significant at the 5% level. The size of the circle is proportional to the magnitude of the trend. Non-significant trends for Lautoka, Fiji (mean and minimum temperature) and La Foa (minimum temperature), New Caledonia are obscured by neighbouring significant trends.

The annual maximum temperature (TX) trend over 1951–2015 (0.12ºC per decade) was similar to the annual minimum temperature (TN) trend (0.13ºC per decade, Table 3.3). On a seasonal basis the strongest TX and TN warming took place in DJF with the weakest in JJA. The annual TX trend over 1983–2015 (0.12ºC per decade) was marginally stronger than that over 1951–82 (0.10ºC per decade). Trends for annual TN were also stronger over 1983–2015 (0.12ºC per decade) when compared with 1951–82 (0.08ºC per decade). Spatially there was little consistency in the annual TX and TN trends although, annual TN trends were markedly stronger east of the Date line (Figure 3.4). As the differences in the TX and TN trends are small, trends in annual and seasonal daily temperature range (DTR) were not statistically significant (Table 3.3).

Table 3.3 Regional trends in annual and seasonal mean and extreme temperature for the western Pacific for 1951–2015 (units per decade). The 95% confidence intervals are shown in brackets. Trends statistically significant at the 5% level are shown in italics. See Table 3.2 for index definitions

| | **TM (ºC)** | **TX (ºC)** | **TN (ºC)** | **TNn (ºC)** | **TNx (ºC)** | **TXn (ºC)** | **TXx (ºC)** | **DTR (ºC)** |
|---|---|---|---|---|---|---|---|---|
| **Annual** | *+0.14* (+0.12, +0.16) | *+0.12* (+0.04, +0.21) | *+0.13* (+0.03, +0.23) | *+0.12* (+0.04, +0.20) | *+0.15* (+0.12, +0.18) | *+0.09* (+0.04, +0.14) | *+0.15* (+0.10, +0.20) | -0.01 (-0.02, 0.00) |
| **DJF** | *+0.14* (+0.12, +0.17) | *+0.15* (+0.12, +0.18) | *+0.14* (+0.12, +0.17) | *+0.14* (+0.08, +0.19) | *+0.16* (+0.07, +0.26) | *+0.12* (+0.05, +0.20) | *+0.14* (+0.10, +0.18) | +0.01 (-0.01, +0.03) |
| **MAM** | *+0.14* (+0.12, +0.17) | *+0.14* (+0.11, +0.16) | *+0.13* (+0.05, +0.23) | *+0.13* (+0.04, +0.21) | *+0.14* (+0.06, +0.22) | *+0.16* (+0.08, +0.24) | *+0.16* (+0.12, +0.19) | 0.00 (-0.02, +0.02) |
| **JJA** | *+0.11* (+0.05, +0.16) | *+0.10* (+0.04, +0.16) | *+0.12* (+0.06, +0.19) | *+0.15* (+0.07, +0.22) | *+0.14* (+0.09, +0.17) | *+0.11* (+0.05, +0.16) | *+0.12* (+0.08, +0.16) | -0.02 (-0.04, 0.00) |
| **SON** | *+0.14* (+0.10, +0.17) | *+0.12* (+0.04, +0.21) | *+0.14* (+0.10, +0.18) | *+0.13* (+0.06, +0.20) | *+0.16* (+0.12, +0.19) | *+0.14* (+0.07, +0.21) | *+0.14* (+0.11, +0.18) | -0.01 (-0.04, +0.01) |

| | TN10p (%) | TN90p (%) | TX10p (%) | TX90p (%) | Txgt50p (%) | TXge30 (days) | CSDId (days) | WSDId (days) | CDDcoldn (degree-days) |
|---|---|---|---|---|---|---|---|---|---|
| **Annual** | *-1.76* (-2.08, -1.48) | *+2.28* (+1.91, +2.67) | *-1.70* (-2.00, -1.46) | *+2.07* (+1.72, +2.45) | *+4.66* (+3.94, +5.33) | *+12.46* (+10.64, +14.42) | *-3.20* (-4.09, -2.34) | *+3.97* (+2.78, +5.19) | *+45.59* (+12.99, +73.91) |
| **DJF** | *-1.75* (-2.74, -0.78) | *+2.36* (+1.80, +2.90) | *-1.80* (-2.13, -1.48) | *+2.27* (+1.79, +2.87) | *+5.16* (+4.03, +6.53) | *+4.24* (+3.20, +5.01) | | | |
| **MAM** | *-1.57* (-2.48, -0.62) | *+2.35* (+1.05, +3.68) | *-1.79* (-2.13, -1.48) | *+2.12* (+1.64, +2.60) | *+5.14* (+4.31, +6.15) | *+3.93* (+3.27, +4.60) | | | |
| **JJA** | *-1.55* (-2.42, -0.71) | *+1.86* (+0.58, +3.16) | *-1.35* (-2.06, -0.74) | *+1.48* (+0.55, +2.44) | *+4.66* (+3.94, +5.33) | *+1.78* (+1.35, +2.18) | | | |
| **SON** | *-1.76* (-2.20, -1.36) | *+2.32* (+1.79, +2.86) | *-1.45* (-2.42, -0.59) | *+1.96* (+0.79, +3.13) | *+4.28* (+1.38, +7.14) | *+2.45* (+0.92, +4.04) | | | |

### 3.3.1.2 Extreme temperature

Remarkably, all the core and additional ET-SCI temperature indices that can be calculated on a regional scale show statistically significant warming on both annual and seasonal timescales (Table 3.3).

On an annual scale, the amount of cold nights (TN10p) and cold days (TX10p) decreased by 1.76 % and 1.70 % per decade respectively, whereas the amount of warm nights (TN90p) and warm days (TX90p) increased by 2.28 % and 2.07 % per decade respectively. TN90p and TX90p also show a marked increase in interannual variability from about 1988 (Figure 3.5).

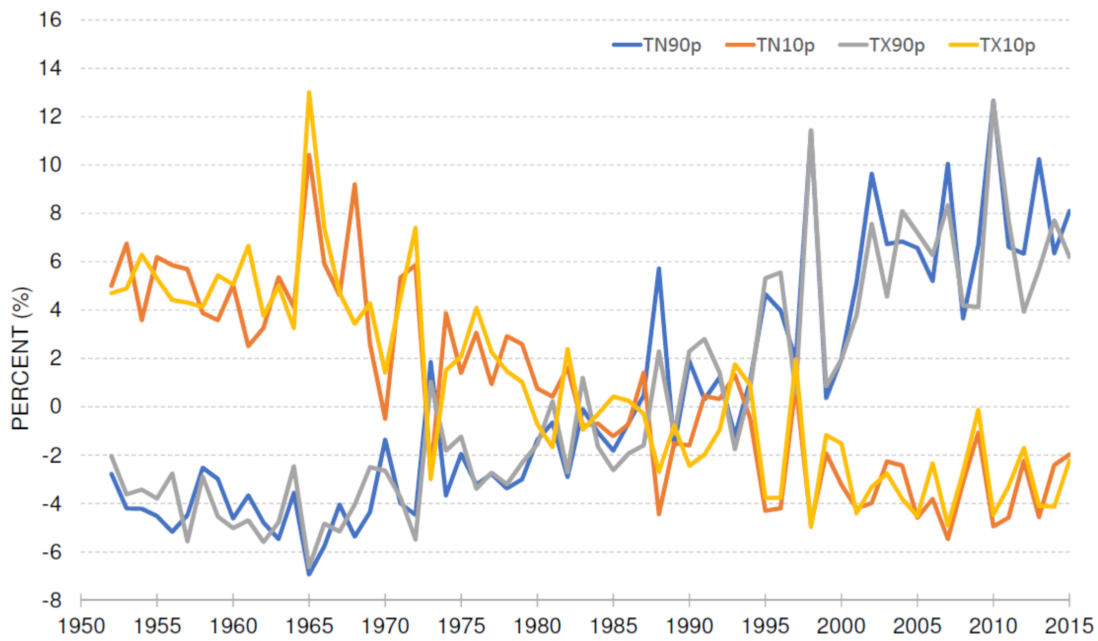


Figure 3.5 Regional amount of warm nights (TN90p), cold nights (TN10p), hot days (TX90p) and cool days (TX10p) anomalies relative to 1971–2000 climatology

For the four percentile-based indices, warming was strongest in DJF and lowest in JJA. These indices also show greatest warming at the upper end of distribution. The fraction of days with above average temperature (TXgt50p) index shows robust warming in all seasons, with the strongest warming in DJF (5.16% per decade). Unlike the other percentile indices, the weakest positive trend is in SON. Warming is southern hemisphere dominated, as DJF is when station trends in the north Pacific are weakest (Figure 3.6). It appears the weakest trends occur in the driest months of the year. For eastern Micronesia

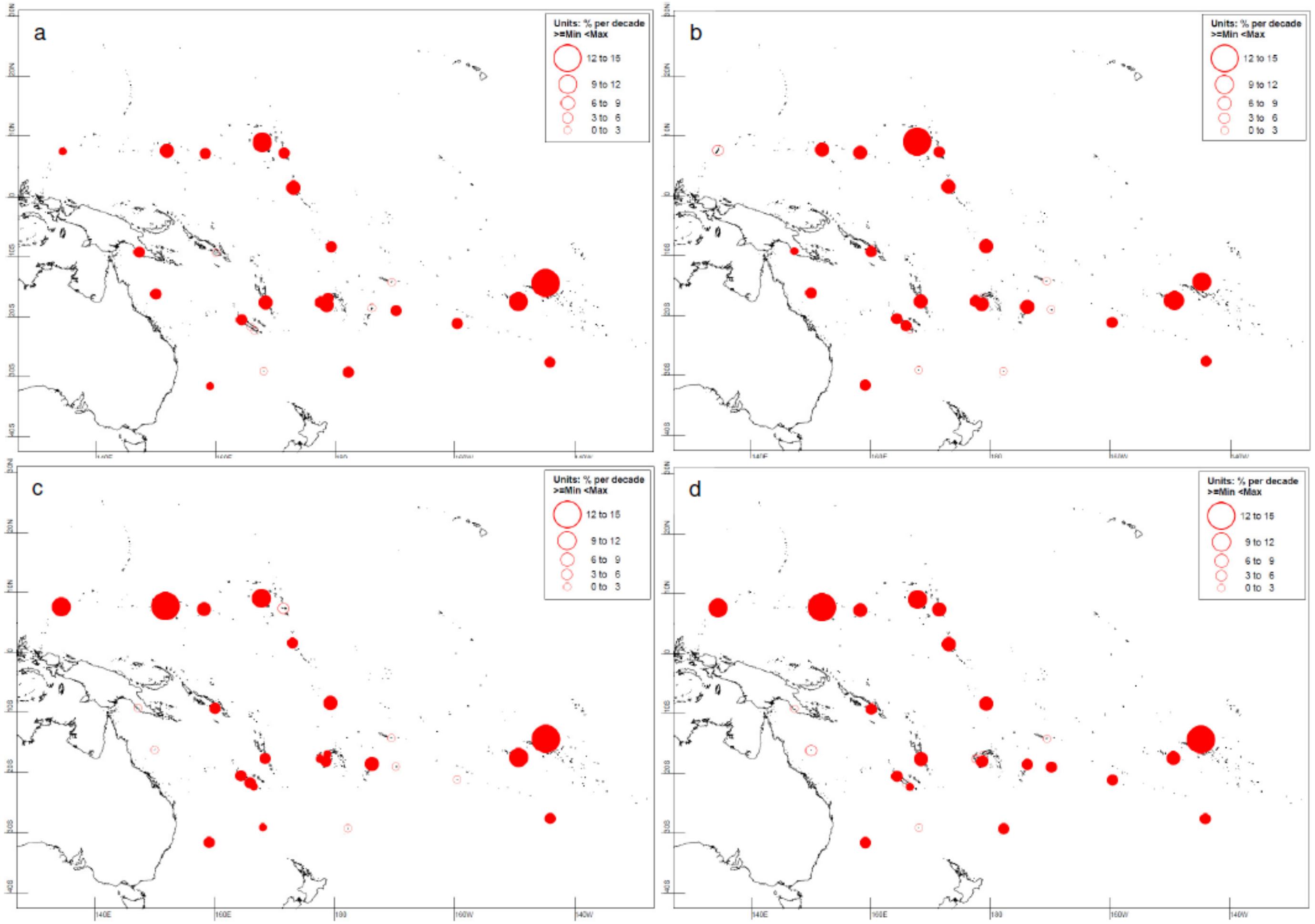


Figure 3.6 Trends in the fraction of days with above average temperature (TXgt50p) over 1951–2015 for (a) DJF, (b) MAM, (c) JJA, and (d) SON. Solid circles represent trends significant at the 5% level. The size of the circle is proportional to the magnitude of the trend.

and the Marshall Islands the driest months are January to March, while for a large part of the south Pacific the driest months are June to August.

The upper end of the absolute indices distribution also shows greatest warming (Table 3.3) with stronger increases in annual maximum TN (TNx) and maximum TX (TXx), both 0.15ºC per decade, then deceases in the annual minimum TN (TNn) and minimum TX (TXn), 0.12ºC and 0.09ºC per decade respectively.

The duration and threshold indices were not calculated at a regional level as trend calculations for some of the station-based indices do not produce meaningful results. For example, at and near the equator almost every day of the year, the mean temperature is above 25ºC, therefore the trends in summer days (SU) index are only viable north of 20°N and south of 20°S. For the same reason, the tropical nights (TR) index was not calculated. Where SU and TR could be investigated, most trends are positive, e.g., at Lord Howe Island, where SU and TR increased by 3.7 and 4.5 days per decade respectively. For regional scale TX of at least 30ºC (TXge30), the subtropical stations were excluded. Like the percentile-based indices, this index shows consistent/robust annual and seasonal warming, strongest in DJF and weakest in JJA (Table 3.3).

The standard warm spell duration indicator (WSDI) index is based on the annual number of days contributing to events where six or more consecutive days experience TX > 90th percentile. The cold spell duration indicator (CSDI) index was calculated in a similar manner. In the tropical Pacific, the number of days meeting this requirement is zero in most years, therefore for the user-specified versions a shorter period, in this case three days was used. On a regional scale, CSDI3 decreased by 3.20 days per decade and while WSDI3 increased by 3.97 days per decade.

As air conditioning is frequently used in the tropical and subtropical Pacific, especially in the summer months, the new ET-SCI cooling degree days (CDDcoldn) index is important. A positive trend of 45.59 degree-days per decade is derived on a regional scale suggesting that demand for air conditioning (and therefore electricity demand) has increased significantly over last 65 years.

Several core and additional ET-SCI indices were not analysed as the timeseries were unusable; this was the case for the entire or part of the region.

These indices have been presented in italics in Table 3.2. The number and frequency of heatwaves and coldwaves in the tropical Pacific was zero for many years, therefore, heatwave and coldwave duration, magnitude and amplitude could not be calculated. At Alofi-Hanan Airport on Niue, for example, there were 19 such annual cases for HWN (TX90) in 65 years, somewhat equally spread across the record, with a further 18 cases of one annual heatwave event. This is likely to be due to the low day-to-day temperature variability on oceanic islands. While there are statistical methods that account for large numbers of zero values in a timeseries, e.g., zero inflation models, they have not been used in this study as a standardised method for trend calculation is preferred. The limitations of indices in detecting heatwave events is well known and discussed in detail in Perkins (2015) and Perkins and Alexander (2013).

### 3.3.2 Annual and seasonal changes in total and extreme precipitation

#### 3.3.2.1 Total precipitation

Of the eight Pacific subregions, only the Southern subtropics and Southwest French Polynesia showed statistically significant annual total PR trends over 1951–2015; both of which were negative (Table 3.4). These were associated with negative trends in JJA in the former and in DJF in the latter. Significant negative trends were also present in SON in the North ITCZ and North PNG subregions (Table 3.4).

Although not associated with statistically significant trends, the annual (not shown), MAM, SON and to a lesser extent the DJF maps show an El Niño-like pattern where the ITCZ is displaced south towards the equator and the SPCZ northeast towards the central Pacific (Figure 3.7).

A notable change in trend pattern is evident from 1981 (Figure 3.8). Positive trends are observed in the Southwest SPCZ and North ITCZ subregions and a negative trend in the Central Pacific subregion. There are seven statistically significant trends (approximately 11% of stations) across the region. There is remarkable spatial similarity between the observed annual PR trends for 1981–2011 and the annual mean (January to December) ERA-Interim reanalysis (Dee et al., 2011) trends for the same period (Figure 3.9). This suggests that these reanalyses (at least first-order) can be used to estimate PR

Table 3.4 Subregional trends for total and extreme precipitation for 1951–2015 (units per decade). The 95% confidence intervals are shown in brackets. Trends statistically significant at the 5% level are shown in italics. NA indicates trend not available due to insufficient data. See Table 3.2 for index definitions

| | **Total PR (mm)** | **Rx1day (mm)** | **Rx2day (mm)** | **Rx5day (mm)** | **R1mm (days)** | **R10mm (days)** | **R20mm (days)** | **CDD (days)** | **CWD (days)** |
|---|---|---|---|---|---|---|---|---|---|
| **Central Pacific** | | | | | | | | | |
| **Annual** | +28.4 (-71.5, +132.7) | *+3.71* (+0.28, +7.85) | +5.76 (-2.99, +14.19) | +4.73 (-2.54, +12.50) | +1.46 (-1.91, +5.06) | +0.67 (-1.99, +3.15) | +0.53 (-1.27, +2.20) | *-1.83* (-3.45, -0.08) | +0.30 (-0.91, +1.52) |
| **DJF** | -9.5 (-47.2, +26.5) | +1.95 (-1.57, +5.52) | +1.01 (-8.45, +8.59) | +0.88 (-6.65, +8.44) | +0.34 (-0.99, +1.62) | -0.05 (-0.84, +0.69) | +0.02 (-0.56, +0.55) | -0.24 (-1.26, +0.62) | +0.20 (-0.48, +0.77) |
| **MAM** | +17.2 (-15.0, +45.5) | +2.69 (-0.83, +6.00) | *+7.42* (+1.34, +13.67) | +5.18 (-0.67, +10.56) | +0.83 (-0.10, +1.72) | +0.56 (-0.16, +1.23) | +0.28 (-0.23, +0.75) | -0.63 (-1.23, +0.02) | +0.31 (-0.24, +0.82) |
| **JJA** | +3.1 (-17.5, +20.2) | +0.67 (-1.72, +3.39) | +0.58 (-5.64, +5.86) | +1.11 (-5.28, +5.43) | +0.16 (-0.60, +0.89) | -0.09 (-0.58, +0.46) | 0.00 (-0.35, +0.34) | -0.01 (-0.53, +0.51) | +0.23 (-0.12, +0.57) |
| **SON** | +11.5 (-9.1, +33.6) | +2.26 (-0.62, +5.15) | +2.31 (-2.78, +8.05) | -1.63 (-8.96, +5.86) | +0.61 (-0.28, +1.44) | +0.19 (-0.41, +0.73) | +0.16 (-0.18, +0.47) | -0.61 (-1.36, +0.24) | +0.27 (-0.16, +0.63) |
| **New Guinea Islands** | | | | | | | | | |
| **Annual** | +4.0 (-102.4, +110.2) | -0.78 (-5.33, +3.44) | -1.78 (-10.92, +5.96) | -1.63 (-8.96, +5.86) | -0.28 (-5.49, +4.78) | +0.47 (-2.71, +3.81) | +1.06 (-1.57, +3.57) | +0.42 (-1.06, +1.96) | *-1.49* (-3.04, -0.19) |

| | Total PR (mm) | Rx1day (mm) | Rx2day (mm) | Rx5day (mm) | R1mm (days) | R10mm (days) | R20mm (days) | CDD (days) | CWD (days) |
|---|---|---|---|---|---|---|---|---|---|
| **DJF** | -12.5 (-42.9, +16.1) | -3.23 (-6.75, +0.50) | -1.04 (-7.76, +5.95) | +0.74 (-5.67, +6.56) | -0.58 (-1.89, +0.83) | -0.47 (-1.47, +0.63) | 0.00 (-0.63, +0.74) | +0.01 (-0.89, +0.85) | -0.66 (-1.55, +0.32) |
| **MAM** | +3.9 (-20.0, +26.2) | -1.47 (-4.62, +1.08) | -0.58 (-5.20, +3.97) | -2.00 (-5.88, +1.21) | -0.97 (-2.30, +0.29) | -0.03 (-0.92, +0.83) | +0.07 (-0.51, +0.61) | +0.40 (-0.39, +1.16) | *-1.17 (-2.10, -0.27)* |
| **JJA** | +26.7 (-13.6, +66.2) | +2.00 (-2.10, +6.29) | *+11.42 (+1.20, +20.95)* | +8.06 (-0.44, +16.02) | 0.00 (-1.35, +1.86) | +0.83 (-0.15, +1.88) | +0.63 (-0.14, +1.43) | +0.15 (-0.53, +0.83) | +0.23 (-0.69, +1.15) |
| **SON** | -3.2 (-50.9, +34.8) | +0.11 (-3.83, +3.54) | -3.00 (-9.13, +3.78) | -3.00 (-8.53, +2.35) | +0.12 (-2.10, +2.05) | +0.01 (-1.18, +1.21) | +0.10 (-0.76, +0.97) | +0.19 (-0.74, +1.09) | +0.23 (-0.82, +1.12) |
| **North ITCZ** | | | | | | | | | |
| **Annual** | -37.3 (-77.1, +6.6) | -0.62 (-5.06, +3.57) | -1.00 (-7.66, +5.24) | -0.46 (-5.81, +6.11) | -1.36 (-3.15, +0.80) | -1.08 (-2.44, +0.55) | -0.71 (-1.69, +0.26) | +0.42 (-0.52, +1.42) | -0.79 (-2.19, +0.60) |
| **DJF** | -3.1 (-21.5, +17.2) | -0.82 (-3.04, +1.70) | -3.91 (-8.70, +0.20) | -3.69 (-8.26, +0.55) | +0.24 (-0.56, +1.05) | +0.13 (-0.50, +0.67) | 0.00 (-0.35, +0.38) | -0.33 (-0.75, +0.13) | -0.15 (-0.65, +0.35) |
| **MAM** | -13.9 (-39.0, +10.4) | -1.44 (-4.61, +2.43) | -4.11 (-10.58, +3.15) | -2.73 (-8.42, +3.00) | -0.23 (-1.22, +0.65) | -0.33 (-1.02, +0.39) | -0.19 (-0.67, +0.23) | -0.11 (-0.61, +0.45) | -0.23 (-0.82, +0.31) |
| **JJA** | -2.3 (-23.0, +16.3) | +0.68 (-1.88, +3.23) | +1.49 (-4.76, +7.43) | +0.91 (-4.66, +6.50) | -0.44 (-0.97, 0.00) | -0.15 (-0.59, +0.24) | -0.13 (-0.45, +0.16) | *+0.22 (+0.02, +0.42)* | -0.06 (-0.54, +0.37) |

| | Total PR (mm) | Rx1day (mm) | Rx2day (mm) | Rx5day (mm) | R1mm (days) | R10mm (days) | R20mm (days) | CDD (days) | CWD (days) |
|---|---|---|---|---|---|---|---|---|---|
| **SON** | *-14.1* (-28.7, -0.3) | -0.61 (-2.78, +1.55) | -1.01 (-0.37, +3.54) | -0.13 (-3.60, +3.42) | -0.36 (-0.98, +0.26) | -0.31 (-0.82, +0.18) | *-0.31* (-0.58, 0.00) | +0.23 (0.00, +0.50) | -0.45 (-0.99, +0.11) |
| **North PNG** | | | | | | | | | |
| **Annual** | -21.8 (-121.8, +92.3) | -2.06 (-6.08, +2.10) | -1.23 (-10.73, +6.42) | NA | NA | NA | -0.71 (-2.50, +0.95) | NA | NA |
| **DJF** | -10.0 (-30.8, +12.0) | +0.71 (-3.86, +6.07) | +0.50 (-6.38, +6.28) | +0.69 (-4.40, +6.06) | 0.00 (-1.14, +0.83) | 0.00 (-0.63, +0.56) | -0.17 (-0.65, +0.38) | +0.27 (-0.81, +1.24) | 0.00 (-0.67, +0.50) |
| **MAM** | +17.5 (-12.9, +55.3) | -1.48 (-4.76, +2.29) | -1.31 (-7.55, +5.25) | -2.41 (-7.70, +2.52) | -0.08 (-1.70, +1.50) | +0.41 (-0.81, +1.53) | +0.25 (-0.37, +0.82) | -0.04 (-0.82, +0.61) | -0.16 (-0.93, +0.60) |
| **JJA** | -9.9 (-48.6, +33.2) | NA | +1.30 (-6.89, +8.78) | +2.17 (-4.08, +8.23) | NA | NA | NA | 0.00 (-0.77, +1.19) | NA |
| **SON** | *-26.7* (-53.6, -0.9) | -3.00 (-6.38, +0.15) | *-9.89* (-17.05, -3.88) | *-8.83* (-14.75, -4.38) | -1.10 (-2.69, +0.33) | -0.64 (-1.60, +0.36) | -0.48 (-1.18, 0.00) | +0.51 (-0.79, +1.90) | -0.32 (-0.97, +0.29) |
| **Southeast SPCZ** | | | | | | | | | |
| **Annual** | -19.0 (-66.7, +25.4) | +0.68 (-3.09, +4.41) | +1.63 (-4.15, +7.58) | +2.41 (-2.89, +7.95) | +0.61 (-1.11, +2.35) | -0.26 (-1.46, +0.95) | +0.12 (-0.60, +0.75) | -0.03 (-1.25, +1.30) | -0.10 (-0.85, +0.62) |
| **DJF** | -4.8 (-25.0, +16.3) | -0.71 (-4.70, +3.06) | -2.11 (-10.89, +5.23) | -4.16 (-10.30, +3.05) | +0.27 (-0.60, +1.08) | +0.09 (-0.54, +0.69) | 0.00 (-0.33, +0.41) | +0.09 (-0.48, +0.60) | +0.08 (-0.45, +0.57) |

| | Total PR (mm) | Rx1day (mm) | Rx2day (mm) | Rx5day (mm) | R1mm (days) | R10mm (days) | R20mm (days) | CDD (days) | CWD (days) |
|---|---|---|---|---|---|---|---|---|---|
| **MAM** | +3.2 (-12.0, +18.4) | -0.71 (-3.34, +2.19) | -3.40 (-9.33, +2.89) | -3.65 (-9.38, +1.71) | -0.25 (-0.86, +0.46) | -0.27 (-0.86, +0.24) | -0.27 (-0.63, +0.12) | +0.10 (-0.24, +0.49) | -0.18 (-0.60, +0.18) |
| **JJA** | -11.0 (-30.4, +8.3) | -0.17 (-2.89, +2.33) | +0.92 (-4.30, +6.22) | +1.44 (-3.06, +5.78) | +0.35 (-0.34, +0.94) | +0.12 (-0.30, +0.54) | +0.08 (-0.18, +0.35) | -0.19 (-0.69, +0.35) | 0.00 (-0.33, +0.34) |
| **SON** | -3.3 (-20.0, +12.9) | -1.12 (-4.12, +1.88) | -1.04 (-7.14, +5.10) | -1.20 (-5.89, +3.56) | -0.04 (-0.72, +0.80) | 0.00 (-0.45, +0.39) | +0.02 (-0.25, +0.33) | +0.02 (-0.73, +0.70) | -0.04 (-0.36, +0.31) |
| **Southern subtropics** | | | | | | | | | |
| **Annual** | *-33.6* (-63.4, -1.9) | -1.50 (-5.31, +1.83) | -2.17 (-7.11, +3.77) | -1.21 (-6.03, +4.00) | *-1.91* (-3.33, -0.37) | *-0.87* (-1.67, -0.11) | -0.54 (-1.11, 0.00) | *+1.43* (0.00, +2.93) | *-0.97* (-1.76, -0.12) |
| **DJF** | -5.0 (-20.0, +10.3) | -1.09 (-5.14, +2.72) | -3.28 (-9.67, +3.74) | -3.24 (-9.19, +3.73) | 0.00 (-0.51, +0.65) | -0.12 (-0.38, +0.14) | 0.00 (-0.26, +0.14) | +0.16 (-0.59, +0.90) | 0.00 (-0.29, +0.27) |
| **MAM** | +1.1 (-13.0, +13.1) | -1.43 (-4.77, +1.62) | -1.38 (-6.25, +3.66) | -0.52 (-5.64, +4.03) | -0.16 (-0.88, +0.60) | +0.07 (-0.20, +0.40) | 0.00 (-0.16, +0.28) | +0.01 (-0.68, +0.66) | +0.09 (-0.19, +0.38) |
| **JJA** | *-18.1* (-30.2, -6.5) | -1.97 (-4.43, +0.24) | *-4.28* (-8.33, -0.24) | -2.92 (-6.50, +0.45) | *-1.09* (-1.67, -0.47) | *-0.51* (-0.83, -0.13) | -0.22 (-0.44, 0.00) | +0.25 (0.00, +0.58) | *-0.60* (-1.08, -0.23) |
| **SON** | -7.1 (-18.8, +3.4) | -0.51 (-3.41, +2.29) | -0.98 (-5.31, +2.96) | -1.13 (-4.20, +2.79) | -0.49 (-1.09, 0.00) | -0.21 (-0.56, +0.10) | -0.16 (-0.38, 0.00) | *+0.54* (0.00, +1.00) | *-0.26* (-0.51, 0.00) |

| | Total PR (mm) | Rx1day (mm) | Rx2day (mm) | Rx5day (mm) | R1mm (days) | R10mm (days) | R20mm (days) | CDD (days) | CWD (days) |
|---|---|---|---|---|---|---|---|---|---|
| **Southwest French Polynesia** | | | | | | | | | |
| **Annual** | *-53.4* (-99.3, -8.9) | -3.50 (-7.31, +0.04) | *-14.19* (-22.98, -4.67) | *-9.18* (-18.09, -1.69) | +1.29 (-0.58, +2.87) | *-1.43* (-2.37, -0.32) | *-1.12* (-2.04, -0.31) | -1.62 (-3.53, +0.66) | -0.04 (-0.94, +0.77) |
| **DJF** | *-23.4* (-46.0, -3.1) | *-4.78* (-8.29, -1.42) | *-13.50* (-22.27, -5.93) | *-10.62* (-20.02, -2.28) | +0.18 (-0.60, +1.00) | -0.49 (-1.09, +0.01) | -0.27 (-0.72, +0.10) | -0.15 (-0.83, +0.40) | -0.39 (-0.81, +0.06) |
| **MAM** | -16.4 (-35.7, +5.0) | -1.97 (-5.62, +1.41) | -5.08 (-14.25, +3.31) | -5.11 (-12.31, +2.13) | +0.48 (-0.33, +1.17) | -0.38 (-0.89, +0.10) | *-0.46* (-0.88, -0.07) | +0.06 (-0.78, +0.83) | +0.18 (-0.28, +0.64) |
| **JJA** | -3.5 (-16.2, +8.1) | -1.84 (-4.78, +1.51) | -4.83 (-11.77, +2.49) | -6.02 (-12.72, +1.34) | *+0.71* (+0.17, +1.33) | 0.00 (-0.37, +0.31) | -0.15 (-0.41, +0.09) | *-0.91* (-1.54, -0.24) | +0.28 (-0.05, +0.57) |
| **SON** | -13.0 (-31.3, +4.7) | -0.31 (-3.50, +2.77) | -3.66 (-9.33, +1.59) | -2.61 (-8.35, +1.85) | +0.03 (-0.70, +0.81) | *-0.40* (-0.80, -0.01) | -0.26 (-0.58, +0.02) | -0.77 (-1.53, -0.01) | +0.06 (-0.32, +0.39) |
| **Southwest SPCZ** | | | | | | | | | |
| **Annual** | -12.7 (-77.2, +56.0) | -0.14 (-3.05, +3.07) | -1.56 (-8.71, +4.37) | -1.21 (-7.22, +4.48) | +0.52 (-2.30, +3.31) | -0.33 (-2.11, +1.43) | -0.25 (-1.37, +0.94) | -0.54 (-2.50, +1.67) | -0.10 (-0.65, +0.48) |
| **DJF** | +4.7 (-22.8, +27.8) | +0.51 (-3.21, +4.26) | -1.00 (-8.02, +5.46) | -1.00 (-7.78, +6.05) | +0.15 (-0.78, +1.03) | +0.10 (-0.55, +0.66) | +0.10 (-0.35, +0.46) | -0.27 (-0.99, +0.37) | -0.01 (-0.44, +0.41) |
| **MAM** | +0.9 (-19.1, +19.2) | +0.59 (-2.15, +3.14) | -2.07 (-8.60, +3.47) | -1.87 (-7.42, +3.70) | +0.37 (-0.30, +1.08) | -0.01 (-0.42, +0.49) | -0.03 (-0.37, +0.28) | -0.25 (-0.89, +0.20) | 0.00 (-0.25, +0.19) |

| | **Total PR (mm)** | **Rx1day (mm)** | **Rx2day (mm)** | **Rx5day (mm)** | **R1mm (days)** | **R10mm (days)** | **R20mm (days)** | **CDD (days)** | **CWD (days)** |
|---|---|---|---|---|---|---|---|---|---|
| **JJA** | -4.3 (-15.0, +7.6) | -0.59 (-2.49, +1.30) | -1.28 (-6.09, +3.55) | -1.46 (-5.69, +2.88) | +0.17 (-0.35, +0.68) | -0.05 (-0.32, +0.28) | -0.05 (-0.27, +0.16) | -0.36 (-1.10, +0.42) | -0.01 (-0.26, +0.32) |
| **SON** | -9.7 (-33.2, +13.3) | -2.59 (-5.23, +0.33) | -4.34 (-9.37, +1.49) | -4.35 (-8.93, +0.69) | -0.28 (-1.42, +0.79) | -0.26 (-0.84, +0.39) | -0.20 (-0.55, +0.20) | +0.64 (-0.57, +1.88) | -0.04 (-0.39, +0.30) |

| **Annual** | **R95p (mm)** | **R95pTOT (%)** | **R99p (mm)** | **R99pTOT (%)** | **SDII (mm/day)** |
|---|---|---|---|---|---|
| **Central Pacific** | +12.55 (-25.80, +56.52) | +0.56 (-0.60, +1.83) | +11.99 (-3.56, +27.24) | +0.56 (-0.06, +1.19) | +0.11 (-0.21, +0.48) |
| **New Guinea Islands** | +20.13 (-29.15, +66.36) | +0.34 (-0.47, +1.16) | -5.30 (-34.44, +25.34) | -0.21 (-1.07, +0.52) | +0.19 (-0.05, +0.42) |
| **North ITCZ** | -15.37 (-44.23, +16.15) | -0.18 (-0.90, +0.60) | -2.56 (-18.40, +16.47) | +0.07 (-1.27, +0.58) | -0.08 (-0.22, +0.06) |
| **North PNG** | -16.13 (-66.68, +30.21) | NA | -20.30 (-43.36, +7.63) | -0.34 (-0.75, +0.31) | +0.03 (-0.26, +0.30) |
| **Southeast SPCZ** | -11.34 (-38.88, +15.09) | -0.30 (-1.02, +0.37) | -6.72 (-22.02, +9.08) | -0.27 (-0.75, +0.31) | -0.14 (-0.39, +0.08) |
| **Southern subtropics** | -18.26 (-37.82, +2.44) | -0.58 (-1.44, +0.28) | -4.70 (-15.33, +5.67) | -0.11 (-0.79, +0.51) | -0.13 (-0.29, +0.03) |
| **Southwest French Polynesia** | *-49.33* (-73.65, -21.19) | *-1.52* (-2.24 -0.62) | *-26.15* (-41.55, -10.30) | *-1.03* (-1.65, -0.38) | *-0.66* (-0.93, -0.37) |
| **Southwest SPCZ** | -7.73 (-32.69, +20.58) | -0.09 (-0.64, +0.40) | -1.03 (-9.81, +11.05) | -0.01 (-0.43, +0.42) | -0.16 (-0.39, +0.07) |

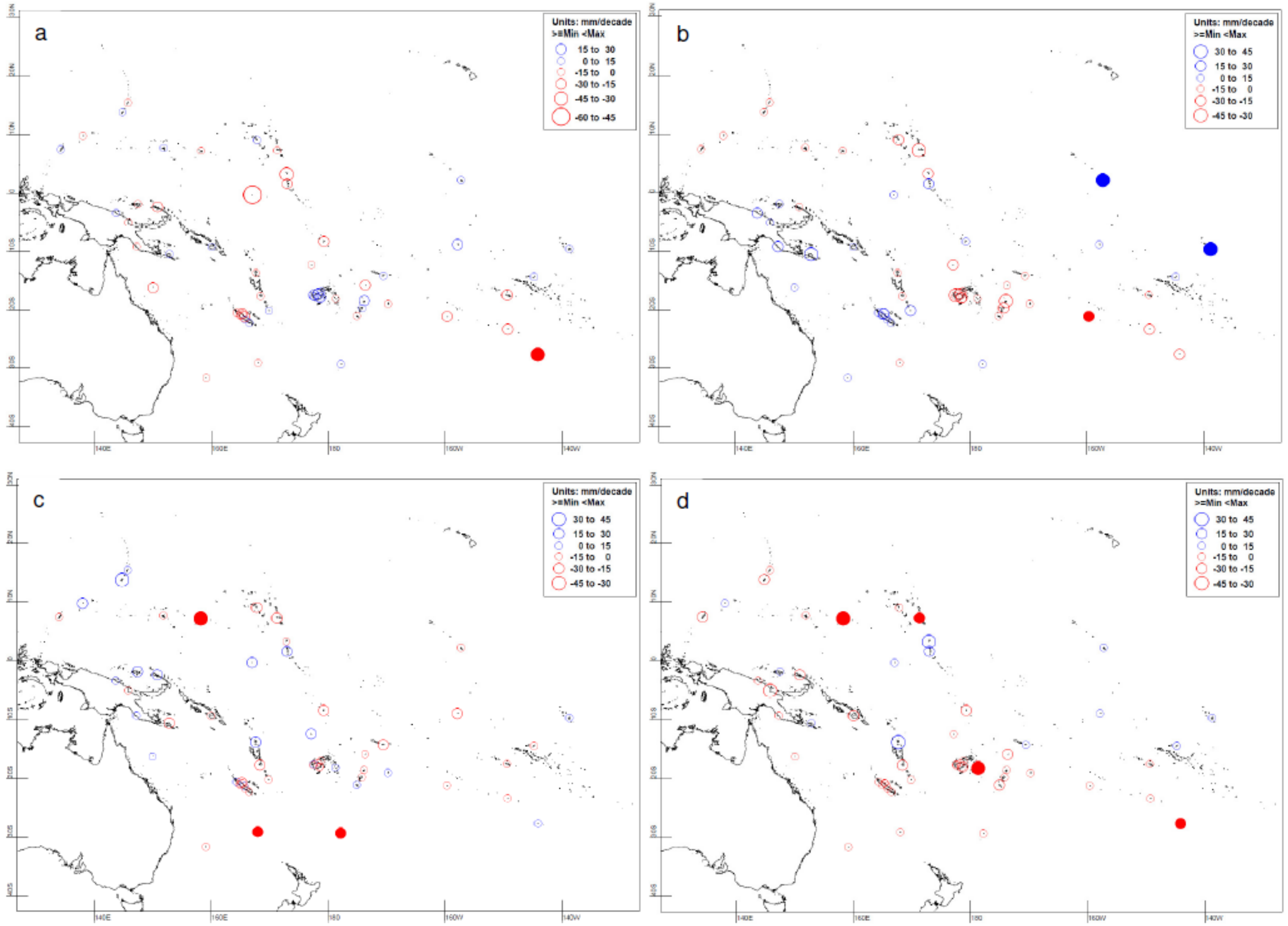


Figure 3.7 Trends in total precipitation over 1951–2015 for (a) DJF, (b) MAM, (c) JJA, and (d) SON. Blue circles represent positive trends and red circles negative trends. Solid circles represent trends significant at the 5% level. The size of the circle is proportional to the magnitude of the trend

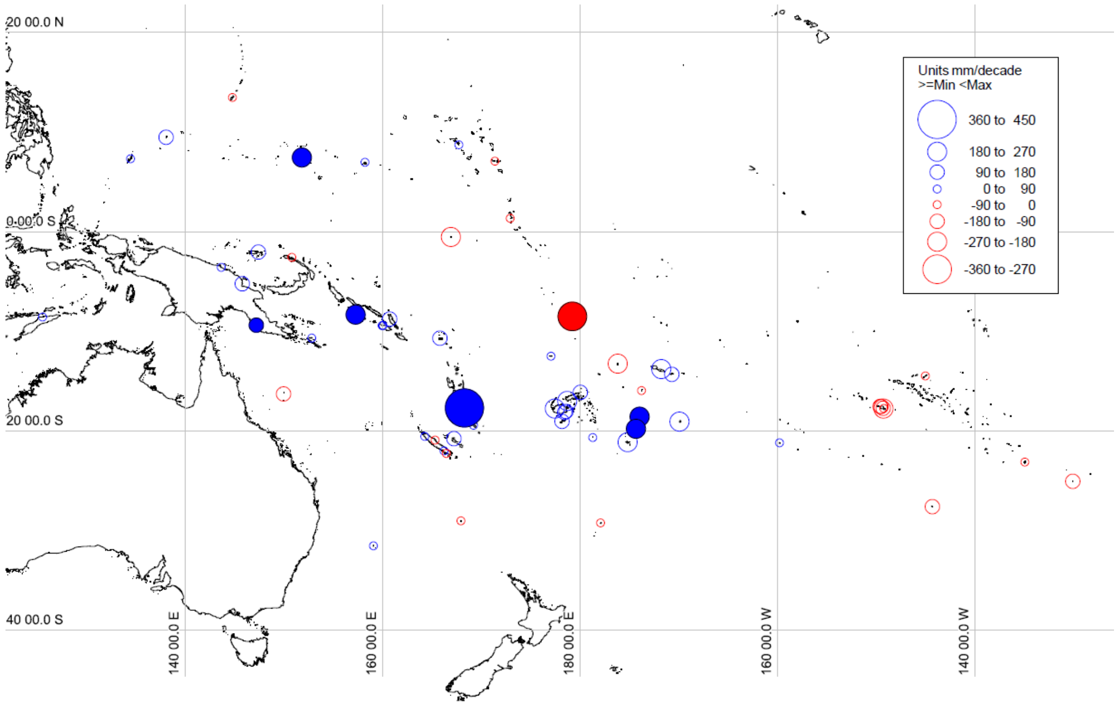


Figure 3.8 Trends in total precipitation over 1981–2011. Blue circles represent positive trends and red circles negative trends. Solid circles represent trends significant at the 5% level. The size of the circle is proportional to the magnitude of the trend

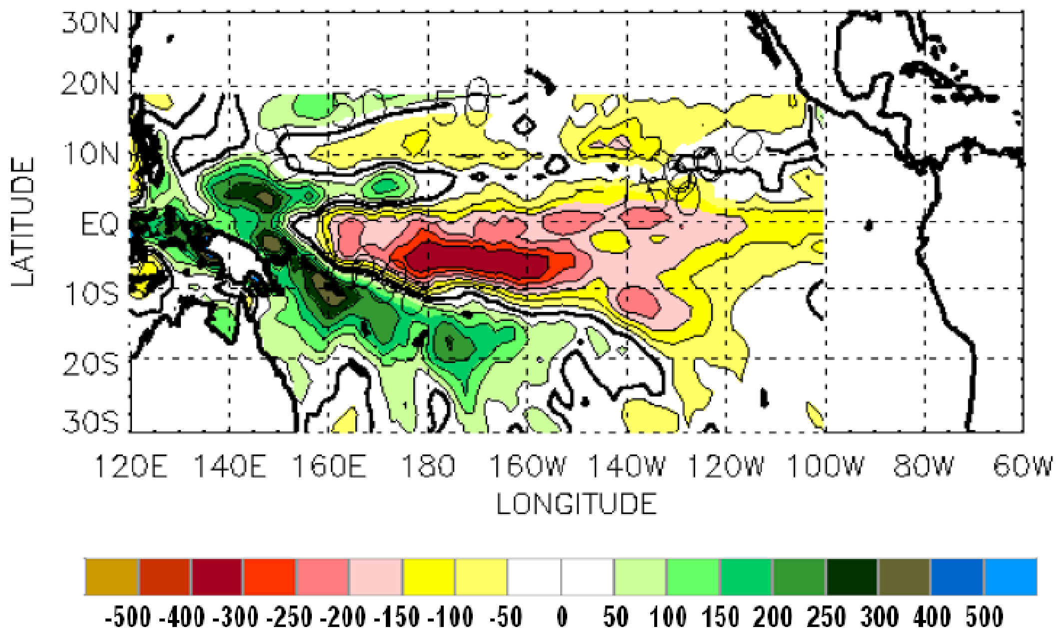


Figure 3.9 Trends in total precipitation from reanalysis ERA-Interim for the period 1981–2011. Units are mm per decade.

trends in the region. However, reanalyses should be used with caution. According to Sillmann et al. (2013), reanalysis data prior to the 1981 should not be used for trends analysis. It is also worth noting that the ERA-Interim model reanalysis trend pattern is similar to the composite La Niña austral summer precipitation pattern (not shown), which is expected to be dominated by La Niña events from the late 1990s.

### 3.3.2.2 Extreme precipitation

Similar to total PR, the proportion of statistically significant extreme precipitation indices trends over 1951–2015 was small. Significant trends were predominately negative and by and large located in the Southern subtropics and Southwest French Polynesia subregions (Table 3.4).

In the case of Southwest French Polynesia, there was a decrease in moderate to high intensity precipitation events, especially those experienced over multiple days. For the duration absolute indices (Rx1day, Rx2day and Rx5day), the negative trends occurred in DJF, whereas for R10mm the negative trends occurred in SON and for R20mm in MAM. Declines are also present in the percentile-based (R95p, R95pTOT, R99p and R99pTOT) and daily PR intensity (SDII) indices. These negative trends contributed to an increase in meteorological drought (SPI-3 Feb and SPI-6 Apr, Table 3.5) over the extended summer. On the other hand, there was an increase in the number of rain days (R1mm) and decrease in the number of consecutive dry days (CDD) in JJA (Table 3.4).

The Southern subtropics showed a similar drying pattern but from different underlying causes: the negative trend in annual total PR was associated with declines in R1mm, R10mm and consecutive wet days (CWD) and an increase in CDD. In other words, a decrease in low to moderate intensity precipitation events was observed. On a seasonal scale there were negative trends in JJA total PR, R1mm, R10mm, CWD and Rx2day and for SON, a positive trend in CDD and a negative trend in CWD. The Southern subtropics drying trend in JJA and SON was also apparent in the drought indices where negative trends were observed for SPI-3 Aug, SPEI-3 Aug, SPI-6 Oct, SPEI-6 Oct, SPI-12 Dec and SPEI-12 Dec (Table 3.5, Figure 3.10). Unlike the Southwest French Polynesia

Table 3.5 Subregional ‘drought’ indices trends 1951–2015 (units per decade). The 95% confidence intervals are shown in brackets. Trends statistically significant at the 5% level are shown in italics. See Table 3.2 for index definitions.

| | **SPI-3 Aug** | **SPI-3 Feb** | **SPI-3 May** | **SPI-3 Nov** | **SPI-6 Apr** | **SPI-6 Oct** | **SPI-12 Dec** | **SPI-12 Jun** |
|---|---|---|---|---|---|---|---|---|
| **Central Pacific** | 0.00 (-0.08, +0.08) | 0.00 (-0.10, +0.11) | +0.08 (-0.01, +0.17) | +0.06 (-0.03, +0.14) | +0.03 (-0.07, +0.12) | +0.02 (-0.08, +0.13) | +0.03 (-0.09, +0.13) | +0.03 (-0.09, +0.14) |
| **New Guinea Islands** | +0.15 (-0.01, +0.31) | -0.03 (-0.20, +0.14) | +0.01 (-0.12, +0.15) | +0.04 (-0.20, +0.24) | -0.04 (-0.20, +0.10) | +0.15 (-0.03, +0.36) | +0.07 (-0.15, +0.31) | +0.12 (-0.15, +0.37) |
| **North ITCZ** | -0.01 (-0.09, +0.09) | 0.00 (-0.08, +0.07) | -0.03 (-0.12, +0.04) | -0.05 (-0.13, +0.02) | -0.03 (-0.12, +0.05) | -0.03 (-0.12, +0.07) | -0.04 (-0.12, +0.04) | -0.03 (-0.13, +0.06) |
| **North PNG** | +0.03 (-0.16, +0.25) | 0.00 (-0.15, +0.13) | +0.08 (-0.15, +0.28) | -0.08 (-0.20, +0.03) | +0.01 (-0.19, +0.21) | -0.05 (-0.18, +0.12) | -0.01 (-0.21, +0.19) | +0.01 (-0.20, +0.20) |
| **Southeast SPCZ** | +0.01 (-0.09, +0.10) | -0.02 (-0.11, +0.07) | -0.05 (-0.13, +0.02) | -0.02 (-0.10, +0.05) | -0.09 (-0.18, +0.01) | -0.01 (-0.10, +0.08) | -0.05 (-0.14, +0.05) | -0.05 (-0.15, +0.05) |
| **Southern subtropics** | *-0.16* (-0.26, -0.06) | -0.02 (-0.10, +0.05) | 0.00 (-0.10, +0.09) | -0.06 (-0.16, +0.03) | +0.02 (-0.06, +0.10) | *-0.18* (-0.30, -0.07) | *-0.10* (-0.18, 0.00) | -0.08 (-0.20, +0.02) |
| **Southwest French Polynesia** | -0.02 (-0.15, +0.09) | *-0.10* (-0.20, 0.00) | -0.08 (-0.16, +0.01) | -0.09 (-0.20, +0.02) | *-0.09* (-0.19, -0.01) | -0.05 (-0.21, +0.08) | *-0.14* (-0.28, -0.02) | *-0.14* (-0.25, -0.03) |

| | SPI-3 Aug | SPI-3 Feb | SPI-3 May | SPI-3 Nov | SPI-6 Apr | SPI-6 Oct | SPI-12 Dec | SPI-12 Jun |
|---|---|---|---|---|---|---|---|---|
| **Southwest SPCZ** | -0.03 (-0.12, +0.05) | +0.02 (-0.07, +0.09) | 0.00 (-0.07, +0.08) | -0.07 (-0.18, +0.04) | -0.02 (-0.12, +0.07) | -0.01 (-0.12, +0.08) | -0.03 (-0.16, +0.09) | -0.03 (-0.14, +0.08) |
| **Central Pacific** | -0.04 (-0.13, +0.03) | -0.03 (-0.17, +0.07) | +0.02 (-0.10, +0.14) | 0.00 (-0.09, +0.08) | -0.02 (-0.14, +0.09) | -0.03 (-0.14, +0.06) | -0.02 (-0.15, +0.10) | -0.10 (-0.19, +0.05) |
| **North ITCZ** | -0.07 (-0.16, +0.02) | 0.00 (-0.09, +0.09) | -0.05 (-0.15, +0.04) | *-0.09* (-0.18, 0.00) | -0.01 (-0.10, +0.09) | *-0.10* (-0.22, -0.01) | -0.09 (-0.17, +0.01) | -0.07 (-0.17, +0.03) |
| **Southeast SPCZ** | 0.00 (-0.12, +0.12) | 0.00 (-0.09, +0.09) | -0.04 (-0.14, +0.06) | 0.00 (-0.09, +0.09) | -0.07 (-0.14, +0.08) | -0.02 (-0.12, +0.09) | -0.02 (-0.12, +0.09) | -0.05 (-0.17, +0.08) |
| **Southern subtropics** | *-0.16* (-0.26, -0.06) | -0.04 (-0.13, +0.04) | -0.01 (-0.10, +0.09) | -0.09 (-0.20, +0.01) | +0.02 (-0.08, +0.10) | *-0.21* (-0.21, -0.02) | *-0.11* (-0.21, -0.02) | -0.10 (-0.23, 0.00) |
| **Southwest French Polynesia** | -0.07 (-0.18, +0.04) | -0.10 (-0.21, +0.02) | -0.07 (-0.21, +0.08) | -0.10 (-0.24, +0.05) | -0.10 (-0.23, +0.04) | -0.09 (-0.24, +0.05) | -0.18 (-0.37, +0.01) | -0.10 (-0.26, +0.05) |
| **Southwest SPCZ** | -0.04 (-0.13, +0.05) | +0.01 (-0.08, +0.10) | -0.02 (-0.11, +0.06) | -0.09 (-0.20, +0.04) | -0.03 (-0.11, +0.06) | -0.03 (-0.13, +0.08) | -0.06 (-0.18, +0.06) | -0.05 (-0.15, +0.06) |

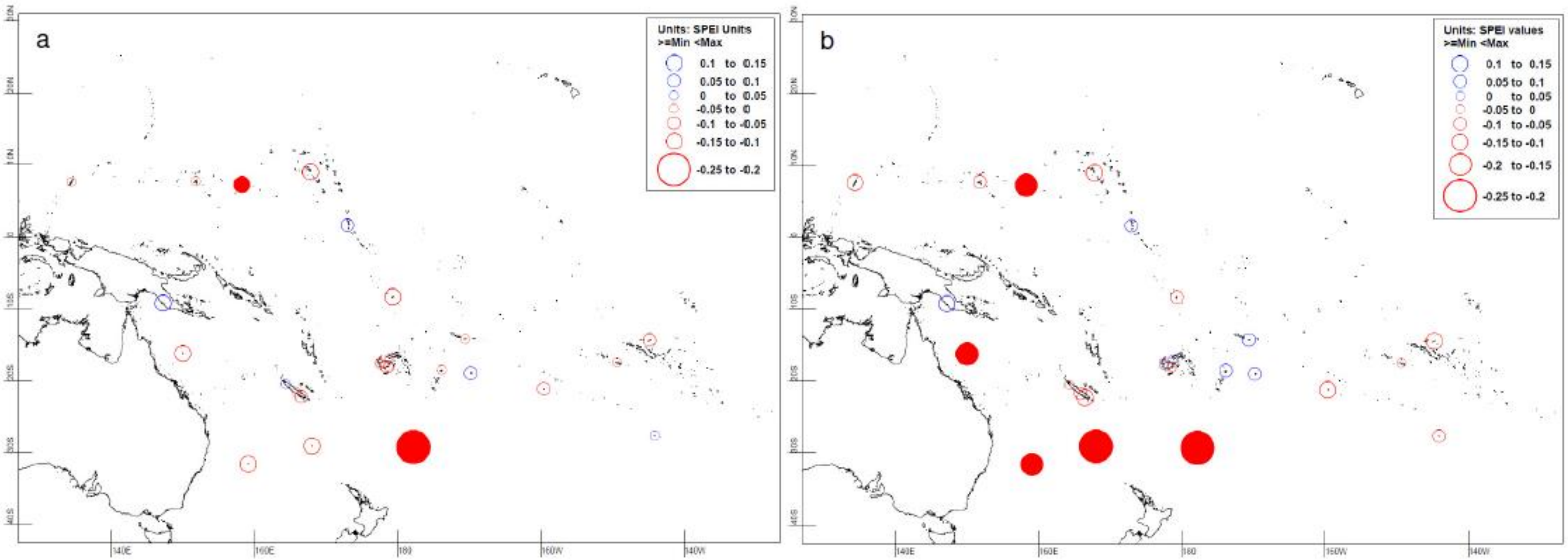


Figure 3.10 Trends in drought over 1951–2015. (a) SPEI-3 Aug, (b) SPEI-6 Oct. Red (blue) circles represent an increase (decrease) in drought conditions. Solid circles represent trends significant at the 5% level. The size of the circle is proportional to the magnitude of the trend

subregion, the drying trend in the Southern subtropics was present in both the precipitation (SPI) and evapotranspiration drought (SPEI) indices.

In the central Pacific there was a decrease in CDD and an increase in annual Rx1day and MAM Rx2day. In the North ITCZ and North PNG subregions, negative trends in SON total PR were associated with declines in SON R20mm and increase in drought (SPEI-3 Nov and SPEI-6 Oct) for the former, and with declines in Rx2day and Rx5day in the latter (Tables 3.2, 3.3). There were no significant total or extreme precipitation trends in the Southwest and southeast SPCZ subregions.

While some indices displayed significant trends on a subregional level (Table 3.4), the same did not apply at a station level. None of the station trends for annual Rx1day, Rx2day and Rx5day, for example, were statistically significant (not shown).

For the period 1981–2011, trends patterns for CDD and for the threshold (e.g., R20mm, Figure 3.11) and percentile-based indices are similar to that for total precipitation, consistent with a change across the mean position of the SPCZ. Based on these results, together with those of Murphy et al. (2014) we infer that since 1999 the WPM has intensified, the SPCZ has been displaced south and west and the ITCZ west of 160°E has strengthened and extended northward west of 140°E. It should be stated however, that few of the station trends are significant for this shorter period. Trends in the absolute indices in the Southwest SPCZ subregion are unlike those of the total precipitation, threshold indices and the percentile indices. Here the trend pattern in Rx1day (Figure 3.12) and Rx5day precipitation are predominately negative, the reverse of the generally positive trend patterns in the total, threshold, CDD and percentile-based indices. These results, although not conclusive as most of the precipitation trends are not significant, suggest that the increase in precipitation since approximately 1999 does not apply to Rx1day and Rx5day precipitation events. Further analysis of Nadi Airport, Fiji daily precipitation and tropical cyclone records for 1981–2011 reveals that 15 of 31 annual Rx1day events are associated with tropical cyclones. Of these, 10 occurred between 1981 and 1993 meaning that the decline in Rx1day precipitation is due to a similar reduction in tropical cyclones activity.

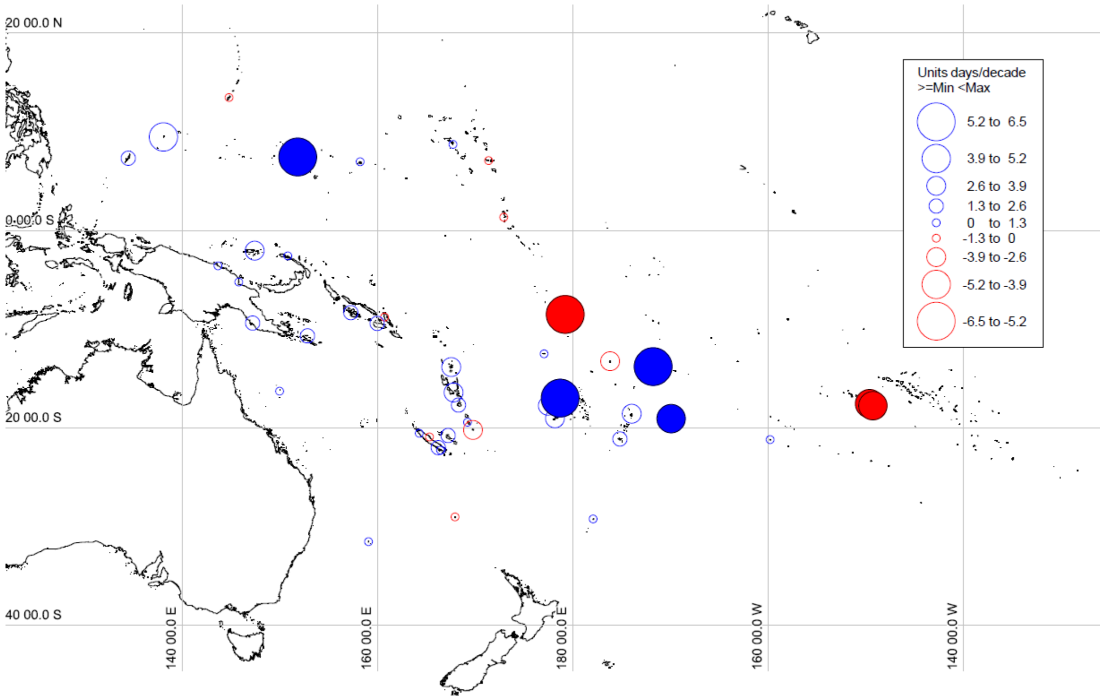


Figure 3.11 Trends in the number of rain days ≥ 10mm (R10mm) over 1981–2011. Blue circles represent positive trends and red circles negative trends. Solid circles represent trends significant at the 5% level.

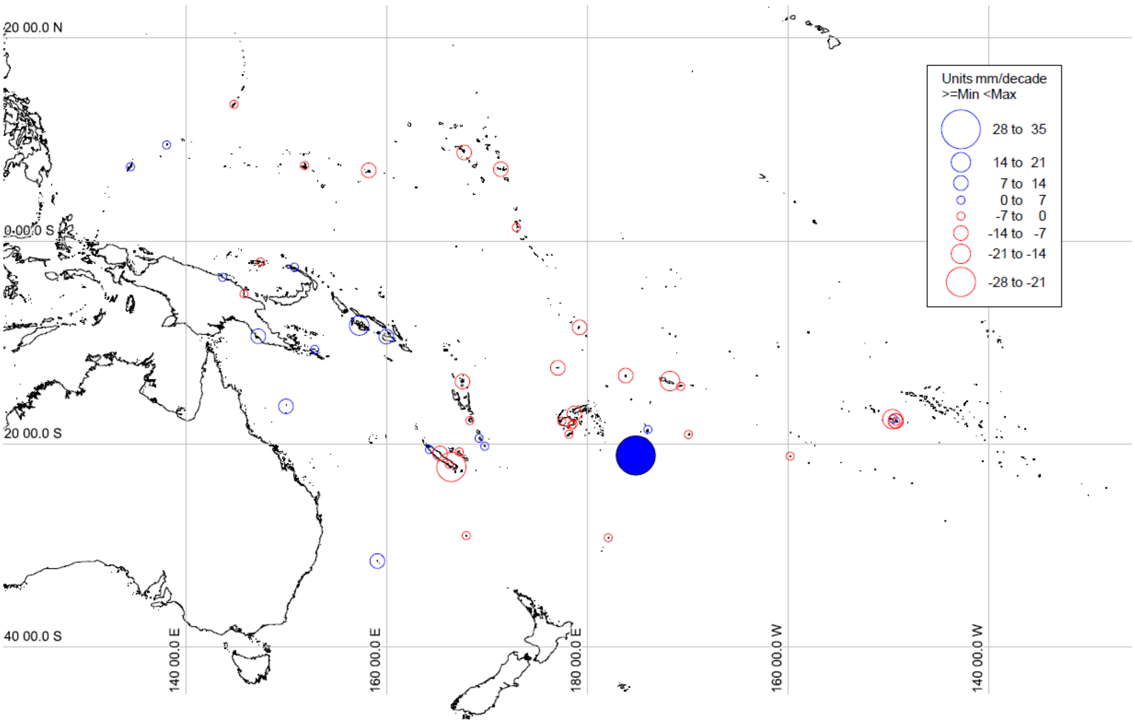


Figure 3.12 Trends in Maximum 1-day precipitation (Rx1day) over 1981–2011. Blue circles represent positive trends and red circles negative trends. Solid circles represent trends significant at the 5% level

### 3.3.3 IPO influence on temperature and precipitation trends

Over the period 1951–2015, trends in the annual and seasonal TPI for the IPO were non-significant.

Apart from TNn (JJA), TNx (MAM), TXx (MAM, SON) and DTR (Annual, MAM, SON) the relationships between the mean and extreme temperature indices and the TPI Index were non-significant. Trends in the temperature indices with IPO removed (not presented) were within 0.02°C per decade of the trends with IPO present, and therefore within the 95% confidence interval of the trends with IPO.

The IPO relationship with total and extreme precipitation varies across the region (strongest closest to the equator) and by season. Where the relationship was statistically significant, the differences in trends in precipitation with IPO and without IPO, were small and within the 95% confidence interval of the trends with IPO. In some cases, statistically significant trends became non-significant and vice versa but only in cases where trends in precipitation with IPO were marginally significant.

### 3.3.4 Changes in magnitude of the most extreme daily precipitation values

On a station scale, the Bin 1 (K1–K20) difference values (1983–2015 median minus 1951–82 median) show significant variability across the region (Figure 3.13). Of those that were statistically significant, most showed increases (8 of 11). Six of the eight locations were in the western and central Pacific and within 10 degrees of the equator. If the *p*-value is increased to 10%, five additional stations in the southwest Pacific region show positive differences.

None of the regional scale differences in the median values (Bins 1–7) for 1951–82 and 1983–2015 were statistically significant. Figure 3.14 shows that on a station scale the magnitudes of increases were also on average greater than magnitudes of decreases.

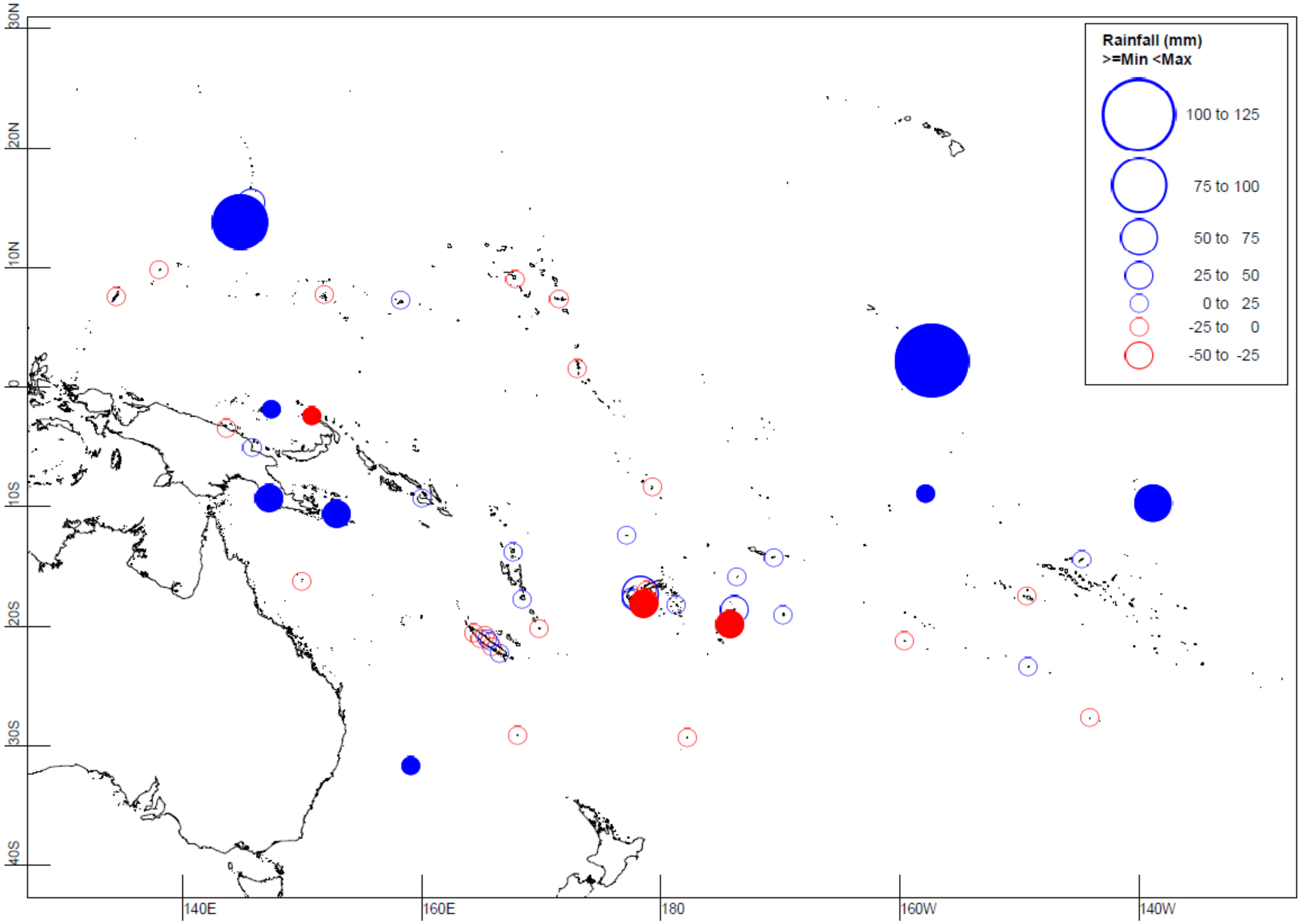


Figure 3.13 Observed changes (differences) in the median values of the 20 largest daily precipitation values (K1–K20, Bin 1) for 1951–82 and 1983–2015. Solid circles represent differences in the median values that are significant at the 5% level. The size of the circle is proportional to the magnitude of the trend.

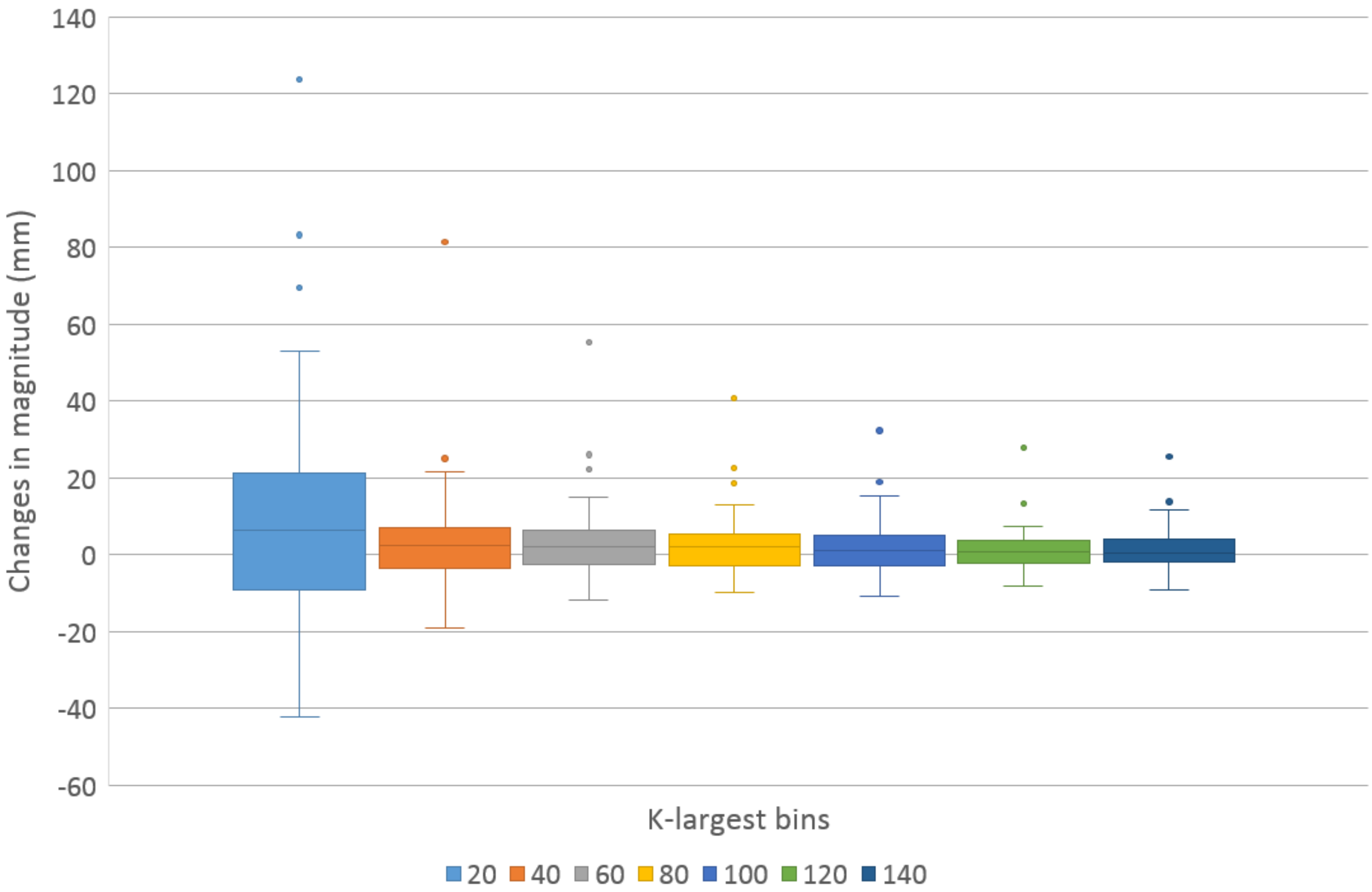


Figure 3.14 Observed changes (differences) in the median values for 1983–2015 and 1951–82 for Bin 1 (K1–K20) to Bin 7 (K120–K140) for the 52 stations.

### 3.3.5 Total and extreme precipitation relationship with ENSO (SSTs and SOI)

The analyses presented in this section is drawn from McGree et al. (2014) where the Pacific Islands region was divided into six regions (Figure 3.15). This work pre-dates the subdivisions shown in Figure 3.3 which is based on cluster analyses and PCA.

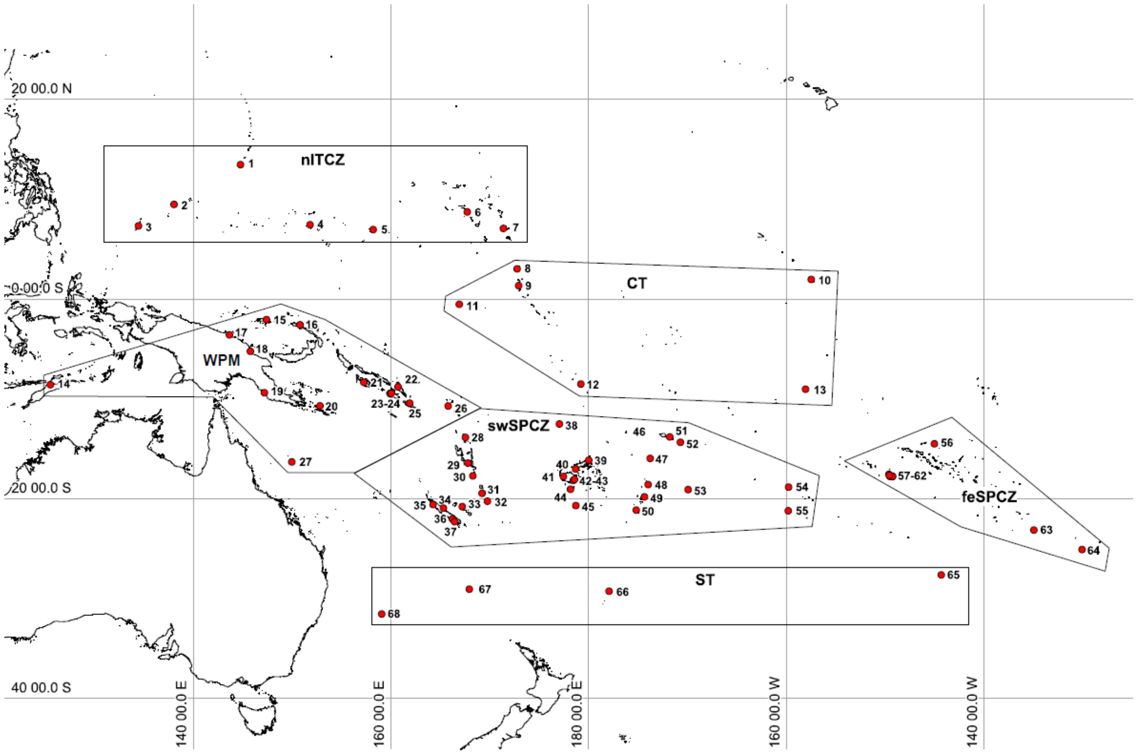


Figure 3.15 Locations of stations and the six subregions used in the McGree et al. (2014) study

The total precipitation time series (Figure 3.16) for the six subregions of the western Pacific show substantial interannual variability which is expected given the well-established role for variations in ENSO (as shown by the relationship with the SOI, Table 3.6) and the IPO in the region. In the Central Tropics (CT) subregion where variability is greatest, annual peaks (dips) are strongly associated with El Niño (La Niña) years or events. An inverse relationship exists between total precipitation and ENSO in the North ITCZ (nITCZ), Southwest SPCZ (swSPCZ), Subtropics (ST) and WPM subregions. In the swSPCZ subregion, greatest precipitation suppression is generally in the

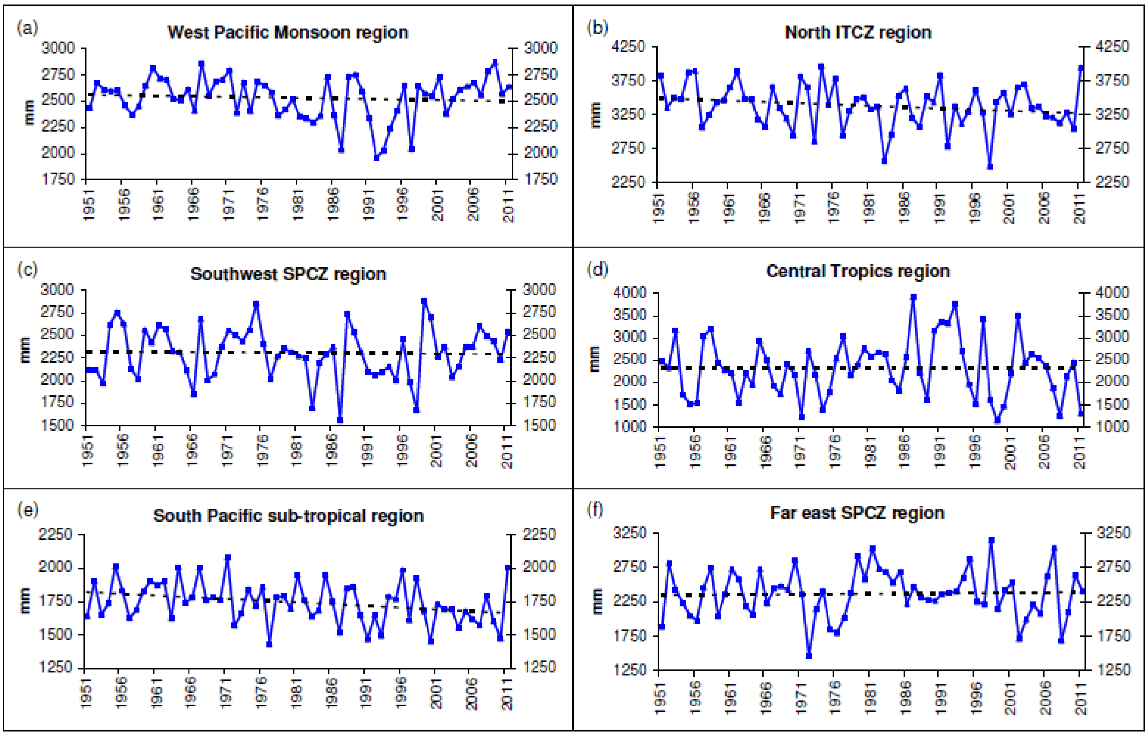


Figure 3.16 Subregional time series for total precipitation (units: mm). Dashed line indicates ordinary least squares fit. (a) WPM, (b) North ITCZ (nITCZ), (c) Southwest SPCZ (swSPCZ), (d) Central Tropics (CT), (e) South Pacific subtropics (SPCZ)

Table 3.6 Relationship between annual average SOI and the variance adjusted subregional (annual) total precipitation and precipitation indices for the period 1951–2011. Trends significant at the 5% level presented in bold print.

| | **North ITCZ** | **Central tropics** | **WPM** | **Southwest SPCZ** | **Far east SPCZ** | **South Pacific subtropics** |
|---|---|---|---|---|---|---|
| **Total precip-itation** | **0.334** | **-0.828** | **0.585** | **0.710** | -0.149 | **0.481** |
| **Rx1day** | -0.242 | **-0.473** | -0.150 | -0.001 | -0.123* | **0.306** |
| **Rx5day** | **-0.263** | **-0.489** | -0.028 | 0.242 | -0.032* | **0.420** |
| **R1mm** | **0.691** | **-0.809** | **0.683** | **0.758** | **0.425*** | **0.535** |
| **R10mm** | **0.597** | **-0.815** | **0.675** | **0.755** | 0.148* | **0.654** |
| **R20mm** | **0.483** | **-0.803** | **0.614** | **0.728** | -0.074* | **0.568** |
| **CDD** | **-0.410** | **0.629** | **-0.553** | **-0.722** | -0.109* | -0.199 |
| **CWD** | **0.452** | **-0.445** | **0.252** | **0.525** | 0.249* | 0.138 |
| **R95p** | -0.157 | **-0.723** | 0.229 | **0.482** | -0.177* | **0.511** |
| **R99p** | **-0.290** | **-0.516** | -0.083 | 0.127 | -0.147* | **0.383** |
| **SDII** | -0.121 | **-0.732** | 0.179 | **0.417** | **-0.365*** | **0.527** |

* Data from 1961–2011

year after the El Niño event for example 1998. The reason for this lag is uncertain at the present time.

Total precipitation is positively correlated with local SSTs in the CT (Figure 3.17a), swSPCZ, WPM, nITCZ (eastern portion only) and ST (excluding Norfolk Is.) subregions but not in the feSPCZ and western portions of the nITCZ and ST subregions. With the exception of the CT (where local SSTs are central Pacific SSTs) there is generally an inverse relationship between total precipitation and central and eastern (CE) Pacific SSTs. Similar relationships exist for the threshold indices. In the case of the feSPCZ subregion, a relationship with CE Pacific SSTs that is not apparent for total precipitation is present for R1mm (Figure 3.17b) and to a lesser extent with R10mm. These findings are in general agreement with those in Table 3.6 where the strength of the relationship between the SOI and total precipitation and the extreme precipitation indices are presented.

There is a clear relationship between ENSO (both SOI and SSTs) and local SSTs and the percentile and absolute indices in the CT and ST subregions. ENSO also appears to have a moderate to strong influence on R95p in the swSPCZ subregion (Figure 3.17c; greater R95p associated with La Niña events) and marginal influence (inverse relationship with the SOI) on R99p and Rx5day precipitation in the nITCZ subregion. The SST plots (not presented) show this influence to mainly be in the western portion of the nITCZ region. The relationship between ENSO and the percentile and absolute indices elsewhere is less noteworthy.

The results of the relationship between annual average SOI and total and extreme precipitation analysis (Table 3.6) also show that for some subregions (nITCZ, WPM, swSPCZ and ST) the threshold indices have a stronger relationship with the SOI than total precipitation. This generally does not apply to the more extreme (absolute and percentile) indices in these subregions.

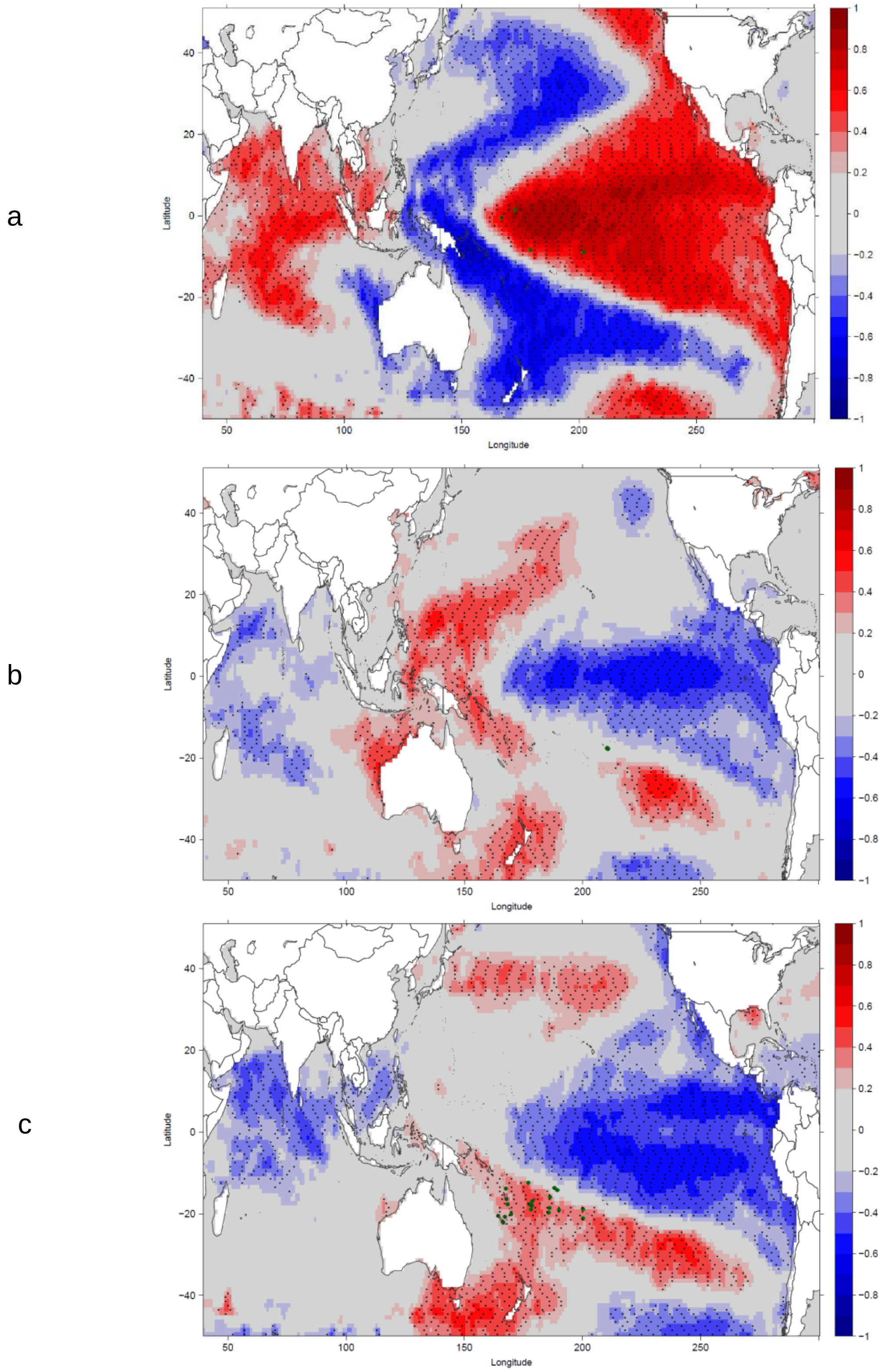


Figure 3.17 Correlation of 1951–2011 regional annual series of HadISST with (a) Total Precipitation in the Central Tropics, (b) R1mm in the Far east SPCZ, and (c) R95p in the Southwest SPCZ subregions. The linear trend has been removed from all series as a means to focus attention on the interannual covariability. Stippling marks significance at the 5% level. Green dots show the sites used for the correlations. The single green dot in (b) represents nine stations in the Society Islands, French Polynesia

## 3.4 Discussion and Conclusion

There is a general perception among Pacific Island communities that changes in weather and climate are occurring in their region. More change is believed to have occurred in the past decade than at any other time in the past. Local perceptions of climate change in their countries include: shifts in seasonal patterns of precipitation and tropical cyclones, more frequent and extreme precipitation causing flooding and mudslides, more drought and fires and more hot days (Australian Bureau of Meteorology and CSIRO 2011).

Changes in mean and extreme temperature documented here are consistent with these perceptions. On a regional scale, we found annual mean temperature increased by 0.14ºC per decade. Trends over 1961–2011 (0.15ºC per decade) were also calculated and compared with that for Whan et al. (2014a, 0.18ºC per decade, 1961–2011) and Jones et al. (2013, 0.16ºC per decade, 1961–2010). Data rescue efforts in recent years, station selection and a weaker positive trend in the last decade (akin to that in the first 15–20 years) are likely responsible for the variance. Increases in mean temperature occurred in all seasons and in both halves of the 1951–2015 study period.

At a regional scale, increases in annual mean maximum and minimum temperature were similar in terms of the rates of increase. Spatially there was little consistency in the annual maximum and minimum temperature trends, although annual minimum temperature trends were markedly stronger east of the Date line. Whether this is a climate phenomenon or the result of unresolved inhomogeneities is unclear. Strong annual mean temperature trends were also present east of the Date line in Jones et al. (2013) and Whan et al. (2014a).

The ET-SCI indices showed strong warming on a regional scale in all seasons. For the percentile-based and absolute indices, the warming was strongest in DJF and lowest in JJA. Both sets of indices showed greatest warming at the upper end of the distribution. According to Whan et al. (2014a) this a recent phenomenon with the reverse occurring in earlier decades.

A noteworthy feature of the new ET-SCI indices is their relevance to industry. The cooling degree days index (CDDcoldn) for example showed a regional scale positive trend of 45.59 degree-days per decade. This suggests electricity demand due to warming alone may have doubled since 1951.

Increase in demand is likely to be even greater when taking into consideration population growth. Noting that in several countries there is limited access to electricity beyond the major towns and cities, and the average income is lower than in the western world, it is likely many Pacific Islanders, especially the elderly, are unable to afford adequate cooling. Higher than normal summer temperatures therefore pose a greater health risk now than they did in the past. Karl and Knight (1997) found that increases in warm nights can contribute substantially to heatwave mortality where air conditioning is uncommon, as the human body depends upon night-time temperatures to cool.

The results of our temperature analyses are largely consistent with global (Alexander et al. 2006), neighbouring (Choi et al. 2009; Caesar et al. 2011) and previous Pacific (Griffiths et al. 2005; Whan et al. 2014a) studies. We found a widespread increase of mean temperature, fewer cool extremes and more warm extremes over the past 65 years, although there were inconsistencies at an index level. For example, the results of this study showed stronger TX90p and TN90p trends (as compared with TX10p and TN10p) which is consistent with the Caribbean (Stephenson et al. 2014) and Indo-Pacific region (Caesar et al. 2011). However, our results contrast with an earlier Indo-Pacific (Choi et al. 2009) study, where TN10p and TN90p trends were strongest, and a Pacific Islands study (Whan et al. 2014a), where there was little difference between the four percentile indices. While differences may be partially due to station selection and an increase in data availability in recent years, Nicholls et al. (2005), found the numbers of warm nights and hot days increased substantially across most of the east Asia–west Pacific region in the year after the onset of El Niño events, while the number of cool days and cold nights tended to decrease. Further, Nicholls et al. (2005) found that the relationship is confounded, at least for warm nights and hot days, by a strong increasing trend in air temperature and the number of extremes, not matched by a trend in the index of the El Niño.

Changes in total and extreme precipitation were more complex. For the period 1951–2015, positive trends were only identified in annual and MAM precipitation at two locations, both in the central Pacific. Annual, MAM, SON and to a lesser extent the DJF total precipitation maps show an El Niño-like pattern where the ITCZ was displaced south towards the equator and the SPCZ northeast towards the central Pacific. Previous studies have attributed this displacement to ENSO and IPO (Salinger et al. 2001, 2014). Increases in mean annual precipitation of 30% or more occurred northeast of the SPCZ between the most recent positive phase of the IPO (1978–98), and the previous negative phase (1946–77). Trends in precipitation from 1951 with IPO removed show little difference to trends in precipitation with IPO present. This may in part be due to there being a non-significant trend in IPO over 1951–2015.

In addition to longer records, the primary reason our results are different from earlier studies is the switch to a negative IPO phase from 1999 with a recent dominance of La Niña events. This is reflected in trends in total precipitation (both observed and reanalysis data) over 1981–2011. It has become wetter in the WPM region and southwest of the mean SPCZ position. In the tropical north Pacific, it has become wetter west of 160°E with the ITCZ/WPM expanding northwards west of 140°E. Northeast of the SPCZ and in the central tropical Pacific east of about 160°E it has become drier.

A statistically significant drying trend in annual total precipitation since the 1950s in the south Pacific subtropics has previously been identified by Jovanovic et al. (2012). They noted a stronger precipitation decline since 1970 which is confirmed in this study (although the trend is not statistically significant). Negative annual total precipitation trends from 1951 were also found in this study, along with declines in annual CWD and a positive trend in annual CDD. Strong drying trends were identified in the low to moderate extremes indices in JJA and SON in this study. The drying trend was also present in the drought indices that cover the JJA and SON periods.

Declines in annual and DJF total precipitation were found in the Southwest French Polynesia region from 1951. There was a decrease in moderate to high intensity precipitation events, especially those experienced over multiple days in this region. For the multi-day absolute indices, the negative trends occurred in DJF, while for R10mm the negative trends occur in SON and for R20mm in MAM. Declines were also present in the annual percentile-based trends (R95p, R95pTOT, R99p and R99pTOT) and SDII. These negative trends contributed to an increase in meteorological drought (SPI-3 Feb and SPI-6 Apr) over the extended summer period. On the other hand, there was an increase in the R1mm and decrease in CDD in JJA. These results suggest there have been fewer tropical disturbances in the Southwest French Polynesia region in recent decades.

Previous studies associated the drying trend in the western southern subtropics with broader trends seen in parts of southern and eastern Australia. This result is consistent with a general intensification of the subtropical ridge of high pressure and associated declines in baroclinicity (Timbal 2009; Timbal and Drosdowsky 2013; Whan et al. 2014b). Austral summer drying in the Southwest French Polynesia subregion, also shown in 1979–2010 20th Century Reanalysis plots in Fyfe et al. (2012), has been linked with anthropogenic greenhouse gas and ozone changes. A clear poleward shift of the southern hemisphere jet stream has also been observed for DJF in reanalyses (Swart and Fyfe 2012). This is attributed largely to a trend in the Southern Annular Mode driven by ozone depletion (Thompson et al. 2011). Drying in the southern French Polynesia region and further east is also evident in CMIP5 21st Century projections. According to Widlansky et al. (2012) this feature can be related to the anomalous transport of dry subtropical air into the SPCZ region, which is shown to be a result of increased meridional SST gradients in the southeastern tropical Pacific.

On a regional scale, differences in the most extreme daily precipitation (largest 140 values) between 1951–82 and 1983–2015 were not statistically significant. On a station scale there was considerable variability across the region. For the largest 20 values, eleven of 52 stations showed significant change, eight of which were positive, including six within the equatorial region. In response to concerns that the most extreme precipitation has increased in recent decades, we find little evidence of such change at a regional level, but on the subregional level, precipitation increased in the equatorial Pacific over parts of PNG and in the central Pacific (eastern Kiribati, northern Cook Islands and northern French Polynesia region). Clearly at the western Pacific scale it is more difficult to show significant changes in climate.

The results from the 'Total and extreme precipitation relationship with ENSO' analyses (Section 3.3.5) confirm a strong relationship between ENSO and total precipitation and the threshold indices as found in the southeast Asia region (Caesar et al., 2011). The percentile-based and absolute indices are influenced by ENSO to a lesser extent and in some cases the influence is negligible. Undoubtedly, larger-scale SST variability is not the only influence on these indices. The results of this study suggest the negative trends in Rx1day precipitation southwest of the SPCZ over 1981–2011 are associated with reduced tropical cyclone occurrence near the Date Line over the same period. Trends in south Pacific tropical cyclone frequency also show a negative trend but lack significance (Kuleshov et al. 2010).

We note with concern the continued decline in data quality and frequency of observations in the western Pacific. Temperature observations >80% complete are now largely limited to the principal observation stations in each country. Notable absences for this study were recent data for Wewak, Momote and Madang in PNG. These temperature records begin in the 1950s but there are significant gaps in the record in the last decade. Compared to earlier decades, little metadata is being documented and this will continue to hinder the homogenisation of meteorological records in the future. Metadata collection is especially important in the current decade as several Pacific national meteorological services have or are in the process of switching to automated observations.

This study will be followed by an investigation into potential relationships between the ET-SCI indices for selected locations and sectoral data for the same location e.g., sugarcane yield near Nadi Airport, Fiji, stream discharge near Noumea, New Caledonia and possibly copra yield around Tahiti, French Polynesia.

*Acknowledgements.* Approval from the respective heads of the Pacific Island National Meteorological & Hydrological Services for the continued use of their meteorological data is greatly appreciated. The authors are particularly grateful to Dr Blair Trewin for his methodological recommendations and Mr Mark Caughey for his analytical assistance. The authors thank the reviewers for their comments and contributions.

## References

Aguilar, E., and M. Prohom, 2011: RClimDex-extraQC (EXTRAQC Quality Control Software). User Manual, Centre for Climate Change, University Rovira i Virgili, Tarragona, Spain. http://www.c3.urv.cat/data/manual/Manual_rclimdex_extraQC.r.pdf (Accessed March 20, 2016).

——, and Coauthors, 2009: Changes in temperature and precipitation extremes in western central Africa, Guinea Conakry, and Zimbabwe, 1955–2006. *J. Geophys. Res. Atmos.*, **114**, D02115, https://doi.org/10.1029/2008JD011010.

Alexander, L., and N. Herold, 2015: *ClimPACTv2 Indices and Software. A document prepared on behalf of the Commission for Climatology (CCl) Expert Team on Sector-Specific Climate Indices (ET-SCI)*. https://github.com/ARCCSS-extremes/climpact2/blob/master/ClimPACTv2_manual.pdf.

Alexander, L. V, 2016: Global observed long-term changes in temperature and precipitation extremes: A review of progress and limitations in IPCC assessments and beyond. *Weather Clim. Extrem.*, **11**, 4–16, https://doi.org/http://dx.doi.org/10.1016/j.wace.2015.10.007.

Alexander, L. V, and Coauthors, 2006: Global observed changes in daily climate extremes of temperature and precipitation. *J. Geophys. Res. Atmos.*, **111**, D05109, https://doi.org/10.1029/2005JD006290.

Alexander, L. V, P. Uotila, and N. Nicholls, 2009: Influence of sea surface temperature variability on global temperature and precipitation extremes. *J. Geophys. Res. Atmos.*, **114**, https://doi.org/10.1029/2009JD012301.

Australian Bureau of Meteorology, and CSIRO, 2011: *Climate Change in the Pacific: Scientific Assessment and New Research. Volume 1: Regional Review. Volume 2: Country Reports.* http://www.pacificclimatechangescience.org/publications/reports/report-climate-change-in-the-pacific-scientific-assessment-and-new-research/.

——, and ——, 2014: *Climate Variability, Extremes and Change in the Western Tropical Pacific: New Science and Updated Country Reports, Pacific-Australia Climate Change Science and Adaptation Planning Program Technical Report*. Australian Bureau of Meteorology and Commonwealth Scientific and Industrial Research Organisation,.

Barry, R., and R. Chorely, 1992: *Atmosphere, Weather and Climate*. Routledge, 421 pp.

Caesar, J., and Coauthors, 2011: Changes in temperature and precipitation extremes over the Indo-Pacific region from 1971 to 2005. *Int. J. Climatol.*, **31**, 791–801, https://doi.org/10.1002/joc.2118.

Cavarero, V., and Coauthors, 2012: Les évolutions passées et futures du climat de la Nouvelle-Calédonie. *La Mètèorologie*, **8**, 13–21, https://doi.org/10.4267/2042/47371.

Choi, G., and Coauthors, 2009: Changes in means and extreme events of temperature and precipitation in the Asia-Pacific Network region, 1955–2007. *Int. J. Climatol.*, **29**, 1906–1925, https://doi.org/10.1002/joc.1979.

Folland, C. K., J. A. Renwick, M. J. Salinger, and A. B. Mullan, 2002: Relative influences of the Interdecadal Pacific Oscillation and ENSO on the South Pacific Convergence Zone. *Geophys. Res. Lett.*, **29**, 21–24,

https://doi.org/10.1029/2001GL014201.
——, M. J. Salinger, N. Jiang, and N. A. Rayner, 2003: Trends and Variations in South Pacific Island and Ocean Surface Temperatures. *J. Clim.*, **16**, 2859–2874, https://doi.org/10.1175/1520-0442(2003)016<2859:TAVISP>2.0.CO;2.
Fyfe, J. C., N. P. Gillett, and G. J. Marshall, 2012: Human influence on extratropical Southern Hemisphere summer precipitation. *Geophys. Res. Lett.*, **39**, https://doi.org/10.1029/2012GL054199.
Griffiths, G. M., M. J. Salinger, and I. Leleu, 2003: Trends in extreme daily rainfall across the South Pacific and relationship to the South Pacific Convergence Zone. *Int. J. Climatol.*, **23**, 847–869, https://doi.org/10.1002/joc.923.
——, and Coauthors, 2005: Change in mean temperature as a predictor of extreme temperature change in the Asia–Pacific region. *Int. J. Climatol.*, **25**, 1301–1330, https://doi.org/10.1002/joc.1194.
Guerreiro, S. B., H. J. Fowler, R. Barbero, S. Westra, G. Lenderink, S. Blenkinsop, E. Lewis, and X.-F. Li, 2018: Detection of continental-scale intensification of hourly rainfall extremes. *Nat. Clim. Chang.*, https://doi.org/10.1038/s41558-018-0245-3.
Henley, B., J. Gergis, D. Karoly, S. Power, J. Kennedy, and C. Folland, 2015: A Tripole Index for the Interdecadal Pacific Oscillation. *Clim. Dyn.*, 1–14, https://doi.org/10.1007/s00382-015-2525-1.
IPCC, 2001: Climate Change 2001: Impacts, Adaptation and Vulnerability. Contribution of Working Group II to the Third Assessment of the Intergovernmental Panel on Climate Change. J.J. McCarthy, Canziani, O.F., Leary, N.A., Dokken, D.J., White, K.S., Ed., Cambridge University Press, p. 1032.
——, 2012: *Managing the Risks of Extreme Events and Disasters to Advance Climate Change Adaptation. A Special Report of Working Groups I and II of the Intergovernmental Panel on Climate Change*. C.B. Field et al., Eds. Cambridge University Press, 582 pp.
Jones, D. A., and Coauthors, 2013: An updated analysis of homogeneous temperature data at Pacific Island stations. *Aust. Meteorol. Oceanogr. J.*, **63**, 285–302.
Jovanovic, B., K. Braganza, D. Collins, and D. Jones, 2012: Climate variations and change evident in high-quality climate data for Australia's Antarctic and remote island weather stations. *Aust. Meteorol. Ocean. J.*, **62**, 247–261.
Karl, T. R., and R. W. Knight, 1997: The 1995 Chicago Heat Wave: How Likely Is a Recurrence? *Bull. Am. Meteorol. Soc.*, **78**, 1107–1120.
Kenyon, J., and G. C. Hegerl, 2008: Influence of Modes of Climate Variability on Global Temperature Extremes. *J. Clim.*, **21**, 3872–3889, https://doi.org/10.1175/2008JCLI2125.1.
Kim, H.-J., B. Wang, and Q. Ding, 2008: The Global Monsoon Variability Simulated by CMIP3 Coupled Climate Models. *J. Clim.*, **21**, 5271–5294, https://doi.org/10.1175/2008JCLI2041.1.
Kuleshov, Y., R. Fawcett, L. Qi, B. Trewin, D. Jones, J. McBride, and H. Ramsay, 2010: Trends in tropical cyclones in the South Indian Ocean and the South Pacific Ocean. *J. Geophys. Res. Atmos.*, **115**, D01101, https://doi.org/10.1029/2009JD012372.
Lough, J. M., G. A. Meehl, and M. J. Salinger, 2011: Observed and projected

changes in surface climate of the tropical Pacific. *Vulnerability of the tropical Pacific fisheries and aquaculture to climate change*, J.D. Bell, J.E. Johnson, and A.J. Hobday, Eds., Secretariat of the Pacific Community.

Mann, H. B., and D. R. Whitney, 1947: On a Test of Whether one of Two Random Variables is Stochastically Larger than the Other. *Ann. Math. Stat.*, **18**, 50–60, https://doi.org/10.1214/aoms/1177730491.

Manton, M. J., and Coauthors, 2001: Trends in extreme daily rainfall and temperature in Southeast Asia and the South Pacific: 1961–1998. *Int. J. Climatol.*, **21**, 269–284, https://doi.org/10.1002/joc.610.

Mataki, M., K. C. Koshy, and M. Lal, 2006: Baseline Climatology of Viti Levu (Fiji) and Current Climatic Trends. *Pacific Sci.*, **60**, 49–68, https://doi.org/10.1353/psc.2005.0059.

McGree, S., and Coauthors, 2014: An updated assessment of trends and variability in total and extreme rainfall in the western Pacific. *Int. J. Climatol.*, **34**, 2775–2791, https://doi.org/10.1002/joc.3874.

McGree, S., S. Schreider, and Y. Kuleshov, 2016: Trends and Variability in Droughts in the Pacific Islands and Northeast Australia. *J. Clim.*, **29**, 8377–8397, https://doi.org/10.1175/JCLI-D-16-0332.1.

McKee, T. B., N. J. Doeskin, and J. Kleist, 1993: The relationship of drought frequency and duration to time scales. *8th Conf. on Applied Climatology*, Anaheim, Canada, 179–184.

Murphy, B. F., S. B. Power, and S. McGree, 2014: The Varied Impacts of El Niño–Southern Oscillation on Pacific Island Climates. *J. Clim.*, **27**, 4015–4036, https://doi.org/10.1175/JCLI-D-13-00130.1.

Nairn, J. R., and R. J. B. Fawcett, 2015: The Excess Heat Factor: A Metric for Heatwave Intensity and Its Use in Classifying Heatwave Severity. *Int. J. Environ. Res. Public Health*, **12**, 227–253, https://doi.org/10.3390/ijerph120100227.

Nicholls, N., and Coauthors, 2005: The El Niño–Southern Oscillation and daily temperature extremes in east Asia and the west Pacific. *Geophys. Res. Lett.*, **32**, 1–4, https://doi.org/10.1029/2005GL022621.

Page, C. M., and Coauthors, 2004: Data rescue in the Southeast Asia and south Region. Challenges and opportunities. *Bull. Am. Meteorol. Soc.*, **85**, 1483–1489.

Perkins, S. E., 2015: A review on the scientific understanding of heatwaves—Their measurement, driving mechanisms, and changes at the global scale. *Atmos. Res.*, **164–165**, 242–267, https://doi.org/10.1016/j.atmosres.2015.05.014.

Perkins, S. E., and L. V Alexander, 2013: On the Measurement of Heat Waves. *J. Clim.*, **26**, 4500–4517, https://doi.org/10.1175/JCLI-D-12-00383.1.

Peterson, T. C., and M. J. Manton, 2008: Monitoring Changes in Climate Extremes: A Tale of International Collaboration. *Bull. Am. Meteorol. Soc.*, **89**, 1266–1271, https://doi.org/10.1175/2008BAMS2501.1.

Rayner, N. A., D. E. Parker, E. B. Horton, C. K. Folland, L. V Alexander, D. P. Rowell, E. C. Kent, and A. Kaplan, 2003: Global analyses of sea surface temperature, sea ice, and night marine air temperature since the late nineteenth century. *J. Geophys. Res. Atmos.*, **108**, 4407, https://doi.org/10.1029/2002JD002670.

Salinger, M. J., R. E. Basher, B. B. Fitzharris, J. E. Hay, P. D. Jones, J. P. Macveigh, and I. Schmidely-Leleu, 1995: Climate trends in the South-west

Pacific. *Int. J. Climatol.*, **15**, 285–302, https://doi.org/10.1002/joc.3370150305.
——, J. A. Renwick, and A. B. Mullan, 2001: Interdecadal Pacific Oscillation and South Pacific climate. *Int. J. Climatol.*, **21**, 1705–1721, https://doi.org/10.1002/joc.691.
Salinger, M.J., Lefale, P., 2005. The Occurrence and Predictability of Extreme Events over the Southwest Pacific with Particular Reference to ENSO BT - Natural Disasters and Extreme Events in Agriculture: Impacts and Mitigation, in: Sivakumar, M.V.K., Motha, R.P., Das, H.P. (Eds.), . Springer Berlin Heidelberg, Berlin, Heidelberg, pp. 39–49. https://doi.org/10.1007/3-540-28307-2_3.
Salinger, M. J., S. McGree, F. Beucher, S. B. Power, and F. Delage, 2014: A new index for variations in the position of the South Pacific convergence zone 1910/11-2011/2012. *Clim. Dyn.*, **43**, https://doi.org/10.1007/s00382-013-2035-y.
Sen, P. K., 1968: Estimates of the Regression Coefficient Based on Kendall's Tau. *J. Am. Stat. Assoc.*, **63**, 1379–1389, https://doi.org/10.1080/01621459.1968.10480934.
Sillmann, J., V. V Kharin, X. Zhang, F. W. Zwiers, and D. Bronaugh, 2013: Climate extremes indices in the CMIP5 multimodel ensemble: Part 1. Model evaluation in the present climate. *J. Geophys. Res. Atmos.*, **118**, 1716–1733, https://doi.org/10.1002/jgrd.50203.
Stephenson, T. S., and Coauthors, 2014: Changes in extreme temperature and precipitation in the Caribbean region, 1961–2010. *Int. J. Climatol.*, **34**, 2957–2971, https://doi.org/10.1002/joc.3889.
Swart, N. C., and J. C. Fyfe, 2012: Observed and simulated changes in the southern hemisphere surface westerly wind-stress. *Geophys. Res. Lett.*, **39**, https://doi.org/10.1029/2012GL052810.
Thompson, D. W. J., S. Solomon, P. J. Kushner, M. H. England, K. M. Grise, and D. J. Karoly, 2011: Signatures of the Antarctic ozone hole in southern hemisphere surface climate change. *Nat. Geosci.*, **4**, 741.
Timbal, B., 2009: The continuing decline in South-East Australian rainfall — update to May 2009. *CAWCR Res. Lett.*, **2**, 4–12.
——, and W. Drosdowsky, 2013: The relationship between the decline of Southeastern Australian rainfall and the strengthening of the subtropical ridge. *Int. J. Climatol.*, **33**, 1021–1034, https://doi.org/10.1002/joc.3492.
Trenberth, K. E., 1976: Spatial and temporal variations of the Southern Oscillation. *Q. J. R. Meteorol. Soc.*, **102**, 639–653, https://doi.org/10.1002/qj.49710243310.
Trewin, B., 2010: Exposure, instrumentation, and observing practice effects on land temperature measurements. *Wiley Interdiscip. Rev. Clim. Chang.*, **1**, 490–506, https://doi.org/10.1002/wcc.46.
——, 2013: A daily homogenized temperature data set for Australia. *Int. J. Climatol.*, **33**, 1510–1529, https://doi.org/10.1002/joc.3530.
Vicente-Serrano, S. M., S. Beguería, and J. I. López-Moreno, 2010: A Multiscalar Drought Index Sensitive to Global Warming: The Standardized Precipitation Evapotranspiration Index. *J. Clim.*, **23**, 1696–1718, https://doi.org/10.1175/2009JCLI2909.1.
Vincent, D. G., 1994: The South Pacific Convergence Zone (SPCZ): A Review. *Mon. Weather Rev.*, **122**, 1949–1970, https://doi.org/10.1175/1520-

0493(1994)122<1949:TSPCZA>2.0.CO;2.
Vincent, L. A., X. L. Wang, E. J. Milewska, H. Wan, F. Yang, and V. Swail, 2012: A second generation of homogenized Canadian monthly surface air temperature for climate trend analysis. *J. Geophys. Res. Atmos.*, **117**, n/a--n/a, https://doi.org/10.1029/2012JD017859.
Waliser, D. E., and C. Gautier, 1993: A Satellite-derived Climatology of the ITCZ. *J. Clim.*, **6**, 2162–2174, https://doi.org/10.1175/1520-0442(1993)006<2162:ASDCOT>2.0.CO;2.
Wang, X. L., 2003: Comments on “Detection of Undocumented Changepoints: A Revision of the Two-Phase Regression Model.” *J. Clim.*, **16**, 3383–3385, https://doi.org/10.1175/1520-0442(2003)016<3383:CODOUC>2.0.CO;2.
——, 2008a: Accounting for Autocorrelation in Detecting Mean Shifts in Climate Data Series Using the Penalized Maximal t or F Test. *J. Appl. Meteorol. Climatol.*, **47**, 2423–2444, https://doi.org/10.1175/2008JAMC1741.1.
——, 2008b: Penalized Maximal F Test for Detecting Undocumented Mean Shift without Trend Change. *J. Atmos. Ocean. Technol.*, **25**, 368–384, https://doi.org/10.1175/2007JTECHA982.1.
Wang, X. L., and Y. Feng, 2013: *RHtestsV4 User Manual*. 28 pp. http://etccdi.pacificclimate.org/software.shtml.
Wang, X. L., Q. H. Wen, and Y. Wu, 2007: Penalized Maximal t Test for Detecting Undocumented Mean Change in Climate Data Series. *J. Appl. Meteorol. Climatol.*, **46**, 916–931, https://doi.org/10.1175/JAM2504.1.
——, H. Chen, Y. Wu, Y. Feng, and Q. Pu, 2010: New Techniques for the Detection and Adjustment of Shifts in Daily Precipitation Data Series. *J. Appl. Meteorol. Climatol.*, **49**, 2416–2436, https://doi.org/10.1175/2010JAMC2376.1.
Whan, K., and Coauthors, 2014a: Trends and variability of temperature extremes in the tropical Western Pacific. *Int. J. Climatol.*, **34**, https://doi.org/10.1002/joc.3861.
Whan, K., B. Timbal, and J. Lindesay, 2014b: Linear and nonlinear statistical analysis of the impact of sub-tropical ridge intensity and position on south-east Australian rainfall. *Int. J. Climatol.*, **34**, 326–342, https://doi.org/10.1002/joc.3689.
Widlansky, M. J., A. Timmermann, K. Stein, S. McGregor, N. Schneider, M. H. England, M. Lengaigne, and W. Cai, 2012: Changes in South Pacific rainfall bands in a warming climate. *Nat. Clim. Chang.*, **3**, 417.
WMO, 2012: *Standardized Precipitation Index User Guide (M. Svoboda, M. Hayes and D. Wood) WMO-No.1090*. 24 pp. http://www.wamis.org/agm/pubs/SPI/WMO_1090_EN.pdf.
Zhang, X., and F. Yang, 2004: RClimDex (1.0) user manual. http://etccdi.pacificclimate.org/software.shtml (Accessed February 20, 2016).
Zhang, X., L. A. Vincent, W. D. Hogg, and A. Niitsoo, 2000: Temperature and precipitation trends in Canada during the 20th century. *Atmosphere-Ocean*, **38**, 395–429, https://doi.org/10.1080/07055900.2000.9649654.
——, and Coauthors, 2005: Trends in Middle East climate extreme indices from 1950 to 2003. *J. Geophys. Res. Atmos.*, **110**, D22104, https://doi.org/10.1029/2005JD006181.
——, L. Alexander, G. C. Hegerl, P. Jones, A. K. Tank, T. C. Peterson, B. Trewin, and F. W. Zwiers, 2011: Indices for monitoring changes in

extremes based on daily temperature and precipitation data. *Wiley Interdiscip. Rev. Clim. Chang.*, **2**, 851–870, https://doi.org/10.1002/wcc.147.

Zhou, Y., and G. Ren, 2011: Change in extreme temperature event frequency over mainland China, 1961−2008 . *Clim. Res.*, **50**, 125–139.

# 4 On the Use of Mean and Extreme Climate Indices to Predict Sugar Yield in Western Fiji

The primary aim of this study is to determine the magnitude of the influence of mean and extreme climate on agricultural productivity in western Fiji. Sugarcane is one of Fiji's largest commercial agricultural crops and greater than 80% of the raw sugar produced is exported. There has been a statistically significant decline in sugar yield since 1975. The proportion of sugar extracted from sugarcane has also declined over the same period. The role of climate in these changes is investigated by first using principal component analysis then stepwise regression to predict sugarcane and sugar yield. ‘Mild drought conditions’, an increase in the diurnal temperature range and cool conditions during the ripening and maturation period are favourable for sugar yield. The impact of future warmer, wetter and drier conditions on sugar yield is also examined. Results show declines in sugar yield with an increase in mean and extreme temperature.

The contents of this chapter have been published in the following peer-reviewed journal. The first author has produced >95% of the work presented:

McGree, S., Schreider, S., Kuleshov, Y., Prakash, B., 2020. On the use of mean and extreme climate indices to predict sugar yield in western Fiji. Weather Clim. Extrem. 29, 100271. https://doi.org/https://doi.org/10.1016/j.wace.2020.100271

## 4.1 Introduction and Background

Pacific Island countries and territories already face a range of challenges in maintaining adequate food security and sustaining commodity exports. Continued population growth with urbanisation, low or stagnant agricultural production/yields and environmental degradation are all risks to food security. The region also faces intense international competition with regards to exports, and the income from most of these products has been relatively flat or falling for some time (SPC, 2011). Climate change is likely to present an additional set of challenges for the agriculture sector, particularly in terms of managing the projected increase in the frequency and intensity of extreme weather events (Taylor et al., 2016). To secure and optimise yields in a changing climate, it is crucial to understand the impact of climate extremes on crop yields in the past and present climate (Vogel et al., 2019).

Investigations into the impacts of extreme weather and climate events on crop yields for individual regions for which high-resolution yield and climate data are available are becoming increasingly common including using statistical (Chakraborty et al., 2019; Troy et al., 2015; Vogel et al., 2019) and biophysical models driven with the same data (e.g., Lobell and Burke, 2010; Salehnia et al., 2020). To date, such studies have largely been undertaken in developed countries in continental settings. To our knowledge, a study modelling crop yield using mean and climate extremes indices has not been undertaken at a small island scale to date.

The aim of this study is to examine sugarcane and sugar yield variability and change since 1975 in western Fiji, model sugarcane and sugar yield using mean and extreme climate variables and use the resulting sugar model to determine the impact of a warmer, wetter and drier climate on future sugar production.

### 4.1.1 Location, climatology and recent changes in climate

Fiji is located in the tropical southwest Pacific Ocean (Figure 4.1, insert) and is made up of 322 islands covering 18,275 square kilometres in land area (Figure 4.1). The two largest islands Viti Levu (bottom left) and Vanua Levu (top right) make up 87% of the land mass. Both islands have mountains rising about 1000–1300m that have a significant impact on the nation’s climate (Terry and Raj, 2002).

Fiji lies in the trade wind belt of predominantly southeasterly winds with the trades relatively strong and persistent during the cool/dry season from May and October. Wind direction has a significant influence on air temperature and precipitation occurrence (FMS, 1995). Air temperatures strongly reflect temperature of the surrounding ocean. Coastal annual mean maximum air temperatures are between 28 and 31°C with annual mean minimum air temperature between 20 and 24°C. On the northwest leeward sides of the main islands, where sugarcane is grown, maximum temperatures rise 1–2°C

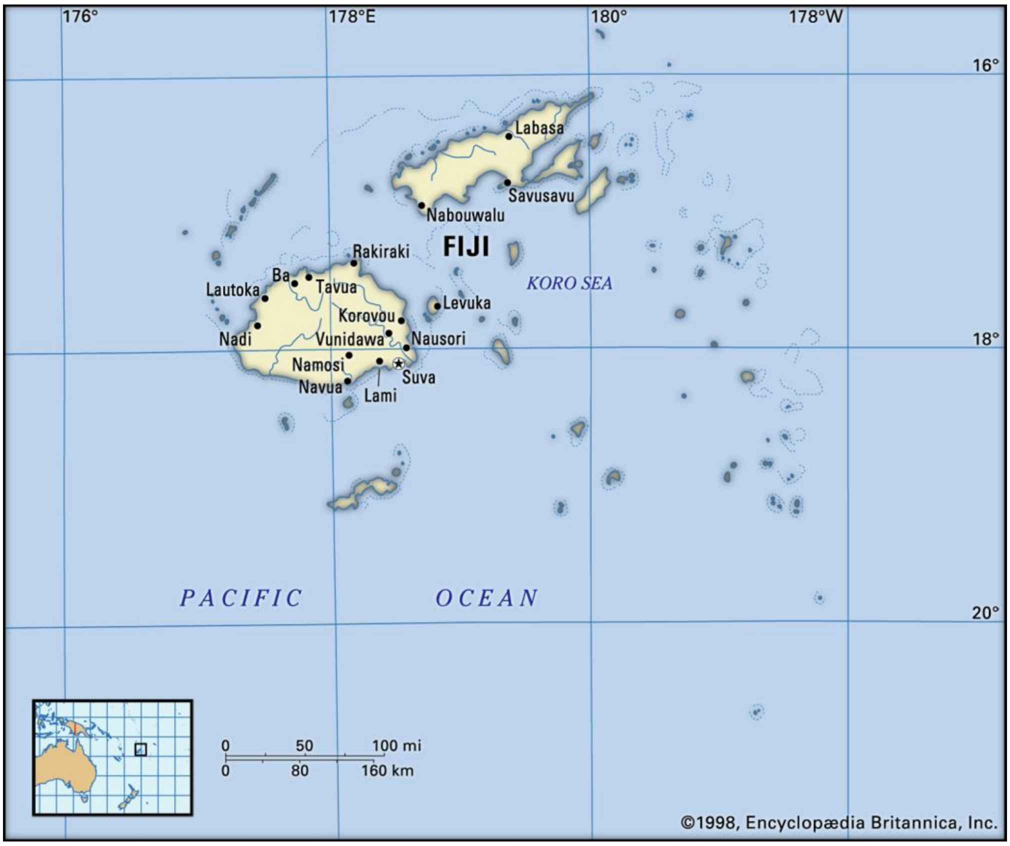


Figure 4.1 Map of Fiji (Source: Macdonald and Foster, 2019)

above those on the leeward side of the islands. Seasonal air temperature range is small, in the order of 2–4°C between the coolest and warmest months (Kumar et al., 2013).

Fiji's sugarcane plantations are largely located in the driest parts of the two main islands. On the western and northwestern coast of Viti Levu less than 2000mm is received on average annually. On the north coast (near Rakiraki) and further inland in western and northern Viti Levu and for most of Vanua Levu the sugarcane plantations receive up to 2500mm. The distribution of precipitation is strongly seasonal with a pronounced maximum during the warmest months, November to April (FMS, 1995). The islands precipitation is subject to large interannual climate variability, mostly associated with El Niño – Southern Oscillation (ENSO, droughts tend to be associated with El Niño events) extremes (Salinger et al., 2001) and directly attributable to shifts in the South Pacific Convergence Zone (SPCZ) (Folland et al., 2002). Seasonal change in precipitation is closely associated with movement in the SPCZ. Fiji also lies in an area often traversed by tropical cyclones. The tropical cyclone season coincides with the wet season and on average 10–12 tropical cyclones affect the country per decade (FMS, 1995).

Over the 65 years to 2015, Fiji's annual mean temperature increased by 0.85°C, with annual mean maximum and minimum temperatures rising at a similar rate. On a seasonal basis, the strongest mean maximum and minimum temperature warming took place over December to February, with the weakest over June to August (McGree et al., 2019). With the exception of negative trends for selected extreme precipitation indices over June to August and September to November at selected locations, there has been little change in total and extreme annual and seasonal precipitation over the last 65 years (McGree et al., 2019).

### 4.1.2 Sugarcane in Fiji and climatic factors affecting sugarcane and sugar production

Sugarcane was the mainstay of Fiji's economy for more than a century (Reddy, 2003) and remains one of Fiji's largest commercial crops today (Singh, 2020). In 2017, 1.63 million tonnes of sugarcane was crushed from an area of 38,040 ha. Greater than 80% of the main product, raw sugar, is exported, mostly at premium prices under preferential arrangements with importers. This accounted for around 10% of country's total exports (FSC, 2019). The sugar industry also plays a significant role in generating internal food supply as cane farmers produce agricultural crops and livestock for their own consumption as well as for cash sale alongside sugarcane production (Reddy, 2003).

Sugarcane has a long growth-maturity period of about 12–15 months (Gawander, 2007) that encounters the complete annual climate cycle. In Fiji, there are two planting seasons. The first is from March to mid-May and the second in September and October. Sugarcane has four-growth phases: germination, tillering (formative), grand growth and maturity and ripening. Under field conditions germination starts from seven to 10 days and usually lasts for about 30–35 days. Warm, moist soil ensures rapid germination. Tillering starts from around 40 days after planting and may last up to 120 days. The grand growth phase starts from 120 days after planting and lasts up to 270 days in a 12-month crop. Drip irrigation, fertigation and warm, humid and sunny climatic conditions favour better cane elongation. Moisture stress reduces internodal length. A temperature around 30°C with a humidity of around 80% is most conducive for good growth. Ripening and maturation phase in a 12-month crop lasts for about three months starting from 270 to 360 days. Ample sunshine, clear skies cool nights and warm days (i.e., more diurnal variation in temperature) and dry weather are highly conducive for ripening (Hogarth and Allsopp, 2000; NETAFIM, 2019; SRA, 2018).

In Fiji, November to March is the grand growth phase and is locally known as the growing season (Koshy et al., 2003). The harvesting season is between June to December in the second year, with the peak ripening season, September and October, within the harvesting season (making delayed harvests favourable). Sugarcane planted late is typically harvested late in the harvesting season (Koshy et al., 2003). The crop planted March to mid-May tends to be well established before it receives essential precipitation during the wet season which is not the case for the latter planted crop (Gawander, 2007).

A majority of the sugarcane harvested each year (80–90%) is ratoon crop which is ‘re-harvested’ for several years (Gawander et al., 2018) at roughly about the same time each year. Ratooning involves cutting most of the above-ground portion but leaving the roots and the growing shoot apices intact to allow the plant to recover/re-sprout and produce a fresh crop in the next season (Hogarth and Allsopp, 2000).

There are several important aspects to sugarcane production, vital to this study. The ideal conditions for sugarcane are a long, warm growing season with a high incidence of solar radiation with adequate precipitation and few to no instances of high winds (Hogarth and Allsopp, 2000). It is essential this be followed by a fairly dry, sunny and cool season for ripening and harvesting. High precipitation during the ripening period is undesirable as it results in poor juice quality (less sugar content), encourages vegetative growth, formation of water shoots and increase in the tissue moisture (Hogarth and Allsopp, 2000). In Fiji, sugarcane is totally rainfed (Gawander et al., 2018), resulting in the crop on occasion being moisture constrained.

Solar radiation is the energy source for photosynthesis and evaporative loss of water from soil and leaf surfaces. Radiation cannot be effectively managed or conserved for crop production. Ideal crop management is directed at optimising interception of radiation by the leaves (SRA, 2018). In Fiji, growers are encouraged to plant the crop by the end of May so that the canopy is closed by mid-late spring and the plant intercepts maximum solar radiation in the warm season (Gawander, 2007).

While radiation provides the energy for photosynthesis, temperature affects the rate of photosynthesis and other biochemical processes governing growth and development. With sugarcane, photosynthetic efficiency increases in a linear manner with temperature in the range from 8 to 34°C. At the upper end, the rate of photosynthesis declines rapidly above 34°C (SRA, 2018). The effect of temperature on sugar production is well recognised in that when leaf growth is constrained at temperatures less than 14–19°C, the available photosynthesis is partitioned to sugar accumulation rather than vegetative growth (SRA, 2018). This explains the role of lower temperature in ripening of sugarcane. Sugar production is also enhanced by a wider range in diurnal temperatures for any given accumulation of thermal time (SRA, 2018). In addition, stalk elongation tends to be more sensitive to lower temperatures than photosynthetic rates (Gawander, 2007).

## 4.2 Data and Methods

### 4.2.1 Data

Yield data in the form of tonnes sugar, tonnes sugarcane and planted land area (in hectares) were obtained for Fiji's sugar mills from the Fiji Sugar Corporation (FSC) and Sugar Research Institute of Fiji (SRIF), Lautoka for the period 1975–2018. Although pre-1975 sugarcane yield data exists, as shown in Figure 3 of Gawander et al. (2018), attempts to obtain this data were unsuccessful. There are currently three sugar mills in Fiji. Lautoka and Rarawai are located on the island of Viti Levu and Labasa on the island of Vanua Levu. A third mill known as Penang (near Rakiraki) on Viti Levu is no longer operational as it was badly damaged during a tropical cyclone in 2016. Sugarcane from the Penang area is now crushed at Rarawai. Only Lautoka yield is used in this study as, the Rarawai yield timeseries is inhomogeneous with the recent inclusion of cane from the Penang milling area, Rarawai milling area boundaries have changed over time and high-quality climate data is not available for the Labasa milling area. Approximately a third of Fijian sugarcane has been crushed at the Lautoka Mill since 2017.

The Nadi Airport meteorological observation site is currently located at the head office of the Fiji Meteorological Service (FMS). Since its establishment in 1942, recordings have been undertaken by highly trained observers. It is located approximately 40km from the northern and 70km from the southern boundary of the Lautoka Mill area (Figure 4.1) and is largely representative of the climate of the Lautoka milling area.

Nadi Airport homogenised daily precipitation, maximum and minimum temperature data from 1974 to 2015 were obtained from the Australian Bureau of Meteorology, Pacific Climate Change Data Portal, www.bom.gov.au/climate/pccsp. Additional Nadi Airport data to 2019, and sunshine and radiation recordings for the same period, were obtained from the FMS. Details on the quality control and homogenisation methodology are presented in McGree et al. (2019). The process of quality control indentifies out of range values based on fixed threshold ranges, outliers based on interquartile range exceedance, coherence between maximum and minimum temperatures (Tmax > Tmin) and consecutive equal values. No major quality control issues were indentified for Nadi Airport. The Nadi Airport precipitation timeseries was found to be homogeneous from 1951 and is therefore no different to the raw quality-controlled record. Two discontinuities in the maximum temperature (Dec. 1985 and Mar. 1998) and two discontinuities in the minimum temperature (May 1965 and Mar. 1998) timeseries were detected. These discontinuities were associated with observation site changes. Both temperature timeseries were adjusted to match the climatology of the current observation site.

The authors acknowledge that the use of one yield and one climate series timeseries to represent a study region is unusual, but obtaining high-quality data in a developing country is challenging. To determine how well Nadi Airport represents the Lautoka Mill area, correlation analyses were applied to annual and seasonal precipitation, maximum and minimum temperature for Nadi Airport and other station records in the milling area (even though lower quality observations). The results showed strong positive correlations, significant at the 99% level.

Nadi Airport gauge precipitation was also compared with satellite observations (TRMM_3B43, v7 dataset, 1998–2019) covering the Lautoka Mill area, obtained from the NASA Goddard Earth Sciences Data and Information Services Center, https://disc.gsfc.nasa.gov/datasets/ TRMM_3B43_7/summary. Strong positive correlation coefficients were found significant at the 99% level. Of concern, though, were the differences in the Nadi Airport gauge and satellite data annual climatologies. While the latter adequately captures seasonal variability, a significant underestimation of precipitation in the wettest months (maximum of 23% in January) as well as an overestimation of precipitation in the driest months (maximum of 46% in June) was found. Chen et al. (2013) and Deo et al. (2017) highlight the inability of TRMM_3B42 observations (the daily and subdaily equivalent of 3B43) to adequately capture high intensity precipitation events on coastal and island high elevation sites in the Pacific. Based on these results satellite data were deemed unsuitable for this study.

### 4.2.2 Methods

#### 4.2.2.1 Calculation of ET-SCI indices, total precipitation and mean temperature timeseries

The World Meteorological Organization (WMO) Commission for Climatology (CCl) Expert Team on Sector-specific Climate Indices (ET-SCI) www.wmo.int/pages/prog/wcp/ccl/opace/opace4/ET-SC I-4-1.php, in cooperation with sectoral experts in agricultural meteorology, water resources and health, has identified and evaluated sector-specific indices, both single- and multi-variable types, to define both simple and complex climate risks of interest to user groups.

The ET-SCI indices for Nadi Airport, referred to as extremes indices in this study, were calculated using ClimPACTv2 (Alexander and Herold, 2015) on the Nadi Airport homogenised series (McGree et al., 2019). ClimPACTv2 facilitates the calculation of over 60 ET-SCI sector-specific (including Expert Team on Climate Change Detection and Indices, ETCCDI) indices. Only indices relevant to Fiji’s climate are used in this study. A descriptive list of the indices used in this study is presented in Table 4.1. Details on the full set of ClimPACTv2 indices are available at https://github.com/ARCCSS-extremes/climpact2.

Table 4.1 Core and additional ClimPACTv2 indices used in this study. Index codes in italics refer to those that are also ETCCDI indices. Duration of bright sunshine is presented as an additional variable.

| **Index Codes** | **Definition** | **Units** |
|---|---|---|
| txgt50p | Percentage of days where maximum temperature > 50th percentile | % |
| txge30 | Number of days when maximum temperature ≥ 30ºC | days |
| *dtr* | Diurnal temperature range (difference between maximum and minimum temperature) | ºC |
| *tmm* | Mean mean temperature | ºC |
| *tnn* | Lowest minimum temperature | ºC |
| *tnx* | Highest minimum temperature | ºC |
| *tnm* | Mean minimum temperature | |
| *txx* | Highest maximum temperature | ºC |
| *txn* | Lowest maximum temperature | ºC |
| *txm* | Mean maximum temperature | |
| *tx10p* | Percentage of time when maximum temperature < 10th percentile (Cool days) | % |
| *tx90p* | Percentage of time when maximum temperature > 90th percentile (Warm days) | % |
| *tn10p* | Percentage of time when minimum temperature < 10th percentile (Cool nights) | % |
| *tn90p* | Percentage of time when minimum temperature > 90th percentile (Warm nights) | % |
| *cdd* | Maximum number of consecutive dry days (precipitation < 1.0mm) | days |
| *cwd* | Maximum number of consecutive wet days (precipitation ≥ 1.0mm) | days |
| *prcptot* | Annual total wet day precipitation (where precipitation is ≥ 1mm) | mm |
| *r10mm* | Precipitation days ≥ 10mm | days |
| *r20mm* | Precipitation days ≥ 20mm | days |
| *rnnmm* | Precipitation days ≥ *nn.* For this study nn = 1mm (Wet day) | days |
| *rx1day* | Maximum 1-day precipitation | mm |
| *rx5day* | Maximum 5-day precipitation | mm |
| rxdday | Maximum *d*-day precipitation. For this study d = 2 days | mm |
| sun | Mean bright sunshine duration | hrs |

ClimPACTv2 outputs the indices in monthly and annual format. Annual indices we also excluded as the sugar cropping cycle does not span the calendar year. Three-month seasonal indices were calculated from monthly values. These were December to February (DJF), March to May (MAM), June to August (JJA), September to November (SON). Duration of bright sunshine data were obtained from the FMS as mean monthly hours of sunshine. Seasonal totals were computed as for the ET-SCI indices. Radiation data were not used due to the large amount of missing data. In total there were 360 climate timeseries. As presented previously, the growth cycle for sugarcane is more than 12 months. This study assumes optimum yield is associated with climate conditions in the final 12 months of sugarcane growth.

#### 4.2.2.2 Selecting predictor variables

As some of the mean and extreme climate variables are highly correlated, multicollinearity needed to be overcome as multicollinearity can affect the extra sums of squares, fitted values and predictions, regression coefficients, and many other parts of multiple linear regression (Kutner et al., 2004). Principal component analysis (PCA) caters for multicollinearity and can be used to reduce the number of climate variables which can be used as variables for modelling sugarcane and sugar yield. PCA is a dimension reduction tool that can be used to reduce a set of correlated predictor variables into a smaller number of uncorrelated variables, ‘principal components’, that still contains most of the information in the larger set. The transformation is defined in such a way that the first principal component captures the largest possible variance, and each succeeding component in turn has the highest variance possible under the constraint that it is orthogonal (uncorrelated) to the preceding components (Kutner et al., 2004).

Prior to running PCA the climate variables were standardised (to mean of zero and standard deviation of 1) as the correlation matrix was used to calculate the principal components. This was essential as the scales of the variables were different.

A scree plot (line plot of the principal components) was used to determine the number of principal components to retain that account for most of the variation. A plot of cumulative variance is presented as Figure 4.2. With no obvious ‘elbow’ before PC32, 100% of the variance or 32 principal components (PCs) were retained. An additional reason for retaining 100% of the variance, is the PCs reflect the variance in Nadi Airport climate, not just the aspects of climate that are important for sugarcane production. Therefore, it is possible the first few PCs do not have role in sugarcane production. The alternative would have been to undertake PCA on climate variables that have a statistically significant relationship with sugarcane and sugar, however, this introduces bias into the analyses.

To interpret each PC, the magnitude and direction of the coefficients for the original variables were examined. The larger the value of the coefficient, the more important the corresponding variable is in calculating the component. The climate variable selected to represent each PC was the one most correlated with the PC timeseries.

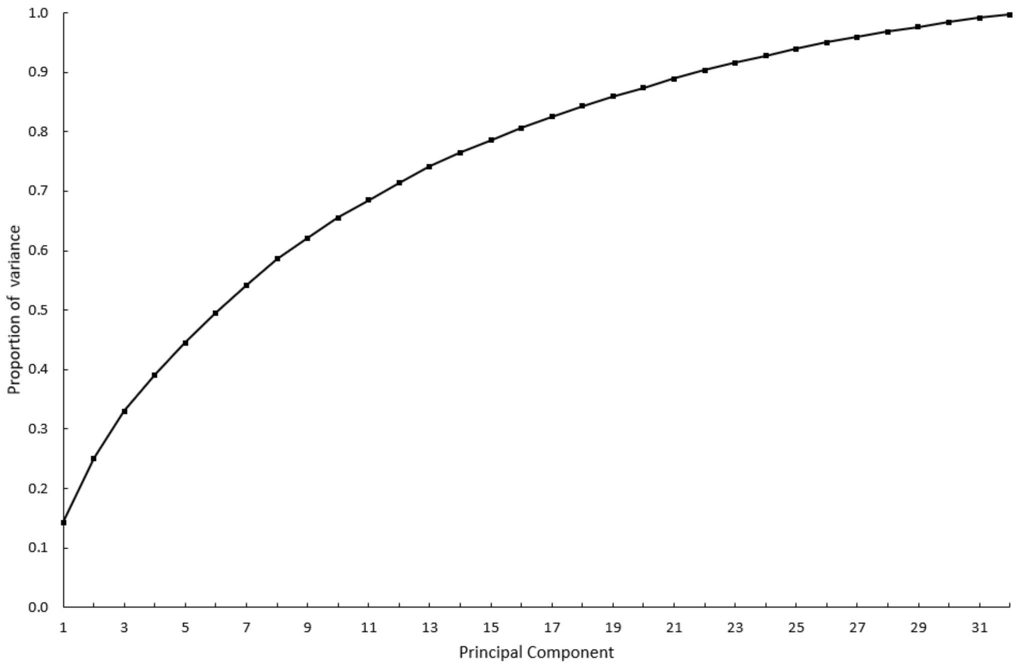


Figure 4.2 Cumulative scree plot for Nadi Airport climate variables

#### 4.2.2.3Multiple linear regression

Stepwise regression backward elimination was used to obtain optimal models and reduce the number of model terms. Backward elimination starts with all the potential terms and removes the least significant term for each step (Draper and Smith, 1981). The step selected was the one with the highest (leave-one out) cross-validated R squared (R-sq) value. The authors note alternative methods for obtaining optimum models such as that proposed by DelSole and Shukla (2009). Both methods have advantages and disadvantages. The method used in this study is less intensive.

As the climate variables and sugar yield timeseries are non-stationary over the study period they were detrended prior to applying stepwise regression by subtracting the trend multiplied by time where t is 0 for 1975, t is 1 for 1976 and so on.

## 4.3 Results and Discussion

### 4.3.1 Variability and change in Lautoka Mill yield

For the period 1975 to 2018, the annual mean, standard deviation and range for sugarcane were 50.64, 9.59, 41.72 tonnes/ha and sugar 5.69, 1.39, 5.72 tonnes/ha, respectively. Annual mean total production was approximately a third of national yield. The trends presented in Figure 4.3a and Figure 4.3c are significant at the 99.9% level and Figure 4.3b at the 95% level.

There has been a decline in sugar (-0.07 tonnes/year, Figure 4.3a) and sugarcane yield (-0.25 tonnes/year, Figure 4.3b) in the last 44 years. Gawander et al. (2018) also found a decline in sugarcane yield over 1961 to 2012 (-0.14 tonnes/year). The proportion of sugar extracted from sugarcane has also declined as shown by the positive trend in the tonnes cane to tonnes sugar ratio (TCTS, +0.07 tonnes/year, Figure 4.3c).

The negative trend in sugarcane yield has strengthened in recent decades. One of several reasons for this is the average age of the ratoon crop, which according to the 2016 FSC annual report is approximately 11 years, whereas the recommended age is less than four. This has apparently had a 'significant impact on yield/hectare' (Singh, 2020). The annual mean TCTS ratio is 9.15, with the ratio increasing from 7.80 in the 10 years to 1985 to 10.16 in the 10 years to 2018. A noticeable interruption in the TCTS trend occurs in 2014 with TCTS remaining below the trend line since that time. This is noted in the 2015 FSC annual report as being due to an improvement in cane production and is perhaps associated with a 'more modern boiling scheme being adopted from India' (FSC, 2015).

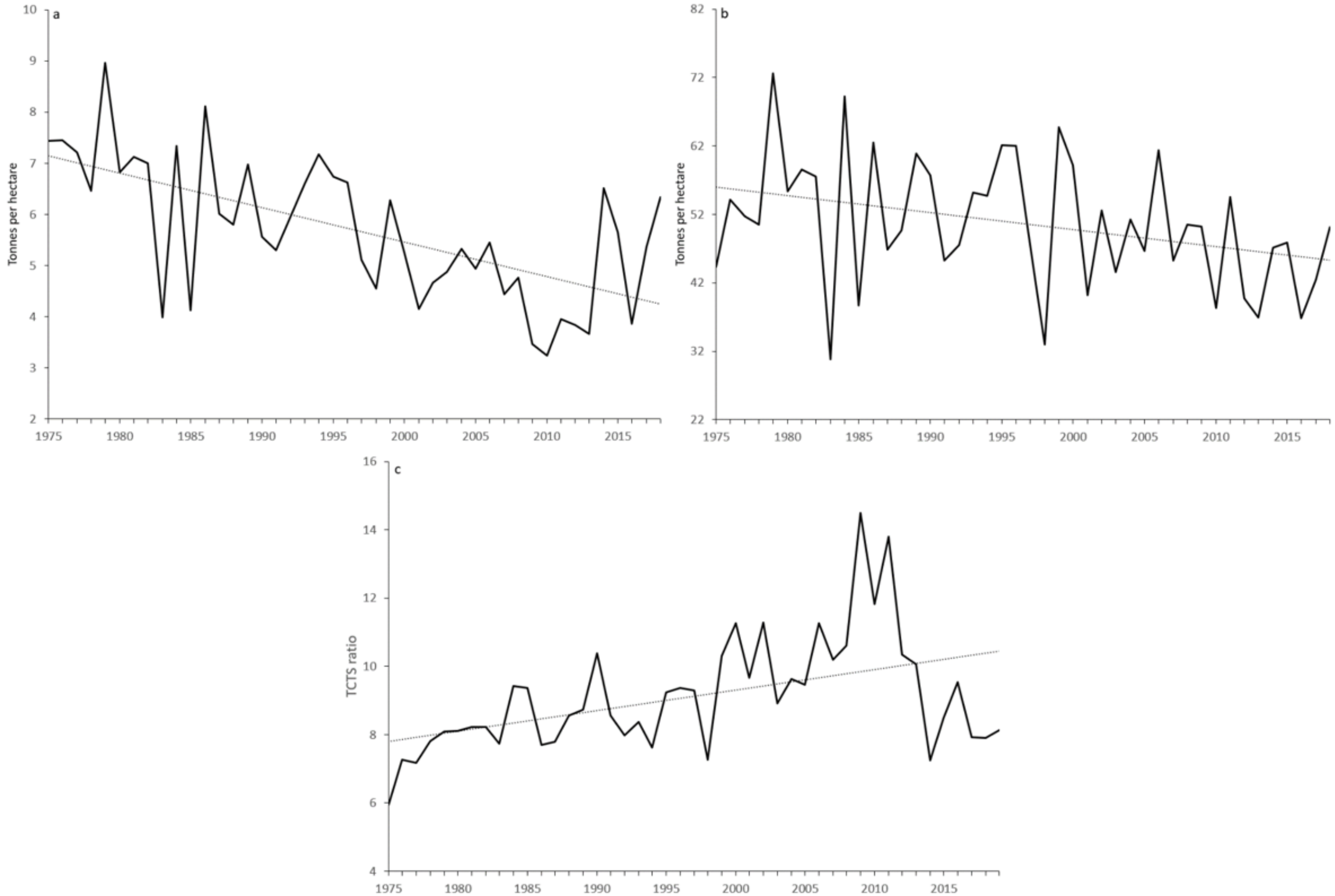


Figure 4.3 Lautoka Mill yield 1975–2018 (a) sugar (b) sugarcane and (c) tonnes sugarcane to tonnes sugar ratio.

### 4.3.2 Modelling sugarcane and sugar yield

From this point forward the focus is on the climate and yield relationship. Multiple linear regression models were created for Lautoka sugarcane and sugar yield using detrended data. Eq. (1) represents the sugarcane model.

$$\text{Sugarcane\_yield} = -90.7 + 6.20\text{txm\_JJA} + 4.34\text{tnn\_Mar} - 0.01746\text{prcptot\_MAM} - 0.535\text{tn90p\_Oct} - 1.143\text{cwd\_Mar} + 1.241\text{r1mm\_Mar} - 7.10\text{tnx\_Jan} - 0.532\text{tx10p\_Mar} + 4.63\text{tnx\_Oct} - 0.1011\text{rx2day\_Oct} - 0.2409\text{cdd\_Jun} + 1.267\text{txn\_Feb} - 1.014\text{cdd\_Apr} - 0.409\text{tn90p\_Jul} - 3.876\text{txn\_May} + 2.237\text{tnn\_DJF} \quad (1)$$

where sugarcane yield is the annual yield of sugarcane (tonnes/ha) and the climate variable terms (and units) are defined in Table 4.2.

Eq. (1) has 16 terms, R-sq 87.4%, adjusted R-sq 79.9% and cross-validated R-sq 66.5%. The maximum variance inflation factors (VIFs) in Table 4.2 are under five indicating low multicollinearity between the model terms. The VIF measures how much the variance of an estimated regression coefficient increases if the climate variables are correlated. A VIF below 10 is considered acceptable.

The terms with the largest effect on the model are rx2day_Oct, txn_May, tnx_Jan, r1mm_Mar and cdd_Apr (Table 4.2). These results suggest that during the late growing season adequate moisture (precipitation) is required for maximum production of sugarcane as is low precipitation and cool conditions during the ripening and maturation period. These findings correspond with known ‘ideal’ climate conditions for sugarcane production summarised in Section 4.1.2. Further, Koshy et al. (2003) refer to ‘mild drought conditions’ as assisting with the ripening process in Fiji. The results also show a negative association between tnx_Jan and sugarcane yield and a positive association between tnn_DJF and tnn_Mar and sugarcane yield which cannot be interpreted at this time. It is possible both unusually warm and cool growing season nights are unfavourable for optimum yield with ideal conditions a narrow climate range in-between. A detailed understanding of sugarcane physiology and further investigation into the relationship between growing season

Table 4.2 Equation 1 coefficients

| **Term** | **Coefficients** | **Standard error coefficients** | **T-Value** | **P-Value** | **VIF** |
|---|---|---|---|---|---|
| Constant | -90.7 | 70.7 | -1.28 | 0.211 | |
| Mean maximum temperature (txm)_June to August (°C) | 6.20 | 1.62 | 3.84 | 0.001 | 2.33 |
| Lowest minimum temperature (tnn)_March (°C) | 4.34 | 1.05 | 4.13 | 0.000 | 2.10 |
| Total wet day precipitation (prcptot)_March to May (mm) | -0.01746 | 0.00503 | -3.47 | 0.002 | 3.56 |
| Percentage of warm nights (tn90p)_October (%) | -0.535 | 0.115 | -4.65 | 0.000 | 4.92 |
| Maximum number of consecutive wet days (cwd)_March (days) | -1.143 | 0.310 | -3.69 | 0.001 | 1.56 |
| Precipitation days ≥ 1mm (r1mm)_March (days) | 1.241 | 0.255 | 4.86 | 0.000 | 2.84 |
| Highest minimum temperature (tnx)_January (°C) | -7.10 | 1.39 | -5.11 | 0.000 | 2.19 |
| Percentage of cool days (tx10p)_March (%) | -0.532 | 0.119 | -4.46 | 0.000 | 1.81 |
| Highest minimum temperature (tnx)_October (°C) | 4.63 | 1.39 | 3.34 | 0.002 | 3.42 |
| Maximum 2-day precipitation (rx2day)_October (mm) | -0.1011 | 0.0171 | -5.93 | 0.000 | 1.27 |
| Maximum number of consecutive dry days (cdd)_June (days) | -0.2409 | 0.0596 | -4.04 | 0.000 | 1.73 |
| Lowest maximum temperature (txn)_February (°C) | 1.267 | 0.634 | 2.00 | 0.056 | 1.68 |
| Maximum number of consecutive dry days (cdd)_April (days) | -1.014 | 0.217 | -4.67 | 0.000 | 2.29 |
| Percentage of warm nights (tn90p)_July (%) | -0.409 | 0.107 | -3.83 | 0.001 | 2.25 |
| Lowest maximum temperature (txn)_May (°C) | -3.876 | 0.737 | -5.26 | 0.000 | 2.33 |
| Lowest minimum temperature (tnn)_December to February (°C) | 2.237 | 0.871 | 2.57 | 0.016 | 1.92 |

temperatures and optimum sugarcane yield is required to confirm the above proposition. Eq. (2) represents the sugar model.

$$\text{Sugar\_yield} = 21.01 + 0.264\text{dtr\_Aug} - 0.2638\text{tnn\_May} - 0.002499\text{prcptot\_MAM} - 0.1751\text{tnn\_Jul} - 0.0276\text{tn90p\_Oct} + 0.1916\text{r1mm\_Mar} - 0.224\text{sun\_Nov} + 0.01131\text{txgt50p\_Nov} - 0.482\text{tnx\_Jan} - 0.1022\text{tx10p\_Mar} - 0.00565\text{rx2day\_Oct} - 0.03316\text{cdd\_Jun} + 0.261\text{txx\_Sep} - 0.4377\text{txn\_May} + 0.403\text{tnn\_DJF} \quad (2)$$

where sugar yield is the annual yield of sugar (tonnes/ha) and the climate variable terms are defined in Table 4.3.

Eq. (2), has 15 terms. R-sq 79.1%, adjusted R-sq 67.2% and cross-validated R-sq 50.6%. The sugar model would appear to be overfitted, however, further reduction of the number of terms decreases both the adjusted R-sq and cross-validated R-sq and increases the difference between the two with the latter a known indicator of overfitting. The highest VIF is 3.16 (Table 4.3). Observed and predicted sugar yield based on Eq. (2) are compared in Figure 4.4.

The terms with the largest effect on the model are tx10p_Mar, r1mm_Mar, txn_May, cdd_Jun and prcp_MAM. As for the sugarcane model, these and other terms suggest a warm late growing season with adequate moisture is favourable for sugar yield, as are low precipitation, an increase in the diurnal temperature range and cool conditions during the ripening and maturation period. The negative prcp_MAM association with sugar yield appears inconsistent with the positive association for r1mm_Mar. This may reflect the transition from growing to ripening period.

A similar moisture contradiction is shown for sugarcane where there is a positive association with yield for r1mm_Mar but a negative association for cwd_Mar. These results suggest some moisture is required, but not excessive amounts, noting the cwd index measures the maximum number of consecutive wet days and January to March is the wettest part of the year. Some climate elements may be proxies for others, e.g., the negative association between tx10p_Mar and sugar yield. This may represent a positive association between

Table 4.3 Equation 2 coefficients

| **Term** | **Coefficients** | **Standard error coefficients** | **T-Value** | **P-Value** | **VIF** |
|---|---|---|---|---|---|
| Constant | 21.01 | 6.33 | 3.32 | 0.003 | |
| Diurnal temperature range (dtr)_August (°C) | 0.264 | 0.147 | 1.79 | 0.084 | 2.06 |
| Lowest minimum temperature (tnn)_May (°C) | -0.2638 | 0.0884 | -2.99 | 0.006 | 1.89 |
| Total wet day precipitation (prcptot)_March to May (mm) | -0.002499 | 0.000716 | -3.49 | 0.002 | 3.16 |
| Lowest minimum temperature (tnn)_July (°C) | -0.1751 | 0.0912 | -1.92 | 0.065 | 1.75 |
| Percentage of warm nights (tn90p)_October (%) | -0.0276 | 0.0110 | -2.50 | 0.018 | 1.97 |
| Precipitation days ≥ 1mm (r1mm)_Mar (days) | 0.1916 | 0.0390 | 4.91 | 0.000 | 2.90 |
| Mean bright sunshine duration (sun)_Nov (hrs) | -0.224 | 0.103 | -2.17 | 0.039 | 1.97 |
| Percentage of days maximum temperature > 50th percentile txgt50p_November (%) | 0.01131 | 0.00631 | 1.79 | 0.084 | 1.30 |
| Highest minimum temperature (tnx)_January (°C) | -0.482 | 0.181 | -2.67 | 0.013 | 1.62 |
| Percentage of cool days (tx10p)_March (%) | -0.1022 | 0.0180 | -5.67 | 0.000 | 1.82 |
| Maximum 2-day precipitation (rx2day)_October (mm) | -0.00565 | 0.00254 | -2.22 | 0.035 | 1.24 |
| Maximum consecutive dry days (cdd)_June (days) | -0.03316 | 0.00918 | -3.61 | 0.001 | 1.80 |
| Highest maximum temperature (txx)_September (°C) | 0.261 | 0.121 | 2.16 | 0.040 | 2.30 |
| Lowest maximum temperature (txn)_May (°C) | -0.4377 | 0.0965 | -4.54 | 0.000 | 1.75 |
| Lowest minimum temperature (tnn)_December to February (°C) | 0.403 | 0.132 | 3.05 | 0.005 | 1.94 |

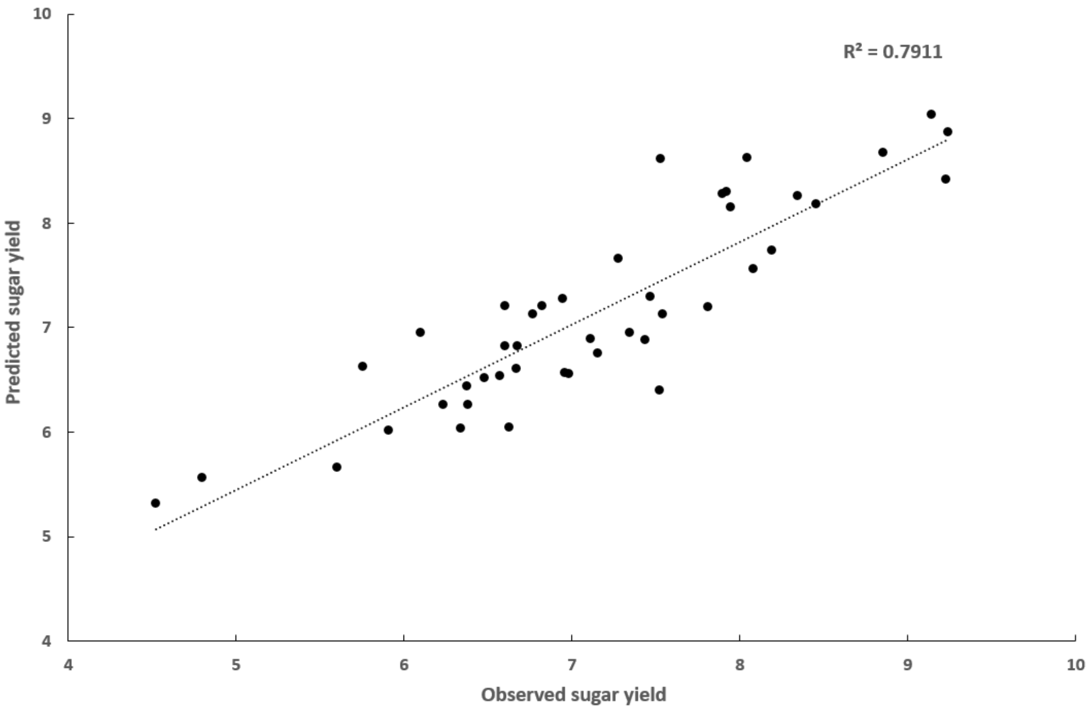


Figure 4.4 Detrended observed and predicted sugar yield (tonnes/ha)

solar radiation and sugar yield as cool days in summer tends to be associated with cloudy days. Further work is required to better understand the climate relationship with this phase of sugarcane production.

With most timeseries, it is highly probable that the observed variable value will be similar to the value at lag 1 and/or longer lag periods. Therefore, when fitting a regression model to timeseries data, it is important to test for autocorrelation in the model residuals. The estimated model would in this case violate the hypothesis of no autocorrelation in the errors, making the forecasts inefficient. The forecasts from such a model while unbiased, would have larger prediction intervals than required. The Durbin-Watson static tests for first-order autocorrelation (Durbin and Watson, 1951, 1950). For Eq. (2), the statistic D is 1.45911. D was then compared with the appropriate lower and upper bounds using the relevant table in Savin and White (1977). The table provides values to test for first-order, positive autocorrelation. The significance level for the test was 0.05. For a sample size of 44 and 15 terms, $D_L$ and $D_U$ are 0.81787 and 2.38581, respectively. As $D > D_U$ no positive correlation exists. First-order negative autocorrelation was also tested. As $4 – D$ is 2.54089 which is greater than $D_U$ no negative correlation with lag 1 exists. While the Durbin–Watson statistic tests for first-order autocorrelation it does not test for autocorrelation at longer lag times. Plots of the autocorrelation (ACF) and partial autocorrelation (PACF) functions and a histogram of the residuals (Figure 4.5) are provided. With the exception of the histogram plot which is not normal, Figure 4.5 shows the residuals have a zero mean and no autocorrelation.

In order to undertake future predictions of sugarcane and sugar yield it is necessary to return the trend and time components to both models. For Eq. (1), - 0.25017553t needs to be added as a model term and for Eq. 2, - 0.0674459t, where t for both equations is the number of years since 1975. 1975 is y = 0. Figure 4.6 shows Eq. (2) with trend and time added. Sugar yield provided by SRIF is labelled Observed.

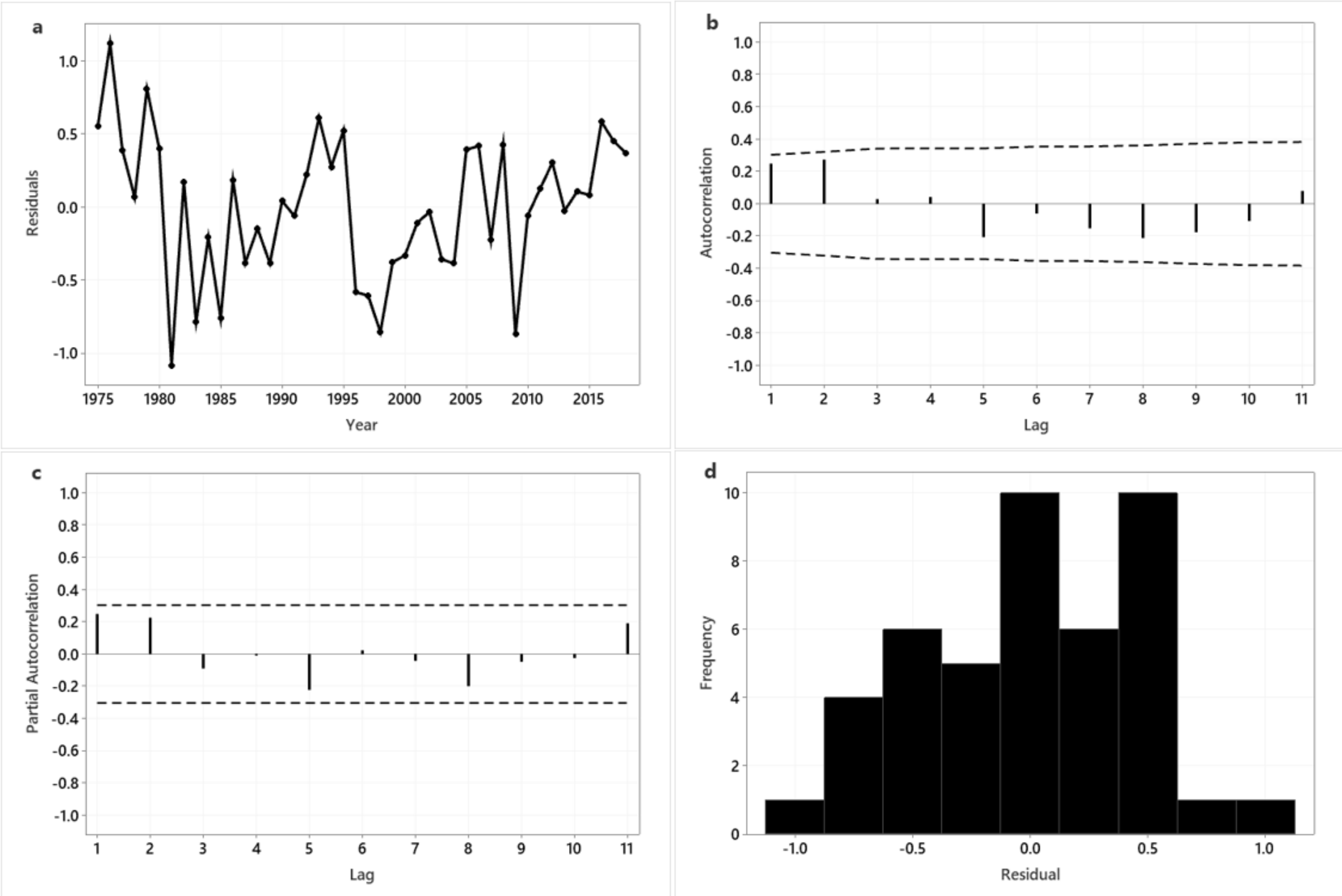


Figure 4.5 Equation 2 residuals (a) Time plot (b) ACF with 11 lag intervals (c) PACF with 11 lag intervals. For (b) and (c), the dashed line represents the 5% significance limits (d) histogram.

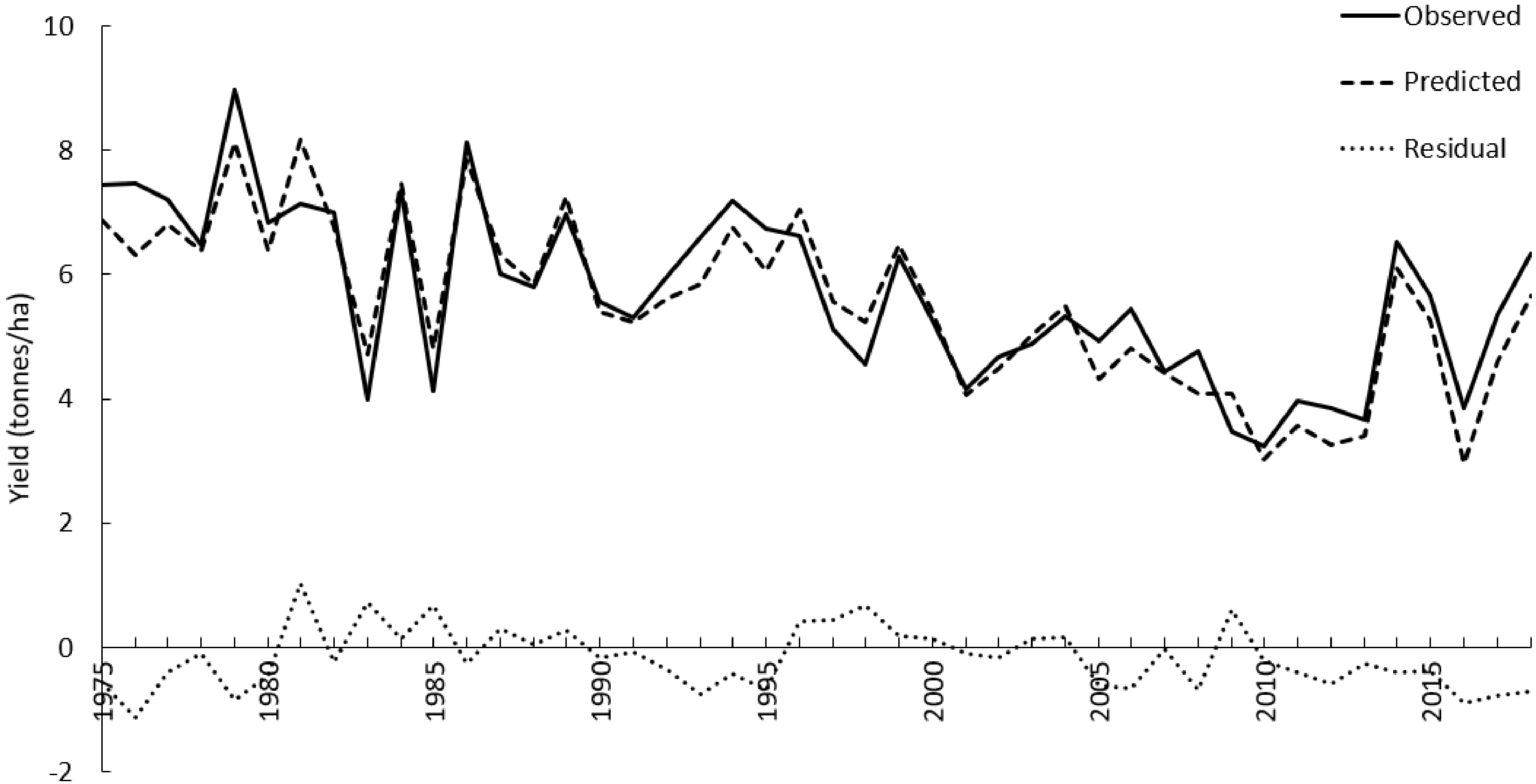

Figure 4.6 Observed and predicted (Eq. 2) sugar yield with the trend and time component added to model.

### 4.3.3 Operational models for sugarcane and sugar yield

Both Eq. (1) and Eq. (2) show potential when it comes to predicting future yield but have October and/or November climate terms, meaning a user would need to wait until late in the crushing season to make a prediction. The crushing season has an average length of 28–30 weeks, extending from late May to early December. A prediction this late in the season has low value even through the actual yield value may take a couple more months to determine.

Multiple linear regression was repeated for both sugarcane and sugar yield with the October and November climate variable terms removed. Eq. (3) is the sugarcane model.

$$\text{Sugarcane\_yield} = 276.6 - 3.01\text{txm\_Feb} + 0.988\text{r1mm\_Mar} - 4.00\text{tnx\_Jan} - 0.709\text{tx10p\_Mar} - 1.254\text{txn\_May} \tag{3}$$

The terms are those for Eq. (1) with the exception of txm_Feb which is mean maximum temperature for February. Eq. (3), has five terms. R-sq 58.4%, adjusted R-sq 53.0% and cross-validated R-sq 45.9%. The highest VIF is 1.60. Eq. (3) displays a lower adjusted R-sq and cross-validated R-sq when compared with Eq. (1) but can be used at the start of the crushing season to provide a preliminary but lower skilled prediction of sugar yield with Eq. (1) used later in the year for a higher skilled prediction. Eq. 4 is the sugar model.

$$\text{Sugar\_yield} = 30.92 - 0.645\text{txm\_Feb} - 0.398\text{txm\_JJA} + 0.415\text{dtr\_Aug} - 0.2226\text{tnn\_May} - 0.001178\text{prcptot\_MAM} + 0.1489\text{r1mm\_Mar} - 0.0952\text{tx10p\_Mar} + 0.318\text{tnx\_Feb} - 0.0211\text{cdd\_Jun} + 0.224\text{txn\_Feb} - 0.2504\text{txn\_May} \tag{4}$$

The terms are those for Eq. (2) with the exception of txm_Feb which is mean maximum temperature for February, txm_JJA the mean maximum temperature over July to August, tnx_Feb the highest minimum temperature in February and txn_Feb the lowest maximum temperature in February. Eq. (4), has 11 terms. R-sq 66.7%, adjusted R-sq 55.2% and cross-validated R-sq 38.6%. The highest VIF is 2.36. Eq. (4) displays a lower adjusted R-sq and cross-validated R-sq compared to Eq. (2) but can used in early September, mid-way through the crushing season to provide a preliminary, but lower skilled forecast of sugar yield with Eq. (2) used in early December for a higher skilled prediction. The trend and time components can be incorporated for future predictions as presented previously for Eqs. (1) and (2).

The above results suggest the late ripening season is important for optimum yield and corresponds with references in the literature, e.g., Koshy et al. (2003) to September and October being the 'peak ripening season' and industry knowledge that a delayed harvest is favourable for yield.

### 4.3.4 Impact of future warmer, wetter and drier conditions on sugar yield

A natural question that arises at this point is, now sugar yield can be modelled, how might yield change in a future warmer, wetter and drier climate. This requires a detailed investigation beyond the scope of this study. In the interim, a succinct analysis is presented below.

According to the Australian Bureau of Meteorology and CSIRO (2014), all Representative Concentration Pathways (RCPs) favour warming up to 1.0°C by 2030 over Fiji, relative to 1995, but after 2030 there is a growing difference between each RCP. By 2090, warming of 1.9–4.0°C is projected for RCP8.5. There is very high confidence that temperatures will rise in this part of the Pacific (Australian Bureau of Meteorology and CSIRO, 2011). The temperature on extremely hot and cool days is projected to increase by about the same amount as mean temperature.

For precipitation, the Coupled Model Intercomparison Project Phase 5 (CMIP5) models show a range of annual precipitation change depending on the emission scenario (RCP2.6, 4.5, 6 or 8.5) selected with the model average for each scenario indicating little change (1–5%). Much like temperature, the range is greater for the highest emissions scenarios. Model agreement is greater for a slight increase in precipitation over November to April. There was a range of projections for May to October with the model average (-1–3%) indicating little change. Year-to-year variability was generally larger than the projected change, except for models with the largest projected change in the highest emission scenario by 2090 (Australian Bureau of Meteorology and CSIRO, 2014). The frequency and intensity of extreme precipitation events are expected to increase with the current 1-in-20-year daily amount projected to increase by approximately 5mm by 2030 for RCP2.6 and by 7mm by 2030 for RCP8.5. By 2090, it is projected to increase by approximately 6mm for RCP2.6 and by 36mm for RCP8.5. While there is high confidence that the frequency and intensity of extreme precipitation events will increase there is low confidence in the magnitude of projected change (Australian Bureau of Meteorology and CSIRO, 2014).

Using Eq. (2), a 20-year baseline of sugar yield centred on 1995 was calculated and labelled Baseline_95 (Table 4.4). Table 4.4 also presents a range of climate scenarios. Scenarios A–C show temperature terms increased at 0.5°C increments. Precipitation and sunshine terms are kept at Baseline_95 levels. Scenarios A–C show a decline in sugar yield of 2–14% relative to the rise in temperature. Table 4.3 shows rain days in March to be the second most influential term in Eq. (2). For scenarios D–F the effect of increasing the number of rain days was investigated. The temperature levels for scenarios D–F are those of A–C. Presented in Table 4.4 are number of rain days required to retain sugar yield close to Baseline_95 levels. March rain days in the order of 17–21 have been experienced in the past with 23 (4) of 44 years receiving >16 (>20) rain days since 1975. These results suggest it may be possible to offset the effects of a warmer climate by increasing soil moisture levels during the growing phase. This finding is consistent with guidelines for optimal sugarcane production where during the growing phase, drip irrigation, fertigation and warm, humid and sunny climatic conditions favour better cane elongation. Moisture stress is known to reduce internodal length. A temperature around 30°C with a humidity of around 80% is most conducive for good growth.

Scenarios G–I show the impact of reducing the number of March wet days by two days where temperatures levels are those of scenarios A–C. The effect is an approximate 4–6% decline in sugar yield. Finally, scenarios J–L show the impact of increasing the number of wet days in March at Baseline_95 temperature levels.

These results suggest that irrigating the sugar crop in the late growing season may increase sugar yield and may offset the impact of ENSO extremes.

Table 4.4 Baseline and simulated sugar yield for the Lautoka Mill. Change is relative to Baseline_95.

| | **Sugar yield** | **dtr_Aug** | **tnn_May** | **prcp_MAM** | **tnn_Jul** | **tn90p_Oct** | **r1mm_Mar** | **Sun_Nov** | **txgt50p_Nov** | **tnx_Jan** | **tx10p_Mar** | **rx2day_Oct** | **cdd_Jun** | **txx_Sept** | **txn_May** | **tnn_DJF** |
|---|---|---|---|---|---|---|---|---|---|---|---|---|---|---|---|---|
| **Baseline _95** | 7.3 | 9.2 | 17.5 | 515.5 | 15.0 | 0.7 | 15.0 | 7.8 | 48.9 | 24.9 | 8.1 | 49.0 | 18.6 | 31.3 | 26.6 | 19.6 |
| **Scenario (units)** | Δ **(%)** | Δ **(°C)** | Δ **(°C)** | Δ **(mm)** | Δ **(°C)** | Δ **(%)** | Δ **(days)** | Δ **(hrs)** | Δ **(%)** | Δ **(°C)** | Δ **(%)** | Δ **(mm)** | Δ **(days)** | Δ **(°C)** | Δ **(°C)** | Δ **(°C)** |
| **A** | -2 | - | +0.5 | - | +0.5 | +0.42 | - | - | +0.04 | +0.5 | -0.08 | - | - | +0.5 | +0.5 | +0.5 |
| **B** | -10 | - | +1.0 | - | +1.0 | +0.84 | - | - | +0.08 | +1.0 | -0.16 | - | - | +1.0 | +1.0 | +1.0 |
| **C** | -14 | - | +1.5 | - | +1.5 | +1.26 | - | - | +0.12 | +1.5 | -0.24 | - | - | +1.5 | +1.5 | +1.5 |
| **D** | -0.1 | +0.5 | +0.5 | - | +0.5 | +0.42 | 16.8 | - | +0.04 | +0.5 | -0.08 | - | - | +0.5 | +0.5 | +0.5 |
| **E** | -0.1 | +1.0 | +1.0 | - | +1.0 | +0.84 | 18.6 | - | +0.08 | +1.0 | -0.16 | - | - | +1.0 | +1.0 | +1.0 |
| **F** | 0.1 | +1.5 | +1.5 | - | +1.5 | +1.26 | 20.5 | - | +0.12 | +1.5 | -0.24 | - | - | +1.5 | +1.5 | +1.5 |

| | Sugar yield | dtr_Aug | tnn_May | prcp_MAM | tnn_Jul | tn90p_Oct | r1mm_Mar | Sun_Nov | txgt50p_Nov | tnx_Jan | tx10p_Mar | rx2day_Oct | cdd_Jun | txx_Sept | txn_May | tnn_DJF |
|---|---|---|---|---|---|---|---|---|---|---|---|---|---|---|---|---|
| **G** | -8 | +0.5 | +0.5 | - | +0.5 | +0.42 | 14.0 | - | +0.04 | +0.5 | -0.08 | - | - | +0.5 | +0.5 | +0.5 |
| **H** | -14 | +1.0 | +1.0 | - | +1.0 | +0.84 | 14.0 | - | +0.08 | +1.0 | -0.16 | - | - | +1.0 | +1.0 | +1.0 |
| **I** | -20 | +1.5 | +1.5 | - | +1.5 | +1.26 | 14.0 | - | +0.12 | +1.5 | -0.24 | - | - | +1.5 | +1.5 | +1.5 |
| **J** | 3 | +0.5 | +0.5 | - | +0.5 | +0.42 | 16.0 | - | +0.04 | +0.5 | -0.08 | - | - | +0.5 | +0.5 | +0.5 |
| **K** | 6 | +1.0 | +1.0 | - | +1.0 | +0.84 | 17.0 | - | +0.08 | +1.0 | -0.16 | - | - | +1.0 | +1.0 | +1.0 |
| **L** | 9 | +1.5 | +1.5 | - | +1.5 | +1.26 | 18.0 | - | +0.12 | +1.5 | -0.24 | - | - | +1.5 | +1.5 | +1.5 |

## 4.4 Conclusions

The aim of this study was to examine sugarcane and sugar yield variability and change for the Lautoka Mill area in western Fiji over the period 1975–2018, to model sugarcane and sugar yield using mean and extreme climate variables, and to use the sugar model to examine the impact of a warmer, wetter and drier climate on sugar production.

There has been a statistically significant decline in sugarcane and sugar yield, continuing a decline in sugarcane production from 1961 (Gawander et al., 2018). The proportion of sugar extracted from sugarcane has also declined as shown by the positive trend in TCTS. It would appear from recent increases in sugar yield and decreases in the TCTS ratio that mill performance is partially responsible for the negative trend in sugar yield. Mill performance though does not explain the decline in sugarcane yield. Singh (2020) suggests the decline in sugarcane yield is in part due to the use of ‘old’ ratoon. Based on the results in Section 3.4 it is likely an increase in temperature over the last half century has contributed to the decline.

Principal component analysis was used to reduce the number of climate variables that were used for modelling sugarcane and sugar yield and to deal with multicollinearity. As some of the 32 climate variables identified through PCA were found to be weakly correlated with sugarcane and sugar yield, stepwise regression backward elimination was used to obtain optimal models while reducing the number of model terms.

The models show significant potential for predicting sugarcane and sugar yield at two stages prior to end of the crushing season. For sugarcane, the first model can be run in early June with lower confidence in the prediction with the second model run in early November with higher confidence in the second prediction. Likewise, for the sugar model with the first run in early September and second model in early December. The cross-validated R-sq for the four models are 46%, 67%, 39% and 51% respectively. Non-climate factors in mill production understandably reduce the predictability of sugar yield.

Model terms and their order of importance correspond with known ‘ideal’ climate conditions for sugarcane and sugar production. Late growing season adequate moisture (precipitation) is highlighted by a positive association with March rain days. As is low precipitation and cool conditions during the ripening and maturation period by the negative association between the lowest maximum temperature in May, and consecutive dry days in June.

Using the ‘higher confidence’ sugar model, the impact of future warmer, wetter and drier conditions on sugar yield was examined. Model scenarios were created to estimate the impact of a warmer climate on sugar yield. Declines in sugar yield in the order of 2–14% were projected with an increase in mean and extreme temperature (precipitation and sunshine kept at baseline levels). Scenarios suggest the impact of rising temperature on sugar yield could be offset by increasing the number of rain days in the late growing season, with irrigation a consideration for the future. This finding is consistent with known benefits of irrigating sugarcane during the growth phase elsewhere in the world. Irrigation is currently not used by the sugar industry in Fiji and substantial investment would be required to establish such a scheme.

Any expansion of irrigation would need to be considered against available water resources, both in terms of the mean and the extremes. In addition, Caribbean studies suggest that while irrigation can contribute to adapting to a warmer climate it should not be the only option as while irrigated sugarcane fairs better than rainfed sugarcane they still found a decline in yield in a warmer climate (Hutchinson et al., 2013). Of course, the thermal limit to photosynthesis in sugarcane places a limit of adaptation, meaning that continued warming will eventually reduce yields to the point at which crops may cease to be viable.

It would be remiss of the authors to not point out the limitations of this study which focuses solely on climate and sugar yield statistical associations. Climate plays a smaller role in sugar production compared to mill efficiency and farm management but is nevertheless an important variable which will become even more important in a future warmer climate. It is possible the results from this work are specific to the Lautoka Mill region and not applicable to other parts of the country, but the chances of this are small noting the findings align with known relationships between climate and sugarcane production.

There are numerous opportunities for future work. These include extending the current study using data prior to 1975, undertaking a similar comparative study for the Labasa Mill area and/or using CMIP5 or later model data to project the impact of a warmer and drier/wetter climate on sugar yield. There is also a clear role for the use of biological models for sugar production, e.g., Marin and Jones (2014) which may better capture non-linearities in relationships and more robustly predict future change.

*Acknowledgements.* Data provided by the Fiji Meteorological Service, Fiji Sugar Corporation and Sugar Research Institute of Fiji is greatly appreciated. The authors are particularly grateful to the former and current Sugar Research Institute of Fiji Chief Executive Officers Mr Jai Gawander and Mr Prem Naidu for the information they provided on sugar production and Mr Mark Caughey for his analytical assistance. The authors thank Dr David Jones and Dr Lynda Chambers for their valuable comments on the initial version of the manuscript as part of the Bureau of Meteorology internal review prior to submission.

*Funding.* This work was partially supported by Australian Department of Foreign Affairs and Trade funded Climate and Oceans Support Program in the Pacific.

## References

Alexander, L., Herold, N., 2015. ClimPACTv2 Indices and Software. A document prepared on behalf of the Commission for Climatology (CCl) Expert Team on Sector-Specific Climate Indices (ET-SCI).

Australian Bureau of Meteorology, CSIRO, 2014. Climate Variability, Extremes and Change in the Western Tropical Pacific: New Science and Updated Country Reports, Pacific-Australia Climate Change Science and Adaptation Planning Program Technical Report. Australian Bureau of Meteorology and Commonwealth Scientific and Industrial Research Organisation, Melbourne, Australia.

Australian Bureau of Meteorology, CSIRO, 2011. Climate Change in the Pacific: Scientific Assessment and New Research. Volume 1: Regional Review. Volume 2: Country Reports. Melbourne, Australia.

Chakraborty, D., Sehgal, V.K., Dhakar, R., Ray, M., Das, D.K., 2019. Spatio-temporal trend in heat waves over India and its impact assessment on wheat crop. Theor. Appl. Climatol. https://doi.org/10.1007/s00704-019-02939-0

Chen, Y., Ebert, E.E., Walsh, K.J.E., Davidson, N.E., 2013. Evaluation of TRMM 3B42 precipitation estimates of tropical cyclone rainfall using PACRAIN data. J. Geophys. Res. Atmos. 118, 2184–2196. https://doi.org/10.1002/jgrd.50250

DelSole, T., Shukla, J., 2009. Artificial Skill due to Predictor Screening. J. Clim. 22, 331–345. https://doi.org/10.1175/2008JCLI2414.1

Deo, A., Walsh, K.J.E., Peltier, A., 2017. Evaluation of TMPA 3B42 Precipitation Estimates during the Passage of Tropical Cyclones over New Caledonia. Theor. Appl. Climatol. 129, 711–727. https://doi.org/10.1007/s00704-016-1803-0

Draper, N., Smith, H., 1981. Applied Regression Analysis, 2nd ed. John Wiley & Sons, Inc., New York.

Durbin, J., Watson, G.S., 1951. Testing for serial correlation in least squares regression. II. Biometrika 38, 159–178. https://doi.org/10.1093/biomet/38.1-2.159

Durbin, J., Watson, G.S., 1950. Testing for serial correlation in least squares regression. I. Biometrika 37, 409–428. https://doi.org/10.1093/biomet/37.3-4.409

FMS, 1995. The Climate of Fiji. Information Sheet No. 35. Climate Services Division, Fiji Meteorological Service, Nadi, Fiji.

Folland, C.K., Renwick, J.A., Salinger, M.J., Mullan, A.B., 2002. Relative influences of the Interdecadal Pacific Oscillation and ENSO on the South Pacific Convergence Zone. Geophys. Res. Lett. 29, 21–24. https://doi.org/10.1029/2001GL014201

FSC, 2019. Fiji Sugar Corporation Annual Report 2018. Lautoka, Fiji.

FSC, 2015. Fiji Sugar Corporation Annual Report 2015. Lautoka, Fiji.

Gawander, J., 2007. Impacts of climate change on sugar-cane production in Fiji. World Meteorol. Organ. Bull. 56, 34–39.

Gawander, J., Salinger, J., Prasad, J., Rounds, P., Kumar, R., 2018. El Nino – Southern Oscillation influences on sugarcane production in Fiji – An exploratory investigation. Int. Sugar J. CXX, 778–784.

Hogarth, D.M., Allsopp, P.G. (Eds.), 2000. Manual of Canegrowing. Bureau of

Sugar Experiment Stations, Brisbane, Australia.
Hutchinson, S., Gomes, C., Alleyne, D., Phillips, W., 2013. An assessment of the economic and social impacts of climate change on the agriculture sector in the Caribbean, Economic Commission for Latin American and the Caribbean Report LC/CAR/L.398. Port of Spain, Trinidad and Tobago.
Koshy, K., Gawander, J., Gosai, A., Pahalad, J., 2003. ENSO Impact on Sugarcane in Fiji, Report on joint research between the University of the Souith Pacific; Fiji Meteorological Service and Fiji Sugar Corporation. Suva, Fiji.
Kumar, R., Stephens, M., Weir, T., 2013. Temperature trends in Fiji: a clear signal of climate change. South Pacific J. Nat. Appl. Sci. 31, 27–38. https://doi.org/10.1071/SP13002
Kutner, M., Nachtsheim, C., Neter, J., 2004. Applied Linear Regression Models, 4th ed. McGraw-Hill/Irwin, New York.
Lobell, D.B., Burke, M.B., 2010. On the use of statistical models to predict crop yield responses to climate change. Agric. For. Meteorol. 150, 1443–1452. https://doi.org/https://doi.org/10.1016/j.agrformet.2010.07.008
Macdonald, B., Foster, S., 2019. Fiji [WWW Document]. Encycl. Br. URL https://www.britannica.com/place/Fiji-republic-Pacific-Ocean (accessed 1.19.20).
Marin, F.R., Jones, J.W., 2014. Process-based simple model for simulating sugarcane growth and production. Sci. Agric. 71, 1–16.
McGree, S., Herold, N., Alexander, L., Schreider, S., Kuleshov, Y., Ene, E., Finaulahi, S., Inape, K., Mackenzie, B., Malala, H., Ngari, A., Prakash, B., Tahani, L., 2019. Recent Changes in Mean and Extreme Temperature and Precipitation in the Western Pacific Islands. J. Clim. 32, 4919–4941. https://doi.org/10.1175/JCLI-D-18-0748.1
NETAFIM, 2019. Sugarcane [WWW Document]. Sugarcane. URL http://www.sugarcanecrops.com/ (accessed 3.3.19).
Reddy, N., 2003. Survival strategies for the Fiji sugar industry. Fijian Stud. A J. Contemp. Fiji 1, 265–285.
Salehnia, N., Salehnia, N., Torshizi, A.S., Kolsoumi, S., 2020. Rainfed wheat (Triticum aestivum L.) yield prediction using economical, meteorological, and drought indicators through pooled panel data and statistical downscaling. Ecol. Indic. 111, 105991. https://doi.org/https://doi.org/10.1016/j.ecolind.2019.105991
Salinger, M.J., Renwick, J.A., Mullan, A.B., 2001. Interdecadal Pacific Oscillation and South Pacific climate. Int. J. Climatol. 21, 1705–1721. https://doi.org/10.1002/joc.691
Savin, N.E., White, K.J., 1977. The Durbin-Watson Test for Serial Correlation with Extreme Sample Sizes or Many Regressors. Econometrica 45, 1989–1996. https://doi.org/10.2307/1914122
Singh, A., 2020. Benefits of crop diversification in Fiji’s sugarcane farming. Asia Pacific Policy Stud. 7, 65–80. https://doi.org/10.1002/app5.291
SPC, 2011. Food security in the Pacific and East Timor and its vulnerability to climate change. Secretariat of the Pacific Community, Noumea, New Caledonia.
SRA, 2018. Sugar Research Australia, The Sugarcane Advisors Information Kit. Indooroopilly, Queensland.
Taylor, M., McGregor, A., Dawson, B. (Eds.), 2016. Vulnerability of Pacific

Island agriculture and forestry to climate change. Pacific Community, Noumea, New Caledonia.
Terry, J.P., Raj, R., 2002. The 1997-98 El Nino and drought in the Fiji Islands, in: Hydrology and Water Management in the Humid Tropics. UNESCO International Hydrology Programme-V, Technical Documents in Hydrology No 52. Paris, France, pp. 80–93.
Troy, T.J., Kipgen, C., Pal, I., 2015. The impact of climate extremes and irrigation on US crop yields. Environ. Res. Lett. 10, 54013. https://doi.org/10.1088/1748-9326/10/5/054013
Vogel, E., Donat, M.G., Alexander, L. V, Meinshausen, M., Ray, D.K., Karoly, D., Meinshausen, N., Frieler, K., 2019. The effects of climate extremes on global agricultural yields. Environ. Res. Lett. 14, 54010. https://doi.org/10.1088/1748-9326/ab154b

# 5 Conclusion

The general objective of this study was to investigate trends and variability in climate extremes, primarily those associated with precipitation and air temperature over the western Pacific region, and determine if there had been a statistically significant change in the characteristics of these extremes in recent decades. This objective has been achieved through conducting four interconnected studies which examined: 1. trends and variability in droughts in the Pacific Islands and northeast Australia; 2. recent changes in mean and extreme temperature and precipitation in the western Pacific Islands; and 3. determine the magnitude of the influence of mean and extreme climate on productivity of agriculture sector in Pacific Island countries using sugarcane and sugar yield in western Fiji as a case study.

This research is important, as the Pacific Islands have been identified as being among the most vulnerable to climate change and climate extremes (Pelling and Uitto, 2001; UNISDR, 2005) with changes in climate extremes likely to impact many sectors (IPCC, 2018, 2014b) including human health (McMichael et al., 2003), agriculture (Barnett, 2011), and fisheries (Singh et al., 2001). In addition, smallness renders island countries at risk of high proportionate losses when impacted by climate extremes (Pelling and Uitto, 2001) and despite the known impacts, relatively little is known about changes in climate extremes in the region (Salinger et. al 1995; Griffiths et al. 2003; Whan et al., 2014).

High-quality timeseries of precipitation and air temperature for the western Pacific have been created then used to investigate change in mean and extreme climate in the since 1951.

Results of the study one are presented in Chapter 2. The research objectives of this study were (i) to determine if there has been a statistically significant change in droughts occurrence, duration and magnitude, and (ii) examine the strength of the relationship between the main climate drivers and Pacific and northeast Australia precipitation on regional/subregional scales.

Trends in drought frequency were mixed spatially (in terms of the direction of change) and largely non-significant. Where there were statistically significant, they were mainly in the subtropics of both hemispheres. The results were similar for total drought duration and total drought magnitude in that a majority of the trends are marginally positive, spatially mixed and largely non-significant. Studies have shown that the subtropics may be expanding as the global climate warms. Climate models project this subtropical drying will continue throughout the 21st century which will place significant stress on ecosystems, agriculture and water supplies (Sniderman et al., 2019) for the islands closest to the poles. Some island communities, e.g., those on the Norfolk Islands are already experiencing significant water stress (CSIRO, 2020).

A significant relationship between the oceanic component of ENSO and precipitation was confirmed for a large part of the western Pacific. A statistically significant lagged relationship in the year following the onset of El Niño was also identified at locations southwest of the SPCZ, e.g., Fiji and Tonga and north of the ITCZ e.g. FSM.

A strong relationship between precipitation and IPO and PDO exists at most locations. Drought was found to be longer and more severe southwest of the SPCZ and north of the ITCZ when the IPO and PDO where in a positive phase (over the 1980s and 1990s). This is an important finding as droughts affect the highest number of people per event in the western Pacific (Wairiu et al., 2011). In Fiji, the 1997/98 drought resulted in 50% loss in sugarcane production and total losses to the industry were around US$50 million while other industry losses were around U$7 million (McKenzie et al., 2005). Also in Fiji, an extension of the dry season by 45 days has been estimated to decrease maize yields by 30–50%, and sugarcane and taro by 10–35% and 35–75% respectively (Hay et al., 2003). Ideally, National Meteorological Services (NMSs) would pay greater attention to drought in the phase of IPO/PDO associated with more severe drought. Knowing the phase more associated with severe drought allows governments, aid agencies and disaster management organisations to better manage limited resources.

The objectives of Chapter 3 (Study 2), were to examine trends in the mean and extremes for the ET-SCI sector-relevant indices from 1951–2015, using quality-controlled and homogenised daily temperature and precipitation data from the western Pacific. This was undertaken for 55 monthly precipitation, 31 monthly temperature, 52 daily precipitation and 29 daily temperature stations in

20 countries. The extremes indices were those recommend by the WMO Expert Team on Sector-specific Climate Indices. These indices are used to highlight variability and trends in moderate-scale climate extremes which are of particular interest to socio-economic sectors, e.g., agriculture, water and health, and to help characterise the climate sensitivity of various sectors.

Mean temperature was found to have increased at most stations, in all seasons and in both halves of the 1951–2015 period. The temperature indices also showed strong warming, which for the majority was greatest over December to February and weakest over June to August. The absolute and percentile-based indices showed greatest warming at the upper end of distribution (>90%ile). The results of the temperature analyses were largely consistent with global (Alexander et al., 2006), neighbouring (e.g., Caesar et al., 2011), and previous Pacific (Griffiths et al., 2003; Whan et al., 2014) studies. Interestingly, strong warming at the upper end of the distribution is consistent with findings in the Caribbean (Stephenson et al., 2014) suggesting this may be a feature of an oceanic climate. Further work is required to confirm this proposition.

Precipitation change was less consistent and trends generally weak at most locations. Annual, March to May, September to November, and, to a lesser extent, the December to February total precipitation maps show an El Niño-like pattern in which the ITCZ was displaced south towards the equator and the SPCZ displaced northeast towards the central Pacific. Previous studies attribute this displacement to IPO variability (Folland et al., 2002; Salinger et al., 2014).

Declines in total and extreme precipitation were found in Southwest French Polynesia and the Southern subtropics. There was a decrease in moderate to high intensity precipitation events, especially those experienced over multiple days, in Southwest French Polynesia from December to February. This finding is consistent with drying of the southeast SPCZ margin which is projected by the CMIP models and has been attributed to increased anomalous transport of dry subtropical air into the SPCZ region in response to increased SST meridional gradients east of the southeast SPCZ margin (Dutheil et al., 2019; Widlansky et al., 2013). Strong drying trends were also identified in the low to moderate extreme indices for both the June to August and September to

November seasons. These negative trends contributed to an increase in the magnitude of meteorological drought in both subregions. The drought trend findings are consistent with those of Chapter 2 even though the trend calculation methods were different.

Finally, the relationship between total and extreme precipitation and Pacific basin sea surface temperatures was investigated with a focus on the influence of the ENSO. A strong relationship between ENSO and total precipitation is established along with similar relationships for the extreme precipitation indices. These findings confirm anecdotal knowledge i.e. La Niña associated with prolonged, high intensity precipitation events and flooding in Fiji (Kuleshov et al., 2014; McAneney et al., 2017). The percentile-based and absolute extreme indices were found to be influenced by ENSO to a lesser extent and in some cases the influence was marginal.

The primary objective of Chapter 4 (Study 3; extension of the work undertaken in Study 2, and presented in Chapter 3), was to examine sugarcane and sugar yield variability and change since 1975 in western Fiji, model sugarcane and sugar yield using mean and extreme climate variables and use the resulting sugar model to determine the impact of a warmer, wetter and drier climate on future sugar production.

Sugarcane is Fiji's largest commercial agricultural crop and there is over 40 years of high-quality yield data available (rare for the Pacific Islands). Greater than 80% of the raw sugar produced is exported (this revenue will be especially important in 2020 noting the impact of the COVID-19 pandemic on tourism revenue in Fiji).

There has been a statistically significant decline in sugar yield since 1975. The proportion of sugar extracted from sugarcane has also declined as shown by the positive trend in the tonnes cane to tonnes sugar ratio. There are several non-climatic reasons for these declines. These include, mill performance and old ratoon as outlined in Chapter 4. Others include the decline in soil fertility and high rates of soil erosion (Ram et al., 2007). The physical conditions (land form, weather) in Fiji are conducive to high rates of soil erosion (Morrison and Clarke, 1990).

This was followed by multiple regressions models of sugarcane and sugar yield being developed using the Nadi Airport mean and extreme climate variables produced in Chapter 3. The Nadi Airport climate station is located near centre in the Lautoka milling region. Principal component analysis was used to reduce the number of climate variables that were used for modelling sugarcane and sugar yield and to deal with multicollinearity. Stepwise regression was then used to obtain optimal models while reducing the number of model terms. The models show significant potential for predicting sugarcane and sugar yield at two stages prior to end of the crushing season. For sugarcane the first model can be run in early June with lower confidence in the prediction with the second model run in early November with higher confidence in the second prediction. Likewise, for the sugar model with the first run in early September and second model in early December. The cross-validated R-sq for the four models are 46%, 67%, 39% and 51% respectively. Non-climate factors in mill production understandably reduce the predictability of sugar yield. Model terms and their order of importance correspond with known 'ideal' climate conditions for sugarcane and sugar production.

The 'higher confidence' sugar model was then used to determine the impact of a warmer, wetter and drier climate on future sugar production. The results show a decline in sugar yield with an increase in mean and extreme temperature. The results also show an increase in the number of rain days in March offsets the increase in temperature suggesting that an increase the number of rain days in the late growing season in a future climate may counter the influence of higher temperatures. As for Australia and other developed sugar producing countries, irrigation in the late growing season may be an option to increase yields and/or adapt to a warmer climate. Any expansion of irrigation would need to be considered against available water resources, both in terms of the mean and the extremes. In addition, Caribbean studies suggest that while irrigation can contribute to adapting to a warmer climate it should not be the only option as while irrigated sugarcane fairs better than rainfed sugarcane they still found a decline in yield in a warmer climate (Hutchinson et al., 2013).

The text on Pacific Islander perceptions of Climate Change in Box 3.1 in Australian Bureau of Meteorology and CSIRO (2011) has been referenced on several occasions through this thesis. It is used here to demonstrate the significance of the work undertaken and to assist with the production of a research synthesis.

There is a general agreement amongst Pacific Islanders that changes in weather and climate are occurring in their region. Pacific Islanders believe more change has occurred over the past decade than at any other time in human memory. This perception from both a mean and extremes temperature change perspective has been broadly confirmed but as Chapter 3, and previous studies e.g., Whan et al. (2014) and Folland et al. (2003) show, IPO can significantly modulate precipitation and temperature trends. IPO positive ‘decades’ for example cause warming in the central Pacific with cooling SSTs in the subtropical north and south Pacific meaning there can be significant change in the rate of temperature change from decade to decade depending on your location and IPO phase. There is also need for caution when analysing short records that span one or two IPO phases. None more obvious than in Griffiths et al. (2003) where precipitation trends over 1961-2000 are clearly influenced by the positive IPO phase from 1978-1998.

Other perceptions include shifts in seasonal patterns of precipitation and tropical cyclones, more frequent and extreme precipitation causing flooding and mudslides, more drought and fires, more hot days and lower crop productivity. These observations are generally supported by findings in Chapters 2–4. It would appear from the manner in which Box 3.1 is presented that the Pacific Islanders are suggesting these changes are associated with anthropogenic climate change. It is possible that these are merely observations of change. From analyses presented Chapter 2–4 it is clear the changes are associated with a combination of interannual (i.e. ENSO) variability, decadal variability and climate change. There is little evidence for example of long-term change in seasonal precipitation in the tropical Pacific. However, there is evidence of prolonged periods droughts (and therefore fires) and conversely prolonged periods of wetter than normal conditions associated with more frequent flooding and landslides in the wet season.

The issues associated with lower crop productivity are more complex. In Chapter 4, declining sugarcane productivity was found to be partly associated with warming temperatures but there are also suggestions in the literature of the declining productively being associated with prolonged use of sugarcane ratoon, declining soil productivity and sugar mill efficiency. This suggests that compared to the developed world, climate change in the Pacific will have a greater impact on agriculture as the islanders have less ability to maintain soil fertility, obtain good quality seed (due to financial limitations) and have less than ideal milling/manufacturing processes.

While some of the perceived climate changes are consistent with findings in Chapter 2-4 it is difficult to scientifically confirm many of these changes due to a lack of sufficient data, highlighting the need for improved observation networks in the region. Detection and attribution of climate changes in the Pacific is further complicated by large changes in ENSO activity over the past century (Power and Smith, 2007). Consequently, it can be difficult to distinguish between natural interdecadal changes and those due to anthropogenic climate change, particularly at the local scale. Some regional-scale changes in the Pacific have been partly attributed to human activities, e.g. weakening of the Walker Circulation (Power and Kociuba, 2011), and warming in the Pacific mean surface temperature (Stott et al., 2010). However, little research has been conducted to determine whether the changes perceived by people in the islands are real, and if so, to quantify the relative contributions from human and natural climate influences.

## 5.1 Limitations of, and/or Improvements to the Analysis and Methods

### 5.1.1 Data quality and quantity

Limited quantity (especially maximum and minimum temperature) and quality of data was an ever-present problem, as such the importance of some findings were downplayed. The author has tried to avoid the temptation of examining changes in the most unusual (<1 percentile and >99 percentile) extremes as these observations are the most questionable. There were also concerns with data completeness. The latter is most obvious in the last 10–20 years. To compound the problem, little metadata is being archived and this has and will continue to hinder the homogenisation of meteorological records in the future.

Numerous issues affect the quality of Pacific observations. For manual observations these include i) insufficient instrument exposure, e.g., trees sheltering a rain gauge, heat (or shelter) source too close to the Stevenson screen, ii) poor maintenance of equipment, e.g., missing louvres in a Stevenson screen, incorrect measuring cylinder for a rain gauge and holes in the inner and/or outer rain gauge, iii) poor observer training and insufficient staff on duty, e.g., thermometer not reset at the conclusion of the 'meteorological' day, observations taken tens of minutes to several hours late and observations entered against the wrong station identification number in the climate data management system.

There has been a rapid increase in the number of automatic weather stations (AWS) installed in the Pacific Islands. The New Zealand National Institute of Water and Atmosphere have installing several hundred AWSs in the last 10 years. While there are significant enticements to transitioning to this method of observation, in that they tend to be donated, enable national meteorological services to reduce staff numbers and provide high frequency observations, they are far more expensive and complex to maintain (often beyond the means of low budget Pacific NMSs). Automated observation data used in this thesis often showed a decline in completeness a year or two after initial installation.

### 5.1.2 Data homogenisation, change point detection and adjustment techniques

If a temperature or precipitation timeseries is to be used for monitoring climate change it is important that it be homogeneous; that is, changes in the temperature as shown in the dataset reflect changes in the climate, and not changes in the external (non-climatic) conditions under which the observations are made. Very few long-term Pacific temperature and precipitation station series are totally free of non-climatic influences, and therefore careful homogenisation is required in order to produce a homogeneous data set.

As outlined in Chapter 3, homogenisation is a two-stage process: firstly, the detection of discontinuities in the timeseries and secondly the adjustment of data to remove those inhomogeneities. The standard scientific practice is to detect potential artificial jumps by comparing data from the station of interest (the candidate station) with data from other nearby stations where the suspected artificial jump is absent (reference stations). If there is an artificial jump in the data, this will be reflected in the candidate station warming or cooling relative to other surrounding stations. This method of detection avoids falsely identifying actual climatic shifts and natural variability (such as that associated with El Niño or La Niña) as spurious artefacts in the data. The comparison with neighbours also serves the valuable purpose of largely rendering the test data free of trends.

The absence of homogeneous neighbouring station records makes it necessary to assess the homogeneity of data without reference series (often the case in the Pacific) e.g., the nearest station to Penrhyn for example is almost 900km away), but using such an approach means that detection and adjustment takes place with a much higher level of uncertainty. Statistical detection using reference stations tests must also take into account the trends in data, otherwise results will be unreliable. Where adjustments have been made without a reference series there have only been carried out if supported by metadata or the changepoint is highly significant.

There are number of ways the quality control and data homogeneous process can be improved but significantly more resources are required then it was allocated to the current PhD project. The involvement of many agencies (e.g., colonial archives, engineering and climate sections of the Pacific NMSs) is needed to implement this task. A detailed examination of the station history and instrument maintenance logs is essential as is the ability to confirm anomalous values. One would ideally confirm digitised anomalous observations with those in the observers' field books (as mistyping is fairly common) and make corrections if required. Finally, the use of multiple homogenisation testing methods is recommended where adjustments are only undertaken where there is agreement between a majority of the methods. Methods that could be used in addition to RHtestsV4 are HOMER and ACMANT which according to Guijarro et al. (2007) provide the most accurate homogenisation results (better than RHtestsV4) for a large number of homogenisation tasks.

### 5.1.3 Drought assessment and trend calculation methods

Drought is one of the most complex and least understood climatic events causing an annual average of USD 6–8 billion of damage globally (Keyantash and Dracup, 2002). There are few direct measurements of soil moisture, stream discharge or dam levels in the Pacific Islands and where available very few are long or complete enough for trend assessment. Therefore, meteorological drought indices such as the percentile index, CDD, SPI and SPEI are used as proxies for agricultural and hydrological drought. Analyses of these proxies come with uncertainties for example, trends in precipitation for a particular region at short timeseries do not necessarily reflect trends in soil moisture as soil type (or lack of soil), wind flow, air temperature, land cover and the state of soil/land degradation influence moisture evaporation (Alexander et al. 2019). Similarly, it is difficult to correlate longer timescales to stream discharge. An ‘unhealthy’ poorly vegetated catchment would likely show drought-like conditions long before a catchment of similar topography that is well vegetated (Saft et al., 2015). While the timescale can be adjusted to the conditions of the catchment, determining the appropriate timescale to use is complex and time consuming (Halwatura et al., 2017). Therefore, it is possible the trends in the 12-month SPI index used in this study (Chapter 2) are not relevant for every location/country in the Pacific. Also, a statistically significant trend for one timescale may not be significant for another as shown in Chapter 3.

Because drought is a complex variable and can at best be incompletely represented by commonly used drought indices, discrepancies in the interpretation of changes can result. Sheffield and Wood (2008) found decreasing trends in the duration, intensity and severity of drought globally. Conversely Dai, (2011) found a general global increase in drought, although with substantial regional variation and individual events dominating trend signatures in some regions (e.g., the 1970s prolonged Sahel drought and the 1930s drought in the USA and Canadian Prairies). Studies subsequent to these continue to provide somewhat different conclusions on trends in global droughts and/or dryness since the middle of the 20th century.

Finally, selecting the ideal method for calculating trends in drought is difficult. In Chapter 2, drought trends were calculated by first determining frequency, total magnitude and total duration for a decade, followed by calculating of the trend through the six decades but this method has statistical limitations as calculating a trend through six data points is problematic. Trends in the SPI and SPEI were calculated in Chapter 3 by simply calculating the trend in the standardised index at a specific timescale from 1951 to 2015 for a particular season. While this is recommended by the WMO ET-SCI, one could argue that this is simply a trend in standardised precipitation for a particular season and not a trend in ‘drought’.

### 5.1.4 Mechanisms for trends and variability

In the process of Chapter 2 undergoing (journal) peer review, one of the reviewers commented on the analysis failing to demonstrate possible mechanisms of the trends and variability. This shortcoming also applies to Chapter 3. Unfortunately, time constraints did not allow the author to implement these recommendations; however, the author intends on continuing this work in the future.

A future study might attempt to exhibit the trends and variability in a large-scale environment. This could be undertaken through the use of reanalysis, satellite or additional station datasets. The results could then be used to support the hypotheses arising from the references in both papers.

In late 2017, the BoM high-resolution Regional Reanalysis for Australia (BARRA) dataset became available. BARRA is a high-resolution multi-decadal atmospheric reanalysis. The reanalysis provides information about surface conditions, information at pressure and model levels, and information on solar radiation and cloud cover. The reanalysis suite is based on the Australian Community Climate Earth-System Simulator and extends 80km into the atmosphere. It is nested within the required boundary and/or initial conditions provided by ERA-Interim reanalysis, Operational Sea Surface Temperature and Sea Ice Analysis, and the Bureau offline soil moisture reanalysis. The region covered by the reanalysis is the Australian continent, the surrounding region including parts of southeast Asia, New Zealand, and south to the ice edge of the Antarctic continent. About one hundred parameters are available at hourly time steps at approximately 12km resolution (Su et al., 2019).

In a recent paper, Acharya et al. (2019), undertook an evaluation of daily precipitation from BARRA-R (regional 12km reanalysis) using a range of evaluation metrics to ascertain its usefulness for further hydrometeorological applications. The precipitation estimates in BARRA-R were area-averaged and benchmarked it against best available point (gauge) and areal precipitation dataset for Australia known as AWAP. They also compared the performance against global (approximately 80km) reanalysis ERA-Interim which provides boundary conditions to drive BARRA-R.

They found that BARRA-R was able to characterise a rich spatial precipitation variation across Australia, far better than displayed by the coarser ERA-Interim global reanalysis. They also found that BARRA-R reproduced unbiased estimates of extreme precipitation. Model performance depended on location with estimates superior in the temperate region compared to the tropics. BARRA-R demonstrated markedly better performance when evaluated at the grid-scale (benchmarked against AWAP) than at point (benchmarked against gauges), suggesting that it represented areal precipitation rather than point precipitation. However, compared to AWAP, BARRA-R was understandably poorer.

There are number of other studies documenting the limitations of using satellite and reanalysis products for studying longer-term trends in extremes. In the case of reanalysis products due in large part to inhomogeneities in the observed data used for assimilation (Alexander et al. 2020). That being said, the same study showed global space-based precipitation products displayed potential for climate scale analyses of extremes and some indices were more robust than others across ground based, satellite and reanalysis products. Daily precipitation intensity showed the least variation and days above 20 mm the largest variation. Alexander et al. (2020) concluded that global space-based precipitation products show potential for climate scale analyses of extremes.

Recent unpublished work at the Bureau of Meteorology shows the ECMWF Reanalysis v5 dataset (weekly to seasonal timescales) to be highly correlated with gauge datasets in the Pacific. Locations with low correlation coefficients happen to be those where confidence in the gauge dataset is also low. In summary, BARRA, ERA and satellite datasets may at some point usefully complement gauge datasets in understanding changes in climate extremes in the western Pacific, especially over the ocean.

As an extension of the analyses undertaken in Chapter 3, cluster and principal component analyses could be used to create temperature grouping as presented in Salinger et al. (1995). The sub-regions could then be used to examine sub-regional temperature variability as in Folland et al. (2003). Folland et al. (2003) found interannual and decadal teleconnections of ENSO and IPO produce definite sub-regional variability, especially since SST patterns are vary significantly across the region. El Niño causes warming along the equatorial Pacific. This is associated with cooler SSTs in the subtropical South Pacific. IPO positive phases are associated with warming in the central Pacific with cooler SSTs in the subtropical north and south Pacific. These teleconnections would also modulate longer term temperature trends.

### 5.1.5 Are the models and findings in Chapter 4 specific to the Lautoka Mill region?

Chapter 4 was the most difficult of the three studies to produce but perhaps the most rewarding as the results have immediate benefit for an industry and Pacific community. A noteworthy limitation is the case study being undertaken for a single sugar mill district. As presented in Chapter 4, there are currently three sugar mills in Fiji. The fourth, Penang is no longer operational as it was badly damaged by a tropical cyclone in early 2016. Sugarcane grown the Penang area is now crushed at Rarawai meaning the Rarawai yield timeseries is now inhomogeneous. A brief investigation found Penang component difficult to separate as milling records are limited.

A similar study to that undertaken in Chapter 4 using data for the Labasa Mill would make an interesting comparative study. The analyses would need to begin with creating homogeneous climate timeseries for one or more locations. This will be difficult noting the Labasa Mill climate station has been relocated on multiple locations and there are limited records detailing site and instrument changes.

It is likely the leading model terms would be those related to the most important aspects of sugarcane production, that being a long, warm growing season with a high incidence of solar radiation with adequate precipitation and few to no instances of high winds followed by a fairly dry, sunny and cool season for ripening and harvesting. While the Labasa milling region has a wetter growing season than southwest Viti Levu and a marginally cooler season ripening season which would appear to be favourable for sugar yield, Gawander et al. (2018) found average yield similar for Lautoka and Labasa, 53 and 50 tonnes/ha respectively. Sugarcane yield trends also over 1961–2012 were 0.14 and 0.16 tonnes per year respectively.

It has been suggested that rotating the principal components using varimax rotation could have produced better results in Chapter 4. Varimax rotation is a statistical technique used at one level of factor analysis as an attempt to clarify the relationship among factors. Generally, the process involves adjusting the coordinates of data that result from a principal components analysis. The adjustment, or rotation, is intended to maximize the variance shared among items. By maximizing the shared variance, results more discretely represent how data correlate with each principal component. To maximize the variance generally means to increase the squared correlation of items related to one factor, while decreasing the correlation on any other factor. In other words, the varimax rotation simplifies the loadings of items by removing the middle ground and more specifically identifying the factor upon which data load. Orthogonal rotation, which varimax achieves, ensures each factor is not correlated. The output then uses loadings on each variable, and a time series of PCA or Factor scores. These can then be used as input into multiple regression. Exploratory factor analysis with varimax rotation and backwards stepwise regression has previously been used in a Fiji study for predicting typhoid occurrence using a range of environmental and health variables (Jenkins et al. 2019).

## 5.2 Outlook

Extreme weather and climate events have significant impacts on Pacific Island society. To be able to learn more about the physics of these events it is necessary to have accurate records of past climate variability. There is still a lot of work to be done to improve the quality of Pacific daily resolution meteorological records. In August 2020, a proposal was presented to Pacific Islands national meteorological service directors where they were asked to make data from at least one climate station for small countries, three to four stations for large countries freely available in the Pacific Climate Change Data Portal www.bom.gov.au/climate/pccsp/ for academic and student research. Currently data for Australian, New Zealand and US affiliated stations are publicly available but this is not the case for the other sites. Improving data sharing is one of several ways of better understanding the climate of the Pacific.

At the same time algorithms are being added to the climate data management system, known as CliDE (Climate Data for the Environment) which will automate the quality checking of data for 14 NMSs. This will include range checks and comparison with neighbouring station observations where possible. While the algorithms in CliDE will not fix dubious data, the quality flags will identify suspect data for future researchers. CliDE also provides the NMSs with the ability to archive metadata and historical station information. Hopefully, these improvements will result in higher quality timeseries for future analyses of trends and variability in climate extremes in the western Pacific.

## References

Acharya, S.C., Nathan, R., Wang, Q.J., Su, C.-H., Eizenberg, N., 2019. An evaluation of daily precipitation from a regional atmospheric reanalysis over Australia. Hydrol. Earth Syst. Sci. 23, 3387–3403. https://doi.org/10.5194/hess-23-3387-2019

Alexander, L. V, Bador, M., Roca, R., Contractor, S., Donat, M.G., Nguyen, P.L., 2020. Intercomparison of annual precipitation indices and extremes over global land areas from in situ, space-based and reanalysis products. Environ. Res. Lett. 15, 55002. https://doi.org/10.1088/1748-9326/ab79e2

Alexander, L. V, Fowler, H.J., Bador, M., Behrangi, A., Donat, M.G., Dunn, R., Funk, C., Goldie, J., Lewis, E., Rogé, M., Seneviratne, S.I., Venugopal, V., 2019. On the use of indices to study extreme precipitation on sub-daily and daily timescales. Environ. Res. Lett. 14, 125008. https://doi.org/10.1088/1748-9326/ab51b6

Alexander, L. V, Zhang, X., Peterson, T.C., Caesar, J., Gleason, B., Klein Tank, A.M.G., Haylock, M., Collins, D., Trewin, B., Rahimzadeh, F., Tagipour, A., Rupa Kumar, K., Revadekar, J., Griffiths, G., Vincent, L., Stephenson, D.B., Burn, J., Aguilar, E., Brunet, M., Taylor, M., New, M., Zhai, P., Rusticucci, M., Vazquez-Aguirre, J.L., 2006. Global observed changes in daily climate extremes of temperature and precipitation. J. Geophys. Res. Atmos. 111, D05109. https://doi.org/10.1029/2005JD006290

Australian Bureau of Meteorology, CSIRO, 2011. Climate Change in the Pacific: Scientific Assessment and New Research. Volume 1: Regional Review. Volume 2: Country Reports. Melbourne, Australia

Caesar, J., Alexander, L. V, Trewin, B., Tse-ring, K., Sorany, L., Vuniyayawa, V., Keosavang, N., Shimana, A., Htay, M.M., Karmacharya, J., Jayasinghearachchi, D.A., Sakkamart, J., Soares, E., Hung, L.T., Thuong, L.T., Hue, C.T., Dung, N.T.T., Hung, P. V, Cuong, H.D., Cuong, N.M., Sirabaha, S., 2011. Changes in temperature and precipitation extremes over the Indo-Pacific region from 1971 to 2005. Int. J. Climatol. 31, 791–801. https://doi.org/10.1002/joc.2118

CSIRO, 2020. Norfolk Island Water Resource Assessment [WWW Document]. URL https://www.csiro.au/en/Research/LWF/Areas/Water/Assessing-water-resources/Norfolk/Overview (accessed 7.19.20).

Dai, A., 2011. Characteristics and trends in various forms of the Palmer Drought Severity Index during 1900–2008. J. Geophys. Res. Atmos. 116. https://doi.org/10.1029/2010JD015541

Dutheil, C., Bador, M., Lengaigne, M., Lefèvre, J., Jourdain, N., Vialard, J., Jullien, S., Peltier, A., Menkes, C., 2019. Impact of surface temperature biases on climate change projections of the South Pacific Convergence Zone. Clim. Dyn. 1–23. https://doi.org/10.1007/s00382-019-04692-6

Folland, C.K., Salinger, M.J., Jiang, N., Rayner, N.A., 2003. Trends and Variations in South Pacific Island and Ocean Surface Temperatures. J. Clim. 16, 2859–2874. https://doi.org/10.1175/1520-0442(2003)016<2859:TAVISP>2.0.CO;2

Folland, C.K., Renwick, J.A., Salinger, M.J., Mullan, A.B., 2002. Relative influences of the Interdecadal Pacific Oscillation and ENSO on the South Pacific Convergence Zone. Geophys. Res. Lett. 29, 21–24. https://doi.org/10.1029/2001GL014201

Gawander, J., Salinger, J., Prasad, J., Rounds, P., Kumar, R., 2018. El Nino – Southern Oscillation influences on sugarcane production in Fiji – An exploratory investigation. Int. Sugar J. CXX, 778–784.

Griffiths, G.M., Salinger, M.J., Leleu, I., 2003. Trends in extreme daily rainfall across the South Pacific and relationship to the South Pacific Convergence Zone. Int. J. Climatol. 23, 847–869. https://doi.org/10.1002/joc.923

Guijarro, J.A., López, J.A., Aguilar, E., Domonkos, P., Venema, V.K.C., Sigró, J., Brunet, M., 2007. Comparison of homogenisation packages applied to monthly series of temperature and precipitation. The multitest project, in: Szentimrey, T., Lakatos, M., Hoffmann, L. (Eds.), Ninth Seminar for Homogenisation and Quality Control in Climatological Databases and Fourth Conference on Spatial Interpolation Techniques in Climatology and Meteorology. WMO Climate Data and Monitoring WCDMP-No.85, Budapest, Hungary.

Halwatura, D., McIntyre, N., Lechner, A.M., Arnold, S., 2017. Capability of meteorological drought indices for detecting soil moisture droughts. J. Hydrol. Reg. Stud. 12, 396–412. https://doi.org/https://doi.org/10.1016/j.ejrh.2017.06.001

Hay, J.E., Mimura, N., Campbell, J., Fifita, S., Koshy, K., McLean, R.F., Nakalevu, T., Nunn, P., de Wet, N., 2003. Climate Variability and Change and Sea-level Rise in the Pacific Islands Region – A Resource Book for Policy and Decision Makers, Educators and Other Stakeholders. Apia, Samoa.

Hutchinson, S., Gomes, C., Alleyne, D., Phillips, W., 2013. An assessment of the economic and social impacts of climate change on the agriculture sector in the Caribbean, Economic Commission for Latin American and the Caribbean Report LC/CAR/L.398. Port of Spain, Trinidad and Tobago.

Jenkins, A.P., Jupiter, S.D., Jenney, A., Naucukidi, A., Prasad, N., Vosaki, G., Mulholland, K., Strugnell, R., Kama, M., Crump, J.A., Horwitz, P., 2019. Environmental Foundations of Typhoid Fever in the Fijian Residential Setting. Int. J. Environ. Res. Public Health 16. https://doi.org/10.3390/ijerph16132407.

Keyantash, J., Dracup, J.A., 2002. The Quantification of Drought: An Evaluation of Drought Indices. Bull. Am. Meteorol. Soc. 83, 1167–1180. https://doi.org/10.1175/1520-0477(2002)083<1191:TQODAE>2.3.CO;2

Kuleshov, Y., McGree, S., Jones, D.A., Charles, A., Cottrill, A., Prakash, B., Atalifo, T., Nihmei, S., Seuseu, F., 2014. Extreme weather and climate events and their impacts on island countries in the Western Pacific: Cyclones, Floods and Droughts. Atmos. Clim. Sci. 4, 803–818. https://doi.org/10.4236/acs/2014.45071.

McAneney, J., van den Honert, R., Yeo, S., 2017. Stationarity of major flood frequencies and heights on the Ba River, Fiji, over a 122-year record. Int. J. Climatol. 37, 171–178. https://doi.org/10.1002/joc.4989

McKenzie, E., Kaloumaira, A., Chand, B., 2005. The Economic Impacts of Natural Disasters in the Pacific Technical Report. Suva, Fiji.

Morrison, R.J., Clarke, W.C., 1990. Soil Erosion in Fiji – Problems and Perspectives. J Eros Control Eng Soc Jpn 43, 54–59.

Ram, A.N., Gawander, J.S., Jokhan, A.D., Garan, K., 2007. Soil loss and declining sugarcane yields on sloping land in Fiji. Proc. Int. Soc. Sugar Cane Technol. 26, 190–198.

Saft, M., Western, A.W., Zhang, L., Peel, M.C., Potter, N.J., 2015. The influence of multiyear drought on the annual rainfall-runoff relationship: An Australian perspective. Water Resour. Res. 51, 2444–2463. https://doi.org/10.1002/2014WR015348

Salinger, M. J., R. E. Basher, B. B. Fitzharris, J. E. Hay, P. D. Jones, J. P. Macveigh, and I. Schmidely-Leleu, 1995: Climate trends in the South-west Pacific. *Int. J. Climatol.*, **15**, 285–302, https://doi.org/10.1002/joc.3370150305.

Salinger, M.J., McGree, S., Beucher, F., Power, S.B., Delage, F., 2014. A new index for variations in the position of the South Pacific convergence zone 1910/11–2011/2012. Clim. Dyn. 1–12. https://doi.org/10.1007/s00382-013-2035-y

Sheffield, J., Wood, E.F., 2008. Global Trends and Variability in Soil Moisture and Drought Characteristics, 1950–2000, from Observation-Driven Simulations of the Terrestrial Hydrologic Cycle. J. Clim. 21, 432–458. https://doi.org/10.1175/2007JCLI1822.1

Sniderman, J.M.K., Brown, J.R., Woodhead, J.D., King, A.D., Gillett, N.P., Tokarska, K.B., Lorbacher, K., Hellstrom, J., Drysdale, R.N., Meinshausen, M., 2019. Southern Hemisphere subtropical drying as a transient response to warming. Nat. Clim. Chang. 9, 232–236. https://doi.org/10.1038/s41558-019-0397-9

Stephenson, T.S., Vincent, L.A., Allen, T., Van Meerbeeck, C.J., McLean, N., Peterson, T.C., Taylor, M.A., Aaron-Morrison, A.P., Auguste, T., Bernard, D., Boekhoudt, J.R.I., Blenman, R.C., Braithwaite, G.C., Brown, G., Butler, M., Cumberbatch, C.J.M., Etienne-Leblanc, S., Lake, D.E., Martin, D.E., McDonald, J.L., Ozoria Zaruela, M., Porter, A.O., Santana Ramirez, M., Tamar, G.A., Roberts, B.A., Sallons Mitro, S., Shaw, A., Spence, J.M., Winter, A., Trotman, A.R., 2014. Changes in extreme temperature and precipitation in the Caribbean region, 1961–2010. Int. J. Climatol. 34, 2957–2971. https://doi.org/10.1002/joc.3889

Su, C.-H., Eizenberg, N., Steinle, P., Jakob, D., Fox-Hughes, P., White, C.J., Rennie, S., Franklin, C., Dharssi, I., Zhu, H., 2019. BARRA v1.0: the Bureau of Meteorology Atmospheric high-resolution Regional Reanalysis for Australia. Geosci. Model Dev. 12, 2049–2068. https://doi.org/10.5194/gmd-12-2049-2019

Wairiu, M., Lal, M., Iese, V., 2011. Climate Change Implications for Crop Production in Pacific Islands Region, in: Aladjadjiyan, A. (Ed.), Food Production: Approaches, Challenges and Tasks. Books on Demand, Rijeka, Croatia, p. 284.

Whan, K., Alexander, L.V., Imielska, A., Mcgree, S., Jones, D., Ene, E., Finaulahi, S., Inape, K., Jacklick, L., Kumar, R., Laurent, V., Malala, H., Malsale, P., Pulehetoa-Mitiepo, R., Ngemaes, M., Peltier, A., Porteous, A., Seuseu, S., Skilling, E., Tahani, L., Toorua, U., Vaiimene, M., 2014. Trends and variability of temperature extremes in the tropical Western Pacific. Int. J. Climatol. 34. https://doi.org/10.1002/joc.3861

Widlansky, M.J., Timmermann, A., Stein, K., McGregor, S., Schneider, N., England, M.H., Lengaigne, M., Cai, W., 2013. Changes in South Pacific rainfall bands in a warming climate. Nat. Clim. Chang. 3, 417–423. https://doi.org/10.1038/nclimate1726

# Appendix A

This appendix provides additional data and information on the changepoint detection and data adjustment processes processes undertaken in Chapter 3 (references for this section presented with those of Chapter 3). The RHtestsV4 (Wang and Feng, 2013) package can be used to detect, and adjust for, multiple changepoints (shifts) that could exist in a data series that may have first-order autoregressive errors. RHtestsV4 is based on the penalized maximal t test (Wang et al., 2007) and the penalized maximal F-test (Wang, 2008a), which are embedded in a recursive testing algorithm (Wang, 2008b), with the lag-1 autocorrelation (if any) of the time series being empirically accounted for. The time series being tested may have zero trend or a linear trend throughout the whole period of record. The problem of uneven distribution of false alarm rate and detection power is also greatly alleviated by using empirical penalty functions. Where available a homogenous time series that is well correlated with the base series may be used as a reference series. Detection of changepoints is also possible with RHtestsV4 when a homogenous reference series is not available. But the results are less reliable and need intensive analysis.

For cases with the reference series the test used is the penalized maximal t test (Wang, 2008b; Wang et al., 2007), which assumes that the time series being tested has zero-trend and Gaussian errors. The base-minus-reference series is tested to identify the position(s) and significance of changepoint(s), but a multi-phase regression (MPR) model with a common trend is also fitted to the anomalies (relative to the mean annual cycle) of the base series at the end to obtain the final estimates of the magnitude of shifts (details provided in the Appendix of Wang (2008b)). In the MPR fit, the annual cycle, linear trend, and lag-1 autocorrelation are estimated in tandem through iterative procedures, while accounting for all the identified mean-shifts (Wang, 2008b).

For cases without a reference series the test used is the penalized maximal F-test (Wang, 2008b, 2008a), which allows the time series being tested to have a linear trend throughout the whole period of data record (i.e., no shift in the trend component; see Wang (2003)), with the annual cycle, linear trend, and lag-1 autocorrelation of the base series being estimated in tandem through iterative procedures, while accounting for all the identified mean-shifts (Wang, 2008b). The time series being tested here can be a base series (the true without a reference series case) or a base-minus-reference series (in a single ready-to-use series).

RHtestV4 has a QMadj_GaussDLY function which is used to apply the quantile-matching (QM) adjustment algorithm (Wang et al., 2010) to daily temperature data (or daily Gaussian data in general) to adjust for a list of significant changepoints that have been identified (e.g., from applying one or more of the six RHtestV4 functions to the corresponding monthly temperature series). The objective of the QM adjustments is to adjust the series so that the empirical distributions of all segments of the de-trended base series match each other; the adjustment value depends on the empirical frequency of the datum to be adjusted (i.e., it varies from one datum to another in the same segment, depending on their corresponding empirical frequencies). As a result, the shape of the distribution is often adjusted (including, but not limited to, the adjustment to the mean), although the tests are meant to detect mean-shifts (thus, a change in the distribution without a shift in the mean could go undetected); and the QM adjustments could account for a seasonality of discontinuity (e.g., it is possible that winter and summer temperatures are adjusted differently because they belong to the lower and upper quartiles of the distribution, respectively). Importantly, the annual cycle, lag-1 autocorrelation, and linear trend of the base series were estimated in tandem while accounting for all identified shifts (Wang, 2008b); and the trend component estimated for the base series is preserved in the QM adjustments when they are estimated without using a reference series. Whenever possible, QM-adjustments are estimated using a reference series that has homogeneous data series for a period encompassing the shift in the base series to be adjusted.

All tests apply to data from 1 January 1951 (or after, if data is not available from this date). Adjustments only apply to the temperature timeseries with QM-adjustments option used in all cases. Changepoints detected in the precipitation timeseries rendered the timeseries unacceptable for further analyses as while the RHtestsV4 developers allow for the adjustment of precipitation, the general consensus among experts at the BoM is that the software fails to make appropriate adjustments.

A timeseries is defined as composite where more than one station record is combined to span the study period. Details on the stations making up the composite are provided. In some cases prior to obtaining the data multiple station records are combined and archived as a single timeseries by the NMS. This is not definded as a composite in this study but the relocation dates are regarded as possible step-change points. The trend is presented as output by RHtestsV4. To convert the monthly (daily) timeseries trend value to °C per decade multiply the trend value by 120 (3652.5).

## A.1 Pago Pago, American Samoa

Precipitation timeseries composite: No

Comments: from 1956

Maximum temperature timeseries composite: No

Comments: from 1957

Minimum temperature timeseries composite: No

Comments: from 1957

### Adjustment details

| Element | Timeseries adjusted? Yes (Y) No (N) | Step changes (YYYY-MM-DD) | Magnitude of step-change (°C) Monthly, Daily | Supported by metadata? Yes (Y), No (N) | Trend before correction (°C/month) Monthly, (°C/day) Daily | Trend after correction (°C/month) Monthly, (°C/day) Daily |
|---|---|---|---|---|---|---|
| Maximum temperature | Y | 1966-03-31<br>1995-06-30<br>2003-03-31 | -0.4157, -0.3934<br>+1.1257, +1.1640<br>-0.8323, -0.8290 | N<br>N<br>Y | +0.001232, +0.000041 | +0.000682, +0.000019 |
| Minimum temperature | Y | 1966-03-31<br>1981-05-31<br>1985-09-31<br>1995-06-30<br>2003-03-31 | -0.2199, -0.1949<br>+0.3290, +0.3543<br>+0.2830, +0.2998<br>+0.5150, +0.5435<br>-0.4611, -0.4590 | N<br>N<br>N<br>N<br>Y | +0.003770, +0.000127 | +0.002344, +0.000074 |

Comments:

## A.2 Lord Howe Island Aero, Australia

Precipitation timeseries composite: Yes

Comments: Lord Howe Island (200440) from January 1951 to October 1988 then Lord Howe Island Aero (200839) from November 1988

Maximum temperature timeseries composite: Yes

Comments: As above

Minimum temperature timeseries composite: Yes

Comments: As above

### Adjustment details

| Element | Timeseries adjusted? Yes (Y) No (N) | Step changes (YYYY-MM-DD) | Magnitude of step-change (°C) Monthly, Daily | Supported by metadata? Yes (Y), No (N) | Trend before correction (°C/month) Monthly, (°C/day) Daily | Trend after correction (°C/month) Monthly, (°C/day) Daily |
|---|---|---|---|---|---|---|
| Maximum temperature | Y | 1954-11-30 | -0.7455, -0.7381 | Y | +0.000404, +0.000013 | +0.001179, +0.000039 |
| Minimum temperature | N | | | | +0.000878, | |

Comments: Observation site moved to the east side of the island in December 1954.

## A.3 Norfolk Island, Australia

Precipitation timeseries composite: No

Comments:

Maximum temperature timeseries composite: No

Comments:

Minimum temperature timeseries composite: No

Comments:

### Adjustment details

| Element | Timeseries adjusted? Yes (Y) No (N) | Step changes (YYYY-MM-DD) | Magnitude of step-change (°C) Monthly, Daily | Supported by metadata? Yes (Y), No (N) | Trend before correction (°C/month) Monthly, (°C/day) Daily | Trend after correction (°C/month) Monthly, (°C/day) Daily |
|---|---|---|---|---|---|---|
| Maximum temperature | N | | | | +0.000498, | |
| Minimum temperature | Y | 1953-11-30 | +0.5379, +0.5447 | | +0.000795, +0.000026 | +0.000618, +0.000020 |

Comments: Possible observation site change in the 1950s, statistical analysis suggests December 1953.

## A.4 Willis Island, Australia

Precipitation timeseries composite: No

Comments:

Maximum temperature timeseries composite: No

Comments:

Minimum temperature timeseries composite: No

Comments:

**Adjustment details**

| Element | Timeseries adjusted? Yes (Y) No (N) | Step changes (YYYY-MM-DD) | Magnitude of step-change (°C) Monthly, Daily | Supported by metadata? Yes (Y), No (N) | Trend before correction (°C/month) Monthly, (°C/day) Daily | Trend after correction (°C/month) Monthly, (°C/day) Daily |
|---|---|---|---|---|---|---|
| Maximum temperature | Y | 1965-12-31<br>1987-12-31 | -0.2861, -0.2662<br>-0.2769, -0.2572 | N<br>N | -0.000068, -0.000003 | +0.000776, +0.000023 |
| Minimum temperature | N | | | | | |

Comments: Small changes in observation site not presented in metadata but noted in Zillman, J.W., Downey, W.K. and Manton, M.J. 1989. Climate Change and its possible impacts in the southwest Pacific region: scientific lecture presented at the tenth session of World Meteorological Organization Regional Association V, Singapore 14–24 November 1989.

## A.5 Penrhyn, Cook Islands

Precipitation timeseries composite: Yes

Comments: The timeseries is made up of manual observations for station number J80000 from January 1951, the 'Warwick Latham' rain gauge from September 1996 to November 2008, the first Penrhyn automatic weather station (J80200) for January and April 1998, September 2004 and December 2008. Penrhyn Marine Office rain gauge from January 2009 to 10 October 2009 and 'Warwick Latham' rain gauge from 11 October 2009 to December 2015.

Maximum temperature timeseries composite: -

Comments: Timeseries ends in 1996, therefore not used

Minimum temperature timeseries composite: -

Comments: Timeseries ends in 1996, therefore not used

### Adjustment details

| Element | Timeseries adjusted? Yes (Y) No (N) | Step changes (YYYY-MM-DD) | Magnitude of step-change (°C) Monthly, Daily | Supported by metadata? Yes (Y), No (N) | Trend before correction (°C/month) Monthly, (°C/day) Daily | Trend after correction (°C/month) Monthly, (°C/day) Daily |
|---|---|---|---|---|---|---|
| Maximum temperature | | | | | | |
| Minimum temperature | | | | | | |

Comments:

## A.6 Rarotonga, Cook Islands

Precipitation timeseries composite: No

Comments:

Maximum temperature timeseries composite: No

Comments:

Minimum temperature timeseries composite: No

Comments: 2012-03 deleted – values too low. Minimum thermometer likely to be faulty.

**Adjustment details**

| Element | Timeseries adjusted? Yes (Y) No (N) | Step changes (YYYY-MM-DD) | Magnitude of step-change (°C) Monthly, Daily | Supported by metadata? Yes (Y), No (N) | Trend before correction (°C/month) Monthly, (°C/day) Daily | Trend after correction (°C/month) Monthly, (°C/day) Daily |
|---|---|---|---|---|---|---|
| Maximum temperature | Y | 1967-06-30 | +0.3520, +0.3350 | Y | +0.001355, +0.000032 | +0.000835, +0.000016 |
| Minimum temperature | Y | 1967-06-30 | +0.2548, +0.3157 | Y | +0.002032, +0.000048 | +0.001645, +0.000033 |

Comments: The timeseries would ideally have been adjusted on 18/8/1967 when the enclosure was moved 1.8km.

## A.7 Chuuk, Federated State of Micronesia

Precipitation timeseries composite: No

Comments:

Maximum temperature timeseries composite: No

Comments:

Minimum temperature timeseries composite: No

Comments:

### Adjustment details

| Element | Timeseries adjusted? Yes (Y) No (N) | Step changes (YYYY-MM-DD) | Magnitude of step-change (°C) Monthly, Daily | Supported by metadata? Yes (Y), No (N) | Trend before correction (°C/month) Monthly, (°C/day) Daily | Trend after correction (°C/month) Monthly, (°C/day) Daily |
|---|---|---|---|---|---|---|
| Maximum temperature | Y | 2001-06-30 | -0.7211, -0.7204 | N | +0.001089, +0.000035 | +0.002051, +0.000067 |
| Minimum temperature | Y | 1996-07-31<br>1999-09-31<br>2004-03-31 | -2.0420, -2.0058<br>+1.4989, +1.4225<br>+0.8833, +0.9124 | Y<br>N<br>N | +0.000719, +0.000023 | +0.000826, +0.000028 |

Comments:

## A.8 Pohnpei, Federated State of Micronesia

Precipitation timeseries composite: No

Comments:

Maximum temperature timeseries composite: No

Comments:

Minimum temperature timeseries composite: No

Comments:

### Adjustment details

| Element | Timeseries adjusted? Yes (Y) No (N) | Step changes (YYYY-MM-DD) | Magnitude of step-change (°C) Monthly, Daily | Supported by metadata? Yes (Y), No (N) | Trend before correction (°C/month) Monthly, (°C/day) Daily | Trend after correction (°C/month) Monthly, (°C/day) Daily |
|---|---|---|---|---|---|---|
| Maximum temperature | N | | | | +0.001383, | |
| Minimum temperature | Y | 1998-04-30<br>2012-04-30<br>2013-06-30 | -0.7322, -0.7235<br>+1.7989, +1.7039<br>-1.5024, -1.3597 | Y?<br>N<br>N | -0.000166,<br>-0.000006 | +0.000879,<br>+0.000028 |

Comments: ? – possible site change.

## A.9 Yap, Federated State of Micronesia

Precipitation timeseries composite: No

Comments:

Maximum temperature timeseries composite: No

Comments:

Minimum temperature timeseries composite: No

Comments:

### Adjustment details

| Element | Timeseries adjusted? Yes (Y) No (N) | Step changes (YYYY-MM-DD) | Magnitude of step-change (°C) Monthly, Daily | Supported by metadata? Yes (Y), No (N) | Trend before correction (°C/month) Monthly, (°C/day) Daily | Trend after correction (°C/month) Monthly, (°C/day) Daily |
|---|---|---|---|---|---|---|
| Maximum temperature | Y | 1958-11<br>1975-02<br>2008-03<br>2009-07<br>2014-06 | -0.8324<br>-0.4172<br>-0.7114<br>+0.3578<br>-1.1871 | Y<br>N<br>N<br>N<br>N | +0.001174, | +0.000993, |
| Minimum temperature | Y | 1968-03<br>1975-02<br>1985-09<br>1995-06<br>2003-11<br>2008-03 | +0.5383<br>+1.0649<br>+1.4383<br>+1.7179<br>+2.8357<br>+2.1010 | Y<br>N<br>Y<br>Y<br>N<br>N | -0.000261, | +0.000873, |

Comments: Only monthly timeseries adjusted. Adjustments made with local sea surface temperature as a reference series. Ideally the 1985-09 adjustment would have been made on 4 October 1985, 1995-06 adjustment would have been made on 17 November 1994, a documented site change. The step changes since 2000 show up as major changepoints in the DTR.

## A.10 Lakeba, Fiji

Precipitation timeseries composite: No

Comments: AWS data used to fill a gap in the manual record in 1999 (July). AWS data used from January 2012.

Maximum temperature timeseries composite: No

Comments: Not available

Minimum temperature timeseries composite: No

Comments: Not available

**Adjustment details**

| Element | Timeseries adjusted? Yes (Y) No (N) | Step changes (YYYY-MM-DD) | Magnitude of step-change (°C) Monthly, Daily | Supported by metadata? Yes (Y), No (N) | Trend before correction (°C/month) Monthly, (°C/day) Daily | Trend after correction (°C/month) Monthly, (°C/day) Daily |
|---|---|---|---|---|---|---|
| Maximum temperature | | | | | | |
| Minimum temperature | | | | | | |

Comments:

## A.11 Laucala Bay (Suva), Fiji

Precipitation timeseries composite: No

Comments:

Maximum temperature timeseries composite: No

Comments:

Minimum temperature timeseries composite: No

Comments:

### Adjustment details

| Element | Timeseries adjusted? Yes (Y) No (N) | Step changes (YYYY-MM-DD) | Magnitude of step-change (°C) Monthly, Daily | Supported by metadata? Yes (Y), No (N) | Trend before correction (°C/month) Monthly, (°C/day) Daily | Trend after correction (°C/month) Monthly, (°C/day) Daily |
|---|---|---|---|---|---|---|
| Maximum temperature | N | | | | +0.001908, | |
| Minimum temperature | N | | | | +0.001940, | |

Comments: As there are no site and/or surrounding environment changes documented, adjustments have not been made even though the raw trends are very strong. The surrounding environment has changed significantly since 1942 beginning with homes developed between the enclosure and sea shore. More recently the mangrove swamp across the road has been covered over. There is significant vegetation around the enclosure which wasn't in the original photographs.

Additional information is required such as when the new Fiji Met. Service double story building construction began. From limited information available sometime between 2009 and 2014. Prior to this single-story building existed from WWII. DTR suggested changepoints Mar 1955 and Apr 2009. These might be the way to go if adjustments are required.

## A.12 Lautoka Mill, Fiji

Precipitation timeseries composite: Yes

Comments: Lautoka Mill AWS data used to fill gaps in the manual record from May to July 2011 and for October 2012.

Maximum temperature timeseries composite: No

Comments:

Minimum temperature timeseries composite: No

Comments:

**Adjustment details**

| Element | Timeseries adjusted? Yes (Y) No (N) | Step changes (YYYY-MM-DD) | Magnitude of step-change (°C) Monthly, Daily | Supported by metadata? Yes (Y), No (N) | Trend before correction (°C/month) Monthly, (°C/day) Daily | Trend after correction (°C/month) Monthly, (°C/day) Daily |
|---|---|---|---|---|---|---|
| Maximum temperature | Y | 1956-10-31<br>1964-11-30<br>1973-08-31<br>1978-08-31<br>1986-09-31 | -0.9910, -0.6927<br>-0.1276, +0.5771<br>-0.1447, +0.4762<br>+0.4389, +0.8597<br>+0.2593, +0.3897 | | +0.001291, +0.000037 | +0.000942, +0.000024 |
| Minimum temperature | Y | 1993-02-28<br>1998-02-28<br>2006-06-30<br>2011-08-31<br>2012-09-30<br>2014-01-31 | , -0.3750<br>+0.1911, +0.1361<br>, -0.4439<br>, -0.2147<br>,+0.4661<br>,+2.1612 | | +0.000307, +0.000010 | +0.000006, +0.000019 |

Comments: A number of mistakes were made in the process of adjusting maximum and minimum temperature that were detected following publication of the analyses in Chapter 3. For example, Nadi Airport maximum temperature was used as a reference series at the daily timescale only. Likewise, for minimum temperature. Also, the changepoints used for minimum temperature monthly and daily adjustments are not the same. In addition to erroneous site-specific trends, there is a small impact on the Pacific-wide regional mean and extreme temperature trends presented in the same chapter. Lautoka Mill ‘homogeneous’ temperature was not used in Chapter 4.

## A.13 Nabouwalu, Fiji

Precipitation timeseries composite: No

Comments:

Maximum temperature timeseries composite: No

Comments: from 1952

Minimum temperature timeseries composite: No

Comments: from 1952

### Adjustment details

| Element | Timeseries adjusted? Yes (Y) No (N) | Step changes (YYYY-MM-DD) | Magnitude of step-change (°C) Monthly, Daily | Supported by metadata? Yes (Y), No (N) | Trend before correction (°C/month) Monthly, (°C/day) Daily | Trend after correction (°C/month) Monthly, (°C/day) Daily |
|---|---|---|---|---|---|---|
| Maximum temperature | Y | 1955-11-30<br>1998-04-30 | -1.0217, -1.0188<br>+0.7494, +0.7475 | N<br>N | +0.001651, +0.000051 | +0.000664, +0.000020 |
| Minimum temperature | N | | | | +0.001055, | |

Comments:

## A.14 Nadi Airport, Fiji

Precipitation timeseries composite: No

Comments:

Maximum temperature timeseries composite: No

Comments:

Minimum temperature timeseries composite: No

Comments:

### Adjustment details

| Element | Timeseries adjusted? Yes (Y) No (N) | Step changes (YYYY-MM-DD) | Magnitude of step-change (°C) Monthly, Daily | Supported by metadata? Yes (Y), No (N) | Trend before correction (°C/month) Monthly, (°C/day) Daily | Trend after correction (°C/month) Monthly, (°C/day) Daily |
|---|---|---|---|---|---|---|
| Maximum temperature | Y | 1985-11-30<br>1998-03-31 | -0.3588, -0.3450<br>-0.3816, -0.4190 | Y<br>Y | +0.000206, +0.000007 | +0.001446, +0.000046 |
| Minimum temperature | Y | 1965-04-30<br>1998-03-31 | -0.4832, -0.4834<br>+0.6646, +0.6591 | Y<br>Y | +0.001263, +0.000042 | +0.000931, +0.000031 |

Comments:

## A.15 Nausori Airport, Fiji

Precipitation timeseries composite: No

Comments: from 1956

Maximum temperature timeseries composite: No

Comments: from 1957

Minimum temperature timeseries composite: No

Comments: from 1957

### Adjustment details

| Element | Timeseries adjusted? Yes (Y) No (N) | Step changes (YYYY-MM-DD) | Magnitude of step-change (°C) Monthly, Daily | Supported by metadata? Yes (Y), No (N) | Trend before correction (°C/month) Monthly, (°C/day) Daily | Trend after correction (°C/month) Monthly, (°C/day) Daily |
|---|---|---|---|---|---|---|
| Maximum temperature | Y | 1976-12-31<br>1998-06-30 | -0.5128, -0.4939<br>+0.3231, +0.3429 | N<br>Y | +0.000826, +0.000028 | +0.001246, +0.000039 |
| Minimum temperature | N | | | | +0.001277, | |

Comments: Documented site change on 3 August 1998, ideally the adjustment would have taken place on this date.

## A.16 Penang Mill, Fiji

Precipitation timeseries composite: No

Comments:

Maximum temperature timeseries composite: No

Comments: Not available

Minimum temperature timeseries composite: No

Comments: Not available

### Adjustment details

| Element | Timeseries adjusted? Yes (Y) No (N) | Step changes (YYYY-MM-DD) | Magnitude of step-change (°C) Monthly, Daily | Supported by metadata? Yes (Y), No (N) | Trend before correction (°C/month) Monthly, (°C/day) Daily | Trend after correction (°C/month) Monthly, (°C/day) Daily |
|---|---|---|---|---|---|---|
| Maximum temperature | | | | | | |
| Minimum temperature | | | | | | |

Comments:

## A.17 Rotuma, Fiji

Precipitation timeseries composite: Yes

Comments: Observations from the AWS used from 12 July 2014

Maximum temperature timeseries composite: No

Comments:

Minimum temperature timeseries composite: No

Comments:

### Adjustment details

| Element | Timeseries adjusted? Yes (Y) No (N) | Step changes (YYYY-MM-DD) | Magnitude of step-change (°C) Monthly, Daily | Supported by metadata? Yes (Y), No (N) | Trend before correction (°C/month) Monthly, (°C/day) Daily | Trend after correction (°C/month) Monthly, (°C/day) Daily |
|---|---|---|---|---|---|---|
| Maximum temperature | N | | | | +0.001042, | |
| Minimum temperature | N | | | | +0.001274, | |

Comments: A large number of step changes identified in both the maximum and minimum temperature timeseries. Both timeseries rejected.

## A.18 Autona, (Hiva Oa, Marquesas Islands), French Polynesia

Precipitation timeseries composite: No

Comments:

Maximum temperature timeseries composite: No

Comments: Too short for analysis

Minimum temperature timeseries composite: No

Comments: Too short for analysis

### Adjustment details

| Element | Timeseries adjusted? Yes (Y) No (N) | Step changes (YYYY-MM-DD) | Magnitude of step-change (°C) Monthly, Daily | Supported by metadata? Yes (Y), No (N) | Trend before correction (°C/month) Monthly, (°C/day) Daily | Trend after correction (°C/month) Monthly, (°C/day) Daily |
|---|---|---|---|---|---|---|
| Maximum temperature | | | | | | |
| Minimum temperature | | | | | | |

Comments:

## A.19 Mataura, (Tubuai, Austral Islands), French Polynesia

Precipitation timeseries composite: No

Comments:

Maximum temperature timeseries composite: No

Comments: Not available from September 2014

Minimum temperature timeseries composite: No

Comments: Not available from September 2014

### Adjustment details

| Element | Timeseries adjusted? Yes (Y) No (N) | Step changes (YYYY-MM-DD) | Magnitude of step-change (°C) Monthly, Daily | Supported by metadata? Yes (Y), No (N) | Trend before correction (°C/month) Monthly, (°C/day) Daily | Trend after correction (°C/month) Monthly, (°C/day) Daily |
|---|---|---|---|---|---|---|
| Maximum temperature | | | | | | |
| Minimum temperature | | | | | | |

Comments:

## A.20 Rapa, (Austral Islands), French Polynesia

Precipitation timeseries composite: No

Comments:

Maximum temperature timeseries composite: No

Comments:

Minimum temperature timeseries composite: No

Comments:

### Adjustment details

| Element | Timeseries adjusted? Yes (Y) No (N) | Step changes (YYYY-MM-DD) | Magnitude of step-change (°C) Monthly, Daily | Supported by metadata? Yes (Y), No (N) | Trend before correction (°C/month) Monthly, (°C/day) Daily | Trend after correction (°C/month) Monthly, (°C/day) Daily |
|---|---|---|---|---|---|---|
| Maximum temperature | Y | 1956-12-31<br>1968-06-30<br>1972-10-31 | -0.8266, -0.8461<br>+0.9394, +0.9676<br>-1.2577, -1.2847 | N<br>N<br>N | +0.000442, +0.000015 | +0.001723, +0.000057 |
| Minimum temperature | N | | | | +0.001654, | |

Comments:

## A.21 Tahiti-Faaa, (Society Islands), French Polynesia

Precipitation timeseries composite: Yes

Comments: Monthly precipitation from January 1951 to May 1957 obtained from Jim Salinger used to extended data obtained from MeteoFrance (from January 1957).

Maximum temperature timeseries composite: No

Comments: from 1957

Minimum temperature timeseries composite: No

Comments: from 1957

### Adjustment details

| Element | Timeseries adjusted? Yes (Y) No (N) | Step changes (YYYY-MM-DD) | Magnitude of step-change (°C) Monthly, Daily | Supported by metadata? Yes (Y), No (N) | Trend before correction (°C/month) Monthly, (°C/day) Daily | Trend after correction (°C/month) Monthly, (°C/day) Daily |
|---|---|---|---|---|---|---|
| Maximum temperature | N | | | | +0.001924, | |
| Minimum temperature | N | | | | +0.002929, | |

Comments:

## A.22 Takaroa, (Tuamotu Group), French Polynesia

Precipitation timeseries composite: No

Comments:

Maximum temperature timeseries composite: No

Comments:

Minimum temperature timeseries composite: No

Comments:

### Adjustment details

| Element | Timeseries adjusted? Yes (Y) No (N) | Step changes (YYYY-MM-DD) | Magnitude of step-change (°C) Monthly, Daily | Supported by metadata? Yes (Y), No (N) | Trend before correction (°C/month) Monthly, (°C/day) Daily | Trend after correction (°C/month) Monthly, (°C/day) Daily |
|---|---|---|---|---|---|---|
| Maximum temperature | N | | | | +0.002359, | |
| Minimum temperature | N | | | | +0.001121, | |

Comments:

## A.23 Agana (Guam International Airport), Guam

Precipitation timeseries composite: No

Comments: from 1957

Maximum temperature timeseries composite: No

Comments: Not available

Minimum temperature timeseries composite: No

Comments: Not available

### Adjustment details

| Element | Timeseries adjusted? Yes (Y) No (N) | Step changes (YYYY-MM-DD) | Magnitude of step-change (°C) Monthly, Daily | Supported by metadata? Yes (Y), No (N) | Trend before correction (°C/month) Monthly, (°C/day) Daily | Trend after correction (°C/month) Monthly, (°C/day) Daily |
|---|---|---|---|---|---|---|
| Maximum temperature | | | | | | |
| Minimum temperature | | | | | | |

Comments:

## A.24 Butaritari, Kiribati

Precipitation timeseries composite: No

Comments: Monthly only

Maximum temperature timeseries composite: No

Comments: Not available

Minimum temperature timeseries composite: No

Comments: Not available

### Adjustment details

| Element | Timeseries adjusted? Yes (Y) No (N) | Step changes (YYYY-MM-DD) | Magnitude of step-change (°C) Monthly, Daily | Supported by metadata? Yes (Y), No (N) | Trend before correction (°C/month) Monthly, (°C/day) Daily | Trend after correction (°C/month) Monthly, (°C/day) Daily |
|---|---|---|---|---|---|---|
| Maximum temperature | | | | | | |
| Minimum temperature | | | | | | |

Comments:

## A.25 Kiritimati, Kiribati

Precipitation timeseries composite: No

Comments: Jun 1995, Jan-Nov 1976, Feb 1987, Jul 1991 to Apr 1995, Oct-Dec 1998 obtained from Mr Tony Falkland (hydrologist consultant)

Maximum temperature timeseries composite: No

Comments: Not available

Minimum temperature timeseries composite: No

Comments: Not available

**Adjustment details**

| Element | Timeseries adjusted? Yes (Y) No (N) | Step changes (YYYY-MM-DD) | Magnitude of step-change (°C) Monthly, Daily | Supported by metadata? Yes (Y), No (N) | Trend before correction (°C/month) Monthly, (°C/day) Daily | Trend after correction (°C/month) Monthly, (°C/day) Daily |
|---|---|---|---|---|---|---|
| Maximum temperature | | | | | | |
| Minimum temperature | | | | | | |

Comments:

## A.26 Tarawa, Kiribati

Precipitation timeseries composite: No

Comments:

Maximum temperature timeseries composite: No

Comments:

Minimum temperature timeseries composite: No

Comments:

### Adjustment details

| Element | Timeseries adjusted? Yes (Y) No (N) | Step changes (YYYY-MM-DD) | Magnitude of step-change (°C) Monthly, Daily | Supported by metadata? Yes (Y), No (N) | Trend before correction (°C/month) Monthly, (°C/day) Daily | Trend after correction (°C/month) Monthly, (°C/day) Daily |
|---|---|---|---|---|---|---|
| Maximum temperature | Y | 1957-05-31 | -0.6541, -0.5256 | Y | +0.000555, +0.000014 | +0.001032, +0.000027 |
| Minimum temperature | Y | 1957-05-31 | -0.3465, -0.2936 | Y | +0.000657, +0.000019 | +0.000891, +0.000026 |

Comments: Site change on 4 July 1957

## A.27 Kwajalein/Bucholz, Marshall Islands

Precipitation timeseries composite: No

Comments:

Maximum temperature timeseries composite: No

Comments:

Minimum temperature timeseries composite: No

Comments:

### Adjustment details

| Element | Timeseries adjusted? Yes (Y) No (N) | Step changes (YYYY-MM-DD) | Magnitude of step-change (°C) Monthly, Daily | Supported by metadata? Yes (Y), No (N) | Trend before correction (°C/month) Monthly, (°C/day) Daily | Trend after correction (°C/month) Monthly, (°C/day) Daily |
|---|---|---|---|---|---|---|
| Maximum temperature | Y | 1954-09-30<br>1960-06-30<br>1992-06-30 | -2.0251, -2.0225<br>+0.7374, +0.7205<br>-0.6341, -0.6413 | Y<br>Y<br>N | +0.000351, +0.000012 | +0.001636, +0.000054 |
| Minimum temperature | Y | 1954-09-30<br>1960-06-30 | +0.1874, +0.1956<br>-1.3130, -1.3411 | Y<br>Y | +0.000922, +0.000029 | +0.002097, +0.000068 |

Comments:

## A.28 Majuro, Marshall Islands

Precipitation timeseries composite: No

Comments:

Maximum temperature timeseries composite: No

Comments:

Minimum temperature timeseries composite: No

Comments:

### Adjustment details

| Element | Timeseries adjusted? Yes (Y) No (N) | Step changes (YYYY-MM-DD) | Magnitude of step-change (°C) Monthly, Daily | Supported by metadata? Yes (Y), No (N) | Trend before correction (°C/month) Monthly, (°C/day) Daily | Trend after correction (°C/month) Monthly, (°C/day) Daily |
|---|---|---|---|---|---|---|
| Maximum temperature | N | | | | +0.001004, | |
| Minimum temperature | Y | 1974-12-31<br>1996-11-30 | -0.9079, -0.8789<br>+0.9606, +1.0042 | N<br>N | +0.001994, +0.000061 | +0.001894, +0.000056 |

Comments:

## A.29 Nauru Arc-2, Nauru

Precipitation timeseries composite: Yes (monthly only as a large amount of daily data missing)
Comments: Nauru Coastal Radio Station to September 1977, Nauru Airport from January 1982 to January 1986, Nauru ARC-2 AWS from July 2003 to December 2008, Nauru manual rain gauge within AWS enclosure January 2009 to October 2009, Topside TB3 rain gauge from November 2009 to December 2015. The gaps between October 1977 to December 1981, February 1986 to June 2003 have been filled with data from Taylor (1973) An atlas of Pacific Island rainfall. Department of Meteorology, University of Hawaii at Manoa, Data Rep. 25, 174 pp.

Maximum temperature timeseries composite: No
Comments: Not available

Minimum temperature timeseries composite: No
Comments: Not available

**Adjustment details**

| Element | Timeseries adjusted? Yes (Y) No (N) | Step changes (YYYY-MM-DD) | Magnitude of step-change (°C) Monthly, Daily | Supported by metadata? Yes (Y), No (N) | Trend before correction (°C/month) Monthly, (°C/day) Daily | Trend after correction (°C/month) Monthly, (°C/day) Daily |
|---|---|---|---|---|---|---|
| Maximum temperature | | | | | | |
| Minimum temperature | | | | | | |

Comments:

## A.30 Houailou P, New Caledonia

Precipitation timeseries composite: No

Comments: from 1952

Maximum temperature timeseries composite: No

Comments: Not available

Minimum temperature timeseries composite: No

Comments: Not available

### Adjustment details

| Element | Timeseries adjusted? Yes (Y) No (N) | Step changes (YYYY-MM-DD) | Magnitude of step-change (°C) Monthly, Daily | Supported by metadata? Yes (Y), No (N) | Trend before correction (°C/month) Monthly, (°C/day) Daily | Trend after correction (°C/month) Monthly, (°C/day) Daily |
|---|---|---|---|---|---|---|
| Maximum temperature | | | | | | |
| Minimum temperature | | | | | | |

Comments:

## A.31 Kone, New Caledonia

Precipitation timeseries composite: No

Comments:

Maximum temperature timeseries composite: No

Comments: Not available

Minimum temperature timeseries composite: No

Comments: Not available

### Adjustment details

| Element | Timeseries adjusted? Yes (Y) No (N) | Step changes (YYYY-MM-DD) | Magnitude of step-change (°C) Monthly, Daily | Supported by metadata? Yes (Y), No (N) | Trend before correction (°C/month) Monthly, (°C/day) Daily | Trend after correction (°C/month) Monthly, (°C/day) Daily |
|---|---|---|---|---|---|---|
| Maximum temperature | | | | | | |
| Minimum temperature | | | | | | |

Comments:

## A.32 Koumac, New Caledonia

Precipitation timeseries composite: No

Comments:

Maximum temperature timeseries composite: No

Comments:

Minimum temperature timeseries composite: No

Comments:

### Adjustment details

| Element | Timeseries adjusted? Yes (Y) No (N) | Step changes (YYYY-MM-DD) | Magnitude of step-change (°C) Monthly, Daily | Supported by metadata? Yes (Y), No (N) | Trend before correction (°C/month) Monthly, (°C/day) Daily | Trend after correction (°C/month) Monthly, (°C/day) Daily |
|---|---|---|---|---|---|---|
| Maximum temperature | Y | 1953-10-31 | -1.4832, -1.4379 | N | +0.000886, +0.000029 | +0.001376, +0.000044 |
| Minimum temperature | Y | 1953-10-31 | +0.9151, +0.9694 | N | +0.001768, +0.000058 | +0.001464, +0.000048 |

Comments:

## A.33 La Foa, New Caledonia

Precipitation timeseries composite: No

Comments:

Maximum temperature timeseries composite: No

Comments: from 1952

Minimum temperature timeseries composite: No

Comments: from 1952

### Adjustment details

| Element | Timeseries adjusted? Yes (Y) No (N) | Step changes (YYYY-MM-DD) | Magnitude of step-change (°C) Monthly, Daily | Supported by metadata? Yes (Y), No (N) | Trend before correction (°C/month) Monthly, (°C/day) Daily | Trend after correction (°C/month) Monthly, (°C/day) Daily |
|---|---|---|---|---|---|---|
| Maximum temperature | Y | 1978-10-31<br>1984-04-30 | +0.2770, +0.4036<br>-0.4716, -0.4684 | Y<br>Y | +0.000801, +0.000026 | +0.001180, +0.000031 |
| Minimum temperature | N | | | | +0.000904, | |

Comments:

## A.34 Noumea, New Caledonia

Precipitation timeseries composite: No

Comments:

Maximum temperature timeseries composite: No

Comments:

Minimum temperature timeseries composite: No

Comments:

### Adjustment details

| Element | Timeseries adjusted? Yes (Y) No (N) | Step changes (YYYY-MM-DD) | Magnitude of step-change (°C) Monthly, Daily | Supported by metadata? Yes (Y), No (N) | Trend before correction (°C/month) Monthly, (°C/day) Daily | Trend after correction (°C/month) Monthly, (°C/day) Daily |
|---|---|---|---|---|---|---|
| Maximum temperature | Y | 1976-05-31 | +0.3101, +3053 | Y | +0.001452, +0.000048 | +0.000885, +0.000029 |
| Minimum temperature | Y | 1976-05-31<br>1995-12-31 | -0.3641, -0.3591<br>+0.5239, +0.5229 | Y<br>Y? | +0.000995, +0.000033 | +0.000782, +0.000025 |

Comments: ? – possible start of AWS

## A.35 Ponerihouen, New Caledonia

Precipitation timeseries composite: No

Comments: from 1952

Maximum temperature timeseries composite: No

Comments: Not available

Minimum temperature timeseries composite: No

Comments: Not available

### Adjustment details

| Element | Timeseries adjusted? Yes (Y) No (N) | Step changes (YYYY-MM-DD) | Magnitude of step-change (°C) Monthly, Daily | Supported by metadata? Yes (Y), No (N) | Trend before correction (°C/month) Monthly, (°C/day) Daily | Trend after correction (°C/month) Monthly, (°C/day) Daily |
|---|---|---|---|---|---|---|
| Maximum temperature | | | | | | |
| Minimum temperature | | | | | | |

Comments:

## A.36 Touho Gend, New Caledonia

Precipitation timeseries composite: No

Comments: from 1952

Maximum temperature timeseries composite: No

Comments: Not available

Minimum temperature timeseries composite: No

Comments: Not available

### Adjustment details

| Element | Timeseries adjusted? Yes (Y) No (N) | Step changes (YYYY-MM-DD) | Magnitude of step-change (°C) Monthly, Daily | Supported by metadata? Yes (Y), No (N) | Trend before correction (°C/month) Monthly, (°C/day) Daily | Trend after correction (°C/month) Monthly, (°C/day) Daily |
|---|---|---|---|---|---|---|
| Maximum temperature | | | | | | |
| Minimum temperature | | | | | | |

Comments:

## A.37 Raoul Island, New Zealand

Precipitation timeseries composite: Yes

Comments: AWS data from January 1997

Maximum temperature timeseries composite: Yes

Comments: AWS data from January 1997

Minimum temperature timeseries composite: Yes

Comments: AWS data from January 1997

**Adjustment details**

| Element | Timeseries adjusted? Yes (Y) No (N) | Step changes (YYYY-MM-DD) | Magnitude of step-change (°C) Monthly, Daily | Supported by metadata? Yes (Y), No (N) | Trend before correction (°C/month) Monthly, (°C/day) Daily | Trend after correction (°C/month) Monthly, (°C/day) Daily |
|---|---|---|---|---|---|---|
| Maximum temperature | Y | 1996-11-30 | +0.2981, +0.2997 | Y | +0.001289, +0.000042 | +0.000811, +0.000026 |
| Minimum temperature | Y | 1996-11-30 | +0.3137, +0.3135 | Y | +0.000752, +0.000025 | +0.000255, +0.000009 |

Comments: Change from manual to AWS observations. Adjustment would ideally have taken place from 1 January 1997. Based on a review of the results ideally only maximum temperature would have been adjusted. The basis for adjustment of both timeseries is weak from a detection of changepoints perspective but there is a clear increase in maximum temperature variability from about 1997.

## A.38 Hanan Airport, Niue

Precipitation timeseries composite: Yes

Comments: Hanan Airport used to extend Alofi timeseries from December 1996

Maximum temperature timeseries composite: Yes

Comments: Hanan Airport used to extend Alofi timeseries from December 1996

Minimum temperature timeseries composite: Yes

Comments: Hanan Airport used to extend Alofi timeseries from December 1996

### Adjustment details

| Element | Timeseries adjusted? Yes (Y) No (N) | Step changes (YYYY-MM-DD) | Magnitude of step-change (°C) Monthly, Daily | Supported by metadata? Yes (Y), No (N) | Trend before correction (°C/month) Monthly, (°C/day) Daily | Trend after correction (°C/month) Monthly, (°C/day) Daily |
|---|---|---|---|---|---|---|
| Maximum temperature | Y | 1971-04-30<br>1976-05-31<br>1996-11-30 | -0.4733, -0.4364<br>+0.4907, +0.4889<br>-0.7395, -0.6809 | Y<br>Y<br>Y | -0.000112, -0.000005 | +0.000953, +0.000026 |
| Minimum temperature | Y | 1971-04-30<br>1976-05-31<br>1996-11-30 | -1.5678, -1.5719<br>+1.1372, +1.1344<br>-0.4568, -0.4271 | Y<br>Y<br>Y | -0.000126, -0.000004 | +0.001123, +0.000036 |

Comments: Step changes associated with relocation inland to Kaimiti, then back to the coastal site Alofi then finally to the current site Hanan Airport.

## A.39 Saipan International Airport, Northern Mariana Islands

Precipitation timeseries composite: No

Comments: from 1954

Maximum temperature timeseries composite: No

Comments: Not available

Minimum temperature timeseries composite: No

Comments: Not available

### Adjustment details

| Element | Timeseries adjusted? Yes (Y) No (N) | Step changes (YYYY-MM-DD) | Magnitude of step-change (°C) Monthly, Daily | Supported by metadata? Yes (Y), No (N) | Trend before correction (°C/month) Monthly, (°C/day) Daily | Trend after correction (°C/month) Monthly, (°C/day) Daily |
|---|---|---|---|---|---|---|
| Maximum temperature | | | | | | |
| Minimum temperature | | | | | | |

Comments:

## A.40 Koror, Palau

Precipitation timeseries composite: No

Comments:

Maximum temperature timeseries composite: No

Comments:

Minimum temperature timeseries composite: No

Comments:

### Adjustment details

| Element | Timeseries adjusted? Yes (Y) No (N) | Step changes (YYYY-MM-DD) | Magnitude of step-change (°C) Monthly, Daily | Supported by metadata? Yes (Y), No (N) | Trend before correction (°C/month) Monthly, (°C/day) Daily | Trend after correction (°C/month) Monthly, (°C/day) Daily |
|---|---|---|---|---|---|---|
| Maximum temperature | N | | | | +0.001035, | |
| Minimum temperature | Y | 2010-05-31 | +0.2844, +0.2808 | N | +0.000864, +0.000028 | +0.000689, +0.000023 |

Comments:

## A.41 Kavieng, PNG

Precipitation timeseries composite: No

Comments:

Maximum temperature timeseries composite: No

Comments: Not available

Minimum temperature timeseries composite: No

Comments: Not available

### Adjustment details

| Element | Timeseries adjusted? Yes (Y) No (N) | Step changes (YYYY-MM-DD) | Magnitude of step-change (°C) Monthly, Daily | Supported by metadata? Yes (Y), No (N) | Trend before correction (°C/month) Monthly, (°C/day) Daily | Trend after correction (°C/month) Monthly, (°C/day) Daily |
|---|---|---|---|---|---|---|
| Maximum temperature | | | | | | |
| Minimum temperature | | | | | | |

Comments:

## A.42 Madang, PNG

Precipitation timeseries composite: No

Comments:

Maximum temperature timeseries composite: No

Comments: Not available

Minimum temperature timeseries composite: No

Comments: Not available

### Adjustment details

| Element | Timeseries adjusted? Yes (Y) No (N) | Step changes (YYYY-MM-DD) | Magnitude of step-change (°C) Monthly, Daily | Supported by metadata? Yes (Y), No (N) | Trend before correction (°C/month) Monthly, (°C/day) Daily | Trend after correction (°C/month) Monthly, (°C/day) Daily |
|---|---|---|---|---|---|---|
| Maximum temperature | | | | | | |
| Minimum temperature | | | | | | |

Comments:

## A.43 Misima, PNG

Precipitation timeseries composite: No

Comments:

Maximum temperature timeseries composite: No

Comments: Not available

Minimum temperature timeseries composite: No

Comments: Not available

### Adjustment details

| Element | Timeseries adjusted? Yes (Y) No (N) | Step changes (YYYY-MM-DD) | Magnitude of step-change (°C) Monthly, Daily | Supported by metadata? Yes (Y), No (N) | Trend before correction (°C/month) Monthly, (°C/day) Daily | Trend after correction (°C/month) Monthly, (°C/day) Daily |
|---|---|---|---|---|---|---|
| Maximum temperature | | | | | | |
| Minimum temperature | | | | | | |

Comments:

## A.44 Momote, PNG

Precipitation timeseries composite: No

Comments:

Maximum temperature timeseries composite: No

Comments: Not available

Minimum temperature timeseries composite: No

Comments: Not available

### Adjustment details

| Element | Timeseries adjusted? Yes (Y) No (N) | Step changes (YYYY-MM-DD) | Magnitude of step-change (°C) Monthly, Daily | Supported by metadata? Yes (Y), No (N) | Trend before correction (°C/month) Monthly, (°C/day) Daily | Trend after correction (°C/month) Monthly, (°C/day) Daily |
|---|---|---|---|---|---|---|
| Maximum temperature | | | | | | |
| Minimum temperature | | | | | | |

Comments:

## A.45 Port Moresby, PNG

Precipitation timeseries composite: No

Comments:

Maximum temperature timeseries composite: No

Comments:

Minimum temperature timeseries composite: No

Comments:

**Adjustment details**

| Element | Timeseries adjusted? Yes (Y) No (N) | Step changes (YYYY-MM-DD) | Magnitude of step-change (°C) Monthly, Daily | Supported by metadata? Yes (Y), No (N) | Trend before correction (°C/month) Monthly, (°C/day) Daily | Trend after correction (°C/month) Monthly, (°C/day) Daily |
|---|---|---|---|---|---|---|
| Maximum temperature | Y | 1966-08-31 | -0.4771, -0.4650 | N | +0.000125, +0.000004 | +0.000815, +0.000026 |
| Minimum temperature | Y | 2013-09-31 | -1.6566, -1.5814 | N | +0.001667, +0.000055 | +0.001987, +0.000065 |

Comments: There is a very obvious drop in minimum temperatures by more than 1.5°C since about October 2013. Cannot confirm if this is an ongoing decline or step-change as there are only 14 more months of data following the step-change. This is not associated with a site change and no obvious change to the surrounding environment. Perhaps Stevenson screen change or fault.

## A.46 Wewak, PNG

Precipitation timeseries composite: No

Comments:

Maximum temperature timeseries composite: No

Comments: Not available

Minimum temperature timeseries composite: No

Comments: Not available

### Adjustment details

| Element | Timeseries adjusted? Yes (Y) No (N) | Step changes (YYYY-MM-DD) | Magnitude of step-change (°C) Monthly, Daily | Supported by metadata? Yes (Y), No (N) | Trend before correction (°C/month) Monthly, (°C/day) Daily | Trend after correction (°C/month) Monthly, (°C/day) Daily |
|---|---|---|---|---|---|---|
| Maximum temperature | | | | | | |
| Minimum temperature | | | | | | |

Comments:

## A.47 Honiara, Solomon Islands

Precipitation timeseries composite: Yes

Comments: Henderson Airport data from October 1974 to July 1979. Composite timeseries homogeneous.

Maximum temperature timeseries composite: No

Comments: See Honiara_Henderson

Minimum temperature timeseries composite: No

Comments: See Honiara_Henderson

### Adjustment details

| Element | Timeseries adjusted? Yes (Y) No (N) | Step changes (YYYY-MM-DD) | Magnitude of step-change (°C) Monthly, Daily | Supported by metadata? Yes (Y), No (N) | Trend before correction (°C/month) Monthly, (°C/day) Daily | Trend after correction (°C/month) Monthly, (°C/day) Daily |
|---|---|---|---|---|---|---|
| Maximum temperature | | | | | | |
| Minimum temperature | | | | | | |

Comments:

## A.48 Honiara_Henderson, Solomon Islands

Precipitation timeseries composite: No

Comments: See Honiara

Maximum temperature timeseries composite: Yes

Comments: Honiara data from January 1951 to December 1974, then March 1987 to December 1998.

Minimum temperature timeseries composite: Yes

Comments: Honiara data from January 1951 to December 1974, then March 1987 to December 1998.

### Adjustment details

| Element | Timeseries adjusted? Yes (Y) No (N) | Step changes (YYYY-MM-DD) | Magnitude of step-change (°C) Monthly, Daily | Supported by metadata? Yes (Y), No (N) | Trend before correction (°C/month) Monthly, (°C/day) Daily | Trend after correction (°C/month) Monthly, (°C/day) Daily |
|---|---|---|---|---|---|---|
| Maximum temperature | Y | 1987-01-31 | +0.5938, +0.6078 | Y | +0.001867, +0.000061 | +0.000722, +0.000023 |
| Minimum temperature | Y | 1974-07-31<br>1987-01-31<br>1998-11-30 | -0.4716, -0.4536<br>+0.9152, +0.9224<br>-0.7711, -0.7537 | Y<br>Y<br>Y | +0.000717, +0.000024 | +0.000969, +0.000029 |

Comments:

## A.49 Ha'apai, Tonga

Precipitation timeseries composite: No

Comments:

Maximum temperature timeseries composite: No

Comments: Not available

Minimum temperature timeseries composite: No

Comments: Not available

### Adjustment details

| Element | Timeseries adjusted? Yes (Y) No (N) | Step changes (YYYY-MM-DD) | Magnitude of step-change (°C) Monthly, Daily | Supported by metadata? Yes (Y), No (N) | Trend before correction (°C/month) Monthly, (°C/day) Daily | Trend after correction (°C/month) Monthly, (°C/day) Daily |
|---|---|---|---|---|---|---|
| Maximum temperature | | | | | | |
| Minimum temperature | | | | | | |

Comments:

## A.50 Keppel (Niuatoputapu), Tonga

Precipitation timeseries composite: No

Comments:

Maximum temperature timeseries composite: No

Comments: Not available

Minimum temperature timeseries composite: No

Comments: Not available

### Adjustment details

| Element | Timeseries adjusted? Yes (Y) No (N) | Step changes (YYYY-MM-DD) | Magnitude of step-change (°C) Monthly, Daily | Supported by metadata? Yes (Y), No (N) | Trend before correction (°C/month) Monthly, (°C/day) Daily | Trend after correction (°C/month) Monthly, (°C/day) Daily |
|---|---|---|---|---|---|---|
| Maximum temperature | | | | | | |
| Minimum temperature | | | | | | |

Comments:

## A.51 Lupepau‘u (Vava‘u), Tonga

Precipitation timeseries composite: Yes

Comments: Vava‘u then Lupepau‘u from January 1995

Maximum temperature timeseries composite: Yes

Comments: Data from 1956, Vava‘u then Lupepau‘u from January 1995

Minimum temperature timeseries composite: Yes

Comments: Data from 1956, Vava‘u then Lupepau‘u from January 1995

### Adjustment details

| Element | Timeseries adjusted? Yes (Y) No (N) | Step changes (YYYY-MM-DD) | Magnitude of step-change (°C) Monthly, Daily | Supported by metadata? Yes (Y), No (N) | Trend before correction (°C/month) Monthly, (°C/day) Daily | Trend after correction (°C/month) Monthly, (°C/day) Daily |
|---|---|---|---|---|---|---|
| Maximum temperature | Y | 1987-03-31 | -0.5896, -0.5332 | Y | +0.000408, +0.000001 | +0.001698, +0.000042 |
| Minimum temperature | Y | 1957-10-31<br>1973-10-31<br>1987-10-31<br>1999-08-31 | +0.9201, +0.8617<br>-0.3956, -0.3754<br>+0.8303, +0.8131<br>-1.4210, -1.3978 | Y<br>Y<br>Y<br>N | -0.000678, -0.000022 | +0.000482, +0.000016 |

Comments:

## A.52 Nuku‘alofa, Tonga

Precipitation timeseries composite: No

Comments: monthly only

Maximum temperature timeseries composite: No

Comments: monthly only

Minimum temperature timeseries composite: No

Comments: monthly only

### Adjustment details

| Element | Timeseries adjusted? Yes (Y) No (N) | Step changes (YYYY-MM-DD) | Magnitude of step-change (°C) Monthly, Daily | Supported by metadata? Yes (Y), No (N) | Trend before correction (°C/month) Monthly, (°C/day) Daily | Trend after correction (°C/month) Monthly, (°C/day) Daily |
|---|---|---|---|---|---|---|
| Maximum temperature | Y | 1988-04-30 | +0.6297, | Y | +0.002359, | +0.001018, |
| Minimum temperature | N | | | | +0.001873, | |

Comments: Site change 1 June 1988

## A.53 Funafuti, Tuvalu

Precipitation timeseries composite: No

Comments:

Maximum temperature timeseries composite: No

Comments:

Minimum temperature timeseries composite: No

Comments:

### Adjustment details

| Element | Timeseries adjusted? Yes (Y) No (N) | Step changes (YYYY-MM-DD) | Magnitude of step-change (°C) Monthly, Daily | Supported by metadata? Yes (Y), No (N) | Trend before correction (°C/month) Monthly, (°C/day) Daily | Trend after correction (°C/month) Monthly, (°C/day) Daily |
|---|---|---|---|---|---|---|
| Maximum temperature | Y | 1960-09-31 | -0.2962, -0.2943 | Y | +0.000994, +0.000032 | +0.001283, +0.000041 |
| Minimum temperature | N | 1967-12-31<br>1973-08-31<br>1976-01-31 | -0.8292, -0.8080<br>-0.9396, -0.9486<br>+1.5747, +1.5668 | N<br>N<br>N | +0.001527, +0.000047 | +0.001394, +0.000046 |

Comments: September 1960 is associated with a site change from the west of the island to the current location. The minimum temperature step changes are very large.

## A.54 Aneityum, Vanuatu

Precipitation timeseries composite: No

Comments:

Maximum temperature timeseries composite: No

Comments: Not available

Minimum temperature timeseries composite: No

Comments: Not available

### Adjustment details

| Element | Timeseries adjusted? Yes (Y) No (N) | Step changes (YYYY-MM-DD) | Magnitude of step-change (°C) Monthly, Daily | Supported by metadata? Yes (Y), No (N) | Trend before correction (°C/month) Monthly, (°C/day) Daily | Trend after correction (°C/month) Monthly, (°C/day) Daily |
|---|---|---|---|---|---|---|
| Maximum temperature | | | | | | |
| Minimum temperature | | | | | | |

Comments:

## A.55 Port Vila, Vanuatu

Precipitation timeseries composite: No

Comments:

Maximum temperature timeseries composite: No

Comments: See Port Vila_Bauerfield

Minimum temperature timeseries composite: No

Comments: See Port Vila_Bauerfield

### Adjustment details

| Element | Timeseries adjusted? Yes (Y) No (N) | Step changes (YYYY-MM-DD) | Magnitude of step-change (°C) Monthly, Daily | Supported by metadata? Yes (Y), No (N) | Trend before correction (°C/month) Monthly, (°C/day) Daily | Trend after correction (°C/month) Monthly, (°C/day) Daily |
|---|---|---|---|---|---|---|
| Maximum temperature | | | | | | |
| Minimum temperature | | | | | | |

Comments:

## A.56 Port Vila_Bauerfield, Vanuatu

Precipitation timeseries composite: No

Comments: Bauerfield short record not used, see Port Vila

Maximum temperature timeseries composite: Yes

Comments: While temperature observations continue to present day in Port Vila the better observation site in terms of exposure in recent years is Bauerfield (Airport). Bauerfield from January 2001.

Minimum temperature timeseries composite: Yes

Comments: While temperature observations continue to present day in Port Vila the better observation site in terms of exposure in recent years is Bauerfield (Airport). Bauerfield from January 2001.

### Adjustment details

| Element | Timeseries adjusted? Yes (Y) No (N) | Step changes (YYYY-MM-DD) | Magnitude of step-change (°C) Monthly, Daily | Supported by metadata? Yes (Y), No (N) | Trend before correction (°C/month) Monthly, (°C/day) Daily | Trend after correction (°C/month) Monthly, (°C/day) Daily |
|---|---|---|---|---|---|---|
| Maximum temperature | Y | 2007-12-31<br>2009-12-31 | +1.5531, +1.5161<br>-1.7061, -1.6737 | N<br>N | +0.002090, +0.000074 | +0.001892, +0.000067 |
| Minimum temperature | Y | 2000-10-31 | -1.5349, -1.5240 | Y | -0.000616, -0.000020 | +0.001494, +0.000050 |

Comments:

## A.57 Sola, Vanuatu

Precipitation timeseries composite: No

Comments:

Maximum temperature timeseries composite: No

Comments: Not available

Minimum temperature timeseries composite: No

Comments: Not available

### Adjustment details

| Element | Timeseries adjusted? Yes (Y) No (N) | Step changes (YYYY-MM-DD) | Magnitude of step-change (°C) Monthly, Daily | Supported by metadata? Yes (Y), No (N) | Trend before correction (°C/month) Monthly, (°C/day) Daily | Trend after correction (°C/month) Monthly, (°C/day) Daily |
|---|---|---|---|---|---|---|
| Maximum temperature | | | | | | |
| Minimum temperature | | | | | | |

Comments: